

HISTOLOGY AND HISTOPATHOLOGY

Cellular and Molecular Biology
Volume 30 (Supplement 1), 2015
<http://www.hh.um.es>



XVIII CONGRESO
DE LA SOCIEDAD ESPAÑOLA DE
HISTOLOGÍA
E INGENIERÍA TISULAR

VI INTERNATIONAL CONGRESS OF
HISTOLOGY
AND TISSUE ENGINEERING

II CONGRESO IBEROAMERICANO DE
HISTOLOGÍA



BILBAO

16-18 SEPTIEMBRE 2015
EDIFICIO BIZKAIA ARETOA



**XVIII Congreso de la Sociedad Española de Histología
e Ingeniería Tisular**

**VI Internacional Congress of Histology and Tissue
Engineering**

II Congreso Iberoamericano de Histología

Bilbao, 16, 17 y 18 de Septiembre de 2015

Organizing Committee

Enrique Hilario Rodríguez, President

Antonia Álvarez Díaz, President

Scientific Committee

Francisco Saéz Crespo, President

Miguel Alaminos Mingorance, vocal

Rafael Álvarez Nogal, vocal

Miguel Ángel Arévalo Gómez, vocal

Julia Buján Varela, vocal

Antonio Campos Muñoz, vocal

Pascual Vicente Crespo Ferrer, vocal

Dámaso Crespo Santiago, vocal

Lucio Díaz-Flores Feo, vocal

María Rosa Fenoll Brunet, vocal

María Pilar Fernández Mateos, vocal

Natalio García Honduvilla, vocal

José M. García López, vocal

Tomás García-Caballero Parada, vocal

Manuel Garrosa García, vocal

José Manuel Juiz Gómez, vocal

M^a Concepción Junquera Escribano, vocal

Juan Francisco Madrid Cuevas, vocal

Inés Martín Lacave, vocal

Alfredo Martínez Ramírez, vocal

Luis Montuenga Badía, vocal

Ana María Navarro Incio, vocal

Rosa Noguera Salvá, vocal

Luis Miguel Pastor García, vocal

Juan Ángel Pedrosa Raya, vocal

José Peña Amaro, vocal

Eloy Redondo García, vocal

Javier F. Regadera González, vocal

Mercedes Salido Peracaula, vocal

Manel Santafé Martínez, vocal

Luis Santamaría Solís, vocal

Jorge Luis Tolvía Fernández, vocal

José Antonio Uranga Ocio, vocal

Juan José Calvo Martín, vocal

Fernando Capela e Silva, vocal

Alberto Enrique D'Ottavio, vocal

María Elsa Gómez de Ferrari, vocal

Carlos R. Morales, vocal.

Juan Ocampo López, vocal

Viktor J. Romero Díaz, vocal

Claudia Sierra Castillo, vocal

Maria Lucia Zaidan Dagli, vocal

INDEX

ORAL SESSIONS

Biología reproductiva.....	1
Docencia.....	5
Histología animal	8
Histología experimental	11
Ingeniería tisular.....	17
Modelos experimentales.....	29
Neurohistología	37
Otros.....	41

POSTER SESSIONS

Biología reproductiva.....	43
Docencia.....	55
Histología animal	60
Histología vegetal.....	70
Histología experimental	72
Ingeniería tisular.....	85
Modelos experimentales.....	106
Neurohistología	122
Técnicas histológicas	133
Otros.....	139

SESIONES ORALES

BIOLOGÍA REPRODUCTIVA

15 HISTOLOGICAL AND ULTRASTRUCTURAL CHANGES IN THE GONADS OF TWO VIVIPAROUS GOODEID FISH AFTER EXPOSURE TO THE 2,4-DICHLOROPHENOXYACETIC ACID HERBICIDE

Guerrero Estévez S.M., López López E.

Instituto Politécnico Nacional, Escuela Nacional de Ciencias Biológicas, Laboratorio de Bioconservación y Manejo

Most of the aquatic systems of the Mexican Central Plateau, the main range of the viviparous Goodeids, are affected by the presence of pesticides. One of these waterbodies is Lake Chapala, where the Goodeids *Goodea atripinnis* and *Chapalichthys encaustus* are distributed and persistent-organochlorine compounds such as 2,4-dichlorophenoxyacetic acid herbicide (2,4-D), a potential endocrine disruptor, has been reported. The aim of this study was to determine the LC₅₀ of 2,4-D for *G. atripinnis* and *C. encaustus* and evaluate their possible sublethal effects on gonadal histology and ultrastructure of these two species, which differ in range and tolerance to environmental conditions. Individuals of *G. atripinnis* and *C. encaustus* were maintained and bred in aquaria under standard conditions. For the LC₅₀ determination (96 hours) static tests were performed by exposing fish to 5 concentrations of a commercial formulation of 2,4-D. Subsequently, acute assays (96 hours) were conducted by exposing *G. atripinnis* to 143.35 and 230.96 mg/L (1/1.45th and 1/0.9th of LC₅₀ value, respectively) and *C. encaustus* to 94.06 and 133.72 mg/L (1/1.45th and 1/1.02th of LC₅₀ value, respectively). All bioassays included a control group and were performed in triplicate. Gonads of individuals from experimental and control batches were dissected and fixed with 2.5% glutaraldehyde in PBS. Tissues were processed for light and electron microscopy. Images were obtained to evaluate the possible alterations after exposure to 2,4-D. The LC₅₀ (96 hours) for 2,4-D for *G. atripinnis* was 207.87 mg/L and for *C. encaustus* was 136.40 mg/L. *G. atripinnis* females exposed to 143.35 mg/L of 2,4-D showed alterations in the cytoplasm and nuclei of oocytes at perinucleolar stage; while in females exposed to 230.96 mg/L, damage was additionally detected in the cytoplasm of oocytes at chromatin-nucleolar stage. Similarly, *C. encaustus* females exposed to 2,4-D exhibited changes in the ovary histology. After exposure to 94 and 133.72 mg/L, *C. encaustus* females showed alterations in perinucleolar oocytes and early vitellogenic oocytes. Ultrastructurally, oocytes from *G. atripinnis* females exposed to 143.35 and 230.96 mg/L of 2,4-D displayed altered mitochondrial and nuclear membranes, as well as a loss of integrity of the cytoplasm of the surrounding follicular cells. Likewise, after exposure of *C. encaustus* females to 94.06 and 133.72 mg/L of 2,4-D, changes in the structure of the mitochondrial membranes and in the continuity of the nuclear membrane of oocytes, as well as in the mitochondrial cristae of follicular cells were observed. Males of *G. atripinnis* and *C. encaustus* exposed to 2,4-D at doses of 143.35 and 94.06 mg/L, respectively, did not show apparent alterations in testis histology. In contrast, exposure of males of *G. atripinnis* to 230.96 mg/L and of *C. encaustus* to 133.72 mg/L led to changes in the spermatogonial and sperm cysts. Ultrastructurally, testes of males of *G. atripinnis* exposed to 2,4-D (143.35 and 230.96 mg/L) and of *C. encaustus* (94.06 and 133.72 mg/L) displayed alterations in the mitochondrial cristae of spermatids. In conclusion: *C. encaustus* is more sensitive than *G. atripinnis* to 2,4-D herbicide; exposure to

this herbicide may cause alterations in gonadal histology and ultrastructure in both studied species, which may affect their reproduction in their natural environment. Viviparous Goodeid species may function as models of endocrine disruption.

88 MOLECULAR CHARACTERIZATION AND EVOLUTIONARY ANALYSIS OF CARNIVORE ZONA PELLUCIDA

(1) Moros C, (1) Izquierdo-Rico MJ, (2) Chevret P, (1) Leza A, (3) Boué F, (1) Ballesta J, (1) Avilés M.

(1) Department of Cell Biology and Histology, Faculty of Medicine, University of Murcia, Campus Mare Nostrum and IMIB Murcia, Spain. (2) Laboratoire de Biométrie et Biologie Évolutive, Université Claude Bernard, Lyon, France. (3) Agence Nationale de Sécurité Sanitaire de l'Alimentation, de l'Environnement et du Travail, Diseases in Wild Animals Unit, France.

Introduction: The zona pellucida (ZP) is an extracellular coat that surrounds mammalian oocytes. This envelope is involved in the interaction between gametes, induction of the acrosome reaction, block to polyspermy and protection of the preimplanted embryo. Previous studies suggested that carnivore ZP was formed of three glycoproteins (ZP2, ZP3 and ZP4), being ZP1 a pseudogene, like in the dog (Goudet et al., 2008). However, molecular evidences showed the expression of four proteins in the ZP of two different carnivores, the ferret and the cat (Leza et al., 2014; Stetson et al., 2015). **Material and methods:** In this study, we performed an *in silico* and a molecular analysis in several species of different carnivore families, to elucidate the ZP composition in this order of mammals. In the *in silico* analysis, the presence of the ZP1 gene in five carnivores (panda, polar bear, tiger, walrus and Wedell seal) was studied using GenBank and Ensembl databases. The existence of ZP1, ZP2, ZP3 and ZP4 mRNAs in the red fox was explored by molecular biology techniques. For the molecular analysis, total RNA was isolated from red fox ovaries (n=2) and cDNA was synthesized with oligo-dT as primer. On the other hand, gDNA was obtained from red fox tissues. Specific primers for ZP2 and ZP3 genes were designed based on fox sequences retrieved from GenBank, ZP1 and ZP4 primers were designed based on sequences from the dog. The cDNA/gDNA was used as template for PCR amplifications and the obtained amplicons were sequenced. **Results:** Our *in silico* analyses demonstrated the presence of a ZP1 gene in panda, polar bear, tiger, walrus and Wedell seal without evidences of pseudogenization. In the molecular analyses conducted in the red fox, the complete mRNA of ZP4 was amplified and partial sequences of ZP2 and ZP3 mRNA were also obtained. Whilst, ZP1 amplification was not possible with cDNA; with gDNA a ZP1 amplification was obtained by PCR. The analysis of this ZP1 amplicon showed the presence of a stop codon that was previously described in the dog, both species belonging to the Canidae family of carnivores. **Conclusion:** The results of this study strongly suggest that four ZP genes are expressed in most carnivores, whilst ZP1 pseudogenization has probably affected only the Canidae family of carnivores, where the dog and fox species are included. Future molecular and proteomic studies should provide more information about when the ZP1 pseudogenization happened in the Canidae family. This work is supported by MICINN (AGL2012-40180-C03-02), the European Commission (FEDER/ERDF) and Fundación Séneca (04542/GERM/06).

93 PROLIFERATIVE AND APOPTOTIC ACTIVITY CHANGES IN SEMINIFEROUS EPITHELIUM OF SYRIAN HAMSTER (MESOCRICETUS AURATUS) DURING RECRUDESCENCE AFTER TO SHORT PHOTOPERIOD

(1) Martínez-Hernández, J., (1) Seco-Rovira, V., (1) Beltran-Frutos, E., (1) Ferrer C., (1) Quesada-Cubo, V., (2) Canteras M., (1) Pastor L.M. (1)

(1) Department of Cell Biology and Histology and (2) Department of Statistics. School of Medicine, IMIB-Arrixaca. Regional Campus of International Excellence. Campus Mare Nostrum. University of Murcia. (30100).

After exposure to short photoperiod in the Syrian hamster there is a period involving testicular regression with involution of the seminiferous epithelium, decreased proliferative activity of spermatogonia and increased apoptosis of germ cells and Sertoli cell. The restoration of complete spermatogenesis occurs spontaneously during recrudescence. The objective of this study was to ascertain how the phenomena of apoptosis and proliferation affect the seminiferous epithelium during recrudescence. A total of 25 hamsters were used (20 treated and 5 controls (CT)). The treated animals were subjected to an 8:16 light-dark photoperiod while the control animals were subjected to a 12:12 light-dark photoperiod. Seven treated animals plus two from the control group were sacrificed at 16, 19 and 21 weeks. Testes were fixed in methacarn and embedded in paraffin. Three recrudescence groups were established: Initial (IR), Advanced (AR) and Total (TR). The proliferative activity was determined by proliferating cell nuclear antigen and the proliferation index of spermatogonia (PI) was calculated. The apoptotic activity was determined by TUNEL. An apoptotic index (AI) of spermatogonia (AI-SG), spermatocyte (AI-SC), round spermatids (AI-SP), AI-SG+SC and AI-SG+SC+SD was determined. The ratio of cells in apoptosis (A) to spermatogonia cells in proliferation (SG-P) was calculated. Also the total number of spermatogonia (TN-SG), spermatocytes (TN-SC) and round spermatids (TN-SD) was determined. Finally total number of apoptotic spermatogonia (TNA-SG), spermatocyte (TNA-SC) and round spermatids (TNA-SD) was calculated. The results showed that the AI-SG in IR only was greater than in TR. No changes in the TN-SG or the TNA-SG in the groups were observed. The AI-SC was higher in IR compared to CT and TR. The TN-SC in IR was lower compared to other groups, while in AR the TNA-SC was higher compared to TR. AI-SD was higher in IR compared to the other groups. The TN-SD was lower in IR whit respect to other groups. In the TNA-SD no changes were found. Regarding to TN in the testis (SG+SC+SD) it was lower in IR compared to other groups, while the TNA (SG+SC+SD) was higher in IR and AR whit respect to TR. The AI-SG+SC and AI-SG+SC+SD were highest in IR. The PI was higher in the three groups of recrudescence compared whit the CT, and no significant differences were found between the three groups. The SG-A/SG-P ratio did not show changes during recrudescence. The SC-A/SG-P, SD-A/SG-P, (SG+SC)-A/SG-P and (SG+SC+SD)-A/SG-P ratio was higher in IR whit respect to CT and TR. In conclusion during recrudescence: a) The SG population has similar apoptotic activity to CT while the proliferative activity is greater; b) in phase IR substantial apoptotic activity remains, in SC and SD; c) and it decreases in AR, allowing complete spermatogenesis in the seminiferous tubule; d) the balance between proliferative and apoptotic activity that exists during the breeding period is reestablished halfway through the recrudescence period. Financed: 04543/GERM/ 06, 04542/GERM/ 06. Fundación Seneca.

(1) Guillén-Martínez, A.; (1) Acuña, O.S.; (2) Soriano-Úbeda, C.; (1) Jara, L.; (3) López Albors, O.; (2) Coy, P.; (1) Ballesta, J.; (1) Izquierdo-Rico, MJ.; (1) Avilés, M.

(1) Department of Cell Biology and Histology, Faculty of Medicine and Nursing. (2) Department of Physiology. Veterinary Faculty. (3) Department of Anatomy and Comparative Pathology, Veterinary Faculty. University of Murcia, Campus Mare Nostrum. (1,2) University of Murcia, Campus Mare Nostrum and IMIB, Murcia, Spain.

INTRODUCTION The oviductal secretions have an active role in the gamete maturation, sperm capacitation and fertilization. Previous studies have reported that genetically modified sperm in mice are sterile in in vitro assay; however, they are fertile in vivo or after incubation of the sperm with uterine secretions. These studies strongly suggest that the female tract secretions contribute to the sperm fertility. Our laboratory has previously identified the mRNA codifying for lactadherin in the porcine oviduct. This sperm plasma membrane protein plays a key role in the fertilization in the mice. The aim of this study was to analyze the presence of lactadherin protein in the porcine oviduct. **MATERIAL AND METHODS** Sample collection Porcine oviducts at the preovulatory phase of the estrous cycle were obtained at the slaughterhouses. The oviductal fluid was collected by aspiration and were centrifuged at 7000 x g for 10 min at 4°C to remove cellular debris, and the supernatant was stored at -80°C. **Immunohistochemistry** The ampullary and the isthmic region of the Fallopian tube were fixed in 10% formalin in PBS (pH 7.4) and embedded in paraplast according to routine protocol. An antigenic retrieval using citrate buffer pH 6.0 and a block of endogenous peroxidase activity was performed. After washing, sections were incubated with a rabbit anti-lactadherin polyclonal antibody (Santa Cruz Biotechnology) overnight at 4°C. After washing in TBS and incubated with a goat anti-rabbit IgG conjugated with HRP secondary antibody (Santa Cruz Biotechnology). Negative controls were done using TBS instead of the primary antibody. Peroxidase was developed with 3,3 diaminobenzidine hydrochloride (DAB kit, Abcam). **Western blot analysis** The different oviductal fluids were separated by SDS-PAGE electrophoresis under reducing condition. The proteins were electrotransferred from the gel to Immobilon-P membrane (Sigma) at 100 V for 1 h. After appropriate blocking with BSA, the membranes were incubated with the previously described primary and secondary antibody at the appropriate dilution. **Proteomic analysis** The lactadherin protein was immunoprecipitated from the oviductal fluid using protein-A sepharose magnetic beads (GE Healthcare Life Science) crosslinked with the anti-lactadherin antibody. The protein fraction bound by the antibody was separated by SDS-PAGE electrophoresis and stained with coomassie blue. The band with a molecular weight of 50 kDa was cut and processed for MS/MS proteomic analysis (Agilent Technologies). **RESULTS** A moderate immunoreactivity was detected in the epithelium of both ampulla and isthmus. The reactivity was mainly detected in the apical surface of the non-ciliated cells. The Western-blot analysis allowed the identification of a specific band of approximately 50 kDa. The proteomic analysis of a band with this apparent molecular weight allow the identification of the lactadherin protein and corroborated the Western blot analysis. **CONCLUSION** In this study, we provide evidences of the presence of the lactadherin in the oviductal fluid and its secretion by the non-ciliated cells of the oviductal epithelium. This protein could modify the sperm membrane during the sperm transit through the female genital tract with a potential effect on the fertilization. This work was supported from the MINECO (AGL2012-40180-C03-01-02-03), FEDER/ERDF and Fundación Séneca (04542/GERM/06).

DOCENCIA

21 STUDENTS' ATTITUDES TOWARDS PREZI® PRESENTATION AS AN INTRODUCTION TO HISTOLOGY LABORATORY

Leiva-Cepas, F.; Giovanetti-González, R.; Ruz-Caracuel, I.; Zurita-Lozano, S.; Casado-Ruiz, J.; Martín, J.D.; Jimena, I.; Peña, J.

(1) Department Morphological Sciences, Section of Histology, Faculty of Medicine and Nursing. University of Cordoba. Spain. (2) Unidad Docente de Medicina Familiar y Comunitaria de Cordoba. SAS. Spain.

Introduction The didactic strategy of Histology Laboratory practical session included the reading by students of an extensive document that explains basics about tissue processing for histology and security measures in laboratories. It considers that its reading is useful because students gain knowledge before attending the practical session and the time dedicated to practice can be employed more efficiently. Nevertheless, a percentage of students failed to read carefully the document. So that, in the course of an innovative project in education, a Prezi ® presentation was developed that contains the same information but in a more visual fashion. After its application, a reaction evaluation was performed to verify objectives achievement. **Material & methods** A questionnaire that contains five items which answers were recorded on a six-point Likert scale from 0 to 5 was administered to 121 students who have completed the histology laboratory practical session. The questionnaire content focus on the welcome given by students to the Prezi ® presentation compared with the previous format. For each item, mean and standard deviation were calculated. **Results** Most of students visualize Prezi ® presentation before attending the practical session. All items of the questionnaire were pointed above four, which is considering very positive. The most valued item was that Prezi presentation is more attractive visually than the previous text document (4,45? 0,77), while the less valued item was that Prezi presentation is easily to use (4,13? 0,78). **Conclusions** Prezi® presentation is visually more attractive for students than plain text document and can ameliorate students? motivation to read information concerning laboratory tasks. Further studies should be made regarding content retention when comparing both tools.

47 INTRODUCTORY SPEECH TO MOTIVATE MEDICAL STUDENTS TO STUDY HISTOLOGY

Garrosa García, M. and Gayoso Rodríguez M.J

Area of Histology. Faculty of Medicine and Institute of Neurosciences of Castile and Leon (INCYL). University of Valladolid. Spain

Medical students are known to be little motivated for the study of Histology since, as a rule, they want to be physicians dealing with patients as soon as possible. They feel more motivated to study clinical matters whereas basic subjects are felt mostly as a must, with the exception of Gross anatomy, which is wrongly considered more necessary by students. We present an introductory speech for the first lecture in Medical Histology with the aim to demonstrate the real relevance of this subject and its beauty. We are trying to make clear the need of Histology

in the curriculum of Medicine as well as to motivate the students to study by using different approaches. No mechanism can be understood without the knowledge of its structure. Furthermore, since Rudolf Virchow it has been established that diseases are based in the cells. Thus, Histology is always the base for Physiology and Pathology, and therefore essential for Medicine. Histology is not only serving the medical specialty Pathologic Anatomy, every physician regardless of his specialty cannot be a real doctor without knowing Histology. Doctors' reports in the different specialties show the constant use of histological concepts to a greater or lesser extent. Other examples of motivation are; the use of questions appeared in the MIR exam, the arterial intima layer changes leading to cardiac infarction, adenopathies occurring in infections or tumors, the patellar reflex, gasses interchange across alveolar-capillary wall, blood-brain barrier, the muscle tissue types making the difference between a long-distance and a speed runner, as well as explaining why Stephen Hawking may be paralyzed in a wheelchair while keeping his sexual functions because his smooth muscle remains intact, etc. Histology is on the ground of all these processes, which appear quite interesting for students in the first years. Histology is not only a source of knowledge about the structure and function of organisms, it also offers the pleasure of gazing at wonderful landscapes, many still unexplored, to which only those ventured into histological observations have access. Together with these beautiful images offered and the already mentioned fundamental importance for Medicine, Histology has the honor of being the discipline of the highest glory which has reached the biomedical field in Spain. Names such as the Nobel Prize Ramón y Cajal, finding the neuron; Río-Hortega, the discoverer of Microglia and Oligodendroglia; Fernando de Castro and Isaac Costero unravelling the carotid body histophysiology and pathology; Tello, Lorente de Nó, Ortiz Picón and others making outstanding findings on Neurohistology, made internationally famous the Spanish Histological School. Therefore, it can be said that the study of Medical Histology is essential, a pleasure and a pride.

126 3D-TECHNOLOGY AS A DIDACTIC INTEGRATIVE PROPOSAL FOR TEACHING THE CONTENTS OF TISSUE AND CELULAR BIOLOGY

(1) Lara Palma I., (1) Espinosa Pedroza M., (1) Lozada Gallegos A., Anzaldúa Arce , S. R., (1) Juárez Mosqueda M. L.

Universidad Nacional Autonoma De Mexico

INTRODUCTION: Throughout the years, the professors that impart the assignments of Veterinary Cellular Biology and Tissue Biology in the Faculty of Veterinary Medicine and Zootechnics on the UNAM have witnessed the difficulties the students face to include the contents of these subjects in the context of a multicellular organism. Therefore, we plan to incorporate in the study of these subjects the three-dimensional technologies (3D). **MATERIALS AND METHODS:** As first step we determined the contents susceptible of being illustrated by interactive simulations. We focused on selecting the contents with the greatest difficulty for the students. To validate the use of 3D technology we used Problem Based Learning (PBL), following the next steps: a) writing rubrics, instructions and work norms; b) explanation and presentation of the subjects developed in 3D; c) selection and presentation of a case. For the assessment of this learning strategy at the beginning and end of the semester a

validation tool was applied. As controls, groups from both assignments were used in which the proposed methodology was not used. **PRELIMINARY RESULTS:** The current study was conducted in students who completed the course in veterinary cell biology, with one group (53 students) in which the proposed methodology was used and 3 control groups (170 students). From the instrument applied on the first day of class, in relation to the importance of the subject in forming Doctors in Veterinary Medicine there was no difference between groups (100 vs. 99.1%, respectively) as well as to the expectation of the course. There were differences in relation to the commitment of the students in regards to the course (72.22% vs. 63.22%, respectively). In relation to the assessment tool applied at the end of the course on the use of teaching resources utilized by teachers, 79.3% of students in the group thought they were appropriate while for the control group only 69.8 %. It is important to note that the 3D material that has been developed corresponds to the structure of biological membranes. Additionally, on questioning students again about the importance of the subjects on their professional training, the percentages remained very similar (96.2% and 97.5%, in the validation and control groups respectively). Interestingly 86.8% of the students in the validation group felt they had the capability to relate the knowledge acquired during the course with their professional life, while in the control group 90.1%. From the validation group 77.4% of students considered to have the ability to relate the contents of the assignment with other subjects while in the control group only 72.7%; finally the question of whether they would be able to pass the subject, the percentages were 52.8 for the validation group and 40% for the control. **CONCLUSIONS:** Preliminary results show a trend towards an improvement of student learning. The use of PBL remains to be analyzed as the key didactic integrator of knowledge. It would also be important to include an analysis of the grade average of the groups and the failure rate. This work is supported by DGAPA-UNAM: PAPIME PE204613

151 DESIGN OF MULTIMEDIA TOOLS, COMPATIBLE WITH MOBILE PHONES AND TABLETS, FOR TEACHING PLANT ORGANOGRAPHY

Pedrosa, J.A., Rus, M.A., del Moral, M.L., Hernández, R., Blanco, S., Peinado, M.A.

Universidad de Jaén

For more than a decade, the authors of the present work have been developing a variety of multimedia tools for teaching Animal and Plant Histology and Microscopic Organography. One of the innovative aspects of these tools is the combination between classic drawing with teaching purposes and the Information and communication technologies, so that the drawings are included in interactive files in flash format. These tools are currently available to public access at the Virtual Teaching Platform of the University of Jaén (http://dv.ujaen.es/docencia/goto_docencia_fold_543004.html). Regarding the current and widespread use of mobile phones and tablets with Internet access, it would be of great interest the design of teaching tools in a format that is compatible with such devices. So far, this was not feasible given the incompatibility between the flash format and the operating systems of mobile phones and tablets. The application iSpring Presenter 7 has been used for creating the teaching tools presented in this work, given in mind that it allows to generate SCORM files (Sharable Content Object Reference Model) directly in a Virtual Teaching Platform, which they interact with in HTML5 format (HyperText Markup Language). The HTML5 format is a new version of the

popular HTML which has new attributes, behaviours, and full compatibility according to the incorporation of multimedia elements. They include flash files, which can be displayed on mobile phones and tablets, as well as downloadable content for later use without an Internet connection. The starting point for the development of self-learning modules for teaching Plant Organography - i.e. the aim of the present work - are PowerPoint slideshows. This application includes iSpring Presenter 7 to the ribbon. The drawings with a sequential animation, along with a brief text description, are the main part of each module. Each one is also accompanied by the corresponding images and/or hyperlinks from an Interactive Histological Atlas (<http://www.ujaen.es/investiga/atlas/>), which is previously developed by the authors. Each module also includes a self-test with different test types designed by iSpring Presenter 7. The results of these tests are sent by SCORM to the Virtual Teaching Platform to be available for the teacher. Hyperlinks to Plant Histology modules, which have previously been developed by the authors, are also included in these modules as additional information. Once the assembly of each module is completed, iSpring Presenter 7 compiles it and generates the SCORM file, which is stored in the Virtual Teaching Platform. So far, all Plant Organography modules have been transformed into the HTML5 format, which are compatible with mobile phones and tablets. The conversion of the other teaching tools - in flash format - from the Virtual Teaching Platform of the University of Jaen to this new format has already begun and it will be completed soon.

HISTOLOGÍA ANIMAL

35 LIVER HISTOPATHOLOGY, LIPID PEROXIDATION AND SOMATIC INDICES OF *Fulica americana* FROM TWO MEXICAN WETLANDS WITH DIFFERENT ENVIRONMENTAL ALTERATIONS

(1) Ibarra-Meza I., (1) López-Islas M. E., (2) Ortiz-Ordóñez E., (3) Sedeño-Díaz J.E., (1) López-López E.

1.- Laboratorio de Bioconservación y Manejo. Escuela Nacional de Ciencias Biológicas del IPN. Prol. de Carpio y Plan de Ayala S/N, Col. Santo Tomás, México 11340. D.F. 2.- Laboratorio de Histología Animal Escuela Nacional de Ciencias Biológicas del IPN. Prol. de Carpio y Plan de Ayala S/N, Col. Santo Tomás, México 11340. D.F. 3.- Coordinación Politécnica para la Sustentabilidad del IPN. Av. IPN esq. Wilfrido Massieu S/N, Edificio de la Biblioteca Nacional, Segundo piso, Unidad Profesional Adolfo López Mateos, Col. Zacatenco, México, D.F

Waterfowl populations have been affected by the decline and degradation of wetlands that receive xenobiotics from anthropogenic activities. Environmental pollutants in wetlands can exert adverse effects on aquatic birds, acting at different levels of biological organization from the molecular to the population levels. This work assesses histopathological alterations and lipid peroxidation (LPO) in liver of two wild populations of *Fulica Americana* in two Mexican wetlands. The results are related to somatic indices (SI): gonadosomatic index (GSI), hepatosomatic index (HSI) and body eviscerated mass (BEM), and physicochemical characteristics of their habitats (wetlands). The study was conducted during an annual cycle in Tecocomulco Lake and Xochimilco Lake, in the Basin of Mexico. The collected organisms

were eviscerated and weighed. Liver portions were obtained for histological analysis and the remaining tissue was kept in liquid nitrogen. The coots were aged. In the laboratory, water samples were analyzed for nutrient levels, biochemical oxygen demand and coliforms. The liver tissue was embedded in liquid paraffin and was stained with hematoxylin and eosin. A discriminant analysis and a Pearson correlation were performed to detect the statistical relationships between LPO, SI, tissue damages and age of birds. The highest nutrient values were observed in Xochimilco, which is considered a hipereutrophic lake. The coots with the higher values of EBM were found in Tecocomulco. The highest LPO levels were detected in Tecocomulco during winter, while both sites showed an increase during summer. Females from spring and summer (reproductive season) exhibited the highest GSI. During the reproductive season, the lowest HSI was reached, while in autumn and winter the highest values of HSI were observed. Two pathologies were detected in three levels each one, leukocyte infiltration (IN) and vasocongestion (V). Both pathologies were found with the higher prevalence in Tecocomulco while in Xochimilco was IN-III, which is related to the highest nutrient levels. A discriminant analysis showed that the highest values for GSI, V-III and both pathologies in the females were present during the reproductive season in Tecocomulco, and the males displayed the higher values for EBM and IN-II and III in the same site. Males and females from autumn and winter presented higher levels for LPO, HSI and IN-I. During the reproductive season, females from Xochimilco exhibited the highest levels of GSI, IN-I and II; while the males showed the highest values of EBM and IN-III. Females and males during autumn and winter had the highest LPO, HSI and both pathologies. In both wetlands, a direct correlation between IN-II and GSI was found and between the age with EBM, LPO and HSI. In addition, in both wetlands, during the reproductive season, females had the highest V and IN prevalence and males had the highest values of EBM. During winter, females and males of both wetlands reached the highest HSI, which can be associated with energy reserves, although they exhibited the highest levels of LPO, which can be explained by food and space competition when migratory birds arrive. The LPO, EBM, HSI and both pathologies increased with age while IN decreased. The studied populations of *Fulica americana* showed differences in histopathology alterations, LPO levels and SI, which is the result of the particular environmental conditions where they inhabit.

72 ANTIOXIDANT TREATMENTS RECOVER THE ALTERATION OF ABR AND REDUCE OLIGODENDROGLIAL DAMAGE AND MITOCHONDRIAL DISRUPTION IN THE INFERIOR COLLICULUS AFTER A PERINATAL ASPHYXIA.

(1) Revuelta Aramberri, M., (1) Arteaga Cabeza, O., (2) Martinez-Ibargüen, A., (1) Hilario Rodriguez, E., (1) Alvarez Diaz, A.

(1)Department of Cell Biology and Histology, (2) Department of Otorrhinolaryngology, School of Medicine and Dentistry, University of the Basque Country, Leioa 48940, Spain.

Introduction Despite improvements in neonatology, perinatal hypoxic-ischemic (HI) encephalopathy remains one of the main causes of disabilities in term-born infants. This specific pathology underlies many neurological disorders such as learning difficulties, language and attention deficit, hyperactivity disorders and cerebral palsy. Moreover, it is also a notable risk

factor for hearing impairments which affect neonates. **Aim** The aim of the present work was to evaluate morphofunctionally the effect of a panel of antioxidants on HI-induced auditory deficits. To this end, we studied the effects of nicotine, melatonin, resveratrol and DHA on the neonatal auditory system via measurement of auditory evoked potentials and characterization of the morphological integrity of the IC. **Material and methods** 7-day-old Sprague-Dawley rats were used for histological and functional studies and the hypoxic ischemic event was induced in perinatal rat pups by the Rice-Vannucci method. Pups were randomly assigned to six experimental groups (n=8): control, HI and the four HI groups administered with the different drug. ABR were measured by GSI Audera equipment and oligodendroglial analyze was performed with MBP staining. Cellular analysis was performed by using mitochondrial membrane potential and integrity markers in the flow cytometer. **Results** The HI event induced a statistically significant decline in ABR latency intervals in the III-V and in the I-V intervals between the peaks, while there were no statistical differences between the treatments and control groups. MBP immunostaining was found to be reduced in subcortical white matter at the level of the ECIC and also in the CIC while treated animals showed a lesser degree of MBP loss in the ipsilateral hemisphere. The mitochondrial membrane integrity and potential are affected in the HI group and also in melatonin and resveratrol treated groups, but treated groups recover the membrane integrity in 3 hours while HI group not. **Conclusions** The present prospective study presents for the first time a correlation between the functional, morphological and molecular aspects underlying the antioxidant induced amelioration of HI induced brainstem damage. Thus, antioxidant treatments were found to provide effective neuroprotection to the immature auditory system before a perinatal hypoxic-ischemic event. **Acknowledgments:** This work was supported by grants from the Basque Country Government (IT773/13)

131 SUBCELLULAR DISTRIBUTION OF THE ACROSOMAL PROTEINS GCNF, FNDC3A AND SP56 IN A GLOBOZOOSPERMIC GOPC-/- KNOCKOUT MOUSE

Bizkarguenaga M(1), Gómez-Santos L(1), Madrid JF2(), Sáez FJ(1) and Alonso E(1)

(1)Department of Cell Biology and Histology, School of Medicine, University of the Basque Country UPV/EHU, Spain. (2) Department of Cell Biology and Histology, School of Medicine, University of Murcia, Spain.

Introduction One of the main causes of infertility in human male is associated with defective spermiogenesis, the process when, among other things, the acrosome is formed and matured. Mammalian spermatozoa penetrate the egg's coat using a number of hydrolytic enzymes that accumulate in a vesicle called acrosome. This organelle is essential for the fertilization of the oocyte; therefore its development must be perfect. Acrosome biogenesis requires a correct interaction between the Golgi complex and the nuclear envelope of early spermatids. Abnormal acrosome formation results in a serious alteration in the sperm head, a disorder of male sterility characterized by the presence of spermatozoa with round head and absence of acrosome, called globozoospermia. GOPC protein is involved in the processes of formation and transport of vesicles from the Golgi apparatus. Knockout *Gopc*^{-/-} mice have a defective vesicular trafficking that give rise to unusual accumulation of proacrosomal vesicles in the perinuclear region, between Golgi apparatus and the nuclear envelope. In the present work we analyze the distribution of some acrosomal proteins during the abnormal spermiogenesis of *Gopc*^{-/-} mice.

Materials and methods To examine the cellular and sub-cellular localization of the acrosomal proteins GCNF, FNDC3A and Sp56, immunostaining was performed on testis sections of adult mice between 8-12 weeks. Testes from wild-type mice (129sv) and knockout *Gopc*^{-/-} mice (provided by Professor Tetsuo Noda of the Department of Cell Biology, Japanese Foundation for Cancer Research (JFCR) Cancer Institute, Japan) were used. For light microscope, testis were fixed in Bouin buffer, embedded in paraffin and sectioned at 4µm. For immunogold electron microscopy, samples were fixed in glutaraldehyde 2%, embedded in Lowicryl K4M and sectioned at 70nm using an ultramicrotome. **Results** Immunohistochemical and immunogold localization of the acrosomal proteins GCNF, FNDC3A and Sp56 in the knockout *Gopc*^{-/-} spermiogenesis reveals differences respect wild type. In wild type mice the acrosome labelling for the acrosomal proteins studied was much stronger than in the proacrosomal vesicles of the GOPC deficient mice in all steps of the round spermatids. Sp56 appeared in compact acrosomes of round spermatids, however GOPC deficient acrosomes were scattered. GCNF appeared strong in the acrosome of round spermatids but no signal when they elongate. Immunogold results revealed GCNF distributed throughout the round spermatid nucleus. FNDC3A protein is detected in acrosomes of round spermatids and residual bodies in the wild type. In mutant *Gopc*^{-/-} mice FNDC3A also is localized in a much lower concentration in proacrosomal vesicles and residual bodies. Immunogold localization of the acrosomal proteins revealed that they remain in the preacrosomal vesicles till late spermatids. **Conclusion** The content of the acrosomal proteins GCNF, FNDC3A and Sp56 during the spermiogenesis in GOPC deficient mice is lower than in the wild type. This is because of the failure of vesicle transport from the Golgi apparatus to the perinuclear region and the wrong fusion of the proacrosomal vesicles to form a mature acrosome. **Acknowledgements** This work was supported by grants from the UPV/EHU (EHUA13/15 and UFI 11/44).

HISTOPATOLOGÍA EXPERIMENTAL

2 MORPHO-FUNCTIONAL ALTERATIONS OF RENAL CORPUSCLES IN AN EXPERIMENTAL MODEL OF UNILATERAL URETERAL OBSTRUCTION.

Ortiz Aranda, M.(1) Pérez Barriocanal, F.(2,3) López Novoa, JM.(2,3) Arévalo Gómez, M. (1,3)

(1) Departamento de Anatomía e Histología Humanas y (2) Departamento de Fisiología y Farmacología. Universidad de Salamanca. (3) Instituto de Investigaciones Biomédicas de Salamanca (IBSAL) Salamanca, España

MORPHO-FUNCTIONAL ALTERATIONS OF RENAL CORPUSCLES IN AN EXPERIMENTAL MODEL OF UNILATERAL URETERAL OBSTRUCTION. **INTRODUCTION:** Chronic kidney disease (CKD) is a pathology that affects nearly 10% of the population. This illness is characterized by a progressive decrease in glomerular filtration rate that eventually leads to renal failure. Tubulointerstitial fibrosis, a major determinant of CKD, occurs by myofibroblast activation and proliferation in the renal interstitium with accumulation of extracellular matrix (ECM). The unilateral ureteral obstruction (UUO) experimental model reproduces the most representative features of tubulointerstitial fibrosis: extracellular matrix (ECM) accumulation, tubular apoptosis myofibroblast activation and proliferation, tubular

deletion and inflammatory cell infiltration. However, up to date, little or none is known about the alterations that occur in renal corpuscles after the OUU. The aim of the present study was to elucidate whether or not the corpuscle is affected after an experimental model of OUU in mice. **METHODS:** OUU was performed in C57BL/6 mice. After 15 days of obstruction, kidneys were extracted and processed either for optical microscopy (Hematoxylin and Eosin, Masson's Trichrome and Sirius Red), immunohistochemical (fibronectin, Collagen I, α -actin, Mib-1, Activated Caspase-3, pSmad 2/3 and WT-1) or electron microscopy. **RESULTS:** No apparent alterations but tubularization of the Bowman's capsule parietal epithelium were detected with hematoxylin and eosin or electron microscopy. However, Masson's revealed an increased mesangial matrix in OUU kidneys. Quantification with Sirius red confirmed a significant increase of mesangial matrix and a decrease in the corpuscular area in OUU corpuscles as compared with controls. Immunohistochemistry against extracellular matrix molecules showed augmented fibronectin and Collagen I in OUU corpuscles. In this way, α -actin was also increased in corpuscles from obstructed kidneys revealing an improved activity of mesangial cells. pSmad 2/3 immunohistochemistry revealed an increased expression of these mediators, implying the TGF- β /Smad pathway in the mesangial expansion observed. Augmented proliferation and apoptosis was detected with Mib1 and activated Caspase-3 respectively maybe owing to the increase of TGF- β . Indeed, a significant detachment of podocytes was observed in OUU corpuscles. **CONCLUSIONS:** In conclusion, it can be said that OUU promotes changes in renal corpuscles, in spite that it is not comprised glomerular functionality.

7 THE ROLE OF PNEUMOCYTES TYPE II AND MACROPHAGES IN VENTILATOR INDUCED LUNG INJURY (VILI)

(1) López, M.; (1) Gutiérrez, R; (1)Rancel, N.; (2) García, C.; (1) (3) Valladares, F

(1) Universidad de La Laguna, (2) Hospital Universitario de Canarias, (3) CIBER de Enfermedades Respiratorias (CIBERES)

BACKGROUND: Mechanical ventilation may induce lung injury that is clinically and pathologically undistinguishable from ARDS. In animal models this injury is called VILI (VENTILATOR-INDUCED LUNG INJURY). VILI may be due to several causes: Barotrauma, Volutrauma, Atelectrauma and Biotrauma. The last one involves inflammatory cells and mediators resulting in a thickening of the alveolar wall that prevents gas exchange. We focused in pneumocytes type II and macrophages. Macrophages activate and attract neutrophils to the site of inflammation, pneumocytes type II can also attract neutrophils however; pneumocytes type II and macrophages carry out many more functions to preserve the alveoli. In the current work the role played by both cell types in ventilator-induced lung injury is assessed. **METHODS:** Random, prospective, controlled study. Adult, healthy Sprague Dawley rats were used; animals were anesthetized and randomly assigned to spontaneous breathing and two strategies of mechanical ventilation for 4h: high tidal volume (VT), 20 ml/kg, low tidal volume, 6 ml/kg and a control group without mechanical ventilation. A histological assessment was carried out (HE and Masson-Goldner) and immunohistochemical staining for Thyroid transcription factor 1 (TTF-1). **RESULTS:** Very obvious changes in the Histology of the three groups were observed for the three different values of ventilation. Macrophages were present in all the various stages of VILI and their number increased with the ventilation volume.

Pneumocytes type II suffered a hyperplasia as part of the reparative process characterizing the last phase of Acute Lung Injury. CONCLUSIONS: pneumocytes type II and macrophages are essential during ventilator-induced lung injury. Their action includes many vital functions like: natural immunity, adaptive immunity, reparation, reepithelialization and fibrosis.

8 STUDY OF ALVEOLAR CHANGES IN SEPTIC RATS, AFTER INTRODUCTION IN A SEALED CHAMBER TO DIFFERENT FiO₂

(1) Acosta, A.; (1) Rodríguez, P.; (1) López, M.; (1) Rancel, N.; (1) (2) Valladares, F.

(1) Universidad de La Laguna, (2) CIBER de Enfermedades Respiratorias (CIBERES)

Background: Mechanical ventilation is a basic measure of support in the treatment of various respiratory conditions; despite its undoubted positive effect, it is not free of adverse effects, such as acute lung injury (currently lung injury induced by the fan). Material and Methods: We will use 4 groups of septic rats (n = 6), with FiO₂ of 0.21, 0.4, 0.6 and 1 for 24 hours in a sealed chamber; previously, after anesthetizing the animal, a blind puncture was performed with the aim of producing a septic phenomenon; 24 hours after the animal sacrifice and extracted the package cardiopulmonary block, processing it and using techniques MO HE and Sirius Red. Results: The main changes we observed in the lung consisted of perivascular edema, inflammatory phenomena, microscopic atelectasis and fibrosis; Conclusions: The morphological features have a direct relationship, in terms of their severity, with hyperoxia received (0.21, 0.4, 0.6 and 1.0), the sealed chamber system in appropriate model for study of acute lung injury.

104 TRANSPLANT OF ES CELLS INTO SEMINIFEROUS TUBULES AS A MODEL TO STUDY EARLY STAGES OF GERM CELL TUMOR INVASION

Moreno Ruiz, P.; Bonilla del Río, Z.; Silván De Pedro, U.; Díez Torre, A.; Arluzea Jauregizar, J. & Aréchaga Martínez, J.

(1) Universidad del País Vasco. (2)ETH Zürich, Instituto de Biomecánica y Universidad de Zürich, Hospital Universitario Balgrist

1. INTRODUCTION Testicular germ cell tumours (TGCTs) are the most frequent malignancies in adolescents and young adult males and its incidence has doubled over the last few decades, but unfortunately the mechanisms underlying their development are still poorly understood. The tumour surrounding stroma, especially cancer-associated myofibroblasts, has been identified as a crucial factor involved in cancer cell growth and invasion, nevertheless, the role of stroma cells in TGCTs development has not been analyzed deeply enough. Among testicular somatic testicular cells, peritubular myoid cells (PTCs) have gained much attention as key players in the stromal response of testicular germ cell tumours (TGCTs). In the healthy testis, these cells regulate testicular homeostasis. Hence, PTCs could play as well a critical role in the early stages of TGCT development in response to CIS-derived signals (Díez-Torre et al. 2011). 2. MATERIALS & METHODS Our laboratory has developed a tumour model that involves the

microinjection of embryonic stem (ES) cells (which are functionally equivalent to CIS cells) into syngenic mouse seminiferous tubules (Silván et al., 2011). After 10 days of cell transplant, we used histology observation of the experimentally induced tumours to characterize stroma-carcinoma response. 3. RESULTS Embryonic stem cells transplanted into seminiferous tubules did not differentiate into germinal cells, but rather they behaved as invasive embryonal carcinoma (EC) stem cells. We present here experimental TGCTs at early stages of development ranging from intratubular growing masses up to mature teratocarcinoma in both intratubular and interstitial localization. These experimental tumours present basement membrane degradation at adjacent areas. 4. CONCLUSION These observations might corroborate our previous in vitro results in co-cultures of embryonic stem (ES) and embryonal carcinoma (EC) cells and testis-derived primary PTCs where MMP-9 expression and release is highly increased. Consequently, this MMPs increment triggers basement membrane degradation during the crosstalk between stroma cells and the embryonal component of TGCTs during early tumor stages as a part of the invasion process. BIBLIOGRAPHY Díez-Torre A, Silvan U, Moreno P, Gumucio J, and Arechaga J (2011). Peritubular myoid cell-derived factors and its potential role in the progression of testicular germ cell tumours. *Int J Androl* 34, 252-265. Silván U, Díaz-Torre A, Andrade R, Arluzea J, Silió M, and Aréchaga J (2011). Embryonic Stem Cell Transplantation Into Seminiferous Tubules: A Model for the Study of Invasive Germ Cell Tumors of the Testis. *Cell Transplant*, 20: 637-642.

138 DOCOSAHEXANOIC ACID IMPROVES LONG-TERM MEMORY IMPAIRMENTS AND NEURONAL CONEXIONS IN HYPOXIA-ISCHEMIC BRAIN INJURY

(1) Arteaga Cabeza, O., (1) Revuelta Aranberri, M., (2) Urigüen Echevarria, L, (1) Hilario Rodriguez, E.,(1) Álvarez Díaz, A. and (3) Martínez Millan, L .

(1). Cell Biology & Histology, (2). Pharmacology, (3).Neuroscience, School of Medicine & Dentistry, University of the Basque Country (UPV/EHU), Leioa, Bizkaia, Spain.

INTRODUCTION: Neonatal hypoxic-ischemic encephalopathy involve primary destructive events, but also secondary maturational disturbances, which lead to subsequent abnormal development and altered functions. Docosahexaenoic acid (DHA) is an essential polyunsaturated fatty acid in the central nervous system that has been shown to possess neuroprotective effects. The aim of the present work was to investigate if short-term protective effects of DHA against HI brain injury in neonatal rats were also persisted in adulthood. To this end we performed long-term behavioral tests related with memory impairments and we evaluated axonal anterograde conexions. MATERIAL AND METHODS: The Rice-Vannucci experimental procedure was used to cause hypoxic-ischemic brain injury in 7-day-old by permanent ligation of the left common carotid artery and subsequent and the subsequent exposure to 8% O₂ for 135 minutes. Pups were randomly assigned to three experimental groups: control, hypoxia-ischemia (HI) and HI animals that received a single dose of 1 mg/kg of DHA 10 minutes before the hypoxic event (HI+DHA). On P90 we evaluated the long-lasting behavioral alterations related with memory, through T-maze and novel object recognition tests. For anterograde tracing experiments, when P100 animals, biotinylated dextran amines (BDA) injections were made in left lateral of the cortex, under anesthesia. RESULTS: Regarding long-

lasting memory, in the first behavioral test, in the T-maze at 40 second delay, HI animals made significantly fewer correct choices comparing to control ones, while pretreated animals made similar number of correct choices to control. In the second one, in a novel object recognition test, animals pretreated with DHA demonstrated a fully reversion of the decrease in discrimination index displayed by HI rats, showing similar values to control animals. Regarding anterograde tracing experiments, changes in the axonal connections of corticofugal neurons following neonatal hypoxic-ischemic injury were detected in HI rats in the talamun and corpus callosum, but these changes were reverted with DHA pretreatment, demonstrating similar patterns to control rats. **CONCLUSIONS:** Taken together, our results indicate that the pretreatment with docosahexanoic acid was able to improve the long-lasting cognitive deficits related with memory and the changes in the axonal connections of corticofugal neurons in the talamun and corpus callosum induced by neonatal hypoxic-ischemic brain injury. **Acknowledgments:** This work was supported by grant from the Basque Government IT 773/13 and BFI-2011-129.

141 HISTOPATHOLOGICAL CHANGES IN GASTRIC MUCOSA IN A ISCHEMIA REPERFUSION MODEL

(1) Peña Mercado, E.; (2) García Lorenzana, M. y (3) Beltrán Vargas, N.E.

(1) Maestría en Ciencias Natural es e Ingeniería. División de CNI. (2) Área de Neurociencias. Departamento de Biología de la Reproducción, División de CBS. (3) Departamento de Procesos y Tecnología, División de CNI. Universidad Autónoma Metropolitana, Ciudad de México.

Introduction Gastric ischemia ? reperfusion injury is an important clinical problem, which is associated with significant morbidity and mortality during the course of hemorrhagic shock, peptic ulcer bleeding, vascular rupture or surgery, or ischemic gastrointestinal disease. Ischemia ? reperfusion (I/R) is caused by interruption of blood supply to an organ or tissue followed by blood reflow into the exposed area. The excessive generation of reactive oxygen species, adhesion of neutrophils to endotelial cells, the activation of various proinflammatory mediators, and the alteration in gastric acid secretion have been implicated in the pathogenesis of I/R ? induced gastric mucosal injury. Impedance spectroscopy is the study of the passive electrical properties of biological tissues as a function of frecuency. Impedance results from the interaction of an electrical current with the tissue at cellular, and molecular levels. Biomedical engineers designed a device to monitor the damage in the gastric mucosa of patients in critical condition. The objetive of this work was to quantify changes in gastric mucosa tissue, associated with changes in impedance generated in a model of ischemia-reperfusion. **Material and methods** Nine rats were randomly assigned to three groups (n=3): control, ischemia, and ischemia-reperfusion. In the ischemia group, the abdominal cavity was exposed, and the celiac artery was isolated. The celiac artery was clamped for 30 min to induce ischemia. In the ischemia- reperfusion group, the celiac artery was clamped for 30 min, and then it was released to allow reperfusion for 30 min. In all three groups, gastric mucosa samples were taken for light microscopy. Also gastric impedance was measured. The histopathological changes were evaluated by an index of gastric injury: cellular edema (score 0-2), cellular necrosis (score 0-2), vascular congestion (score 0-2), glandular disruption (score 0-2), and epithelial erosion (0-2).

Kruskal-Wallis analysis of variance was used to detect differences among groups, and statistical comparisons were made using the Mann-Whitney U test. Results: Histological evaluation of the gastric mucosa revealed that gastric ischemia triggers cellular edema, and vascular congestion. During ischemia - reperfusion epithelial erosion, cellular edema, necrosis, and glandular disruption are observed. There were statistically significant differences among the groups with respect to the index of gastric injury, which was greater in the I/R group. Also, impedance parameters increased in the I/R group with respect to control, and ischemia groups. Conclusion: The proposed index of gastric injury allowed to quantify the gastric mucosa damage generated in a I/R model. Furthermore, this injury was related with impedance increase, which is an objective method to evaluate tissue injury.

145 MODULATION OF THE INNATE IMMUNE CELLS BY THE VAGUS NERVE IN EXPERIMENTAL HEPATIC AMOEBIASIS IN RATS.

(1) Martínez-Jaimes M. D., (2) Javier Ventura-Juárez J. (2) Muñoz-Ortega M. H., (3) Quintanar-Stephano A., (2) Ávila-Blanco M. E., (4) García-Agueda C. E., and (5) García-Lorenzana M.

(1) Doctorado en Ciencias Biológicas y de la Salud, Universidad Autónoma Metropolitana. (2) Laboratorio de Morfología, Departamento de Morfología, (3) Departamento de Fisiología y Farmacología. Centro de Ciencias Básicas, Universidad Autónoma de Aguascalientes. (4) Unidad de Investigación en Gerontología. FEZ, Universidad Nacional Autónoma de México. (5) Laboratorio de Neurobiología Tisular, Departamento de Biología de la Reproducción, Universidad Autónoma Metropolitana, Iztapalapa.

INTRODUCTION: Amebiasis is an illness caused by the protozoan parasite *Entamoeba histolytica* and it is considered the third cause of death in the world. At experimental level, various animal models have been identified in which the pathology of amebiasis is reproduced: 1) susceptible (hamster and gerbil), the inflammatory tissue damaged seems to be related to the lysis of the hepatocytes and neutrophils; 2) resistant (rats and mice), the inflammatory cells succeed in lysing the parasite provoking minor tissue damage. The parasympathetic nervous system has a crucial role in immunomodulation by the vagus nerve, their structure provides a pathogen detection system, and a negative feedback to the immune system after the pathogen has been eliminated. **OBJETIVE:** The aim of this study is to analyze *in vivo* interaction of *Entamoeba histolytica* with neutrophils, macrophages, and NK cells in livers from intact, and vagotomized rats. **MATERIAL AND METHODS:** Twenty four Wistar male rats were used in this study, with a weight of 350-450 g. The animals were maintained in a room with a controlled temperature of 24 ± 2 °C with light/dark cycles of 12h/12h. For parasympathetic denervation of the liver, surgery began with a linear incision below the sternum in aseptic conditions. The stomach was partially externalized, and in the anterior surface of the esophagus, the hepatic branch of the vagus nerve was dissected microscopically. Six groups were formed (n=4): Intact (I), Intact + amoeba (IA), Sham (S), Sham + amoeba (SA), Vagotomized (V), and Vagotomized + amoeba (VA). Inoculation via intraportal with 1×10^6 trophozoites of *Entamoeba histolytica* of the HM-1: IMSS strain. Sacrifice times were previously standardized in a kinetic study at various development times: 1, 4, 8, 12, and 24 hours. It was determined that eight hours post-inoculation of *E. histolytica* was the best time for study. Livers obtained, fixed in 4% paraformaldehyde, and processed by routine histological techniques. The tissue liver slides were stained with H-E, PAS, and Masson. Amoeba was identified with monoclonal anti lectin *E. histolytica* 220 kDa. Neutrophils were identified with rabbit anti-human neutrophil

myeloperoxidase, macrophages with anti-CD68 antibody, and NK cells with anti-NK. RESULTS: Stomachs weight and liver glycogen was higher in V. Collagen increased in VA, whereas vascular and neutrophilia areas were decreased. There were fewer neutrophils, macrophages, NK cells around the amoeba in the following order IA> SA> VA ($p<0.05$ between IA and VA). CONCLUSION: To finish, we propose that the absence of parasympathetic innervations causes an early decrease of the innate immune response against infection by *E. histolytica* in amebic liver abscess, apparently by parasympathetic inhibition in cellular functions, and probably by participation of sympathetic activity.

This work was performed as part of the Doctorado en Ciencias Biológicas y de la Salud de la Universidad Autónoma Metropolitana (standard of excellence CONACYT) and supported by CONACYT.

INGENIERÍA TISULAR

19 REGENERATIVE RESPONSE OF SKELETAL MUSCLE TO THE IMPLANT OF OSTEOVIT®: PRELIMINARY RESULTS.

Leiva-Cepas, F.; Ruz-Caracuel, I.; Jimena, I.; Cámara-Pérez, J.; Villalba, R.; Villatoro, A. y Peña, J.

(1) Department Morphological Sciences, Section of Histology, Faculty of Medicine and Nursing, University of Córdoba. Spain. (2) Research Group in Muscle Regeneration, University of Córdoba, Spain (3) Regional Blood Transfusion Center and Tissue Bank Sector. Córdoba. Spain. (4) IMIBIC, Reina Sofia University Hospital, University of Córdoba. Spain. (5) Terapia Regenerativa Veterinaria REGVET. Malaga. Spain.

Introduction Skeletal muscle has a robust capacity for remodeling, repair, and regeneration following injury. However, when a significant loss of muscle mass occurs, this regenerating response is inadequate and the injured area is replaced by fibrosis. To solve this problem some studies have shown that the implant of myoblasts incorporated into a porous collagen scaffold in an extent muscle defect. This implant produced a biocompatible host response that contributes to in situ fiber formation, demonstrating collagen potential for delivering myoblast. In this communication we present preliminary results of the regenerating power of a collagen matrix implanted in a muscle defect. **Material & methods** Dark Agouti rats were anesthetized and cylindrical punch ($\varnothing 6 \times 5$ mm length) was extracted of the belly from anterior tibial muscles. A porous collagen scaffold (Osteovit®) was used to replace muscle defect. Adipose tissue-implantation was used as control. Animals were sacrificed 30 and 45 days after implantation; muscles were removed, frozen in isopentane previously cooled in liquid nitrogen and sectioned at $8\mu\text{m}$. Cryosections were stained using histological, histochemical and immunohistochemical techniques. **Results** Our results showed that muscle defect had been occupied by muscle tissue in both groups (Osteovit®-implant and adipose tissue implant), although they differed with histology of a normal muscle. Even though in both cases they were observed areas of fibrosis, atrophy, cytoarchitectural abnormalities into and myofibers spatial disorientation, these were fewer when Osteovit® was used. **Conclusions** Our study shows that using only a porous

collagen scaffold, skeletal muscle is able to develop a powerful regenerating response able to reconstruct a volumetric defect with muscle tissue, reducing the appearance of fibrosis. However, a combined strategy (e.g. with rehabilitation) is required to improve muscle histological organization.

43 PLATELET-RICH PLASMA PROMOTES NESTING OF CHONDROCYTES ON CHITOSAN SCAFFOLDS

(1) Martorell Tejedor, S.; (1,2) Carda Batalla, C.; (1,2) Ruiz Saurí, A.; (1,2) Martín de Llano, J.J.; (1,2) Mata Roig, M.; (3) Gamboa-Martínez, T.C.; (3) Gámiz-González, A.; (3,4) Vidaurre, A.; (3,4) Gómez Ribelles, J.L.; (1,2) Sancho-Tello Valls, M.

(1) Departament de Patologia, Facultat de Medicina i Odontologia, Universitat de València; (2) INCLIVA, Hospital Clínico Universitario, Valencia; (3) Centre for Biomaterials and Tissue Engineering, CBIT, Universitat Politècnica de València, Valencia; (4) CIBER-BBN, Bioingeniería Biomateriales y Nanomedicina, Valencia.

INTRODUCTION. Cartilage pathologies have a high incidence in the world's population. Numerous studies point to tissue engineering as a good alternative for the repair and regeneration of articular cartilage by using biomaterials. Chitosan has been proposed as an adequate biomaterial for regeneration of cartilage. The aim of this study was to assess the behaviour of Chitosan scaffolds coated with platelet-rich plasma (PRP) as a biodegradable scaffold material for cartilage regeneration. **MATERIALS AND METHODS.** Chitosan scaffold were manufactured as 3-mm diameter discs, made of 3% chitosan, containing pores in order to lodge chondrocytes. **Obtaining PRP:** PRP was obtained from whole blood collected with 3.8% sodium citrate as anticoagulant. Anticoagulated blood was centrifuged 8 min at 360 xg at room temperature, and the obtained plasma was separated into four fractions by pipetting very meticulously in order to avoid turbulence in the fractions obtained. The deepest fraction (number 4), located immediately above the red series, is the most enriched fraction in platelet-derived growth factors. **PRP activation:** PRP was used for clot formation by adding 50 µl of 10% CaCl₂ per ml of plasma fraction, which originated a clot in 5-8 min over either coverslips or over chitosan scaffolds. **Chondrocyte culture:** human chondrocyte were obtained from healthy areas of articular cartilage of donors. Cell suspension was obtained by successive enzymatic digestion, filtered through a 70 µm pore nylon filter, and finally isolated cells were used for primary cultures, as previously described. Cells were seeded over chitosan scaffolds (20x10³ cells/disc) or over coverslips, and cultured in static conditions for 1, 3, 7, 14 and 21 days; some of the discs and coverslips had been previously covered with PRP. Cellular morphology, adhesion and proliferation were studied with optical and electron microscope. **RESULTS.** PRP promotes the formation of a fine fibrillar mesh covering either scaffold pores or coverslips, that could be observed either by optic and scanning electron microscopy. Chondrocytes cultured after PRP covering presented a polygonal and starry morphology, with abundant long processes that spread out over the PRP fibrillar mesh. In the absence of PRP, cells presented a more rounded morphology and fewer processes. Moreover, the number of chondrocytes observed within scaffold pores along the time of culture was higher in chitosan scaffolds covered with PRP in comparison to non-PRP-covered ones. **CONCLUSION.** PRP promotes a starry morphology of cultured chondrocytes over chitosan scaffold along with a

higher number of cells with respect to the cells cultured in the absence of PRP. GRANT. This study was supported by MAT2013-46467-C4 grant from Ministerio de Economía y Competitividad, Spain.

60 THREE DIMENSIONAL DIFFERENTIATION MODEL OF HUMAN ADIPOSE-DERIVED MESENCHYMAL STEM CELL SPHEROIDS FOR CARTILAGE REPAIR

Zubillaga Marañón, V., Alonso-Varona, A., Palomares Casado T.

Universidad de País Vasco

Introduction Human adipose-derived mesenchymal stem cells (ADSCs) are widely used in cartilage regeneration due to their capacity of differentiation toward chondrogenic phenotype. Although ADSCs are commonly cultured in a two-dimensional (2D) monolayer, this culture system does not mimic the in vivo environment of chondrogenic mesenchymal stem cells. In order to improve chondrogenic differentiation protocols, we have used spherical clusters of cells. This model provides a three dimensional (3D) environment that allows direct cell-cell interactions observed in the cartilaginous condensations during the embryonic development¹. The aim of this study is to evaluate the use of hanging drop (HD) culture system in chondrogenic differentiation of ADSCs in terms of analyzing its viability and further chondrogenic differentiation. Material and methods ADSCs kindly supplied by HistoCell SL were seeded in 9 cm diameter petri dishes at a density of 15×10^3 in droplets of 30 μl in complete culture media (DMEM+Glutamax supplemented with 10% FBS)². The HD cultures allow forming cell spheroids due to gravity. After spheroids have been formed, the diameter was quantified via bright-field microscopy and analyzed with ImageJ software. Cell viability within the spheroid was determined by Live/Dead assay. In another set of experiments, after 48 h of spheroids formation, medium was replaced by chondrogenic specific culture medium for 7 days and a histological analysis (hematoxylin-eosin, safranin-O and alcian blue) was done in order to evaluate the chondrogenic differentiation of cells forming the spheroids. Results ADSCs cultured in HD system and forming spheroids were viable and proliferate during 7 days in culture. The quantification of the diameter of the spheroids gives an approach of the cell proliferation. Thus, we found a progressive increase (1.2-fold) in the diameter of spheroids from day 5 to day 7 ($305,787 \pm 21,877 \mu\text{m}$ vs $383,23 \pm 14,103 \mu\text{m}$, respectively) (Figure 1). Moreover, at the times 5 and 7 days, the Live/Dead assay shows that most cells in the spheroid were viable.

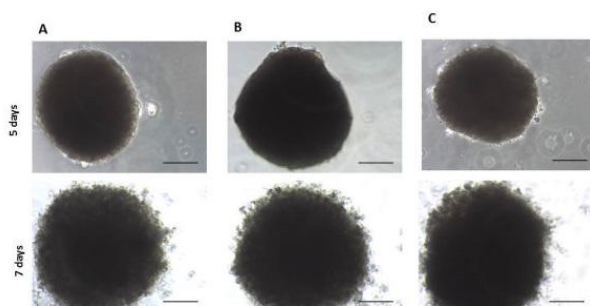


Figure 1: Bright field of ADSCs cultured in spheroids using HD technique. The scale bar represents 100 μm .

Finally, after chondrogenic stimulus, the histological analysis showed positivity in alcian blue and safranin-O staining at 7 days of culture, indicating pre-chondrogenic phenotype of the ADSC differentiated in the spheroids.

Conclusions 1. The 3D model provides a more physiological environment, partially mimicking the in vivo conditions of the mesenchymal stem cells. 2. ADSCs in the 3D spheroids are viable, proliferate under appropriate conditions and exhibit chondrogenic phenotype.

Acknowledgments V. Zubillaga is the recipient of an UPV/EHU predoctoral grant. Part of this work has been supported by Jesús Gangoiti Barrera Foundation. References 1. Liangming Z. et al. *Biotechnol Lett* 2010; 32:1339-1346. 2. Murphy K.C. et al. *Cell Tissue Res* 2014; 357:91-99.

61 AN IN VITRO COMPARATIVE STUDY OF THE EFFECTS OF ULTRAVIOLET B IRRADIATION ON HUMAN FIBROBLASTS AND ADIPOSE DERIVED MESENCHYMAL STEM CELLS

Burón Aizpiri, M., Palomares Casado, T., Alonso-Varona, A.

Universidad del País Vasco

AN IN VITRO COMPARATIVE STUDY OF THE EFFECTS OF ULTRAVIOLET B IRRADIATION ON HUMAN FIBROBLASTS AND ADIPOSE DERIVED MESENCHYMAL STEM CELLS (1) Burón Aizpiri, M., (2) Palomares Casado, T., (1) Alonso-Varona, A. (1) Department of Cell Biology and Histology, Faculty of Medicine UPV/EHU, Leioa, Vizcaya, Spain (2) Department of Surgery, Radiology and Physic Medicine, Faculty of Medicine UPV/EHU, Leioa, Vizcaya, Spain INTRODUCTION Ultraviolet B (UVB) irradiation is responsible for a variety of dermal pathologies, ranging from sunburn or skin aging to cancer development [Schuch et al. 2014]. Part of UVB is absorbed by the epidermis and mainly affects epidermal cells. However, 10-30% of UVB can penetrate the epidermis damaging the dermis and hypodermis, where fibroblasts and adipose derived mesenchymal stem cells (ADSCs) are, respectively [Mao et al. 2015]. In this study we investigate the effects of UVB on human fibroblasts (HFF) and ADSCs viability and cell damage. The goal is to design an in vitro model to study the effects of UVB in order to evaluate the protective effect of natural and renewable biomaterials. MATERIALS AND METHODS Cells. HFF were cultured in DMEM without phenol red supplemented with 10% FBS, L-glutamine (4mM), sodium pyruvate (1mM) and penicillin-streptomycin (100U/ml); and ADSCs in DEMEM + Glutamax, both at 37°C in an atmosphere containing 5% CO₂. Cells were sub-cultured to about 90-95% confluence by detaching with trypsin-EDTA solution. UVB irradiation. Cells at a density 1x10⁴ cells/well were irradiated in a range of 20 to 100mJ/cm² with 302nm UVB using a UVLM-26 lamp (Ultra-Violet Products, UK, Cambridge). After UVB irradiation, cells were incubated during 72h. Non-irradiated cells (control) were maintained in the same culture conditions without UVB exposure [Ahn et al. 2012]. MTT ASSAY. Cell viability was evaluated using the colorimetric MTT assay. Cells were irradiated as previously described, and cell viability was measured at 1, 24, 48 and 72h, in terms of absorbance at 540nm using a microplate reader (Biotek, HT Synergy, USA). LDH ASSAY. Cell damage was determined by quantifying the amount of

LDH released, using a commercial LDH cytotoxicity detection kit (Roche, Germany). Cells were exposed according to the experimental design. The absorbance of the supernatant was measured at 490nm using a microplate reader. RESULTS Results indicate that exposure of cells to UVB energy reduced cell viability and increased LDH release in a dose dependent manner. At 24h, cell viability was similar in both cell types. However, at 72h the cytotoxic effects are higher in HFF and AMSCs. Thus, the dose of radiation that causes 50% reduction on cell population (LD50) at 72h was 2,6 times higher in the case of ADSCs compared to HFF (38,8mJ/cm² vs 14,6mJ/cm², respectively). CONCLUSIONS UVB exposure induces delayed damage in both cell populations but AMSCs show more resistance to such damage. REFERENCES Ahn BN. et al. Naunyn Schmiedebergs Arch Pharmacol, 2012;385: 95-102. Mao GX. et al. International Journal of Cosmetic Science, 2015; 37:321-328. Schuch AP. et al. Environmental Science & Technology, 2014; 7;48: 11584-11590.

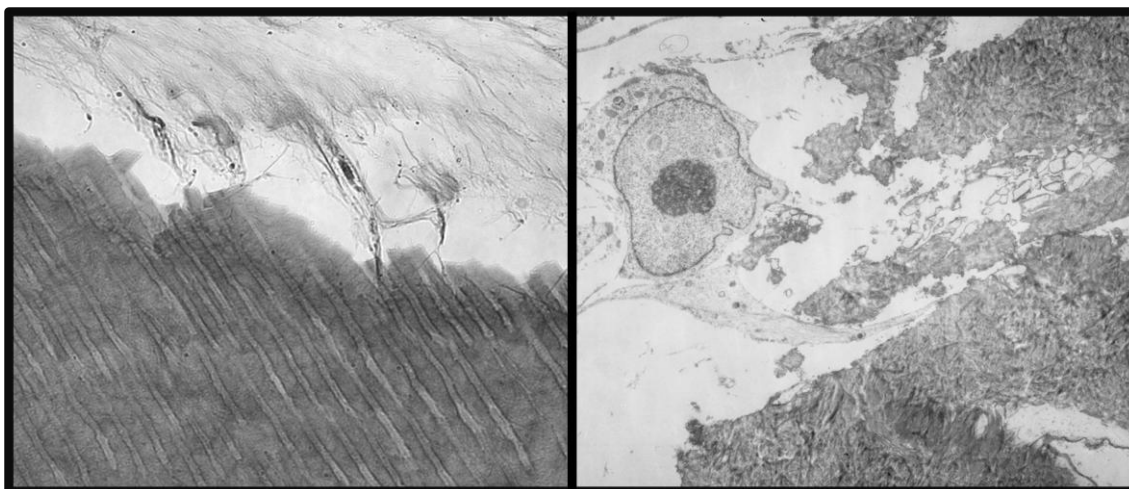
103 DENTIN MATRIX INDUCES HUMAN DENTAL PULP STEM CELLS DIFFERENTIATION

(1) Peydró S.; (1,2) Martín de Llano J.J; (1,2) Carda C.

(1) Departament de Patologia, Facultat de Medicina i Odontologia, Universitat de València, Spain. (2) Instituto de Investigación Sanitaria INCLIVA, Valencia, Spain.

Introduction The dentin matrix contains hydroxyapatite, calcium phosphate and other mineral components as well as biological molecules including several chemotactic and growth factors as TGF- β , FGF, IGF, etc. These matrix components and the tridimensional structure of the dentin may have an effect on human dental pulp stem cells (hDPSC) differentiation. The aim of our work was to study the adhesion, proliferation and differentiation of the hDPSC on a dentin surface. **Materials and methods** hDPSC obtained from young patient's third molars extracted for prophylactic reasons were cultured, from 1 to 6 weeks, on dental-derived matrices in basal medium containing ascorbic acid. Transversal sections of dental roots were obtained from human teeth from which the soft tissues, dental pulp and periodontal ligament, had been mechanically removed. Samples were processed for both light and transmission electron microscopy (TEM) using standard procedures. Cell adhesion, proliferation, morphology and secretory activity were evaluated. **Results** Phase contrast microscopy observation of the samples showed a high cell proliferation rate and adhesion to the dentinal surface at early stages of cell culture. Nevertheless, when these early samples were processed for paraffin embedding most of the cells were lost during the sample processing. At six weeks of cell culture hDPSC formed dense and complex layers completely surrounding the dental fragments with a strong and stable adhesion at this time. On dentin with tubules orientated perpendicularly to the surface hDPSC adopted an odontoblast-like morphology, developing cytoplasmic prolongations inside the tubules with a low production of matrix. These findings were confirmed at an ultrastructural level through TEM, demonstrating the presence of cytoplasmic prolongations, similar to those corresponding to odontoblastic processes, containing secretory vesicles. On the other hand, on dental sections in which the dentin layer had the tubules orientated in parallel to the surface, hDPSC formed flat layers with a high production of collagen matrix between them and the dentin surface. **Conclusions** Dentin surfaces constitute a favorable biological environment for hDPSC adhesion and proliferation and may induce cell differentiation into dental tissue forming

cells. The three-dimensional structure and dental matrix composition both are factors that influence the likely differentiation of hDPSC.



111 GENERATION OF A FULL-THICKNESS SUBSTITUTE OF THE HARD PALATE BY TISSUE ENGINEERING

(1) Garzón, I.; (1) Martín-Piedra, M.A.; (2) Liceras, E.; (1) Alfonso-Rodríguez, C.A.; (1) García-Martínez, L.A.; (1) Sánchez-Quevedo, M.C.; (3) España, A.; (1) Alaminos, M.; (1,3) Fernández-Valadés, R.

(1) Tissue Engineering Group, Department of Histology, University of Granada, Spain, and Instituto de Investigación Biosanitaria ibs.GRANADA, Spain; (2) Division of Pediatric Surgery, University Hospital of Granada, Spain; (3) Craniofacial Malformations and Cleft Lip and Palate Management Unit, University Hospital of Granada, Spain

Introduction: Cleft palate is one of the most common congenital defects. Clinical management of this condition is challenging and multiple surgical interventions are often required. Current therapeutic strategies include the use of muco-periosteal flaps obtained from healthy palatal areas to repair the hard palate cleft. However, one of the major problems in cleft palate repair is the bone reconstruction of the medium palate cleft and alveolar bone. In this work, we have developed for the first time a full-thickness hard palate substitute consisting of a bioengineered oral mucosa and an underlying bone with potential usefulness for cleft palate reconstruction. Materials and Methods: Primary keratinocyte and fibroblast cell cultures were established from rabbit palate biopsies using enzymatic digestion with trypsin-EDTA and type-I collagenase and adipose tissue-derived stem cell cultures were generated from small adipose tissue biopsies. Then, a bioengineered oral mucosa substitute was generated by combining fibrin-agarose hydrogels with oral mucosa fibroblasts. Once the hydrogel had jellified, cultured oral mucosa keratinocytes were subcultured on top. To develop a bone substitute, fibrin-agarose biomaterials containing adipose tissue-derived stem cells were induced during 28 days with StemPro Osteogenesis Differentiation Kit. Both tissues -oral mucosa and bone- were subjected to controlled nanostructuration to permanently attach both structures and generate a full-thickness hard palate substitute. Histological analyses were carried out to determine the differentiation

level of each bioengineered structure. Results: Histological analysis of the full-thickness substitutes revealed the presence of an epithelial cell layer on top of the stromal substitute. Immunofluorescence results showed the expression of typical markers of oral mucosa such as cytokeratins CK4 and CK3 as well as CK19 and CK5 at the epithelial layer of the hard palate substitute. In addition, subjacent bone substitutes revealed the presence of calcium deposits by the positive expression of alizarin red and osteocalcin. Conclusion: All these findings suggest that bioengineered hard palate substitutes generated by tissue engineering show relevant markers of epithelial and bone differentiation *ex vivo*. Therefore, these substitutes could have translational clinical potential for the reconstruction of cleft palate defects. Acknowledgments: This study was supported by the Spanish Plan Nacional de Investigación Científica, Desarrollo e Innovación Tecnológica from the Spanish Ministry of Economy and Competitiveness (Instituto de Salud Carlos III), grant FIS PI14/2110 (co-financed by FEDER funds, European Union).

116 BIOCOMPATIBILITY OF NOVEL MAGNETIC NANOPARTICLES IN 2D MODELS FOR USE IN TISSUE ENGINEERING

(1) Campos, F.; (2) López-López, M.T.; (2) Rodríguez-Arco, L.; (2) Bonhome-Espinosa, A.B.; (3) Fernández-Valadés, R.; (1) Alaminos, M.; (1) Campos, A.; (1) Carrie I, V.; (4) Rodríguez, I.A.

(1) Tissue Engineering Group, Department of Histology, University of Granada, Spain, and Instituto de Investigación Biosanitaria ibs.GRANADA, Spain; (2) Department of Applied Physics, University of Granada, Spain; (3) Division of Pediatric Surgery, University Hospital of Granada, Spain; (4) Cátedra de Histología B, University of Córdoba, República Argentina

Introduction: Magnetic nanoparticles (MNP) are promising tools for the generation of novel biomaterials for use in tissue engineering. The possibility of controlling the orientation and alignment of these nanoparticles may allow the efficient generation of artificial tissues with tunable biomechanical properties. However, magnetite has been suggested to be partly cytotoxic, and novel functionalization methods are in need to prevent these particles from releasing any toxic compounds to cells and tissues. In this sense, the objective of this study is to determine the biocompatibility of MNP on cultured human gingival fibroblast by using a panel of cell viability assays. Materials and Methods: Human gingival fibroblasts were isolated from human oral mucosa biopsies and cultured in 24-well plates (2×10^5 cells and 500 μ l DMEM culture medium per well) and randomly assigned to one of the following experimental groups: Group A: 1% of Magnetite MNP (MAG); Group B: 1% of magnetite MNP functionalized with polyethylene-glycol (MAG+PEG). In both cases the cells were exposed to the MNP during 24h. Fibroblasts without MNP were used as positive controls (CM) and Fibroblasts exposed to 2% triton X-100 were used as negative controls (CT). Cell morphology in each group was analyzed by phase contrast microscopy. In order to evaluate the nuclear membrane permeability, released DNA was quantified by spectrophotometry. Finally, cell proliferation was analyzed with WTS-1 technique. Results: Fibroblasts exposed to MAG+PEG and CM showed the orthotypical spindle-like shape of normal fibroblasts. In contrast, fibroblasts exposed to MAG and CT displayed a rounded morphology, and their attachment to the culture surface was affected. DNA

quantification technique did not show any alteration in MAG and MAG+PEG as compared to CM. Cell proliferation analysis showed similar levels of cell activity for MAG+PEG and CM ($p > 0.05$), but cell proliferation was significantly lower in MAG than in the CM group ($p < 0.001$). Conclusions: The morphological analysis, DNA quantification and cell proliferation assays demonstrated that magnetic nanoparticles functionalized with polyethylene-glycol did not affect the normal function and morphology of human gingival fibroblasts. Functionalized magnetic nanoparticles showed *ex vivo* biocompatibility and they could be used for the generation of novel bioartificial substitutes for several tissue engineering applications. Acknowledgements: This study was supported by the Spanish Plan Nacional de Investigación Científica, Desarrollo e Innovación Tecnológica from the Spanish Ministry of Economy and Competitiveness (Instituto de Salud Carlos III), grants FIS PI14/0955, FIS PI14/2110 and FIS PI14/1343 (co-financed by FEDER funds, European Union).

120 GENERATION OF BIOLOGICALLY ACTIVE ABDOMINAL MESHES FOR ABDOMINAL WALL SURGERY. EVALUATION OF THE SYNTHESIS OF EXTRACELLULAR MATRIX COMPONENTS

(1) Martín-Piedra, M.A.; (1) Garzón, I.; (1) Alfonso-Rodríguez, C.A.; (1) Campos, F.; (2) López-Cantarero, M.; (1) Sánchez-Quevedo, M.C.; (1) Crespo, P.V.; (1) García, J.M.; (1) Alaminos, M.

(1) Tissue Engineering Group, Department of Histology, University of Granada, Spain, and Instituto de Investigación Biosanitaria IBS-GRANADA, Spain; (2) Department of Surgery and its specialties, University of Granada, Spain.

Introduction: Abdominal wall defects due to congenital disease, traumatic injury, surgical resection and hernia are among the most frequent situations in abdominal surgery. However, current therapeutic approaches based on the use of inert surgical meshes are not able to stimulate healing and have clinical disadvantages such as fibrosis, inflammation and intestinal adhesions. Tissue engineering may allow the generation of biological tissue substitutes for use in abdominal surgery without the drawbacks of inert meshes. In the present study, we generated two types of biologically active abdominal meshes (BAAM) for use in abdominal wall surgery and we evaluated the expression of key extracellular matrix (ECM) components in these bioengineered meshes. **Materials and Methods:** Biologically active abdominal meshes were generated by using polyglycolic/polypropylene (PGA-PP) and polypropylene (PP) commercially available surgical meshes immersed in fibrin-agarose scaffolds with rat fibroblasts (2.4×10^5 cells/mL). These BAAM were grafted on the abdominal wall of Wistar rats for histological study after 2 and 4 weeks. Inert PGA-PP and PP meshes were grafted *in vivo* as controls. In all cases, synthesis of several ECM components was analyzed by picrosirius (collagen fibers), orcein (elastic fibers), alcian blue (proteoglycans) and PAS (glycoproteins and carbohydrates) histochemical methods. Expression of type-I collagen (COL1) was analyzed by immunohistochemistry. **Results:** First, the use of PP meshes was associated to an increased synthesis of proteoglycans and carbohydrates and a decreased expression of fibrillar components as compared with PGA-PP. Then, inert meshes had higher synthesis of collagen and elastic fibers as determined by picrosirius and orcein and of type-I collagen as determined by immunohistochemistry than BAAM. The same pattern was found for the presence of non-

fibrillar components of the ECM, including proteoglycans, glycoproteins and carbohydrates. Conclusions: These results suggest that the use of BAAM in abdominal surgery is associated to less fibrosis than inert meshes and support the use of these bioengineered tissues in abdominal wall surgery. Acknowledgments: This study is supported by CTS-115, Tissue Engineering Group, University of Granada, Spain

124 CELL VIABILITY ASSESSMENT IN THREE-DIMENSIONAL ARTIFICIAL TISSUES GENERATED BY TISSUE ENGINEERING

(1) Martín-Piedra, M.A.; (1) Campos, F.; (1) Jaimes-Parra, B.D.; (1) Alaminos, M.; (1) Crespo, P.V.; (1) García, J.M.; (1) Campos, A.; (2) Warley, A.; (1) Sánchez-Q uevedo, M.C.

(1) Tissue Engineering Group, Department of Histology, University of Granada, Spain, and Instituto de Investigación Biosanitaria ibs.GRANADA, Spain; (2) King's College, London, UK

Introduction: Development of biological artificial tissues is the main objective of tissue engineering. Although isolated cells used to build artificial tissues have been evaluated for their viability in bidimensional cultures, methods to evaluate cell viability within three-dimensional tissue constructs should be developed. Electron probe X-ray microanalysis is one of the most sensitive techniques for determination of cell viability, as it allows accurate quantification of the intracellular ionic content in cell cultures. Live-dead methods combine the use of exclusion dyes for determination of cell membrane integrity and metabolic compounds to analyze cytoplasmic cell fu nction. In this work, we optimized two highly-sensitive methods (Electron Probe X-ray microanalysis -EPXMA- and Live-Dead) to evaluate cell viability in fibrin-agarose artificial tissues with gingival fibroblasts. Materials and Methods: Primary cultures of human gingival fibroblasts were generated by enzymatic digestion of human gingival biopsies. A stromal substitute made of human fibrin and 0.1% agarose with gingival fibroblasts immersed within was generated and cultured for 21 days. Artificial tissues were evaluated at day 7 and 21 of development by EPXMA and Live-Dead. For EPXMA, tissue constructs were sectioned in thin slices, washed for 5 seconds with distilled water at 4°C, plunge-frozen in liquid nitrogen and freeze-dried. Specimens were then mounted on a carbon stub and sputter coated with a thin layer of carbon in an argon atmosphere. Quantification of the ionic concentrations of Na, K, S, P, Ca, Mg and Cl in cells within the artificial tissue was carried out by electron probe X-ray microanalysis using a Philips Quanta 200 scanning electron microscope with an energy-dispersive detector EDAX, using the P/B ratio method with reference to standards of inorganic salts. For Live-Dead, art ificial tissues were sectioned, washed in PBS, incubated in a mixture of calcein AM and ethidium homodimer-1 for 3 min and analyzed in a fluorescence microscope Nikon Eclipse Ti-U. Results: Our results show that the ionic content of gingival fibroblasts cultured on three-dimensional systems of artificial tissues was as follows (expressed as mmol/kg of dry weight): Na: 87.87, P: 219.01, Mg: 24.24, K: 169.84, Cl: 88.92, Ca: 47.00, S: 130.66 at 7 days, and Na: 59.96, P: 347.94, Mg: 18.24, K: 193.71, Cl: 119.75, Ca: 182.23 S: 121.33 at 21 days. The K/Na ratio was 1.93 at day 7 and 3.23 at day 21 of development in culture. For the Live-Dead method, results showed 87% of alive cells at day 7 and 61.4% at day 21. Conclusions: These results suggest that highly-sensitive EPXMA and Live-Dead methods

can be used for the evaluation of three-dimensional artificial tissues. Results also show that cell viability is high in fibrin-agarose, thus confirming that these biomaterials are highly biocompatible. Acknowledgements: This study was supported by the Spanish Plan Nacional de Investigación Científica, Desarrollo e Innovación Tecnológica from the Spanish Ministry of Economy and Competitiveness (Instituto de Salud Carlos III), grant FIS PI14/2110 (co-financed by FEDER funds, European Union).

125 GENERATION OF A TISSUE-LIKE BIOLOGICAL MEMBRANE BY WHARTON'S JELLY STEM CELLS FOR TISSUE ENGINEERING

(1) Jaimes-Parra, B.D.; (1) García, J.M.; (1) Alfonso-Rodríguez, C.A.; (2) Fernández-Valadés, R.; (1) Martín-Piedra, M.A.; (1) Alaminos, M.; (1) Campos, A.; (1) Sánchez-Quavedo, M.C.; (1) Garzón, I.

(1) Tissue Engineering Group, Department of Histology, University of Granada, Spain, and Instituto de Investigación Biosanitaria ibs.GRANADA, Spain; (2) Division of Pediatric Surgery, University Hospital of Granada, Spain.

Introduction: The human umbilical cord is gaining increasing attention in regenerative medicine mainly due to the presence of undifferentiated stem cells with important differentiation capability. In this context, Wharton's jelly mesenchymal stem cells (WHJSC) are among the most promising cell populations of the umbilical cord and they have been extensively used in tissue engineering protocols. In this study, we describe and evaluate a novel Wharton's jelly stem cell-based biological membrane as a novel tissue-like biomaterial for use in different tissue engineering protocols. **Materials and Methodology:** WHJSC were obtained from umbilical cords corresponding to newborns delivered by cesarean section. Umbilical cord samples were cut into small fragments and digested in collagenase type I to obtain primary cell cultures. Once primary cell cultures were established, cells were allowed to reach 100% confluence to let WHJSC form a homogeneous cell-membrane. WHJSC-based tissue-like biological membranes were stained with haematoxylin-eosin, alcian blue, picosirius, Verhoeff and PAS to evaluate the presence of relevant extracellular matrix components. Immunohistochemistry for PCNA, vimentin and type I-collagen was used to analyze cell proliferation, phenotype and collagen fibers synthesis. **Results:** Our results showed that the WHJSC-based tissue-like biological membranes consisted of an abundant cell population surrounded by a dense pericellular extracellular matrix material synthesized by the WHJSC. The analysis of the extracellular matrix components confirmed the strong presence of collagen fibers and the lack of elastic fibers, with few proteoglycans and glycoproteins. Cells were vimentin-positive and a high percentage of cells were positive for PCNA. **Conclusions:** WHJSC-based tissue-like biological membranes obtained by culturing human WHJSC demonstrated to have numerous viable cells with proliferative capability and a very abundant extracellular matrix mainly consisting in collagen fibers. These results suggest that these membranes could have potential usefulness for tissue engineering purposes in the fields of ophthalmology, peripheral nerve repair, palate surgery and other areas where stem cells and collagen may contribute to tissue regeneration. **Acknowledgements:** This study was supported by the Spanish Plan Nacional de Investigación Científica, Desarrollo e Innovación Tecnológica from the Spanish Ministry of Economy and Competitiveness (Instituto de Salud

Carlos III), grants FIS PI14/0955, FIS PI14/2110 and FIS PI14/1343 (co-financed by FEDER funds, European Union).

135 BONE REGENERATION OF CRITICAL MANDIBULAR DEFECTS USING TISSUE ENGINEERING TECHNIQUES: PORCINE EXPERIMENTAL STUDY.

García-Honduvilla N1,2,5, Coca A3, Ramírez-Varela S3, Peña J4, 5, Ca bañas MV4, 5, Román J4, 5, Buján J1, 5.

(1) Dpto. Medicina y Especialidades Médicas (UAH); (2) CUD-ACD; (3) Dpto. Química Inorgánica y Bioinorgánica (UCM); (5) CIBER-BBN.

INTRODUCTION: Reconstruction of bone by autologous bone transplants has been established as the “gold standard” due to their osteogenic properties. However, bone grafting is only applicable to relatively small defects, and can be accompanied by donor site morbidities, such as infection, bleeding, pain, swelling, nerve damage, bony non-union and pain upon movement. Therefore, the objective of this work is to design constructs bound for bone repair - regeneration critical mandibular defects using autologous mesenchymal cells from adipose tissue on nanoapatitas hidrocarbonatadas arrays (L1). **MATERIAL AND METHODS** Adipose stem cells were isolated from the subcutaneous neck fat from 6 female mini-pigs and cells were incubated in DMEM for 7 days. To induce the differentiation, ADSC were cultured with specific osteogenic differentiation medium. The cell identification and the degree of differentiation were assessed by histological techniques (von Kossa, alkaline phosphatase) and immunohistochemical (RUNX2, OCT3 / 4, Nanog, osteopontin).

For in vivo studies, we performed (n=6), 4 critical mandibular defects (35 mm x 15 mm) (2 hemiarcade) on which they were implemented, at random, the various constructs (total number of defects = 24):

A. Control Group (n = 6 defects): animals which underwent the defect and are not subjected to any treatment.

b.- Group I (n = 6): L1 prosthesis.

c.- Group II (n = 6): L1 prosthesis colonized with undifferentiated adipose mesenchymal cells (MSCAT).

d.- Group III (n = 6): L1 prosthesis colonized with mesenchymal cells from the same animal previously differentiated in vitro for 7 days.

Radiological controls at 3 and 6 months after the creation of the bone defect using CT were performed. The animals were sacrificed at 6 months. The samples obtained were decalcified and processed for histological examination (hematoxylin-eosin, Masson's trichrome and Sirius Red) and immunohistochemical (osteopontin, osteocalcin, and TRAP RANK).

Data were analyzed using statistical package version 15.0 SPSS

RESULTS: The rate of in vitro proliferation, histological stains and immunohistochemical

studies showed mesenchymal nature of cells isolated from porcine adipose tissue. The expression of osteopontin and osteocalcin , together with Von Kossa staining, demonstrated a certain degree of differentiation into osteogenic MSCAT line after 7 days of culture .

Two of the six animals showed an abnormality (33.33 % morbidity) .

The CT images showed a greater bone regeneration in those groups treated with the cell-colonized L1 biomaterial versus the control group and group I. Histology showed better bone remodeling in the groups treated with cells (Groups II and III) characterized by higher amounts of cortical bone and by Haversian channels surrounded by several lamellae and among these. In contrast the other groups biopsies were constructed from more cancellous (spongy) bone, consisting in interrupted lamellae and numerous large spaces filled with marrow and arranged in a more or less regular pattern. The best performance in terms of regeneration was observed in the treatment group L1 + undifferentiated MSCAT (Group II) where we observed a high osteoblast and osteoclast activity confirmed by immunohistochemical techniques.

CONCLUSION: The tissue engineering techniques suggest an improvement in the process of bone regeneration. The addition of MSCAT into scaffolds should improve the quality and quantity of the regenerated bone.

(Proyecto IMIDEF-2014)

155 CORNEAL RIMS FOLLOWING HYPOTHERMIC STORAGE FOR SEVEN DAYS AS A SOURCE OF STEM-LIKE LIMBAL EPITHELIAL CELLS

(1) Hernández-Moya, R.,(1,2) Etxebarria Ecenarro, J.,(1) Asumendi Mallea, A.,(1) Boyano Lopez, M.D.,(1) Andollo Victoriano, N.

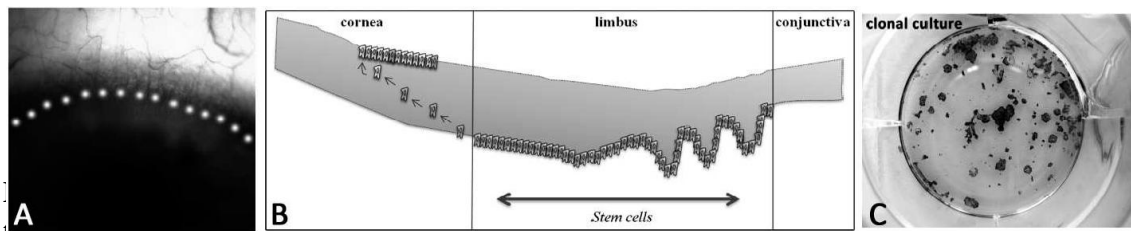
(1) Department of Cell Biology and Histology, School of Medicine and Dentistry, University of the Basque Country, BioCruces Health Research Institute. Leioa, Spain.

Introduction: Availability of donor corneal-scleral rims is essential for the progression of basic research in stem cell therapies for the treatment of corneal disease. However, a worldwide shortage of corneal donors for transplantation reflects a shortage of corneal-scleral rims available to the research community. In the present study, we have analyzed the presence and capability for growing *in vitro* of limbal epithelial stem/progenitor cells (LSC) retrieved from limbal rims remaining after corneal transplantation. These corneal rims have been stored in hypothermic conditions in Optisol-GS medium for long time (7 days), and are usually discarded.

Materials and Methods: Protein expression of putative limbal stem cell markers (K15, Δ Np63 α and ABCG2) and terminally differentiating suprabasal cells (K3 and involucrin) was assessed using immunofluorescent staining in frozen histological sections of the corneal rims, as well as in limbal epithelial cultures established from these corneal rims and maintained up to 3 cell passages. Colony forming efficiency (CFE) assays were performed to corroborate the presence of colony-forming cells in the primary culture.

Results: In the basal layer of the limbal epithelium, we have detected cells that stained positively for the putative stem cell markers K15 and $\Delta Np63\alpha$, and negatively for the differentiation markers K3 and involucrin. Isolated cells in primary cultures also expressed the putative LSC markers K15 and ABCG2 after several culture passages. Furthermore, isolated cells seeded at clonal dilution were able to grow forming holoclon-like colonies, demonstrating the presence in the culture of cells with self-renewing capability.

Conclusions: We have demonstrated that limbal rims remaining after corneal transplantation that have been conserved in hypothermic conditions for as long as 7 days can be a valuable source for LSC cultures for research and even for stem cell therapy purposes, that would have otherwise been ignored.



the location of the limbus as well as the migration and differentiation of the LSCs, from the limbal area to the cornea, to become corneal epithelial cells. (C) Clonal culture showing cell growth into holoclon-like colonies.

MODELOS EXPERIMENTALES

16 HISTOLOGICAL CHANGES TO THE CORNEA CAUSED BY EXPERIMENTAL CONDUCTIVE KERATOPLASTY.

Usón Gracia, A., Abellán Rubio, E., Crisóstomo Ayala, V., Álvarez Pérez, V., Borrega Hernández, M., Sanchez-Margallo, F.M.

Stem Cell Therapy Unit, “Jesús Usón” Minimally Invasive Surgery Centre

INTRODUCTION: Conductive keratoplasty (CK) is a technique that uses radiofrequency to modify collagen fibers, thus adjusting the curvature of the cornea in cases of presbyopia, hypermetropia and astigmatism.

Its short- to mid-term efficacy is not clear, since there are cases in which the effect is lost, and the defect regresses. Our aim was to evaluate the histological changes caused by the application of this therapy to rabbit's cornea as a way to determine its mid-term efficacy.

MATERIAL AND METHODS: Five New Zealand White rabbits, were subjected to a CK treatment on the right eye, with the left eye acting as control. Animals were followed up for 6 months using serial ophthalmological tests (slit-lamp and pachymetry) and were then euthanized for histological analysis.

After fixation, samples were divided at the mid corneal line, and were processed and included in paraffin using standard techniques. Transversal 4 μm sections were then obtained using a semi-

automatic microtome. All samples (treated and control) were stained with Hematoxylin-Eosin for cell nuclei visualization and assessment, as well as Masson's trichromic and Toluidine blue stains for collagen fibers evaluation.

Blinded microscopical evaluation was performed by the same operator in all cases, evaluating the degree of epithelialization, presence of epithelial alterations, loss of keratinocytes, inflammatory infiltrate, degree of apoptosis, presence of neovessels and integrity of the Descemet membrane. Changes were assessed using a 0 to 4 score, where 0 represents no changes and 4 was graded when changes to the normal architecture were severe and extensive.

RESULTS: Clinical data obtained during the follow up suggested that CK therapy had been effective in terms of corneal curvature modification. In terms of histopathological assessment, no changes to normal corneal architecture were seen in any control sample. Treated corneas however, presented different degrees of changes in all cases. Individual scores from all studied parameters are presented in the table.

At the level of the epithelium, two of the samples showed a localized thickening with cytoplasmatic vacuolization at the basal membrane along with increased number of cellular layers. The remaining samples also presented with cytoplasmatic vacuolization, albeit with a normal number of layers. In one case, keratin did not adhere completely to the epithelium.

No stromal thickening was seen. All studied samples exhibited decreased cellularity, increased intercellular spaces, loss of the collagen lamellae horizontal structure and increased extracellular matrix. These alterations were located anteriorly in two cases. A focal inflammatory infiltrate was also detected in one sample.

Regarding the corneal endothelium, localized tears on the Descemet membrane and poor adherence were seen in two cases, while the remaining samples were normal.

CONCLUSIONS: Despite good clinical results, CK's effectivity is not stable on the mid-term, as shown by the poor healing and lack of complete recovery of corneal architecture.

- Longer term studies are needed to evaluate the time needed for complete tissue regeneration and stability of the therapy.

Table 1. Histological assessment of changes to the rabbit's cornea after CK

	6 months				
Animals	R14-038	R14-041	R14-042	R14-43	R14-044
Epithelialization degree	1	2	3	3	2
Epithelial alteration	1	2	3	3	2
Loss of keratinocytes	3	1	2	2	1
Inflammatory infiltrate	0	0	0	0	2
Apoptosis degree	0	0	0	0	0
Vascularization	0	0	0	0	0
Descemet membrane	2	0	0	0	0

Score:

- 0 (no changes): There are no evident alterations, or changes can be considered normal.

- 1 (slight): Isolated changes to the normal pattern, but beyond what would be considered normal.

- 2 (mild): Clearly identifiable alterations that nonetheless span a limited amount of the sample

- 3 (moderate): Obvious changes occupying a great percentage of the sample

- 4 (severe): Severe lesions that span most of the sample.

32 PATHOPHYSIOLOGICAL STUDY MYOFASCIAL PAIN SYNDROME: PRELIMINARY RESULTS

(1) Santafe Martinez, M, (1) Margalef Perez, R, (1) Sisquella Basagaña, M, (1) Bosque Alberich, M, (1) Romeu Escolá, C, (2) Mayoral del Moral, O, (1,3) Monterde Perez, S, (1) Priego Luque, M, (1,4) Ortiz Castellon, N, (1) Tomàs Ferrer, J.

(1) Unidad de Histología y Neurobiología, Departamento de Ciencias Médicas Básicas, Facultad de Medicina y Ciencias de la Salud, Universidad Rovira i Virgili, Calle St. Lorenzo 21, 43201 Reus. (2)Unidad de terapia física, Hospital Provincial de Toledo, Cerro de San Servando s / n, 45006 Toledo. (3)Unidad de Fisioterapia, Departamento de Medicina y Cirugía, Facultad de Medicina y Ciencias de la Salud, Universidad Rovira i Virgili, Calle St. Lorenzo 21, 43201 Reus. (4) Sección de Neurología, Departamento de Medicina, Hospital Universitario de San Juan. Reus.

An abnormal release of acetylcholine (ACh) in the synaptic cleft seems responsible for localized increase in diameter of muscle fibers located below the synapse. There are called "contraction knots" and the existence of a sufficient number of them is considered a myofascial trigger point identifiable by palpation and electromyography in humans.

Objective: The increase of acetylcholine in the synaptic cleft into muscles of mice generates contraction knots comparable to those described in humans.

Methodology: We increase ACh in the synaptic cleft by the anticholinesterase neostigmine both *in vivo* and *ex vivo* samples. For *in vivo* experiments, neostigmine is injected subcutaneously in adult male Swiss mice.

- Electrophysiology study: intracellular recordings are performed to evaluate the spontaneous release of ACh.
- Morphological experiments: to evaluate the morphology of synaptic contacts the AChR are stained with α -bungarotoxin rhodaminated in the LAL muscle. Moreover, the presence of glycosaminoglycans (GAGs) is assessed with the PAS- Alcian technique.

Results:

- Electrophysiology study: When neostigmine is applied subcutaneously (*in vivo*, *in toto*): spontaneous ACh release is strongly increased in the LAL muscle.
- Morphological experiments: With α -bungarotoxin rhodaminated we observe abundant contracted synaptic contacts. With PAS-Alcian technique we have obtained images of contraction nodes rich in GAGs.

Conclusion. Mice treated with a single subcutaneous injection of neostigmine can be a good model for the study of myofascial trigger points because they showed an increase in spontaneous ACh release and contraction knots.

This work is funded by a grant from FISS (PI13 / 02084)

54 WNT SIGNALING PATHWAY IS CRITICAL AT SEVERAL STAGES OF ODONTOGENESIS

Aurrekoetxea Campo, M., Irastorza Epelde, I., García Gallastegui P., Uribe-Etxebarria Zubizarreta, V., Ibarretxe Bilbao G., Unda Rodríguez F.

Department of Cell Biology and Histology. Faculty of Medicine and Dentistry. University of the Basque Country. Leioa 48940, Vizcaya. Spain.

Introduction: Odontogenesis or tooth development is a complex process controlled by numerous inter-cellular signaling pathways such as BMP, FGF, Hedgehog and Wnt families. Particularly, Wnt/ β -catenin signaling is a highly conserved pathway, and the precise control of this route is required for normal dental development. In mouse, tooth development begins around embryonic day (E) 10.5. Epithelial tooth buds occurs at the E12.5-13.5 stage. After the bud stage, the tooth germ progresses to the morphogenesis stage at E14.5, odontoblast differentiation stage at E17.5 and ameloblast differentiation stage at E19.5. Therefore, these stages are crucial during tooth development. Methodology and materials: To investigate the effects of controlled overactivation of the Wnt/ β -catenin route we used a 6-bromoindirubin-3'-oxime (BIO), a specific pharmacological inhibitor of glycogen synthase kinase-3 IX (GSK-3), on first molar cultures at different stages of odontogenesis. Results: Overactivation of the Wnt/ β -catenin pathway induced a deregulation and ectopic expression of some odontogenenic target genes, such as Fgf4, Fgf10, Msx1, Dkk1, Wnt10b, Shh, Bmp4 and Epipofin/Sp6. At the initiation stage, Wnt overactivation promoted the formation of regulatory centers, which control extra teeth. Furthermore, in the morphogenesis and cell differentiation stages alterations of tooth

development and disorders were detected, and changes in gene expression occurred. Conclusions: We propose a feedback loop between Wnt, Efn and BMP, which would determine the correct tooth morphology, and the development of the ameloblasts and odontoblasts.

70 A 3D EXPERIMENTAL MODEL OF COLORECTAL CANCER FOR DRUG SCREENING USING FLUORESCENCE-BASED MEASUREMENT

(1) Garrido-Pascual, P ; (2) Calle, Y; (1) Palomares, T.,;(1) Alonso-Varona, A.

(1) Faculty of Medicine and Dentistry, University of the Basque Count ry UPV/EHU, Bizkaia, Spain and (2) Department of Life Sciences, Health Sciences Research Centre, University of Roehampton, London, UK.

Introduction. In the field of drugs development, it has been pointed out the relevance of experimental model used to assess the efficacy of the chemotherapeutic agents¹. Thus, it has been demonstrated a lack of correlation between the results obtained in vitro 2D culture models and those obtained in the clinic. 3D multicellular model, which includes both tumor and stromal cells, reflect better the *in vivo* tumor microenvironment, and allow investigation of cell-cell interactions, cell metabolism or the matrix synthesis². This approach permits to analyze more precisely the drug efficacy.

Herein, we report a novel fluorescence-based 3D model of colorectal cancer suitable for *High-Throughput Screening* (HTS) drug discovery.

Materials and Methods. In this study we developed a 3D model that includes human colon tumor cells (DLD-1), previously labelled with eGFP, grown as multicellular spheroids and embedded in a collagen I gel solution in 96-well plates. Also, we used a standard 2D culture of these tumor cells, in order to compare the results obtained in both models. Cell proliferation was determined by two methods: *i*, measurement of fluorescence intensity (FI) from eGFP-labelled tumor cells and, *ii*, measurement of absorbance on MTT assay. In addition, we evaluated apoptosis by using Annexin V immunodetection.

Results. Firstly, we compare the data of cell proliferation obtained by measuring the FI and absorbance in the MTT assay, showing that both methods correlated well, both in 2D and in the 3D culture systems. To validate this model for HTS, a pilot study was carried out using a library of the most common anti-colorectal cancer drugs. The drugs had the expected effect in 2D and 3D culture systems.

Discussion and Conclusions. This fluorescence-based 3D model has proved to be as sensitive as MTT when quantifying cell proliferation. Besides, it provides useful information to identify cytotoxic drugs *in vitro*, which shows the potential of this 3D model as a platform for drug development.

Acknowledgments: This work has been partially supported by Fundación Jesus Gangoiti Barrera.

References: 1. Chitcholtan K, Sykes PH, Evans JJ. The resistance of intracellular mediators to doxorubicin and cisplatin are distinct in 3D and 2D endometrial cancer. *J Transl Med.* 2012;10:38.

2. Hoffmann OI, Ilmberger C, Magosch S, Joka M, Jauch KW, Mayer B. Impact of the spheroid model complexity on drug response. *J Biotechnol.* 2015; 205: 14-23.

82 HIGHLY EFFICIENT GENERATION OF DUAL GLUTAMATERGIC/CHOLINERGIC NT2-DERIVED POSTMITOTIC HUMAN NEURONS BY SHORT-TERM TREATMENT WITH CYTOSINE β -D-ARABINOFURANOSIDE

González-Burguera I., Aretxabala X. , Barrondo S., Ricobaraza A., García del Caño G., López de Jesús M., Sallés J.

Universidad del País Vasco / Euskal Herriko Unibertsitatea

Introduction Upon retinoic acid (RA) treatment, pluripotent NTERA2/D1 (NT2) cells generate postmitotic neurons (RA/NT2N), which can be functionally integrated in the host tissue when grafted into the rodent and human brain, thus representing a promising source for neuronal replacement therapy. However, this model presents two major limitations: the lengthy differentiation procedure and its low efficiency. Recent studies suggest that differentiation can be shortened to 6 days using the nucleoside analogue cytosine β -D-arabinofuranoside (AraC). Here, neuronal phenotypes generated by treatment of NT2 progenitors with AraC or RA were characterized and compared. Specifically, the expression of neuron-specific and neurotransmitter phenotype markers was evaluated and combined with a detailed morphometric analysis of terminally differentiated neurons. Material and Methods NT2 cells were maintained in complete medium (DMEM, 10% FBS, 100 U/mL penicillin and 100 μ g/mL streptomycin) at 37°C under a humidified atmosphere containing 5% CO₂. To induce differentiation, NT2 cells were treated with RA, as previously described by Pleasure et al. (1992), or with AraC, as reported by Musch et al. (2010). Cells were collected at different time points along the process and analyzed by high-resolution fluorescence microscopy and western blot. Given that a low cell density can compromise neuronal survival and differentiation, it was tested whether increased confluence improves the yield of terminally AraC-differentiated neurons (AraC/NT2N). For this purpose, NT2 cells treated with AraC during 3-days were replated to a higher density and treated for 3 additional days with AraC. This modification resulted in a 2-fold increase of surviving cells yielded a culture highly enriched in cells with neuronal morphology. Cell size, nuclear and soma area, and neurite length and number morphometric parameters were measured manually using ImageJ software. Results Our results show that short-term exposure of NT2 cells to AraC could be a suitable method to efficiently generate mature neurons. The morphometric analysis performed in RA/NT2N and AraC/NT2N, showed a larger soma and nucleus in AraC/NT2N vs. RA/NT2N along with a lower ratio of nuclear to body area. Neurites of AraC/NT2N neurons were also shorter and fewer than in RA/NT2N. Of particular interest, cells committed to differentiate by short treatment with AraC displayed a completely different neurotransmitter phenotype when compared with RA/NT2N neurons. In fact, AraC/NT2N were essentially composed of dual glutamatergic/cholinergic neurons,

whereas RA/NT2N were mainly GABAergic. Conclusions Taken together, these results further reinforce the notion that NT2 cells are a versatile source of neuronal phenotypes and provide a new encouraging platform for studying neuronal differentiation mechanisms and for exploring neuronal replacement strategies. References Musch T et al. (2010). PLoS One, 5:e10726. Pleasure SJ et al. (1992). J Neurosci, 12:1802-1815. Funding: Basque Government grants GIC/IT-589/13 and SAIOTEK S-PE11UN124-125, Instituto de Salud Carlos III, Centro de Investigación Biomédica en Red de Salud Mental, CIBERSAM.

147 MORPHOLOGICAL ALTERATION IN BLOOD CELLS OF FISHES EXPOSED TO CADMIUM.

Hernández Díaz, M., Hernández Calderas, I., Becerra Amezcua, M. P., Jerónimo-Juárez, J. R., y Guzmán García, X.

Universidad Autónoma Metropolitana. Unidad I ztapalapa. División de Ciencias Biológicas y de la Salud. Departamento de Hidrobiología. Lab. de Ecotoxicología. Av. San Rafael Atlixco. No. 186. Colonia Vicentina. C.P. 09340. Delegación Iztapalapa. México. D.F.

Heavy metals are considered critical pollutants in aquatic ecosystems, due to its ionic form and ability to be absorbed by organisms. Among the most dangerous heavy metals is cadmium, which affects the cell membrane and cell metabolism enzymes in aquatic animals such as fish. Fish are used as models for experimental and ecotoxicological research due to their hematopoietic system and blood tissue are highly sensitive to environmental stress. The aim of this study was to determine morphological alterations of blood cells caused by this pollutant through a cell bioassay and hemolysis microassay in cadmium concentrations. We collected 10 fish in Tecolutla, Veracruz, Mexico, and extracted a blood samples with heparinized syringes. The samples were transported at 4 ° C to be processed in the laboratory. The bioassay was performed by placing 1mL of fish blood (*Trichurus lepturus*) a 1.5 mL eppendorf tube in duplicate, for as control batch, and 1 mL of blood, 0.5 ml of PBS and 0.33 µg/mL in duplicate, as cadmium experimental batches. Later blood smears were performed with 50 µL at 6, 12 and 24 h, they were stained with Giemsa. Morphological analysis was performed and microphotographs of the observed alterations were obtained. The hemolysis microassay was performed with human and common carp erythrocytes to determine their sensitivity exposing to 0.33 µg/mL, 0.99 µg/mL and 1.65 µg/mL of cadmium. Reading was performed in a plate spectrophotometer to obtain the concentration and percent hemolysis of the cells. The results were treated statistically using the U test of Mann-Whitney. The results showed that the cadmium in concentration of 0.33 µg/mL cause changes in erythrocytes as poikilocytosis, Heinz bodies, decreased cytoplasm, lobulation of nucleus and hemolysis, polymorphonuclear cells showed disintegration of nucleus and monomorphonuclear cells were not observed. The cadmium has a percentage of 34% hemolysis while human erythrocytes have 0.9% hemolysis in the presence of metal. The blood cells of fish in a 0.33 µg/mL sublethal concentration of cadmium presents morphological changes in erythrocytes, polymorphonuclear and monomorphonuclear cells, besides producing alteration in nucleus and cell membrane rupture. Fish erythrocytes according to hemolysis microassay are statistically more sensitive compared to cadmium human erythrocytes.

150 USEFULNESS OF QUANTITATIVE MICROANALYTICAL STUDY TO EVALUATE CANCELLOUS BONE IN OSTEOPOROTIC PATIENTS

(1) Crespo PV, (1) Sánchez Quevedo, MC, (2) Crespo-Lora V, (1) García JM, (3)CanoJR, (3) Cruz E, (3) Guerado E

(1) Tissue Engineering Group, Department of Histology, University of Granada, Spain. (2) Division of Pathology, University Hospital San Cecilio, Granada, Spain. (3)Division of Traumatology and Orthopedic Surgery, Hospital Costa del Sol, Marbella, Spain

INTRODUCTION: Adult cancellous bone consists of a series of trabeculae of mature lamellar bone. Lamellar bone tissue is hard, and it is considered as a biphasic tissue composed of a mineralized matrix and an organic material. The mineralized matrix component is mostly hydroxyapatite. Scanning electron microscopy (SEM) associated to microanalytical detectors has been suggested as an excellent approach to obtain information on mineralized tissue. The objective of this work is to determine the concentration of calcium and phosphorus in mature lamellar bone corresponding to cancellous bone, both in osteoporotic patients and in normal native bone.

MATERIAL AND METHODS: 20 cancellous bone tissue biopsies were obtained from the femoral head of patients with hip fractures. 10 of these biopsies were diagnosed as normal bone, whereas 10 samples were classified as osteoporotic according to their histological features and the total area corresponding to bone trabeculae. Each sample was analyzed using two representative images obtained by light microscopy at 40X augmentation using the ImageJ1 software. For the microanalytical study, each biopsy was fixed in liquid nitrogen and cryopreserved at -80°C. Then, specimens were washed in 3% H₂O₂ for 24h to eliminate the organic component, air-dried, sputter-coated with carbon in an argon atmosphere (P=0.1 torr) and examined in a FEI Quanta 200 scanning electron microscope (voltage= 15 kV; spot size = 50nm; tilt angle = 35°; take-off angle = 50°) with an EDAX microanalytical detector. Spectra were collected by pin-point electron beam at 40,000X magnification. Ten analyses were taken per specimen. The peak-to background ratio (P/B) method was used to measure the concentrations of calcium and phosphorus in each group of patients. Microcrystalline salt standards were used to quantify Ca and P as described in previous publications. All results were calculated as weight fraction percentage of Ca and P. Statistical comparison was carried out using Student t test.

RESULTS: All spectra showed significant peaks for calcium and phosphorus. Quantitative analyses with the approach described in material and methods showed that the average Ca concentrations for the 100 determinations taken for each study group were 29.39% for normal bone and 29.91% for osteoporotic bone. In turn, the concentrations of P were 11.65% for normal bone and 11.76% for osteoporotic bone. The Ca/P ratio was identical (2.56) for both the normal and the osteoporotic bone. Microanalytical differences were non-significant for the comparison of both bone types -Ca, P and Ca/P ratio-, but the size of the bone trabeculae and area were statistically significant (p=0.00025 and 0.00026, respectively).

CONCLUSIONS: These results reveal that the microanalytical values were similar for the normal bone and the osteoporotic bone, whereas the microscopy analysis showed significant differences between both bone types. Therefore, we hypothesize that different types of bone

may have the same concentration of Ca, P and Ca/P ratio. Microanalysis is a valid method for the study of ionic concentrations in human bone.

ACKNOWLEDGEMENTS: This work was supported by grant SAS PI-0808-2010 from Consejería de Salud y Bienestar Social, Junta de Andalucía, Spain.

NEUROHISTOLOGÍA

29 HISTOLOGICAL CHANGES IN HUMAN DIAPHRAGM MUSCLE IN DEATH BY DROWNING. AN AUTOPSY CASE.

Ruz-Caracuel, I. (1,3); Beltrán, C. (2); Leiva-Cepas, F. (1,3); Agüera, A. (1,3); Jimena, I. (1,3,4); Girela, E. (2); Peña, J. (1,3,4)

(1) Department Morphological Sciences, Section of Histology, Faculty of Medicine and Nursing, University of Córdoba. Spain (2) Section of Legal and Forensic Medicine. Faculty of Medicine and Nursing, University of Córdoba. Spain (3) Research Group in Muscle Regeneration, University of Cordoba. Spain (4) Maimónides Institute for Biomedical Research IMIBIC, Reina Sofia University Hospital, University of Cordoba. Spain

Introduction The determination of the cause and manner of death for a body recovered from the water is hampered by a lack of autopsy findings specific for drowning. In an experimental study we have found the presence of histological changes in skeletal muscles that suggest that death by drowning prompts rhabdomyolysis and rapid anoxia of skeletal muscle. We hypothesized that these changes could be specific of this type of death. In the present communication we showed a human case where we confirmed those findings. **Material & methods** The study was approved by the 'Comisión de Docencia e Investigación del Instituto de Medicina Legal de Córdoba'. Diaphragms muscles from an autopsy case of drowning (case A) and a case of heart attack (case B) were analysed. Case A was an old female 83 y. who committed suicide by drowning in a well. Case B was a middle aged man of 51 y. who suffered a sudden cardiac death, without previous antecedents of cardiomyopathy. Both cases had a similar post-mortem interval (about 20 h). Four independent samples were taken from each muscle, fast frozen in isopentane cooled with liquid nitrogen and sectioned at 8µm in a cryostat. A panel of histological (haematoxylin-eosin, modified Gomori trichrome) and histochemical (oxidative enzymes, PAS, myosin adenosine triphosphatase) techniques were performed. Frequency of changes was counted in nine areas of 0,24mm² per sample at x20 magnification. Some fragments were selected for study using transmission electron microscopy. **Results** While in case B no abnormalities were detected in diaphragm using histological and histochemical techniques, in case A there were changes that consist of the presence of ragged red fibers, whorled fibers and hypercontracted fibers. The frequency of these changes was 0,92± 1,05; 0,36±1,13 and 1,44±1,32 fiber per area, respectively. **Conclusion** Given the fact that changes found in the autopsy case of drowning are coincident with those described in our experimental study, we think that these findings could be useful for forensic diagnosis of suspicious death by drowning. Nevertheless, it would be necessary to increase the number of autopsy cases analysed in order to establish a well documented inference.

30 EVALUATION OF NATALIZUMAB TREATMENT IN EXPERIMENTAL AUTOIMMUNE ENCEPHALOMYELITIS USING SKELETAL MUSCLE HISTOLOGY

Ruz-Caracuel, I. (1,2); Leiva-Cepas, F. (1,2); Aguilar-Luque, M. (3,4); Luque, E. (1,4); Peña-Toledo, M.A. (2); Jimena, I. (1,2,4); Túnez, I. (3,4); Peña, J. (1,2,4)

(1) Department Morphological Sciences, Section of Histology, Faculty of Medicine and Nursing, University of Córdoba. Spain (2) Research Group in Muscle Regeneration, University of Cordoba. Spain (3) Department Biochemistry and Molecular Biology, Faculty of Medicine and Nursing, University of Córdoba. Spain (4) Maimónides Institute for Biomedical Research IMIBIC, Reina Sofia University Hospital, University of Córdoba. Spain

Introduction Experimental autoimmune encephalomyelitis is an experimental model for multiple sclerosis. Although the pathogenic cause resides in central nervous system, there are plenty of peripheral signs and symptoms related to musculature, so that we have previously studied skeletal muscle histology in relation to disease course. We have characterized lesions that can help to monitor disease activity and in the present communication we show effects of natalizumab treatment on skeletal muscle histology. **Material & methods** Experimental autoimmune encephalomyelitis was induced in Dark Agouti rats (n=4) with MOG + Freund's adjuvant. Fourteen days after induction, when first disease signs appeared, natalizumab treatment was started for 24 days. After treatment completion, animals were sacrificed and soleus muscles were excised and processed by freezing for light microscopy and for transmission electron microscopy. Histological and histochemical techniques were performed on cryosections. Lesions were counted per area and the following histomorphometrical parameters were calculated: cross-sectional area, minimum diameter and fiber typing. Results were compared with control groups previously published by us. Image Pro Plus 6.0 and Sigma Stat 3.1 were employed for morphometrical and statistical analysis, respectively. Results Some scattered target and core-targetoid fibers and spot lesions were observed using oxidative techniques. Nevertheless, number of those lesions was lower than in untreated animals. Histomorphometrical parameters were also favorable to Natalizumab treated animals. **Conclusion** Natalizumab treatment ameliorates skeletal muscle histological lesions in experimental autoimmune encephalomyelitis. Skeletal muscle histology is a useful tool to analyze response treatment in this experimental model; further studies should be made comparing other treatment strategies repercussions on these parameters.

81 DIACYLGLICEROL LIPASE α IS LOCALIZED TO NUCLEAR SPECKLES OF ADULT CORTICAL NEURONS

(1) Aretxabala X, (1) García del Caño G, (1) González-Burguera I., (1,2) Montaña M., (1,2) López de Jesús M, (1,2) Barrondo S., (1) Ricobaraza A, (1,2) Sallés J. (1)UPV/EHU (2)CIBERSAM

INTRODUCTION: It is well known that the phosphoinositide cycle coupled to diacylglycerolipase alpha (DAGL α), which is the responsible for the synthesis of 2-arachidonoliglycerol (the most abundant endocannabinoid in the mammalian brain), is located in the neuronal plasma membrane in the mammalian central nervous system. In spite of this fact, the idea of the presence of the same cycle in the neuronal cell nucleus has gained reliability sheltered by the fact that some independent laboratories have already demonstrated the presence here and its importance in some processes like mRNA export, DNA repair and gene transcription of phosphoinositide cycle (biosynthetic and hydrolytic machinery). Another fact is that classical biochemical techniques provided evidence of DAGL α activity in the mentioned cellular compartment. This evidences led us to consider the possibility of the presence of DAGL α in neuronal nucleus. With these facts in mind we directed our research so that we could obtain evidences of the presence of the DAGL α and its importance together with PLC β in the synthesis of the 2-AG in neuronal nucleus.

MATERIALS AND METHODS: To obtain the results in the present work placed, we first performed a centrifugation-based subfractionation to isolate nuclei from other cellular fractions or got sections of 40 μ m wide from previously washed (0.37% sodium sulphide buffer) and fixed (4% PF) from adult rat cortex homogenates. Then we performed experiments of Immunohistochemistry, immunofluorescence and western blotting.

RESULTS: Antibodies against DAGL α c-terminal showed best immunoreaction in previously washed tissue in immunohistochemical assays. After probing a battery of different commercially available antibodies, DAGL α -RbAf380 (Frontier Science) was the one which gave us better immunoreactivity. It marked the protein in a specifically way and in a perinuclear-like pattern in the somatosensorial cortex of sections of Sprague-Dawley adult rats. The tissue was washed with a solution containing 0.37% (w/v) sulphide solution (Sodium Sulphide Washing Buffer) before been fixed with 4% paraformaldehyde solution.

Immunoreactivity augmented in SSWB treated sections of somatosensorial cortex in immunofluorescence assays. Assays were performed in adult rat brain sections washed and without been washed with the SSWB letting us see the improvement of the immunoreactivity due to the pretreatment. DAGL α located apparently in the nuclei and not along the nuclear membrane because they not colocalized.

DAGL α locates in the adult neuronal nuclei in low-cromatin domains. Double immunofluorescence performed in isolated nuclei of adult rat brain showed immunopositivity of DAGL α antibody only in those NeuN (adult neuron marker) positive cells. When the same experiment was performed with DAGL α and Lamin B1 antibodies, we did not see colocalization between them, Lamin B1 antibody always appearing surrounding DAGL α one. The same no-colocalization result was obtained when DAGL α antibody and Hoesch staining (Chromatine marker) were probed together. In contrast, this kind of experiment showed us the colocalization between DAGL α and SC35 (nuclear speckle marker) antibodies.

Western blot assay corroborates the suitability of the subfractionation procedure and the presence of DAGL α in neuronal nucleus in poor chromatine locations. Western blot analysis of isolated nuclei subjected to sequential fractionation and crude membranes (P2) obtained from homogenates of rat brain cortex run in parallel.

Some fraction markers (BiP, NPCx, H3, NeuN/FOX-3) were tested to analyce the suitability of the subfractionation procedure getting a clear band at the expected molecular weight

84 CLASSIFICATION OF CENTRAL AND PERIPHERAL AXONS USING TRANSMISSION ELECTRON MICROSCOPY AND ARTIFICIAL INTELLIGENCE METHODS

(1) De Juan Herrero, J.; (2) David Gil Mendez, D.; (1) Girela López, J.L. ; (2) Azorín López, J., (3) Pérez-Cañaveras, R.M.

Departamentos de Biotecnología (1), Tecnología Informática y Computación (2) y Enfermería (3) Universidad de Alicante, Spain

INTRODUCTION The published articles, related to nerve fibers, have grown progressively from the beginning of XX century, until right now. During this period, about 130,000 papers have been published. 40% of them have been issued during the first 14 years of the XXI century, 78% of them in the last decade. The first works registered in PubMed using morphometric techniques for the axon study is dated in 1969. Since then, the number of articles published about morphometry in nerve fibers, has been around 1,600. The articles published, using morphometric methods, associated with electron microscopy have been around for 400 issues. Finally, we have only found three articles that relate the keywords axon, morphometric and artificial intelligence. The morphometric study of nerve fibers is a useful tool to research several subjects related to the nervous system: development, aging, and pathological conditions in both peripheral and central nerve fibers. These studies have shown the existence of a close relationship between functional aspects of nerve fibers and the morphologic and morphometric parameters (axon and fiber caliber, myelinated, cytoskeletal components, etc.). Here we used Artificial Intelligence (AI) methods to classify optic and cochlear nerve fibers of the rat using morphometric parameters obtained with transmission electron microscopy. The aim of this work is double: (1) to determine the importance of the several morphometric parameters used and clustering of both, optic and cochlear nerve fibers. (2) to determine what are the most efficient axonal parameters capable to discriminate between central (optic nerve) and peripheral (cochlear nerve) nerve fibers. **MATERIAL AND METHODS** Adult Wistar rats were anesthetized, transcardially perfused and its optic and cochlear nerves removed and processed for ultrastructural microscopy studies. Axons were analyzed with a computer-linked planimeter. Several parameters were obtained for each axonal cross-section, using a computer program: axon diameter, myelin sheath thickness, G-Ratio, microtubule number (Mtn), neurofilament number (Nfn) and R-proportion ($R = Nfn/[Nfn+Mtn]$). Data were processed with a set of AI methods, to improve the distinction between nerve fibers from optic and cochlear nerves. We use two supervised techniques, Multilayer Perceptron (MLP) and Decision Trees (DT), and an unsupervised one, K-Means clustering. All the computations of the decision tree were developed using the WEKA software (Machine Learning Group at the University of Waikato). **RESULTS** The supervised methods classify the type of nervous fibers whereas the unsupervised ones divide different kinds of fiber within the optic and cochlear nerves in clusters. The AI methods achieve a high accuracy, being MLP slightly more exact (around 2% more, in general) than DT. The K-Means clustering is also tested by checking the correct classification and prediction of these groups, with excellent results, in many cases with accuracy very close to 100%. **CONCLUSIONS** This work contributes with the AI methods to create nerve fiber clusters (unsupervised methods) and decision tree (supervised methods) to make the results more visible and easy to interpret.

OTROS

1 RELATIONSHIP OF A METASTASIS SUPPRESSOR GENE AND TWO MARKERS OF THE IMMUNE SYSTEM IN BREAST CANCER.

(1) Durán Mateos, E.M; (2) Reina Perticone, M.A; (3) Cárdenas Rebollo, J.M; (1) Arriazu Navarro, R.

(1) Department of Basic Medical Sciences, School of Medicine, CEU-San Pablo University, Madrid, Spain. (2) Department of Anesthesiology, Madrid-Montepíncipe University Hospital, Madrid, Spain. (3) Department of Quantitative Methods, School of Pharmacy, CEU-San Pablo University, Madrid, Spain.

Nm23 is a metastasis suppressor gene whose downregulation promote metastatic progression. Many reports suggest that cancer development is controlled by the host immune system, underlying the importance of including immunological biomarkers for the prediction of prognosis and response to therapy. The aim of this study was to investigate the expression of Nm23 in breast carcinomas and its relationship with tumor microenvironment through immune system markers, CD8 a marker of cytotoxic T lymphocyte and CD 68 a tumor-associated macrophages marker (TAM). A retrospective study was done with 200 breast cancer patients in early stages of disease. Nm23, CD8 and CD68 protein expressions were evaluated using immunohistochemistry. Image analysis was used to determine: the area of immunopositive epithelial cells to Nm23 marker and the number of CD8+ and CD68+ cells. The mean \pm SE was calculated. Cases were divided into two groups: Nm23+ and Nm23-; the differences among groups were evaluated using ANOVA test. Numbers of T CD8+ cells were increased when Nm23 was present while the number of macrophage CD68+ cells were increased when Nm23 was absent. It has been demonstrated that CD8+ patients are significantly associated with improved survival, which means that such cells has tumor inhibitory effect when are present in the microenvironment. Nevertheless, TAM recruitment changes the tumor microenvironment, and that includes the enrichment of cytokines and growth factors that can stimulate the proliferation of malignant cells; that may have effects in tumor progression, increasing the risk of metastasis. Therefore, Nm23 loss could be associated with a more favorable environment for the development and dissemination of breast cancer. Our results suggest that Nm23 could be a role on the immune system. However, more studies are needed to determine this association. Acknowledgments: This study was supported by financial grant from San Pablo-CEU University and Santander Bank (USP-BS-PPC04/2011).

154 ULTRASTRUCTURAL MODIFICATIONS OF BOVINE OOCYTES MATURED UNDER

(1) Hernández Garduño S., (1) Lara Palma I., (2) Cote Vélez M. A., (3) Viguera Villaseñor R. M., (4) Córdova Izquierdo A., (5) Cornejo Cortés, M.A., (1) Juárez Mosqueda M. L.

(1) FMVZ–UNAM; Departamento de Morfología (México, Distrito Federal), (2) IBT-UNAM; Fisiología Molecular (México, Morelos), (3) INP; Biología de la Reproducción (México, Distrito Federal), (4) UAM-Xochimilco; Departamento de Producción Agrícola y Animal (México Distrito Federal), (5) FES-CUAUTITLÁN-UNAM; Departamento de Ciencias Biológicas (México, Estado de México)

INTRODUCTION: Heat stress is considered an important factor in the reduction of fertility of bovine cattle. The *in vitro* increase of temperature (40-42°C) during oocyte maturation has been related to changes that affect its growth potential, like the variations in the function of the cumulus cells, the cytoplasm and the chromatin configuration. Considering that during stress, large amounts of glucocorticoids are produced, it has been proposed that they could be mediating the response to temperature changes, and that these events can influence the appropriate oocyte maturation. To our knowledge there are no studies focused on the direct effect of glucocorticoids on the ultrastructure of cow's oocytes. The main objective of this investigation was to determine if glucocorticoids affect the ultrastructural maturation of bovine oocytes subjected to heat stress. **MATERIALS AND METHODS:** Bovine oocytes were matured at a physiological temperature of (38.5°C) and at (41°C) to produce heat stress. Oocytes were incubated with the presence of a synthetic glucocorticoid (dexamethasone) and dimethyl sulfoxide (DMSO) as a vehicle, at a concentration of 10^{-7} M for 24 hours. After the *in vitro* procedure the oocytes were immediately fixed and processed for transmission electron microscopy (TEM). **RESULTS:** TEM revealed that bovine oocytes that underwent heat stress, the controls, DMSO and dexamethasone groups, showed loss of integrity of the cumulus cells with damage to its nuclear and cytoplasmic ultrastructure. In regards to the oocyte ultrastructure, numerous vacuoles were seen in the ooplasm, giving rise to the formation of large empty spaces. Electron dense material was also seen as well as alterations in the mitochondria, which were found in the cell periphery. Oocytes matured under physiological conditions (38.5°C) showed an adequate ultrastructure, including the ones incubated with dexamethasone. **CONCLUSIONS:** The results obtained in the present study seem to indicate that glucocorticoids have little or no influence during bovine oocyte maturation when cultured under heat stress (41°C), since the observed ultrastructural changes seem to be more related to the effects of temperature and possibly to the incubation time (24hours).

This work was supported by DGAPA-UNAM: PAPIIT IN215012

SESIONES DE PÓSTER

BIOLOGÍA REPRODUCTIVA

14 COLLECTION, EVALUATION AND FREEZING OF ADULT SPERM ANTILOPE (*Addax nasomaculatus*) FROM ZOO-PARK LECOCQ OF MONTEVIDEO, URUGUAY. (1) Calvo-Marin, J., (3) Modernell-Mateu, A., (2) Elordhoy-Rodriguez, D., (3) Tavares-Lusiardo, E., (1) Robert-Zelmano wicz, D., (1) Viqueira-Pazos, M., (1) Lombide-Bossio, P.

(1) Área Histología y Embriología, Facultad de Veterinaria, Montevideo, Uruguay. (2) Área Teriogenología, Facultad de Veterinaria, Montevideo, Uruguay. (3) Zoo-Parque Lecocq, Intendencia Municipal de Montevideo, Uruguay.

INTRODUCTION: *Addax nasomaculatus* is a species of African antelope found in the list of threatened and endangered by the International Union for Conservation of Nature and Natural Resources (IUCN). Currently, only less than one hundred animals live in freedom, limiting its presence to the national park in Morocco and some zoo specimens. In Zoo Park Lecocq from Montevideo-Uruguay we found the South America larger captivity population, the third in number after Texas and San Diego in the United States. The authorities and veterinary professionals of Zoo Park have been making efforts to increase the number of individuals performing a reproductive management which could give sufficient variability antelope populations. Currently Faculty of Veterinary Medicine professors and veterinarians from Zoo Park Lecocq established a framework of cooperation for the preservation of gametes of this and other endangered species. In this work, preliminary data on the evaluation of male reproductive antelopes are presented. The aim of this work was the procurement, testing and freezing of adult semen antelope (*Addax nasomaculatus*).

METHODS AND MATERIALS: In the facilities of the Zoo Park de Montevideo-Uruguay Lecocq semen was obtained by electroejaculation stimulation from three adult male antelope. Semen obtained was diluted 1: 1 in semen extender refrigerated at 4°C and transferred to the laboratory of Histology and Embryology, Faculty of Veterinary Medicine for evaluation and subsequent freezing. Primary evaluation of volume, mass motility (on a scale of 1 to 5) and single motility and vigor was performed. The concentration by counting in heamocytometer, total number of sperm, viability test using the eosin-nigrosine dye and morphological examination (percentage of abnormalities) were made from a sample, keeping the rest of the semen in the refrigerator to complete the cooling at 4°C for two hours. The freezing of semen was done in 0.25 ml straws which were loaded, sealed and cooled in nitrogen vapors for thirty minutes. Later they were identified and preserved in liquid nitrogen container to -196°C.

RESULTS: The variables measured in semen analysis are given in Table I

CONCLUSIONS: First, it is significant that the animals have responded well to manipulation and extraction protocol semen given its wild nature. Second it is distinguished that the primary evaluation and semen freezing using standardized protocols for other species of the family *bovidae* have shown acceptable preliminary data that not only validate the methodology but encourage us to continue working with this species because of their status of animals in captivity and danger of extinction.

Table I: Semen analysis of *Addax nasomaculatus*

Male	Volume (ml)	Mass motility	Single motility and vigor	Concentration (mm ³)	N° of zoids	Viability (%)	Morphologic exam (% abnormalities)
1	7	4/5	80% - 4/5	40.000	2.380 x 10 ⁶	70	50 (head and tail)
2	3,8	3/5	50% - 4/5	240.000	1.642x 10 ⁶	95	62 (cytoplasmic droplet)
3	1,6	4/5	80% - 4/5	730.000	745x10 ⁶	80	45 (head and tail)

39 ZP2 BEADS: DESIGN OF A NEW TOOL TO STUDY THE MOLECULAR MECHANISMS OF SPERM-OVOCYTE INTERACTION

(1) Canha A., (2) Zamorano L., (2) Algarra B., (2) Aviles M., (1) Romar R., (3) Olivares M.C., (2) Jimenez-Movilla M.

(1) Departamento de Fisiología, Facultad de Veterinaria, 30071 Campus Espinardo, \"Campus Mare Nostrum\". IMIB (Instituto Murciano de Investigación Biomédica). Universidad de Murcia. Murcia. IMIB. España. (2) Departamento de Biología Celular e Histología, Facultad de Medicina, Universidad de Murcia. IMIB. España (3) Departamento de Bioquímica y Biología Molecular, Facultad de Medicina, Universidad de Murcia. IMIB. España

INTRODUCTION: The oocyte is encapsulated by a filamentous structure composed of several glycoproteins termed zona pellucida (ZP), which acts as a matrix that mediates interaction of the sperm (1). It has been shown that processing of ZP2 at N terminal position (LADEN) mediates recognition between gametes (2, 3). The study of these molecular mechanisms is very limited due to the human oocytes ethical problems, the difficulty of obtaining mature oocytes in many mammalian species, the high cost of genetically modified mice and the inability to transfer this knowledge to other species such as swine and human [4]. Therefore, we propose a novel in vitro model that mimics the oocyte shape, allowing the research on the interaction of gametes, identification and characterization of the structure of ZP2 and the conditions for sperm recognition. In this work, the proposed model is developed by combining magnetic beads conjugated with ZP2 recombinant protein. This novel model besides increasing our knowledge of the sperm-oocyte interaction could also be industry-wide implemented as an evaluator of mammalian sperm quality.

MATERIALS AND METHODS For this study were designed two different conformation of porcine ZP2 protein. ZP2N and ZP2C recombinant proteins were marked with a Flag tag recognition on N- and C-terminal position, respectively, to identify the role of each protein region on sperm-oocyte interaction. These recombinant proteins were also marked with a histidine tag for easy identification and adhesion to the His Mag Sepharose Ni magnetic beads. These proteins were expressed in mammalian cells (CHO). Secreted proteins were identified by electrophoresis and western blot. The secreted recombinant proteins were conjugated with His Mag Sepharose Ni magnetic beads. The efficiency and stability of this adhesion were evaluated over time by western-blot and confocal analysis.

RESULTS: Secreted proteins ZP2N and ZP2C were identified by electrophoresis and western blot with Anti-Flag antibody. The ZP2C showed a molecular weight of 100 kDa and ZP2N displayed two different sizes: 100kDa and 75kDa. This can be explained because the processing site LADEN is located in N-terminal region. The recombinant proteins efficiently secreted were conjugated with His Mag Sepharose Ni magnetic beads. We observed an efficient adhesion of proteins to the beads by confocal microscopy and by western blot. This adhesion is stable overtime.

CONCLUSIONS: A novel in vitro model that mimics the three dimensional morphology of the oocyte, combining magnetic beads with ZP proteins (i.e. ZP1-4) was developed in order to study the role ZP2 protein on sperm-oocyte interaction. Future studies will be performed in order to incubate this model with sperms, which will increase our knowledge of the oocyte-sperm interaction and could be also implemented as an in vitro selection and quality evaluation technique of potentially fertile mammalian spermatozoids.

This work was funded by Seneca Foundation "Young Leaders in Research 2013"

40 CRYOPRESERVATION OF TAIL EPIDIDYMIS SEMEN FROM YOUNG ANTELOPE (*Addax Nasomaculatus*) OF ZOO-PARK LECOCQ OF MONTEVIDEO-URUGUAY.

(1) Calvo-Marin, J., (3) Modernell-Mateu, A., (2) Elordhoy-Rodriguez, D., (3) Tavares-Lusiardo, E., (1) Robert-Zelmanowicz, D., (1) Viqueira-Pazos, M., (1) Lombide-Bossio, P

(1) Área Histología y Embriología, Facultad de Veterinaria, Montevideo, Uruguay. (2) Área Teriogenología, Facultad de Veterinaria, Montevideo, Uruguay. (3) Zoo-Parque Lecocq, Intendencia Municipal de Montevideo, Uruguay.

INTRODUCTION: Sperm cryopreservation is an important reproductive biotechnology, which seeks to promote the conservation of male germplasm indefinitely. However, the cryopreservation process results in the decrease in fertility when compared to fresh semen. The cooling curve type used during freezing has direct influence on the degree of cell damage. The traditional way of freezing semen is a biotechnology widely used in the field of reproduction. The *postmortem* sperm retrieval is important for the preservation of male germplasm from animals with high zootechnical value who may die unexpectedly; this procedure is also considered an important tool in the use of sperm from endangered animals. In this work, using standardized protocols for freezing male gamete of species of *bovidae* family, preliminary data

is presented from the cryopreservation of *Addax nasomaculatus* semen, a species of African antelope found in the list of threatened and endangered species present extinction by the International Union for Conservation of Nature and Natural Resources (IUCN). The aim of this work was the procurement, testing and cryopreservation of tail epididymal sperm of a young antelope from Zoo-Park Lecocq of Montevideo Uruguay.

METHODS AND MATERIALS: A pair of epididymis of young antelope, who had an accident and failing to respond favorably to the treatments used, must be slaughtered according to the rules of bioethical handling under the Uruguayan legislation in force. Epididymis tails were isolated from the testes, washed in Petri dish and sectioned with a scalpel. A preliminary evaluation was performed of volume, motility mass (on a scale of 1 to 5), single motility and vigor of semen obtained, which was diluted and refrigerated at 4°C subsequently transferred to the laboratory of Histology and Embryology, Faculty of Veterinary Medicine. The conventional method of freezing was done and the semen was packed in 0.25 ml straws. These were cooled in liquid nitrogen vapor by placing them on a metal grid in a polystyrene box with nitrogen at a distance of 6 cm from the liquid surface for thirty minutes. Then straws were identified, immersed and preserved in liquid nitrogen container to -196°C.

RESULTS: The results of the semen primary evaluation are shown in Table I.

CONCLUSIONS: The tail of the epididymis is storage of sperm before ejaculation, allowing these cells to remain viable and mobile for several weeks. This region has accumulated a sufficient number of sperm for several ejaculations, what becomes a source of germplasm, yet little explored in species of wild *bovidae* family. These preliminary data may be considered acceptable and validate the methodology, encouraging us to continue working with this species because of their status of animals in captivity and in danger of extinction.

Table I: Semen analysis from *Addax nasomaculatus* epididymal tail

Volume (ml)	Mass motility	Single motility	Vigor	Morphologic exam (% abnormalities)
0,05	3/5	70-80%	4/5	50% (loose heads, tails, cytoplasmic droplet)

42 CAN THE INTRATESTICULAR INJECTION OF ANTIBODIES BE AN ALTERNATIVE TO THE PRODUCTION OF KNOCKOUT MICE?

(1)Bizkarguenaga M., (1)Gianzo M., (1)Gómez-Santos L., (2)Madrid J.F., (3) Díaz-Flores L, (1)Sáez F.J. and (1)Alonso E.

(1)Department of Cell Biology and Histology, UFI 11/44, School of Medicine and Dentistry, University of the Basque Country UPV/EHU, Spain. (2) Department of Cell Biology and Histology, School of Medicine, University of Murcia. Spain. (3) Department of Anatomy, Pathology, Histology and Radiology, University of La Laguna (Tenerife), Spain.

Introduction Globozoospermia is characterized by sperm cells with round heads and a defective acrosome. Anomalies in only one gene, as *gopc* can produce globozoospermia. *Gopc*-/-

knockout mice have round spermatids and sperm cells, showing a deficient fusion of proacrosomal vesicles and a lot of vesicles between the Golgi apparatus and the nucleus. Production of knockout mice may be difficult, because deletion of a gene in all the cells can produce severe disorders or dead, thus to develop new methods to inhibit a protein only in spermatogenic cells to obtain globozoospermic sperm cells will be welcome. The objective of this work was to develop a new method to obtain globozoospermic sperm cells by microinjection of an anti-GOPC antibody in the seminiferous tubules of mouse testis. The testes were analyzed to confirm the presence of globozoospermic cells, acrosomal proteins were identified by means of immunohistochemistry and their localization was compared with wild type and knockout *Gopc*^{-/-} mice. Methodology and materials An anti-GOPC antibody (1 µg in PBS and 0.5% w/v bromophenol blue) was microinjected into the seminiferous tubules of a testis from each mouse. The contralateral testis of each mouse was microinjected with the same quantity of PBS and bromophenol blue. Thirty five days after injection, testes were dissected and fixed in Bouin solution and embedded in paraffin and 4 µm thick sections were obtained. Histological sections from microinjected, knockout *gopc*^{-/-}, and non-microinjected wild type mice were stained with haematoxylin and eosine to analyze the presence of globozoospermic cells. Other sections were processed with Schiff periodic acid (PAS) stain to analyze the presence of the glycoconjugates in the acrosome of spermatids. Some sections from microinjected, knockout *Gopc*^{-/-}, and non-microinjected wild type mice were analyzed by immunohistochemistry using specific antibodies to Sp56, GCNF and FNDC3A, to localize the distribution of these proteins in spermatids. Results The only difference observed by histological analysis of testes from microinjected, wild type and knockout mice was the presence of globozoospermic spermatids in knockout *Gopc*^{-/-} (100% of the seminiferous tubules) and microinjected testis (50% of the seminiferous tubules). PAS staining showed most of the glycoconjugates in the acrosome of spermatids in wild type testes, but a disperse distribution of glycoconjugates in spermatids of microinjected testes similar to that of knockout, due to dispersed proacrosomal vesicles. The analysis of acrosomal proteins Sp56, GCNF and FNDC3A showed a localization of these proteins similar to that observed with PAS staining: the proteins were located in the acrosome of wild type spermatids, but disperse in small proacrosomal vesicles in the globozoospermic spermatids of both knockout and microinjected mice. Conclusions Microinjection of an anti-GOPC antibody into the seminiferous tubules of mouse testis produce spermatids with a globozoospermic phenotype and disrupts the formation of the acrosome in this cells, in a similar way as occurs in *Gopc*^{-/-} knockout mice. These results show that intratesticular microinjection of antibodies in mouse testis could be an alternative to knockout mice, and a useful tool to study spermiogenesis. Acknowledgements Supported by UPV/EHU (GIU09/64 and UFI 11/44), and Basque Government (SAIOTEK S-PE12UN010). The GOPC knockout mouse (No. RBRC01253) was provided by the RIKEN BRC, Japan.

89 HETEROGENEITY OF MESENCHYMAL CELLS IN THE HUMAN AMNIOTIC MEMBRANE

(1) Cortes*, S., (2) Insausti, C.L., (1) Seco-Rovira. V., (1) Beltrán-Frutos, E., (2) García-Bernal D, (2) Blanquer, M., (1) Ferrer, C., (1) Hernández- Martínez, J., (2) Moraleda, J.M., (1) Pastor, L.M.

(1)Department of Cell Biology and Histology, School of Medicine, IMIB-Arrixaca, University of Murcia. Regional Campus of International Excellence. Campus Mare Nostrum. University of Murcia.30100. (2)Unidad de Terapia Celular. Servicio de Hematología. Hospital Universitario Virgen de la Arrixaca (HUVA). IMIB-Arrixaca.

Introduction: The capacity to culture epithelial and mesenchymal cells from amniotic membrane (AM) and their peculiar immune privilege has stirred the regenerative medicine field. Recently, some authors have considered that there is a degree of heterogeneity in mesenchymal cells. This communication aims to morphologically discriminate different types of mesenchymal cells in human AM. Material and Methods: AM from placentas at 39 weeks of gestation were processed for conventional light microscopy, carbohydrate histochemistry, lectin histochemistry, immunohistochemistry, and transmission electron microscopy study (TEM). Also a semiquantitative study was made by light and electron microscopy. Results: Three types (I, II, III) of mesenchymal cell were characterized by conventional light microscopy. However, in semithin sections, a fourth type (IV, Hofbauer cell) was observed. The cytoplasm of mesenchymal cells was PAS positive; increasing gradually the positivity from type I to type III. A similar staining pattern was observed with the Concanavalin-A lectin. Several growth factors were identified in the cytoplasm of these cells: VGF, TGF- β 2, PDGF-C, FGF-2, this positivity gradually increased from Type I to Type III cells. Similarly these mesenchymal cells also showed an increase of positivity from type I to type III for fibronectin, vimentine and connexin 43. Ultrastructurally, it was possible to characterize four types of mesenchymal cells and Hofbauer cell. Semiquantitatively by light microscopy, type II cells were significantly more numerous than those of type III, both being significantly more numerous than type I and IV. By TEM, type III cells were significantly more frequent than the other types. Type I and II cells were less frequent. Conclusions: a) It was possible to morphologically characterize heterogeneity in the population of mesenchymal cells from human amniotic membrane; b) such cellular heterogeneity is in relation with a higher synthesis of diverse growth factors and extracellular matrix proteins; c) it is very likely such heterogeneity implies a gradual differentiation of the population of mesenchymal cells into fibroblasts. Financed: 04543/GERM/06, 04542/GERM/06. Fundación Seneca. CARM. *Becario de colaboración del Ministerio de Educación, Cultura y Deporte 2014-15.

90 DEATH OF SERTOLI CELLS BY APOPTOSIS IN SYRIAN HAMSTER (MESOCRICETUS AURATUS) IN NORMAL PHYSIOLOGICAL CONDITIONS.

(1) Seco-Rovira V, Beltrán-Frutos E, Martínez-Hernández J, Quesada-Cubo, V., Ferrer C, Pastor LM

(1) Department of Cell Biology and Histology, School of Medicine, IMIB-Arrixaca, University of Murcia. Regional Campus of International Excellence. Campus Mare Nostrum. University of Murcia. 30100. bioetica@um.es.

Introduction: It is known that Sertoli cells, the somatic cells of the seminiferous epithelium, vary in number during postnatal development, while they are considered as quiescent and fully differentiated in adults, where their numbers remain constant. In the Syrian hamster

(*Mesocricetus auratus*), Sertoli cell death by apoptosis was observed during testicular regression. This observation led us to wonder whether Sertoli cells suffered a similar fate in the adult Syrian hamster during the breeding season. **Material and Methods:** For this purpose, nine 6-month-old Syrian hamsters under a photoperiod of 16:8h light-dark were used. The testes were removed and processed for light microscopy study (H&E, TUNEL and vimentin immunohistochemistry) and an index of Sertoli cells in apoptosis was determined. **Results:** The qualitative results identified some H&E Sertoli cells with a clearly altered morphology. Using the TUNEL histochemical technique, TUNEL + cells were observed in basal position of the seminiferous epithelium with morphology similar to that of Sertoli cells. By means of vimentin immunohistochemistry in the same histological sections, these TUNEL + cells were confirmed to be apoptotic Sertoli cells. The apoptotic index of Sertoli cells was $0.86 \pm 0.12\%$. **Conclusions:** These findings confirm that in the Syrian hamster the Sertoli cell is not a totally quiescent cell and that it undergoes cell death by apoptosis during adulthood. Moreover, this apoptotic index is lower than that found during the early phases of testicular regression. Finally, this observation suggests the existence of a cellular mechanism that would explain the age-related loss of Sertoli cells that has been observed in several species of mammal. **Financed:** 04543/GERM/ 06 and 04542/GERM/ 06. Fundación Seneca. CARM.

95 ULTRASTRUCTURAL CHANGES IN LEYDIG CELLS OF SYRIAN HAMSTER DURING TESTICULAR REGRESSION DUE TO EXPOSURE TO SHORT PHOTOPERIOD (1) Beltrán-Frutos, E., Seco-Rovira, V., Martínez-Hernández, J., Ferrer, C., Pastor, L.M.

(1) Department of Cell Biology and Histology, School of Medicine, IMIB-Arrixaca. Regional Campus of International Excellence. Campus Mare Nostrum. University of Murcia. 30100

Testicular regression occurs in the Syrian hamster exposed to a short photoperiod. The Leydig cell population decreases and ultrastructural changes are associated with the decreased production of testosterone. The aim of our study was to analyze the ultrastructure of Leydig cells throughout the period of regression. For this a transmission electron microscopy study was made of the testicular interstitium in states of middle regression (MR), strong regression (SR) and total regression (TR). During testicular regression, 3 types of Leydig cell could be differentiated ultrastructurally: normal, necrotic and involuted. In the MR stage, normal, involuted and necrotic Leydig cells could be seen, the last mentioned being the most numerous. In the SR and TR stages most Leydig cells were characterized by a smaller nucleus and cytoplasm, and fewer organelles related with testosterone synthesis (involved). In conclusion, the different ultrastructure of Leydig cells observed during testicular regression differentiates 3 types of the same in the testicular interstitium: normal, necrotic and involuted. The decrease in the Leydig cell population suffering testicular interstitium after exposure to short photoperiod mainly takes place at the start of regression (MR), probably as a result of the increase in necrotic cells observed in this study. **Financed:** 04543/GERM/ 06, 04542/GERM/ 06. Fundación Seneca.

96 CHANGES IN THE PRESENCE OF GAP JUNCTIONS BETWEEN LEYDIG CELLS DURING TESTICULAR REGRESSION AFTER EXPOSURE TO SHORT PHOTOPERIOD IN THE SYRIAN HAMSTER

(1) Beltrán-Frutos, E., (1) Llor-Alcazar, D., (1) Seco-Rovira, V., (1) Martínez-Hernán dez, J., (1) Ferrer, C., (2) Canteras, M., (1) Pastor, L.M.

(1)Department of Cell Biology and Histology and (2) Department of Statistic. School of Medicine, IMIB-Arrixaca. Regional Campus of International Excellence. Campus Mare Nostrum. University of Murcia. 30100

Gap junctions are a means of direct intercellular communication between Leydig cells. These junctions appear to be modified with changes in steroidogenesis in Leydig cells. The Syrian hamster undergoes testicular involution accompanied by reduced steroidogenesis after exposure to short photoperiod. Therefore our aim was to make a semiquantitative study of the expression of connexin 43 protein present in the Gap junctions during testicular regression to check the possible changes in the same. For this, 17 Syrian hamsters were divided into 4 groups: control (C), middle regression (MR), strong regression (SR) and total regression (TR). The presence of connexin 43 was detected immunohistochemically, and a semiquantitative study was made of their positivity (number of GAP junctions relative to number of Leydig cells observed). Data were analyzed statistically. The control group had a higher number of junctions per number of Leydig cells than the TR group ($p < 0.05$). No other significant differences were observed. In conclusion, the lower number of Gap junctions in the TR group compared with group C may be related to the decreased in testosterone synthesis by Leydig cells in regression. Furthermore, the fact that there was no significant decrease in the number of junctions in the MR and SR groups suggests that only when the testis is in an advanced state of regression and steroidogenesis has been greatly reduced, is intercellular communication among Leydig cells considerably reduced. Financed: 04543/GERM/ 06, 04542/GERM/ 06. Fundación Seneca. CARM

99 TESTIS TISSUE AND GENE EXPRESSION ALTERATIONS IN ADULT MICE INDUCED BY ZEARALENONE.

(1)García-Suárez, M.D, (1) Mora-Ramiro, G., (1) Peña-Corona, S.I., (1) Gaona Domínguez, S., (2)Pérez Martínez, M., (1)Gómez Olivares, J.L.,(1) Serrano, H.

(1)Universidad Autónoma Metropolitana-Iztapalapa, CBS; (2) Universidad Nacional Autónoma de México, FMVZ

INTRODUCTION. Xenoestrogens are compounds that alter the physiological function exerted by endogenous steroid hormones, mainly those involved in reproduction. One major group of natural xenoestrogens is the phytoestrogens or plant-derived estrogen-like regulators. Whereas most phytoestrogens are produced through the secondary higher plant metabolism, others are toxins made by Fungi, as is the case of Zearalenone. Ingestion is the usual exposure via to phytoestrogens and mycoestrogens and most plant and fungus-exposed foods are prone to have important amounts of estrogen disruptors. The goal of the present work is to evaluate the effect of oral zearalenone treatment on the general architecture of adult mice testis, and the relative gene expression of their isolated Leydig and Sertoli cells.

MATERIAL AND METHODS. Twenty adult mice were distributed in control group or three experimental groups. Along 4 weeks, the experimental groups received a daily oral dose of 10, 20 or 40 µg/Kg body weight of zearalenone or vehicle. After treatment, testes were dissected. Right testis was fixed in PBS formalin, dehydrated, paraffin included, and 5 µm slices were obtained. Masson's trichrome stain was used for sample processing. Left testes were minced in Krebs-Ringer-Glucose solution and small fragments were collagenase digested. After a Ficoll gradient sedimentation, interstitial and tubule fractions were obtained. Leydig cells were obtained through a 13% Ficoll column whereas Sertoli cells were obtained after pancreatin digestion and separated as the 4 and 5% fractions of a 2 to 6% sucrose gradient column. RNA from Leydig and Sertoli was isolated with Silica membrane spin columns. Similar amounts from all treatments were used for cDNA synthesis and amplification for aromatase, αER, βER, and βActin as endogenous gene. Amplified material was analyzed and relative expression was obtained.

RESULTS. Histological analysis showed severe alterations in testes from treated animals when compared to control mice. Tubule diameters from treated animals were significantly reduced ($220 \pm 2 \mu\text{m}$) than control animals ($290 \pm 2 \mu\text{m}$). The area covered by the germinative epithelium was reduced from $2.2 \pm 2 \times 10^3 \mu\text{m}^2$ in control animals to $1.4 \pm 2 \times 10^3 \mu\text{m}^2$ in either three treatments. As a consequence of the zearalenone treatment, the area covered by the tubular component was reduced to 65% of the control group. No sperm cells were observed in the tubular lumen from treated animals although all the differentiation steps germinal epithelium cells can be detected. Leydig cells were also reduced in treated animals. Aromatase and ERα expression was reduced in zearalenone treated animals.

CONCLUSIONS. Oral xenoestrogens have now been considered as a major public health concern attending their negative effects on reproduction. Adult male mice treated with low doses of zearalenone show an organismic impairment in fertility potential. Reduction of the seminiferous tubule, and the area of the germinal epithelium drastically affect sperm production at doses as low as 10 µg/kg body weight. At the molecular level, the induction of βER in both Leydig and Sertoli cells indicate that these effects are through the interaction of zearalenone with this type of ligand-dependent transcription factor.

107 IMMUNOHISTOCHEMICAL EVALUATION OF HYPOXIA IN THE PORCINE OVIDUCT AND UTERUS WITH THE EXOGENOUS MARKER PIMONIDAZOLE

(1) Lorenzana Canales, J., (1,2) Gutiérrez Trujillo, H. A., (1) Ayala, M^a D., (1) Latorre Reviriego, R., (3) Morcillo Martín, E., (3) Soria Gálvez, F., (1) López Albors, O.

(1) Dept. Anatomy & Comparative Pathology, Faculty of Veterinary Science, International Excellence Campus for Higher Education and Research "Campus Mare Nostrum", University of Murcia, Murcia, Spain. (2) Dept. Animal Health, Faculty Veterinary Medicine, University National of Colombia. (3) Minimally Invasive Surgery Center Jesús Usón, Ctra. N 501 SN, 10071 Cáceres, Spain

INTRODUCTION. Pimonidazole is an exogenous marker broadly used in mammals to characterize the tissue oxygen gradients by immunohistochemical techniques. It has been established that pimonidazole binds to cells in severe hypoxic conditions lower than 10 mmHg oxygen pressure. In the female reproductive organs regulation of oxygen levels has proved crucial for the optimal development of oocytes and the survival and quality of the embryos. In a previous work where pimonidazole binding to the female reproductive tract has been evaluated (rat, Gillies et al. 2011, J. Mol. Hist. 42:341-354), different staining was observed for certain cell types and organs. In this work pimonidazole was used in pre-pubertal and mature pigs to reveal hypoxic areas in the uterine tube (oviduct) and uterus. **MATERIAL AND METHODS** Three pre-pubertal pigs (40-56 Kg), two gilts (90-105 Kg) and one sow (230 Kg) were used. According to visual inspection of the ovary the gilts and sow were at peri-ovulatory stage. After anaesthesia all pigs were intravenously injected 0.3-0.5 g/m² body surface of pimonidazole (Hypoxyprobe, Inc®). All specimens belonged to parallel studies where the reproductive organs were not manipulated and according to their protocols pigs were euthanized at the end of the study. Samples of the oviduct ampulla, ampulla-isthmic junction, isthmus and uterine horn were fixed in 4% paraformaldehyde, and then processed for paraffin embedding, sectioned and finally incubated with the primary monoclonal antibody anti-pimonidazole (FITC-Mab, Hypoxyprobe, Inc®). Anti-FITC-Mab (Hypoxyprobe, Inc®) secondary antibody and diaminobenzidine were used to visualize positive staining. Two authors independently evaluated the staining intensity as none (-), weak (+), moderate (++) and strong (+++). **RESULTS** In the uterine tube different staining between pre-pubertal and sexually mature pigs (gilts and sow) was observed. While in pre-pubertal pigs hypoxic areas were hardly observed, in sexually mature pigs the intensity and extension of staining was higher. On those mature pigs moderate to strong staining was currently found in the oviduct epithelium, weak to moderate in the lamina propria and no staining in the muscularis. In the uterus, independently of the sexual maturity, the staining was always strong in the epithelium and endometrial glands, but moderate in the myometrium and absent in the endometrial stroma. **CONCLUSIONS.** For the first time the exogenous hypoxia marker pimonidazole allowed visualizing highly hypoxic areas in the porcine uterine tube and uterus. The epithelium was always the most hypoxic layer. While in the uterine tube the staining pattern for hypoxia was not achieved until the onset of puberty, in the uterus it was independent of the pig's sexual maturity. This work was funded by project AGL2012-40180-C03-03 (Ministerio de Economía y Competitividad).

108 SELECTION OF MORPHOLOGICALLY NORMAL SPERM WITHIN THE PORCINE UTERUS

(1, 2) Hernández-Caravaca, I., (3, 4) Izquierdo-Rico, M.J., (1, 4) Matás, C., (1, 4) Soriano-Úbeda, C., (1) Abril-Sánchez, S., (5) Gutiérrez Trujillo, H.A, (1, 4) García-Vázquez, F.A

(1) Department of Physiology, Faculty of Veterinary Science, International Excellence Campus for Higher Education and Research “Campus Mare Nostrum”, University of Murcia, Murcia, Spain, (2)Boehringer-Ingelheim S.A., Barcelona, Spain. (3)Department of Cell Biology and Histology, Faculty of Medicine, International Excellence Campus for Higher Education and Research “Campus Mare Nostrum”, University of Murcia, Murcia,

Spain. (4) Institute for Biomedical Research of Murcia (IMIB-Arrixaca), Murcia, Spain. (5)Dept. Animal Health, Faculty Veterinary Medicine, University National of Colombia.

Introduction: After sperm deposition within the uterus through natural or artificial insemination (AI), billions of sperm begins a competition looking for the oocyte. Of the total of sperm deposited, only few of them are able to reach the place where the fertilization occurs, the oviduct. The influx of polymorphonuclear neutrophils and the backflow (reflux of the semen out of the sow after insemination) are two of the known mechanism by which the sperm population within the uterus is reduced. However, little is known about the role of sperm characteristics which make them able to reach the oviduct and fertilize. The ejaculate is composed by different sperm subpopulations based on their motility, morphometry or morphology characteristics among others. In the present study, we examine whether sperm morphology could be involved in their selection within the female genital tract. For this purpose, sperm morphology was evaluated in the backflow (60 min after insemination) and within the utero-tubal junction (UTJ) (collected ~24h after insemination) following intrauterine sperm deposition (n=6). These groups were compared with the morphology of the sperm in the dose before insemination.

Material and methods: Sperm rich fractions were obtained from two fertile boars and diluted in commercial extender. Sperm doses (1500×10^6 sperm/40 ml) were deposited in the uterus body (post-cervical AI) of the 6 sows. Backflow was collected in each sow during 60 min after insemination. The collection was performed using a human colostomy bags fixed around the vulva. Approximately ~24 h after AI sperm were collected within the UTJ. For that, the genital tract was exposed through a mid-ventral incision (laparotomy) a UTJs were flushed with Phosphate-Buffered Saline. Sperm were classified as normal, having a cytoplasmic droplet (proximal-PCD or distal-DCD) or with tail defects (TD). A total of 2800 sperm were evaluated (insemination dose=800, backflow=1000 and UTJ=1000).

Results: Sperm morphology was examined in the three experimental groups: 1) insemination dose (previous to be deposited in the uterus); 2) backflow (during 60 min after AI); and 3) UTJ (sperm reaching the UTJ 24 h after AI). The results are presented in Table 1. The sperm collected in the backflow have an increased of ~10% of morphologically abnormal sperm compared to the insemination dose ($P<0.05$), mainly due to an increase in TD. Moreover, almost the totally of the sperm reaching the UTJ has normal morphology ($97.88 \pm 1.09\%$), pointing to a reduction of ~15% compared with the insemination dose ($P<0.05$). No differences were found in the morphology of sperm collected from right and left UTJ.

Conclusions: In conclusion, the data of the present study suggests that uterus acts as a barrier against morphologically abnormal sperm. Some of the sperm are discarded in the backflow and within the uterine horns, ensuring an adequate population of normal sperm in the oviduct able to fertilize the oocyte.

Table 1. Sperm morphology in the original dose compared with the backflow and the sperm in the uterus. Data expressed as mean \pm SEM.

	Normal morphology (%)	Proximal cytoplasmic droplet (%)	Distal cytoplasmic droplet (%)	Tail defects (%)
Insemination Dose	82.25 \pm 2.41 ^a	7.12 \pm 3.15	8.25 \pm 3.26 ^{ab}	2.37 \pm 0.59 ^a
Backflow	72.30 \pm 2.53 ^b	10.15 \pm 3.99	9.35 \pm 2.67 ^a	8.30 \pm 2.51 ^b
UTJ	97.88 \pm 1.09 ^c	1.54 \pm 0.67	0.56 \pm 0.56 ^b	0.00 \pm 0.00 ^a

a, b, c letters in the same column indicate significant differences ($p<0.05$)

134 GENE EXPRESSION OF THE VEGF SYSTEM IN THE PORCINE OVIDUCT AT PRE- AND POST-OVULATORY STAGES

(1) Olsson, F., (2) Izquierdo Rico, M.J., (1-3) Gutiérrez Trujillo, H.A., (1) Latorre Reviriego, R., (2) Avilés Sánchez, M., (2) Gu illén Martínez, A., (1) López Albors, O.

(1) Dept. Anatomy & Comparative Pathology, Faculty of Veterinary Science, University of Murcia (2) Dept. Cell Biology and Histology, Faculty of Medicine, University of Murcia. (1-2) International Excellence Campus for Higher Education and Research “Campus Mare Nostrum”, University of Murcia, Murcia, Spain. (3). Dept. Animal Health, Faculty Veterinary Medicine, University National of Colombia.

INTRODUCTION: The vascular endothelial growth factor (VEGF) has been postulated as a key factor involved in the local regulation of the oviduct physiology. The VEGF system includes several isoforms of the VEGF family (VEFG-A) and two main binding receptors, the Flt-1 (c-fms-like tyrosine kinase) and the KDR (fetal liver kinase-1). In the female reproductive tissues VEGF₁₂₀ and VEGF₁₆₄ are the most expressed isoforms, while the KDR receptor has been postulated as the major receptor. The role of the VEGF system in the oviduct is still poorly understood and precise information about their expression throughout the estrous cycle is still lacking in the swine. The present work was aimed at analysing the relative expression of VEGF-A, Flt-1 and KDR during one pre-ovulatory and two post-ovulatory stages of the porcine estrous cycle.

MATERIAL AND METHODS: Oviducts from adult sows were collected from the slaughterhouse. On-site careful inspection of the ovary allowed allocating the samples into the late follicular pre-ovulatory stage (LF, n=4), and the early luteal (EL, n=4) and late luteal (LL, n=4) post-ovulatory stages. The ampulla (Amp) and isthmus (Isth) were sectioned and immediately frozen in liquid nitrogen. Total RNA was isolated from oviducts and cDNA was synthesized with oligo-dT as primer. Gene expression of different genes were analyzed by RT-qPCR: VEGF-A (accession number: ENSSSCT00000001892) Flt-1 (ENSSSCT00000010212) and KDR (ENSSSCT00000036588). Anova was carried out for RT-qPCR relative to GADPH expression values considering the estrous phase (LF, EL, LL) and oviduct region (Amp, Isth) as fixed factors for a significance level of $p < 0.05$.

RESULTS: The relative expressions for the three tested genes have been summarized in Table 1 (mean \pm standard deviation). VEGF-A, Flt-1 and KDR expression were consistently lower in the pre-ovulatory (LF) than in the post-ovulatory EL and LL stages ($p < 0.01$). While VEGF-A and KDR expressions were higher in the ampulla than in the isthmus ($p < 0.01$), the opposite result was observed for Flt-1 expression at the post-ovulatory EL and LL stages ($p < 0.01$).

		VEGF-A	Flt-1	KDR
LF	Amp	11,45 ± 6,08	2,92 ± 0,81	10,62 ± 7,56
	Isth	5,22 ± 2,47	3,52 ± 1,87	3,07 ± 1,88
EL	Amp	14,95 ± 3,94	3,29 ± 1,71	23,95 ± 3,82
	Isth	9,12 ± 2,74	8,01 ± 3,67	11,78 ± 4,05
LL	Amp	15,46 ± 2,89	6,65 ± 2,6	29,07 ± 13,94
	Isth	12,93 ± 2,37	11,97 ± 0,97	20,48 ± 8,93

CONCLUSIONS: The increasing expression of the VEGF system throughout the estrous cycle suggests a maximum activity in the porcine oviduct during the post-ovulatory period. The higher expression of VEGF-A and KDR in the ampulla and Flt-1 in the isthmus demonstrate a regional compartmentalization of this factor, which might be related with the different functions of these two oviduct regions. Further studies including the localization of the proteins in the oviduct are required to elucidate its role in the regulation of the oviduct physiology during the estrous cycle of pigs.

This work was funded by project AGL2012-40180-C03-03 (Ministerio de Economía y Competitividad).

DOCENCIA

31 REACTION EVALUATION TO NEAR-PEER TEACHING IN HISTOLOGY LABORATORY

Ruz-Caracuel, I. (1); Leiva-Cepas, F. (1,2); Cambrón-Carmona, M.A. (1); Tallón de Lara, C. (1); Cámara-Pérez, J. (1); Agüera, A. (1); Jimena, I. (1); Peña, J. (1)

(1) Department Morphological Sciences, Section of Histology, Faculty of Medicine and Nursing. University of Córdoba. Spain (2) Unidad Docente de Medicina Familiar y Comunitaria de Córdoba. SAS. Spain

Introduction Histology Laboratory experience consisted of a practical session where students in groups of 5-6 performed the steps for solid tissue and citology processing. The session was traditionally taught by professors, laboratory technician and intern students; and it was noticed that students preferred to interact with intern students. Based on the hypothesis that students will create a more comfortable educational environment, a near-peer teaching educational strategy, where only intern students and recently graduated students acted as teaching staff, was designed for the current 2014-2015 academic year. A students' reaction evaluation was performed to analyse achievement of objectives. Materials & Methods After finishing Histology Laboratory sessions a total amount of 121 students who has completed it were asked to answer a survey.

The survey consisted of eight items valued using a Likert 0-5 scale, one yes/no question and a request for suggestions. A descriptive analysis was performed. Results Students felt comfortable and relaxed during the practical session (4,37? 0,78 of 5) and they felt confident to ask questions (4,23? 0,90 of 5). The best valued item was that intern students communicate confidently (4,45? 0,62 of 5); whereas the less valued item was that students preferred the session to be driven by a intern student with a 3,61? 1,01. Only a 5,79% of students would like to modify something, and the most common modification, cited by only three students, was shortening the time dedicated. Conclusions Students valued very positively the educational environment created by intern students in the histology laboratory session. In conjunction with results that showed similar and better acquisition of concepts compared with previous academic years, we have proven that this near-peer teaching strategy applied has advantages for students.

49 AN AUDIOVISUAL NOTEBOOK ON ARTIFICIAL CORNEA TRANSLATION AS A MODEL OF LEARNING INTEGRATION IN TISSUE ENGINEERING

(1) Garzón, I.; (1) Carriel, V.; (1) González-Andrades, E.; (1) Campos, F.; (1) González-Andrades, M.; (2) Fernández-Valadés, R.; (1) García, J.M.; (1) Campos, A.; (1) Alaminos, M.

(1) Tissue Engineering Group, Department of Histology, University of Granada, Spain, and Instituto de Investigación Biosanitaria ibs.GRANADA, Spain; (2) Division of Pediatric Surgery, University Hospital of Granada, Spain.

Introduction: Active participation of students in their learning-teaching process has been emphasized to promote self-discovery learning. One of the innovative didactic resources used to stimulate the participation of the students is the elaboration of audiovisual notebooks, in which students can participate in different stages with different roles. Furthermore, audiovisual notebooks are excellent tools to promote integration of different knowledge, especially in medical curricula. In the present work, we developed an audiovisual notebook focused on the elaboration of an artificial human cornea by tissue engineering and the sequential steps that are necessary to generate and translate to the clinical setting this artificial tissue product. Materials and methods: A novel model of human artificial cornea was generated in the University of Granada tissue engineering laboratory following previously developed protocols. Then, quality control analyses were carried out in vitro and in vivo in laboratory animals. Later, artificial corneas were constructed in a GMP facility approved by the Spanish Medicines Agency (AEMPS) using pharmaceutical grade reagents and conditions. Finally, artificial corneas were implanted in selected patients with cornea damage at the Division of Ophthalmology of the Granada University Hospital Complex. Selected pre and postgraduate students participated in the elaboration of the script of an audiovisual notebook and in the different stages of its elaboration (design, film making, animation figures, dialogues, etc.). Seminars and discussion sections were implemented to follow the progress of the process. Results: An integrated audiovisual notebook was generated taking into account both the basic and the clinical phases of the process. For the students, elaboration of this notebook contributes to the development of a new didactic model allowing not only the acquisition of basic and clinical competences, but also the basic-clinical integration in tissue engineering. Our results enable a translational conception of a basic science and develop a cooperative learning, which is an important transversal

competence that is very difficult to implement in medical curricula. An added value is the active implication of the students in the project and their very positive performance when they are evaluated. Conclusions: Elaboration of audiovisual notebooks on basic-clinical approaches such as the use of an artificial cornea generated by tissue engineering is an useful integrative model that may contribute to the acquisition of cognitive and skill competences in a specific issue and to acquire transversal competences that are not easy to reach in medical curricula. Acknowledgements: This work was supported by grant UGR13-115, Secretariado de Innovación Docente, University of Granada, Spain.

119 SERVICE-LEARNING IN HISTOLOGY. THE BLOOD AND HEMATOPOIETIC SYSTEM AS A MODEL

(1) Martín-Piedra, M.A.; (1) Campos, F.; (1) Campos-Sánchez, A.; (1) González-Andrades, E.; (2) López-Berrio, A.; (2) López-Candia, M.D.; (3) López-Núñez, J.A.; (4) Ruyffelaert, A.; (1) Carriel, V.

(1) Tissue Engineering Group, Department of Histology, University of Granada, Spain, and Instituto de Investigación Biosanitaria ibs.GRANADA, Spain; (2) Blood and Tissue Bank of Granada-Almería, Granada, Spain; (3) Department of Didactics and Scholar Organization, University of Granada, Spain; (4) University of Granada, Spain (1)

Introduction: Service-learning has been defined as a structured learning experience that combines community services with explicit learning objectives, preparation and reflection¹. Students engaged in service-learning are expected not only to provide direct community service but also to learn about the context in which the service is provided, the connection between the service and their academic coursework and their roles as citizens. Service-learning helps medical students² to rediscover their initial, altruistic reasons for studying medicine and for all these reasons is being progressively incorporated to medical school curricula as a model of teaching without classical reception learning lectures. Because service learning could be a useful model to acquire scientific and social competences in blood and hematopoietic system for medical students in histology the perceptions of teachers and professionals involved in Blood Banks regarding this activity is investigated. Methods: Teachers of histology and professionals of a Blood Bank (20) completed a questionnaire regarding their perceptions about the cognitive, attitudinal, procedural, social and solidarity competences that students could acquire in lectures about blood and haematopoietic system or in different activities linked to the Blood Bank. The questionnaire includes several items that are related to the topics that should be evaluated by the teachers and professionals in a scale ranging from 1 to 5. The results were analyzed and compared using a nonparametric Mann-Whitney test. Results: The results highlight significant differences between teachers of histology and professionals linked to Blood Banks in connection with cognitive ($p=0.0010$) and solidarity ($p=0.0030$) competences which are perceived for the professional as more correlated to the service-learning. Conclusion: To know the perceptions of teachers and professional about the competences that students could acquire in a service-learning program linked to Blood Banks, should contribute to designing their learning process not only concerning scientific cognitive competences about the blood and haematopoietic system but also regarding the solidarity competences they could obtain while they are actively participating in the community. This is in agreement with the Stanford model

which is supported on teaching without classical reception lectures. References: 1. Furco A. Institutionalizing service-learning in higher education. *J Pub Affairs*. 2002; 6: 39-47. 2. Sarena D, Seifer MD. Service-learning: Community-campus partnerships for health professions education. *Acad Med*. 1998; 73: 273-277. Acknowledgements: This work was supported by grant UGR 13-116, Secretariado de Innovación Docente, University of Granada, Spain.

122 EPISTEMOLOGICAL BELIEFS OF POSTGRADUATE STUDENTS OF A TISSUE ENGINEERING MASTER PROGRAM

(1) Campos-Sánchez, A.; (1) Alfonso-Rodríguez, C.A.; (2) Ángeles, B.; (1) Jaimes-Parra, B.D.; (1) Martín-Piedra, M.A.; (2) Ruyffelaert, A.; (1) García, J.M.; (1) Crespo, P.V.; (1) Sánchez-Quevedo, M.C.

(1) Tissue Engineering Group, Department of Histology, University of Granada, Spain, and Instituto de Investigación Biosanitaria ibs.GRANADA, Spain; (2) University of Granada, Spain

Introduction: Students' epistemological beliefs are defined as personal and implicit beliefs systems or students' Assumptions about nature of knowledge and learning. (1). Research has shown that epistemological beliefs are related to problem solving, conceptual change, motivation, learning strategies and academic performance (2). Although epistemological beliefs have been investigated in primary, secondary school and universities, a very scarce research have been done in postgraduate students. In this sense, it is important to identify the students' epistemological beliefs in postgraduate programs, especially to plan future teaching strategies for these students. In the present work, two epistemological dimensions -the source of knowing and justification for knowing- are investigated in postgraduate students in a health sciences program in Tissue Engineering and a Social Sciences program. Methods: Students (20 per master program) completed a validated questionnaire related to two epistemological dimensions -source and justification of knowing- that students had to link to their epistemological beliefs. Each item had to be scored by the students from 1 to 5. The test was carried out at the beginning of each master program, and results in both groups were statistically evaluated by a non-parametric Mann-Whitney test. Results: Students in health sciences and social sciences significantly differed ($p=0.0069$) in the epistemological beliefs related to the source of knowing, specifically on the role of books as sources of knowing, which was more importantly scored by Tissue Engineering students (3.54 ± 0.73) as compared to students of Social Sciences (2.78 ± 0.91). Science books contents are therefore considered by science students as a more consolidated knowledge that the content present in social sciences books. In addition, both groups of students also differed ($p=0.0020$) in the epistemological beliefs related to justification of knowing, which was more important for Tissue Engineering students (4.27 ± 0.33) than for Social Sciences postgraduate students (3.92 ± 0.33). Conclusion: As epistemological beliefs have important effects on learning strategies, the results found in this study should be taken into account to design postgraduate programs. In this sense, clearly-established tissue engineering concepts and their justification should be incorporated to reference books used in the Tissue Engineering programs. References: 1. Schommer, M. The influence of age and education on epistemological beliefs. *Br J Educ Psychol*. 1998; 68: 551-562. 2. Chan K-W. Preservice teacher education students' epistemological beliefs and conceptions about learning. *Instr Sci*.

2011; 39:87-108. Acknowledgements: This study is supported by CTS-115, Tissue Engineering Group, University of Granada, Spain.

123 INNOVATIVE DIDACTIC RESOURCES IN A STANFORD MODEL OF TISSUE ENGINEERING

(1) Garzón, I.; (2) Campos-Sánchez, A.; (1) Jaimes-Parra, B.D.; (1) Alfonso-Rodríguez, C.A.; (1) Martín-Piedra, M.A.; (2) Ruyffelaert, A.; (2) Sola, M.; (1) Crespo, P.V.; (1) Sánchez-Quevedo, M.C.

(1) Tissue Engineering Group, Department of Histology, University of Granada, Spain, and Instituto de Investigación Biosanitaria ibs.GRANADA, Spain; (2) University of Granada, Spain

Introduction: The recent development of novel disciplines such as Tissue Engineering still lacks of clearly defined threshold concepts. These concepts must be transformative, irreversible, integrating and bounded, and their establishment may require long times to be recognized. In this regard, a recent innovation in health science education -the Stanford didactic model- is based on the use of imaginative didactic resources that can be used to replace classical lectures for teaching new disciplines in which threshold concepts need to be characterized. The recent incorporation of Tissue Engineering to medical curricula in medical schools make this innovative discipline a good candidate to apply the Stanford model and therefore to experiment with new imaginative didactic resources. In the present work male and female students' perceptions about some of these innovative resources are investigated in order to evaluate which of them should be incorporated in future differentiated learning programs. **Methods:** 70 Tissue Engineering medical students filled a questionnaire related to the use of 10 different innovative didactic resources such as a representation of theatre, imitation of a film or TV program, the use of YouTube or audio-visual notebooks elaborated by the students, etc. Each question had to be rated in a Likert-like scale from 1 to 5. The results were evaluated with ANOVA test to identify differences in the responses obtained between male and female students. **Results:** Our results showed statistically significant differences between male and females students for 3 of the 10 items analyzed here. The three items were related to the use of audio-visual models such as movies, TV contests and TV series, which were highly rated by females (3.66, 3.69 and 3.47, respectively) as compared to male students (3.29, 3.19 and 3.09, respectively). Differences were statistically significant ($p=0.0170$ for the use of movies, $p=0.0010$ for TV contests and $p=0.0020$ for TV series, respectively). **Conclusions:** These results suggest that female students would prefer TV-linked audio-visual models as innovative didactic resources in Tissue Engineering using the Stanford model. This may point out that TV-based audio-visual models could be used in future differentiated learning programs in Tissue Engineering. **Acknowledgements:** This work was supported by grant UGR13-116, Secretariado de Innovación Docente, University of Granada, Spain.

HISTOLOGÍA ANIMAL

3 HISTOMORPHOMETRIC AND IMMUNOHISTOCHEMICAL STUDY OF *Dama dama* RUMEN DURING PRENATAL DEVELOPMENT

(1) Redondo García, E.; (2) García González, A.; (3) Gázquez Ortiz, A.; (4) Franco Rubio, A.; (5) Masot Gómez-Landero, A.J. (1, 2, 3 and 5)

Department of Veterinary Histology, Faculty of Veterinary Medicine, Extremadura University (Cáceres); (4) Department of Veterinary Anatomy, Faculty of Veterinary Medicine, Extremadura University (Cáceres).

INTRODUCTION: Common or European fallow deer (*Dama dama*) is a species of deer native to the Mediterranean region. It differs from other major European deer, red deer in its smaller size, its palmate antlers and your reddish-brown pelage dotted with white flecks in spring and summer (occasionally with a dark stripe on the back).

A detailed study of the ontogenesis of *Dama dama* stomach has not been undertaken to date, and our aim was to sequence several histological phenomena that occur during the ontogenesis of the rumen.

METHODOLOGY: Histomorphometric and immunohistochemical analyses were carried out on 50 embryos and fetuses of *Dama dama* from the initial stages of prenatal life until birth. For the purposes of testing, the animals were divided into five experimental groups: group I, 30-60 days, 1-25% of gestation; group II, 67-90 days, 25-35% of gestation; group III, 97-135 days, 35-50% of gestation; group IV, 142-191 days, 45-70% of gestation; and group V, 205-235 days, 75-100% of gestation. Samples of the rumen were fixed in 10% neutral buffered formalin, processed using routine histological methods, sectioned at 2 µm and stained with hematoxylin and eosin.

RESULTS: The rumen of the primitive gastric tube was observed at approximately 50 days. At 57 days the rumen consisted of three layers: internal or mucosal, middle or muscular, and external or serosal layer. The stratification of the epithelial layer was accompanied by changes in its structure with the appearance of ruminal pillars and papillae. The outline of the ruminal papillae began to appear at 132 days of prenatal development as evaginations of the basal zone toward the ruminal lumen, pulling with it in its configuration the stratum basale, the lamina propria and the submucosa. From the pluripotential blastemic tissue at 50 days we witnessed the histodifferentiation of the primitive tunica muscularis, composed of two layers of myoblasts with a defined arrangement. It was also from the pluripotential blastemic tissue, at 87 days, that the lamina propria and the submucosa were differentiated. The serosa showed continuity in growth as well as differentiation, already detected in the undifferentiated outline phase. The tegumentary mucosa of deer rumen was shown without secretory capacity in the initial embryonic phases; neutral mucopolysaccharides appeared from 57 days. The presence of neuroendocrine cells (non-neuronal enolase) in the ruminal wall of deer during development was not detected until 87 days. The glial cells were detected at 132 days for glial fibrillary acidic protein and at 57 days for vimentin. The immunodetection of vasointestinal peptide and neuropeptide Y, progressively increase from the 87 days until the end of gestation.

CONCLUSIONS: In terms of the rumen structure of the primitive gastric tube, our observations revealed that the red deer is less precocious than small and large domestic

ruminants. Thus its secretory capacity, detected by the presence of neutral mucopolysaccharides, and its neuroendocrine nature, determined by the presence of positive non-neuronal enolase cells, were evident in minor advanced stages of prenatal development than those detected in the sheep, goat, cow and red deer.

4 HISTOMORPHOMETRIC AND IMMUNOHISTOCHEMICAL STUDY OF *Dama dama* RETICULUM DURING PRENATAL DEVELOPMENT

(1) Redondo García, E.; (2) García González, A.; (3) Gázquez Ortiz, A.; (4) Franco Rubio, A.; (5) Masot Gómez-Landero, AJ.

(1, 2, 3 and 5) Department of Veterinary Histology, Faculty of Veterinary Medicine, Extremadura University (Cáceres); (4) Department of Veterinary Anatomy, Faculty of Veterinary Medicine, Extremadura University (Cáceres).

INTRODUCTION: Common or European fallow deer (*Dama dama*, sometimes called *Cervus dama*) is a species of deer native to the Mediterranean region. It differs from other major European deer, red deer (*Cervus elaphus*) in its smaller size, its palmate antlers and your reddish-brown pelage dotted with white flecks in spring and summer (occasionally with a dark stripe on the back).

A detailed study of the ontogenesis of *Dama dama* stomach has not been undertaken to date, and our aim was to sequence several histological phenomena that occur during the ontogenesis of one of the gastric compartments, the reticulum.

METHODOLOGY: Here we describe a histomorphometric and immunohistochemical analysis of the stomach of 50 *Dama dama* embryos and fetuses from 30 days of gestation until birth (235 days). For the purposes of testing, the animals were divided into five experimental groups: group I, 30-60 days, 1-25% of gestation; group II, 67-90 days, 25-35% of gestation; group III, 97-135 days, 35-50% of gestation; group IV, 142-191 days, 45-70% of gestation; and group V, 205-235 days, 75-100% of gestation. Samples of the reticulum were fixed in 10% neutral buffered formalin, processed using routine histological methods, sectioned at 2 μ m and stained with hematoxylin and eosin.

RESULTS: Differentiation of the reticular compartment from the primitive gastric tube begins at 57 days, forming a three-layered structure: epithelium, pluripotential blastemal tissue and serosa. The primitive reticular cells are initiated as small epithelial evaginations (primary ribs) at 107 days. At 132 days, lateral growths appear from the primary reticular ribs, forming the corneum papillae. The secondary reticular ribs form at 132 days as growths from the primary ribs. The uneven height of primary and secondary reticular ribs leads to the formation of cells of varying size. Growth of the reticular ribs involves the lamina propria but not the submucosa, so clear separation of these layers is maintained during histodifferentiation. Formation of the tunica muscularis from the pluripotential blastemal tissue begins at 57 days of intrauterine life, as two layers of longitudinally and circularly arranged myoblasts. Differentiation of the muscularis from the mucosa occurs at approximately 195 days, as longitudinal projections of the internal bundles of the tunica muscularis form the musculature of the primary ribs. The secretion of neutral and acid mucopolysaccharides by the reticular epithelial layer begins at 57 days,

establishing the gradual adaptation of the mucosa to its protective function in postnatal life. Neuroendocrine (non-neuron enolase) and glial cells (glial fibrillary acidic protein and vimentin) were detected by immunohistochemistry, in a similar localization and intensity to that reported in the rumen. The neuropeptides vasoactive intestinal peptide and neuropeptide Y showed a positive immunoreaction in the reticular epithelium from 132 days of prenatal life, again earlier than reported for the rumen.

CONCLUSION: In comparison with domestic ruminants, deer were shown to be more precocious with regard to development of gastric tube, in their capacity to secrete neutral mucopolysaccharides, and in their neuroendocrine nature, as determined by the detection of positive neuroendocrine and/or glial cells.

5 HISTOMORPHOMETRIC AND IMMUNOHISTOCHEMICAL STUDY OF Dama dama OMASUM DURING PRENATAL DEVELOPMENT

(1) Redondo García, E.; (2) García González, A.; (3) Gázquez Ortiz, A.; (4) Franco Rubio, A.; (5) Masot Gómez-Landero, AJ.

(1, 2, 3 and 5) Department of Veterinary Histology, Faculty of Veterinary Medicine, Extremadura University (Cáceres); (4) Department of Veterinary Anatomy, Faculty of Veterinary Medicine, Extremadura University (Cáceres).

INTRODUCTION: Common or European fallow deer (*Dama dama*, sometimes called *Cervus dama*) is a species of deer native to the Mediterranean region. It differs from other major European deer, red deer (*Cervus elaphus*) in its smaller size, its palmate antlers and your reddish-brown pelage dotted with white flecks in spring and summer (occasionally with a dark stripe on the back)

A detailed study of the ontogenesis of *Dama dama* stomach has not been undertaken to date, and our aim was to sequence several histological phenomena that occur during the ontogenesis of one of the gastric compartments, the omasum.

METHODOLOGY: 0 embryos and fetuses of *Dama damma* from the initial stages of prenatal life until birth. For test purposes, the animals were divided into five experimental groups: group I, 30-60 days, 1-25% of gestation; group II, 67-90 days, 25-35% of gestation; group III, 97-135 days, 35-50% of gestation; group IV, 142-191 days, 45-70% of gestation; and group V, 205-235 days, 75-100% of gestation. Samples of the omasum were fixed in 10% neutral buffered formalin, processed using routine histological methods, sectioned at 2 μ m and stained with hematoxylin and eosin.

RESULTS: At 57 embryonic days, the omasum wall was differentiated, and comprised three layers: the epithelial layer, pluripotential blastemic tissue and serosa. The stratification of the epithelial layer was accompanied by changes in its structure, with the appearance of four laminae of different sizes; in order of appearance these were: primary at 57 days, secondary at 80 days, tertiary at 87 days and quaternary at 125 days. At around mid-gestation, lateral evaginations were formed from the stratum basale of the primary and secondary smaller laminae. These were the primitive corneum papillae. From 195 days, the corneum papillae were

present in all four sizes of laminae. The histodifferentiation of the lamina propia-submucosa, tunica muscularis and serosa showed patterns of development similar to those reported for the rumen and reticulum of red deer. The omasum of red deer during prenatal life, especially from 57 days of gestation, was shown to be an active structure with full secretory capacity. Its histological development, its secretory capacity (detected by the presence of neutral mucopolysaccharides) and its neuroendocrine nature (detected by the presence of positive non-neuronal enolase cells and the neuropeptides vasoactive intestinal peptide and neuropeptide Y) were parallel to the development of the rumen and the reticulum.

CONCLUSION: However, its prenatal development was evident at earlier stages than that of the omasum in sheep, goat, cow and iberian red deer.

24 NEUROPROTECTIVE EFFECT OF THE COMBINATION OF RESVERATROL AND DOCOSAHEXANOIC ACID AGAINST NEONATAL HYPOXIA-ISCHEMIA

(1) Arteaga Cabeza, O.; (1) Revuelta Aramberri, M.;(2) Urigüen Echevarria, L., (1) Álvarez Díaz, A.; (3) Martínez Ibargüen, A and (1) Hilario Rodriguez, E.

(1). Cell Biology & Histology, 2. Pharmacology, 3.Otorrhinolaryngology, School of Medicine & Dentistry, University of the Basque Country (UPV/EHU), Leioa, Bizkaia, Spain.

INTRODUCTION: Despite pediatric advances in neonatal care, perinatal hypoxia-ischemia (HI) brain injury continues being a serious problem, remaining responsible of a great percentage of neonatal mortality and neurocognitive deficits. Resveratrol (RVT), a natural polyphenol found especially in red wine, and docosahexanoic acid (DHA), a long-chain omega-3 fatty acid, commonly found in fish, are both antioxidants with neuroprotective properties. The main goal of our study was to evaluate in a prospective way the protective effects of the combination of resveratrol and docosahexanoic acid when administered before HI brain injury in neonatal rats using the Rice-Vannucci model.

MATERIAL AND METHODS: 7-day-old (P7) rats were assigned to three experimental groups (n=8): Control, Hypoxia-Ischemia (HI) and a group of HI animals that received a single dose of a combination of DHA (1 mg/kg) and RVT (20 mg/kg) 10 minutes before hypoxia (RVT+DHA). The HI injury was induced by permanent ligation of the left common carotid artery and the subsequent exposure to 8% O₂ for 2 hours and 15 minutes. Animals were sacrificed immediately (0 h), 3 h, 12 h and 7 days after HI event. Fixed brains were stained with Nissl for morphological studies and non-fixed brains were dissociated and studied by flow cytometry to analyze inner membrane integrity (NAO) and membrane potential (Rh123) of mitochondria. $P < 0.0001$ was considered statistically significant after having performed one-way analysis of variance followed by Bonferroni-Dunn correction.

RESULTS: Coronal sections of HI group demonstrated a damage area in the ipsilateral hemisphere with loss of brain tissue, while no macroscopic differences were shown between pretreated group and control one. Regarding mitochondrial inner membrane integrity, HI group underwent a statistically significant decrease in the percentage of NAO positive cells at 12 h

with respect to the Control group, while animals pretreated with the combination of antioxidants maintained similar values to Control one. In regards to mitochondrial transmembrane potential, pups subjected to the HI event underwent an important reduction in the percentage of Rh 123 positive cells, but rats pretreated with the antioxidants showed similar values to those of the controls.

CONCLUSIONS: Taken as a whole, the present study present for the first time that the pretreatment with a combination of resveratrol and docosahexanoic acid led to a neuroprotective effect in the hypoxic-ischemic brain injury in rats by reducing the infarct damage and by maintaining mitochondrial inner membrane integrity and potential.

Acknowledgments: This work was supported by grant from the Basque Government IT 773/13 and BFI-2011-129.

34 MORPHOMETIC STUDY OF THE FOLLICLE-ASSOCIATED EPITHELIUM AND THE INTRAEPITHELIAL LYMPHOCYTIC POPULATION IN RABBIT APPENDIX

Roma, S.M.; Pérez, F.A.; D'Ottavio, A.E.

Cátedra de Histología y Embriología. Facultad de Ciencias Médicas. Universidad Nacional de Rosario. Argentina

Rabbit appendix, a main lymphoid organ in the gastrointestinal tract, is highly related with mucosal immunity. It reveals a collection of lymphocytes covered by the follicle-associated epithelium (FAE), a single layer containing membranous (M) cells, specialized in sampling and transporting luminal antigens to the underlying lymphoid tissue for the induction of IgA antibody response. In this regard, M cells evidence basolateral membrane folds harboring immunocompetent cells. These membranous pockets constitute the interface between the lumen and the immune system and contain lymphoid cells (i.e: larger cells called blasts and smaller ones, localized nearby the basal membrane, identified as lymphocytes). This morphological modification in lymphocytes entering to the intraepithelial compartment occurs after the transport of small amounts of antigens from the lumen to the abovementioned pockets via M cell cytoplasm (transcytosis). At present, no information was found regarding possible changes in FAE area and/or morphological modifications in the intraepithelial lymphocytic population of rabbit appendix when exposed to antigens administered parenterally. This communication deals specifically with this type of procedure. Twenty adult New Zealand rabbits were divided as follows: G1: control. G2: adjuvant only. G3: sensitized and euthanized 24 hours after the first sensitization G4: sensitized and euthanized 24 hours after the second sensitization. Sensitization was performed with 100 µg of ovalbumin in Freund's complete and incomplete adjuvant administered twice subcutaneously at a 15 days interval. Appendix specimens were stained with H&E for histopathological study, with Giemsa for identifying immunocompetent cells and with Anti-Vimentin antibody as M cell cytoskeleton marker. FAEs in two histological slices per animal were analyzed in every group. Taking advantage of digital photography at high magnification and image analysis software, FAE area was measured and intraepithelial smaller lymphocytes (diameter: 7-10 µm), blasts (diameter > 10 µm) and total lymphocytes were

quantified. Results, expressed as mean per animal \pm standard error were statistically processed through ANOVA test with a 0,05 significance level. FAE area was $2105,39 \pm 95,2 \mu^2$ in G1; $1954,10 \pm 164,33 \mu^2$ in G2; $1899,67 \pm 12,62 \mu^2$ in G3 and $1944,45 \pm 49,32 \mu^2$ in G4 (ns). Total intraepithelial lymphocytes were: $10,10 \pm 0,67$ in G1; $9,72 \pm 0,72$ in G2; $9,15 \pm 0,53$ in G3 and $7,92 \pm 0,45$ in G4 ($p=0,04$). Blasts were: $8,1 \pm 0,38$ in G1; $7,6 \pm 0,49$ in G2; $7,1 \pm 0,29$ in G3 and $5,9 \pm 0,40$ in G4 ($p=0,0008$). Cytes were: $2,02 \pm 0,47$ in G1; $2,1 \pm 0,31$ in G2; $2,08 \pm 0,39$ in G3 and $2,01 \pm 0,33$ in G4 (ns). In conclusion, while FAE did not show changes, parenterally immunized rabbits would produce reverse effects in relation to lumen antigen challenge. This effect was put into evidence through a lower afflux of immunocompetent cells to the M basolateral pocket-like structures and its lower activation, revealed by the significant blast decrease. Consequently, these modifications could influence the typical mucosal immune response since blasts are precursors of the effector/memory cells which later colonize the lamina propria.

37 IDENTIFICATION OF UNDIFFERENTIATED CELLS IN THE THYROID GLAND OF THE RAT.

Vázquez Román V, Utrilla Alcolea JC, Fernández Santos JM, Bernabé Caro R, Conde Amiano E, Martín Lacave I.

Dpto . Citología e Histología Normal y Patológica. Facultad de Medicina. Universidad de Sevilla.

INTRODUCTION: The thyroid is an organ of low proliferation; however it can change its size under different physiological conditions. This ability to renew the gland can be due to the fact that both the follicular cells and C cells retain their capacity to divide by mitosis and, also, this might be justified by the presence of a population of stem cells that could respond to proliferative stimuli. Several authors have proposed the main cells of the Solid Cell Nests (SCN) as resident adult thyroid stem cells. These authors support the idea that SNC main cells may possess capacity for self-renewal and differentiation into more than one cell type and even those, they could act as cancer stem cells. This affirmation is supported by p63 expression, confined at the basal and parabasal cell layers, whereas remaining negative for thyroid differentiation markers such as thyroglobulin (TG) and calcitonin (CT). The SCNs are considered to be remnants of the ultimobranchial body (UBB) and are equivalent to the ultimobranchial follicles (UBF) identified in rat thyroid glands.

The aim of this study was to analyze the presence of undifferentiated cells with stem cell potential in UBF walls. To this end, immunohistochemistry and immunofluorescence of different morphological patterns of UBF throughout postnatal life of the rat were performed.

MATERIAL AND METHODS: Wistar rats aged 0-24 months were used. After formaldehyde fixation and paraffin embedding, thyroid glands were serially sectioned and stained by double immunohistochemistry or double immunofluorescence using the following primary antibodies: anti-CT (Dako), anti-TG (Dako), anti-Cytokeratins (clone 34 β E12-Dako), anti-p63 (Santa Cruz) and anti-TTF-1 (Santa-Cruz). Immunohistochemical staining was carried out by using the Envision Flex system (Dako) and diaminobenzidine and Fast-Red as substrates. Immunofluorescence staining was carried out by using the anti mouse Cy2-conjugated and anti rabbit Cy3-conjugated (Jackson) secondary antibodies. Microscopic analysis was performed

using the Olympus BX50 fluorescence microscope using the Hamamatsu ORCA-03G digital camera and image processing software Image Pro-Plus 7.0 (Infaimon).

RESULTS: In all UBF, immunopositive cells for the undifferentiated basal cell markers p63 and CK-34 β E12 were detected regardless of the UBF size and morphological pattern. As opposite to normal follicular and C cells, UBF cells remained negative for TTF-1. Finally, in mixed follicles, positive cells for TG were observed and TG was also recognized in some UBF lumen.

CONCLUSION: Our results demonstrate the presence of undifferentiated cells within the thyroid UBF throughout the life of the rat. These results support the hypotheses that there is a resident population of stem cells in the UBF of the rat thyroid glands.

38 COMPARATIVE STUDY OF THE PRIMARY CILIA IN THYROCYTES OF ADULT MAMMALS.

Utrilla Alcolea JC, Gordillo Martínez F, Fernández Santos JM, Vázquez Román V, Gómez Pascual A, Garnacho Montero C, García Marín R, Morillo Bernal J, Martín Lacave I.

Dpto. Citología e Histología Normal y Patológica. Facultad de Medicina. Universidad de Sevilla. Spain

INTRODUCTION: Since their discovery in different human tissues in 1898 by Zimmermann, primary cilia have been reported to exist in the vast majority of cell types in vertebrates. They are considered like cellular antennae that occupy an ideal cellular location for the interpretation of information from both the environment and cells. So far, in mammal thyroid glands, cilia have been found in the thyrocytes of humans and dogs (fetuses and adults), as well as in rat embryos. The present study was planned to investigate whether the existence of this organelle in follicular cells is a general event in the postnatal thyroid gland of different mammals.

MATERIAL AND METHODS: Normal adult thyroid glands from several mammalian species have been analyzed: human, guinea pig, rat, mouse, rabbit and pig. The samples were fixed in 4% neutral buffered formalin, embedded in paraffin, sectioned at 4-5 μ m and mounted on silane-coated glass slides. For the immunofluorescence (IF) study, an antigen retrieval step was performed. As primary antibody, a monoclonal anti-acetylated α -tubulin, which labels the axoneme, was used, followed by Cy3-labeled donkey anti-mouse IgG secondary antibody. When double IF was performed, the slides were then incubated with polyclonal rabbit anti-E-cadherin antibody and, subsequently, with Cy2-labeled donkey anti-rabbit IgG antibody. Samples were visualized with the fluorescent microscope (Olympus, BX50) or with a laser scanning confocal microscope (Leica, TCS-SP2), and analyzed with Leica Confocal Software. Primary cilia lengths were morphometrically assessed using the Image Pro-Plus 7.0 software (Infaimon).

RESULTS: In human thyroid glands, primary cilia were detected in most thyroid follicles. Generally, every follicular cell had a unique primary cilium, although there were some cells which showed more cilia, the mean length being $7.3 \pm 1.2 \mu$ m. In pigs and rabbits, a very similar distribution pattern was observed, the mean length in rabbits was $5.2 \pm 2.4 \mu$ m and $4.6 \pm 0.7 \mu$ m in pigs. Nevertheless, in guinea pigs, most thyroid follicles lacked primary cilia and for those sporadically present ciliated cells, the mean length of the primary cilium was $4.9 \pm 1.4 \mu$ m.

Finally, and surprisingly, in rat and mouse thyroid samples no primary cilia were found, not even sporadically.

CONCLUSION: According to our results, primary cilia are present in the adult thyroid gland of most mammal species studied by us, usually as a single copy per follicular cell. We hypothesize that primary cilia could be involved in the regulation of normal thyroid function through specific signaling pathways.

57 ELECTRON MICROSCOPE ANALYSIS OF PRIMARY CILIA IN THE THYROID GLAND

(1) Gómez Pascual A, (1) Utrilla Alcolea JC, (1) Fernández Santos JM, (1) Garnacho Montero C, (1) Vázquez Román V, (2) Jiménez García A. and (1) Martín Lacave I.

(1)Dpto. Citología e Histología Normal y Patológica, Facultad de Medicina, Universidad de Sevilla. (2) Dpto Cirugía Endocrina, Hospital Universitario y Área "Virgen Macarena", Facultad de Medicina, Universidad de Sevilla

INTRODUCTION: Two main classes of cilia are considered based on their structure and function: “secondary cilia”, with a 9+2 pattern, which are motile and present on multi-ciliated epithelial cells; and “primary cilia”, with a 9+0 pattern, which are usually solitary and non-motile. Thyroid primary cilia have been described, since their discovery by Zimmermann in 1898 in humans, as emerging from the apex of thyroid follicular cells. Subsequently, ciliated follicular cells were reported in other vertebrate species, such as fish, amphibians, birds and reptiles. Up to date, no other species of mammals have been reported to present primary cilia in thyrocytes. The present study was therefore planned to investigate the existence and morphology of primary cilia in follicular cells of different mammals by electron microscopy.

MATERIAL AND METHODS: We have analyzed normal adult thyroid glands from humans, pigs and rats. For transmission electron microscopy (TEM) studies, thyroid glands were fixed for 4h in 2.5% glutaraldehyde in 0.1M cacodilate buffer at 4°C, post-fixed 1 h in 1% osmium tetroxide, embedded in Spurr, ultrasectioned and observed with a Philips CM 10 microscope. For scanning electron microscopy (SEM) studies, the samples were fixed in the same glutaraldehyde solution, but extended for several days at room temperature, followed by post-fixation in 1% osmium tetroxide. Specimens were dried with the critical point method using CO₂, then sputter coated with vacuum-evaporated gold, and photographed with a JEOL 6460 LV microscope.

RESULTS: TEM analysis of specimens of human and pig thyroid glands revealed a sporadic presence of primary cilia, located on the apical surface of follicular cells and protruding into the colloid. Usually, only one cilium per cell was present although occasionally two cilia together were observed. When cross-sectioned, the typical 9+0 pattern of primary cilia was clearly recognizable at the base of the shaft.

When thyroid samples from human and pig were observed by SEM, follicular cells showed a polyhedral outline. The cell surface, generally convex, presented numerous microvilli and, emerging among them, from the geometric center of the cell, one primary cilium protruded into the follicular lumen. In human thyroid cells, occasionally more than one cilium was observed, which often emerged according to the characteristic “V” shape pattern. Conversely, follicular cells from the rat thyroid gland always lacked primary cilia, although they shared the same

polygonal morphology and the presence of numerous microvilli with the other above-described species.

CONCLUSION: In the present study we show the ultrastructural characteristics of primary cilia by TEM and by SEM, not only in human follicular cells but also in pig thyrocytes. These features are in sharp contrast with rat thyroid glands where primary cilia are absent. On the basis of these findings, such a relevant dissimilarity among species should be taken into account when using rat models for the study of normal thyroid activity and thyroid cancer biology.

58 IMMUNOFLUORESCENCE STUDY OF THE PRIMARY CILIA IN THYROID CELL LINES

Utrilla Alcolea JC, Gordillo Martínez F, Fernández Santos JM, Vázquez Román V, Gómez Pascual A, Garnacho Montero C, García Marín R, Morillo Bernal J, Martín Lacave I.

Dpto. Citología e Histología Normal y Patológica. Facultad de Medicina. Universidad de Sevilla.

INTRODUCTION In the thyroid gland, primary cilia have been described, since their discovery in different human tissues, as emerging from the apex of follicular cells. It is known that the primary cilia resorption and protrusion is regulated by cell cycle transitions. In culture cells, the primary cilia have been observed in serum-starved and confluent cultures, in the stationary phase of the cell cycle (G₀); it is generally accepted that primary cilia are disassembled prior to mitosis so that the centrioles can function at the poles of the mitotic spindle. It has also been recently observed that cancer cell lines and cells in primary tumors, which have deregulated cell growth, commonly lack cilia. In the present study, we aimed at analyzing the presence of the primary cilium in the most widely used established cell-line models in the study of thyroid cell function, using double immunolabeling by immunofluorescence. **MATERIAL AND METHODS** Several thyroid cell-lines were cultured: (1) Follicular cells of human (normal, Nthy-ori 3-1; anaplastic thyroid carcinoma, 8505C; follicular thyroid carcinoma, FTC-133) and rat (FRT, PC-C13) origins. (2) C cells of human (medullary thyroid carcinoma, TT) and rat (C-cell carcinoma, CA77) origins. For experiments, cells were seeded at approximately 70% of confluence in a slide chamber and grown until confluence to allow for ciliogenesis. For the double immunofluorescence (IF) study, a monoclonal anti-acetylated γ -tubulin antibody, which labels the axoneme, was used, followed by Cy3-labeled donkey anti-mouse IgG secondary antibody. Then, the slides were incubated with a polyclonal goat anti- γ -tubulin antibody to label the basal bodies, and, subsequently, with a FITC-labeled anti-goat secondary antibody. Samples were visualized with the fluorescent microscope (Olympus BX50), and analyzed with the Image Pro-Plus 7.0 Software (Infaimon). **RESULTS** Primary cilia were observed in all human follicular cell lines tested, both normal and cancerous, although at a clearly lower frequency in cancer cell lines. Specifically, the approximate percentage of ciliated cells was 43% for Nthy-ori 3-1, 21% for FTC-133, and 7% in the case of 8505C cell line. Strikingly, primary cilia were not found in the rat thyroid cell lines tested (FRT and PC-C13). As expected, primary cilia were absent in human thyroid cells Nthy-ori 3-1 grown in the presence of serum. In relation to C-cell cultures, no primary cilia

were detected in any species. **CONCLUSION** As shown before, primary cilia were only detected in thyroid follicular-cell cultures. We also confirm that primary cilia were only observed when cells were serum starved for two days, to induce cell cycle arrest. Therefore, we consider that primary cilium is an organelle of cells in a quiescent or differentiated state.

71 HYPOXIA ISCHEMIA ALTERS THE AUDITORY EVOCATED POTENTIALS AND PRODUCE MORPHOLOGICAL AND CELLULAR DAMAGE IN THE INFERIOR COLLICULUS IN RATS.

(1) Revuelta Aramberri, M., (1) Arteaga Cabeza, O., (1) Alvarez Diaz, A., (1) Hilario Rodriguez, E., (2) Martinez-Ibargüen, A.

(1) Department of Cell Biology and Histology, School of Medicine and Dentistry, University of the Basque Country, Leioa 48940, Spain. (2) Department of Otorrhinolaryngology, School of Medicine and Dentistry, University of the Basque Country, Leioa 48940, Spain.

Introduction Perinatal asphyxia is a problem that leads to neurodevelopment deficits or disabilities, such as learning difficulties, language and attention deficit, hyperactivity disorders and cerebral palsy in newborn infants. It is also a notable risk factor for hearing impairment that affected neonates and affecting the brainstem. The brainstem auditory pathway has been shown to be very sensitive to low blood oxygen concentrations with the consequent damage in the Organ of Corti or loss of brainstem neurons, such as inferior colliculi neurons. This neuronal damage may interfere with nerve conduction and synaptic transmission of the brain producing an acute impairment. Aim Our objective was to analyze the differences in the ABR and to see with histological and cellular methods the damage in the inferior colliculus after a perinatal asphyxia in Sprague ?Dawley rats. Material and methods 7 day rats were randomly assigned to two experimental groups: SHAM operated animals (pups with neither ischemic nor hypoxic injury) and hypoxic-ischemic (HI) group, animals submitted to both ischemia (permanent left carotid occlusion) and hypoxia (reduction of O₂ to 8%) by Rice-Vannucci method. The AEPs were measured by the GSI Audera equipment at 14 days and then, animals were sacrificed and the cochlear nuclei isolated, paraformaldehyde fixed, paraffin included, sectioned and stained with Hypoxi probe-kit. Cellular integrity was analyzed with flow cytometer at 0h, 3h and 12h after the damage. Results The Auditory Pathway was altered during the hypoxic-ischemic insult, with retardation in the latency of the waves. Hypoxia/ischemia seemed to induce auditory functional damage in the neural integrity of the brainstem by increasing the latency of the I-V and III-V waves? ratio. At histological level, the hypoxi-probe kit stained cell exposure to a reduction of the oxygen, so we observe in the HI group a different staining comparing to the SHAM group due to the hypoxic event. Besides we observed differences in the mitochondrial integrity at 0h, 3h and 12h after the damage with a decrease in the membrane potential and integrity. Conclusions Our results suggest that the HI event reduces the auditory capacity and generate morphological and cellular damage in the inferior colliculus. These results are an interest start point for the development of future assays in order to reduce neonatal hypoxic-ischemic induced hypoacusia. Acknowledgments: This work was supported by grants from the Basque Country Government (IT773/13).

HISTOLOGÍA VEGETAL

97 MORPHOLOGY, VIABILITY AND HISTOCHEMICAL PROPERTIES OF ENDEMIC ORCHID SEEDS FROM MEXICO.

(1) Garcia-Suárez, M.D.; (1) Buendía López, Y.O.;(1) Serrano Garcia F.M (2) Mora Ramiro G.; (2) Peña Corona, S.; (3) Lechuga Corchado, J.A.; (4) Gómez Olivares, J.L. y (4) Serrano, H.

(1) Departamento de: Biología, (2 y 4) Ciencias de la Salud y (3) Biotecnología. Universidad Autónoma Metropolitana-Iztapalapa, Av. San Rafael Atlixco 186. México, 09340, D.F., México.

INTRODUCTION. Orchids are one of the three largest of flowering plants with over 25 000 species worldwide ordered in 850 genera, in Mexico we can find 1,260 species distributed on 164 genera that inhabit several vegetation types from semiarid zones up to mesic environments; they are famed for their beautiful and fascinating flowers that are intensively collected. Orchid seeds hold the world record for the smallest seeds of all flowering plants and present a transparent testa with a fusiform aerodynamic morphology, its embryo take up little space within them, relatively undifferentiated when mature with neither endosperm nor cotyledon present. Here we studied orchid seed size; its viability and describe morphology and histochemical properties of several Mexican epiphytic orchids: *Lalelia albida* Batem ex Lindl., *Laelia gouldiana* Reichb.f., *Laelia speciosa* (Kunth) Schltr, *Laelia autumnalis* (Lex.) Lindl. , *Prostechea vitellina* (Lindl.) Higgins and *Cuitlauzina pendula* Lex. in P.de La Llave & J.M.de Lexarza. **MATERIAL AND METHODS.** Seeds were obtained from a local nursery at México City, they were measured in dimensions length and width, tested for their viability with tetrazolium 1% and 10% sucrose solution after three hours exposure. As seeds lack food reserve as an endosperm, food reserves are at the embryo proper, besides embryos do not germinate on their own. Embryo was tested in order to observe oil droplets, starch grains and protein bodies, which were evaluated with histochemical tests using differential dyes: eosine, lugol, sudan III and silver nitrate; observed under a Zeiss light microscope and photographed with a digital camera, measured with Motic Image 2.0 and Image J programs. **RESULTS.** Tetrazolium test is one of the most reliable for evaluation for seed quality and vigour, all seeds proved viable in different percentages, except for *Laelia gouldiana* which presented mock seeds. Seed morphology showed a fusiform testa formed by one-layered irregular reticulated cells, seeds measured between 370-563 μm in length and 88-182.5 μm in width. Embryos length 80.6-292.3 μm and 37-171.0 μm width, being *Laelia autumnalis* the smallest and *Cuitlauzina pendula* the largest. Mature embryos are globular and covered with cuticular sheath, soluble carbohydrates, lipid and protein bodies were found differentially for each species tested. **CONCLUSIONS.** Orchids produce a vast number of this tiny seeds perfectly adapted for wind dispersal and with the strategy to meet their specific obligate mycorrhizal symbiont fungi like *Rhizoctonia* genus, in order to be able to germinate and encounter a suitable host tree and a suitable location. The observed reticulated testa, showed a particular pattern that might be useful as an indicative for systematic studies, particularly for epiphytic orchids. The studied orchid species are endemic to México with limited distribution, some are considered as endangered species, *Laelia speciosa* is under special protection NOM- 059 (Norma Oficial Mexicana); all the viable seeds of these epiphytic orchids might be germinated under in vitro tissue culture techniques in order to promote their conservation.

98 MORPHO-ANATOMY OF THREE Tillandsia SPECIES (BROMELIACEAE) FROM THE ZAPOTITLÁN VALLEY AT PUEBLA MEXICO.

(1) Garcia-Suárez, M.D.; (1) Fraile Ortega, M.E.; (2) Laguna Hernandez G.; (3) Collazo Ortega, M.; (4) Gómez Olivares J.L. Y (4) Serrano,H.

Departamento de: (1) Biología y (4) Ciencias de la Salud, Universidad Autónoma Metropolitana-Iztapalapa, Av. San Rafael Atlixco 186. México, 09340, D.F., México. (2) Laboratorio de Estructura y Fisiología de Plantas y (3) Laboratorio de Desarrollo de Plantas, Facultad de Ciencias, Ciudad Universitaria. Universidad Nacional Autónoma de México. México, 04360, D.F., México.

INTRODUCTION. Within the Zapotilán Valley Puebla a semiarid region located in Central southwest part of Mexico, three epiphytic species of the Tillandsioideae family coexist in two plant communities whose environments are slightly different., the ?Izotal? and the ?Cardonal?, in the first their phorophyte is *Beaucarnea gracilis* Lem and in the second plant community the columnar cacti *Cephalocereus columna-trajani* (Karw) K Schum, *Neobuxbaumia tetetzo* (J M Coult) Backeb and their putative hybrids. Here we studied the morpho-anatomy that has allowed *Tillandsia dasyliiriifolia* Baker, *Tillandsia califanii* Rauh and *Tillandsia recurvata* (L.)L., inhabit in a semiarid land. MATERIAL AND METHODS. Adult plants of the three *Tillandsia* epiphytes were taken out for anatomical studies, leaves and roots were fixed in FAA for transversal semi-thin cuts and a differential dyes: toluidine blue, neutral red and Sudan III ; also synthetic resine was used. Observations and photographs were done with an optical microscope Zeiss and Olympus camera. RESULTS. Leaf anatomy, structure of the three Bromeliaceae were investigated, pelltate scales with shield and wings were observed, the three specie present one-layered epidermis *T. dasyliiriifolia* and *T. califanii* with spherical silica bodies, parenchymatic hypodermis, aquiferous parenchyma, chlorenchyma in median region sometimes with idioblasts with rafidia, interfascicular air canals spherical shaped, filled with irregular stellate cells. Leaves present collateral vascular bundles with sclerified cells, *T. dasyliiriifolia* present bundle sheath of parenchyma, the three present an homogenous mesophyll with large vacuoles, *Tillandsia dasyliiriifolia* *T. califanii* showed sunken stomata and *T. recurvata* is hipostomatic and stomata are at epidermis cells level. Roots present a multi-layered cell rhizodermis forming a velamen, cotex has a multi layered exodermis with transfer cells with thickened walls , below a massive ring of cortical fibers as resistance tissue, parenchyma wit h wide open spaces form the cortex; endodermis present Caspari bands without wall thickenings; one- layered pericyclic cells for *T.dasyliiriifolia* and *T. califanii* multi-layered for *T. recurvata*. CONCLUSIONS. All three species were capable to grow and coexist on the same phorophyte *B. gracilis*, at the Izotal plant community and at the Cardonal, on the *Cephalocereus columna trajai* columnar cacti as support. The morpho-anatomical studies show the characteristics that have allowed these species to grow and develop in a high light, temperature and transpiration environment. The anatomy of the three *Tillandsia* indicate that they may be using the CAM photosynthetic mechanism and the presence of a bundle sheath around the vascular tissue of *Tillandsia dasyliiriifolia* suggest it may be as well using a C4 phothosynthetic pathway as an alternative. The presence of pelltate scales protecting stomata area help to perform a better water use efficiency and a well developed aquiferous parenchyma is related with succulence and water storage. The roots are mainly used as anchors to hold on to a perch, leaves act as collectors for dew and water trickles to the base of the stem where it is abso rved, moisture and nourishment enter through scales on the leaves. All morpho-anatomic characteristics show evidence of several adaptations that enables these three plants to survive in a harsh semiarid environment where temperatures are above 40°C.

HISTOPATOLOGÍA EXPERIMENTAL

20 MUSCLE HYPERTROPHY AND ATROPHY INDUCED BY EXTRACTS FROM RED AND WHITE MUSCLES RESPECTIVELY ON NORMAL RATS

Leiva-Cepas, F.; Ruz-Caracuel, I.; Agüera, E.; Tallón de Lara, C.; Zurita-Lozano, S.; Jimena, I.; Luque E.; Peña J.

(1) Department Morphological Sciences, Section of Histology, Faculty of Medicine and Nursing. University of Cordoba. Spain. (2) Clinical Unit of Neurology. Reina Sofia University Hospital, Cordoba, Spain. (3) Research Group in Muscle Regeneration, University of Cordoba, Spain. (4) Maimónides Institute for Biomedical Research IMIBIC, Reina Sofia University Hospital, University of Cordoba. Spain.

Introduction The soleus and extensor digitorum long (EDL) muscles are very often used in studies of experimental myology and myopathology, especially for comparative purposes because the former is a typical red muscle (85-100% of slow fibers) while the second is a white muscle (95% fast twitch fibers). Both muscles differ in their regenerative capacity, response to denervation and pathological reactions to the same type of injury. Since previous studies have shown that an extract of soleus muscle denervated induce a hypertrophic response in soleus muscle of normal rat, we wonder whether similar extracts obtained from different types of muscles could induce a similar response or whether different types of muscles respond equally to these extracts. **Material & methods** Following a methodology previously published we obtained four types of muscle extracts from Wistar rats: Extracts from normal soleus (mEx-nSOL) and EDL (mEx-nEDL) muscles and extracts from soleus (mEx-dSOL) and EDL (mEx-dEDL) muscles after 4 days of denervation. 16 Wistar rats were divided in four groups (n=4) and were injected for 10 consecutive days with 1 ml i.p. of these extracts; normal untreated rats were used as control. The soleus and EDL muscles were then dissected and processed for light microscopy. Cryosections were stained with histological, histochemical and immunohistochemical techniques for skeletal muscle. Morphometric analysis was performed with ImagePro Plus 4.5 software and measured the following parameters: mean fiber cross-sectional area, mean fiber minor diameter, number of muscle fiber /area and number of myonuclei / fiber; the data were analyzed statistically with SigmaStat 3.1 software. **Results** Data from morphometric and statistical analysis revealed that the same muscle responds differently to different extracts. Thus, extracts derived from soleus muscle induced a hypertrophy response in both soleus and EDL muscles, while extracts obtained from EDL induced muscle atrophy. Both types of response (hypertrophy and atrophy) were significantly more potent when extracts were obtained from denervated muscles. **Conclusion** Our results suggest that muscle atrophy and hypertrophy response may depend, at least in part, to factors specific of muscle type, which are to some extent controlled by innervation.

22 MONITORING AND DIAGNOSIS BY ULTRASOUND OF HISTOLOGICAL CHANGES IN MUSCLE CONTUSION LESIONS

Jimena, I (1, 3, 5); Ruz-Caracuel, I (1, 3); Leiva-Cepas, F (1, 3); Jiménez-Fermín, M.(2); Agüera, A. (1, 3); Benito-Ysamat, A (1,4); (7) Jiménez-Díaz F.J (2); Peña J (1, 3, 5)

(1) Research Group in Muscle Regeneration, University of Córdoba, Spain (2) Laboratory of Performance and Sports Readaptation, Faculty of Sport Sciences, University of Castilla-La Mancha, Spain (3) Department Morphological Sciences, Section of Histology, Faculty of Medicine and Nursing. University of Córdoba. Spain (4) Section of Musculoskeletal Radiology, Reina Sofia University Hospital, Córdoba, Spain (5) Maimónides Institute for Biomedical Research IMIBIC, Reina Sofia University Hospital, University of Cordoba. Spain

Introduction Muscle ultrasound (US) is a well-known validated imaging technique for the evaluation of patients with suspected neuromuscular disorders, diagnosis of sports muscle injuries and follow-up studies to evaluate the results of treatment in muscle. In a previous study we correlated US findings with histological changes taking place during an experimentally induced degeneration?regeneration process in rat skeletal muscle using a myotoxic agent. Sequential histological study allowed controlling US characterization in terms of basic sonographic criteria and facilitates ultrasound interpretation of muscle healing process. However, conflicting results with other studies may be explained by the type of muscle injury. Therefore the aim of this study was to analyze the eco-histologic correlation in an experimental model of muscle contusion injury, since direct contusion is one of the most common mechanisms of muscle injury in sports. Material & methods Wistar rats were subjected to an injury in the gastrocnemius muscle using a falling ball technique in a system designed by us, based on similar models. Seven groups (n=4 each) were sacrificed at different times after injury (immediately, 1, 3, 6, 10, 15 and 20 days); uninjured rats were used as control. All animals were sacrificed immediately after performing ultrasonographical analysis with a portable ultrasound machine to proceed to the extraction of the muscles, that were processed for microscopic study with histological, histochemical and immunohistochemical techniques. Results In this contusion injury model, ultrasonographic changes were not evident in relation to changes in echotexture and eointensity on different days; nor the color flow and power Doppler sonography showed clear changes indicative of increased blood flow. Conversely, lesions were observed and subsequent regeneration times were analyzed histologically: degenerative changes (degeneration and necrosis of muscle fibers, edema and inflammation) were evident in the early stages (0, 1 and 3 days) and regenerative changes were observed at later stages (6, 10, 15 and 20 days). However, all these changes were found scattered, alternating with histologically normal muscle fibers. 20 days after injury, small fibrotic nodules surrounded by small regenerative muscle fibers were observed in two rats. Conclusion Our results suggest that the absence of muscle changes in US, or some defined sonographic appearance, does not guarantee the absence of tissue lesion. This implies that some patterns of muscle lesions that could be related to the types of myopathological changes, frequency and territorial distribution in the muscle can not be well recognized by US.

26 PRIMARY CILIA ORGANIZATION IN TWO DIFFERENT MODELS OF TUMORS

Junquera C., Muñoz G., Luesma MJ., Monleón E., Berga C., Gómez A., Castiella T.

University of Zaragoza

INTRODUCTION The primary cilium is a non-motile organelle whose axoneme is made of nine peripheral doublets of microtubules (9+0). Primary cilia (PC) are found in many differentiated cells, acts as sensory cellular antennae that could co-ordinate some cellular signaling pathways. The finding that PC are linked to cell cycle regulation and progression has led to suggestions that they may play a role in tumor formation. Hedgehog, Wnt and PDGFR?? signaling can promote cell proliferation, and excessive signaling can lead to cancer. The ultrastructural characterization and location of these cilia in tumoral cells therefore provide interesting data for cancer research. We investigated by electron microscopy PC structure and organization in two different model of tumors, with mesenchymal (gastrointestinal stromal tumor, GIST) and epithelial (vesical urothelial carcinoma) origins. **MATERIAL AND METHODS** A total of 8 GIST and 8 bladder cancer biopsies were processed following standard TEM protocol. All samples were provided by the Hospital Clínico Lozano Blesa from Zaragoza. All the protocols developed were approved by the Ethical Committee of Clinical Research of Aragón (CEICA). **RESULTS** In bladder carcinoma, tumoral cells presenting PC have specific location, just on top of basal lamina. The beginning of the ciliogenesis is observed in some epithelial cells where centrioles have moved and lost their typical perpendicular layout. They laterally present many satellites to which microtubules are anchored in some occasions. The cilium appears to grow within the cell body, upon docking of the mother centriole appendices to a vesicle of Golgi origin. The mother centriole moves until the membrane surface contacting by means of transitional fibers giving rise to the ciliary basal body. The axoneme lacks the central pair of microtubules and extends to the outer surface of the membrane in a short length (100 - 200 nm), making really difficult to locate this nanostructure. On the other hand, a high percentage of tumoral cells from GISTs present PC (1 - 2 μm length) projected into the extracellular space and emerged close to nucleus. The axoneme is a direct extension of a typical basal body and contains nine outer doublet microtubules, exhibiting a 9+0 pattern. The parental and daughter centrioles display peripheral satellites from basal body; transitional fibers (alar sheets) extended outwards from each microtubular triplet and establish contact with plasma membrane. The cilium remains partially intracellular within a membrane invagination, the ciliary pocket. The axoneme of the cilium lies parallel to the cellular membrane, where multiple pinocytic vesicles appear. No decrease of number of cilia has been observed depending on the tumoral progression. **CONCLUSIONS** An increasing number of tumors harboring primary cilia are now being found. Thus, at present, new lines of research have branched off to investigate the role of primary cilia adult homeostasis and tumor formation. Figure 1.- Transmission electron microscopy. Ultrastructure of the primary cilium A) Urothelial cell carcinoma. B) GIST tumoral cell. G: Golgi apparatus; bb: basal body; C2: daughter centriole. tf: transitional fibers; ax: axonema; pv: pinocytic vesicles; s: satellites.

44 EBULIN F CAUSES PNEUMONIA, INTESTINE ATROPHY AND FOCAL MYOCARDIAL DEGENERATIONS IN ELDERLY MICE

(1) Vaca Fernández, P.L.; (2) Garrosa García, M.; (3) Jiménez López, P.; (4) Tejero del Río, J.; (5) Cabrero Lobato, P.; (6) Córdoba Díaz, D.; (7) Quinto Fernández, E.J.; (8) Gayoso Rodríguez, M.J.; (9) Girbés Juan, T.

Area of Histology, Faculty of Medicine and INCYL. University of Valladolid (1, 2 and 8). Nutrition and Bromatology, Faculty of Medicine and CINAD. University of Valladolid (3, 4, 5, 7 and 9). Pharmacy and Pharmaceutic Technology, Faculty of Pharmacy and IUFI. Complutense University of Madrid (6). Spain

INTRODUCTION Ebulin f is a type-2 ribosome-inactivating protein (RIP) present in dwarf elder fruit. It is composed of an A and a B polypeptide chains, the former showing N-glycosidase activity, while the B-chain selectively bonds to D-galactose, which confers the nature of lectin to the protein. The function of these RIPs in the plant has been proposed to be defensive against insects, viruses and fungi by causing the irreversible inactivation of ribosome and promoting apoptosis. The presence of ebulin f in certain food products and its potential application in medicine to cause selective apoptosis in transformed cells make the study of the toxicology of this protein of special interest. **METHODOLOGY AND MATERIALS** Highly purified ebulin f was isolated from green fruits and injected via i.p. to 6- and 12 month-old female Swiss mice as follows: a single dose of either 1.4, 2.1, 2.8 or 5.0 mg/Kg body weight dissolved in 0.1 M phosphate buffer saline pH 7.4. Control animals of both ages were injected with the vehicle only. Two weeks after administration of the toxin, all surviving animals were anesthetized with isoflurane and sacrificed by decapitation. Samples of lung, stomach, small and large intestine and heart were taken and fixed by immersion in 4% paraformaldehyde. Pieces were processed for paraffin embedding, sectioned at 7 µm and stained for light microscopy with hematoxylin and eosin, Masson trichrome or TUNEL method. Care and manipulation of animals followed the guidelines of the 2010/63/EU directive. **RESULTS** A reduction in body weight was observed in all experimental groups after treatment, the weight being recovered in 3 to 4 days. The injection of ebulin f at 1.4 mg/Kg killed half of the animals in 14 days, whereas at 2.1 mg/Kg killed all the animals in 8 days. Experimental animal lungs showed pneumonia at different phases independently of the dose injected, albeit it appeared more severe in 12-month old animals. Doses equal or higher than 2.1 mg/Kg caused a mild atrophy of Lieberkühn's crypts and increased number of apoptosis both in enterocytes and in Paneth cells. The decrease in cell renewal and resulting atrophy led to a shortening of both intestines. Myocardium appeared slightly altered in experimental animals, in which scattered foci of cardiac muscle degenerations could be observed. **CONCLUSIONS** Elderly mice appear more sensitive to ebulin f than young animals since, after treatment, the former die around one week earlier than the latter. The toxicity of ebulin f as compared to ricin is considerably lower when injected i.p. Our study suggest that the action mechanism of ebulin f does not seem to be a simple arrest of protein synthesis, but comprises the promotion of other mechanism triggering apoptosis. When dwarf elder fruits are ingested, special care must be taken, such as boiling, to inactivate the protein. Finally, taking into account its lectin activity and its promotion of apoptosis in the small intestine, there is an interesting research line open to address its potential use as specific drug against intestinal tumors.

55 HEPATIC ENDOTHELIAL CELL IN LIVER TISSUE TARGETED BY SPECIFIC NANOPARTICLES

Marquez Clavijo, J.(1); Fernández Piñeiro,I.(2); Unda Rodriguez, F.(1); Ibarretxe Bilbao, G.(1); Sánchez Barreiro, A.(2); Badiola Etxaburu, I.(1).

(1) Department of Cell Biology and Histology. Faculty of Medicine and Dentistry. University of the Basque Country. Universidad del País Vasco/Euskal Herriko Unibertsitatea. Leioa 48940, Bizkaia. SPAIN. (2) Department of Pharmacy and Pharmaceutical Technology. Faculty of Pharmacy. Praza Seminario de Estudos Galegos, s/n. Campus sur. 15782 Santiago de Compostela. SPAIN

Introduction: Endothelial cells recover blood vessel and maintain the physiology and architecture of vasculature. In the case of the liver, the blood vessels and sinusoids are recovered internally by endothelial cells. The role of endothelial cells in the blood pressure regulation, immune response, coagulation or hormone synthesis has been described. Endothelial cells are very important cells not only for the homeostasis of the body but also in some pathologies. In this project, we studied the presence of cell membrane proteins in different endothelial cells of liver tissue, comparing the endothelial cells of sinusoid respect to endothelial cells of blood vessels of portal triad. Methodology and Materials: We used nanoparticles based on sorbitans esters, coated with different molecules to analyze the differential protein expression of endothelial cells from the great vessels respect to endothelial cells of sinusoid. Nanoparticles were coated with different molecules such as xantane, chondroitin sulphate and pullulan. To ensure the interaction of the nanoparticle with the cell, nanoparticles were loaded with a GFP-plasmid. Different nanoparticles were injected systemically into the mouse tail vein and after 72 hours, green fluorescence signal was produced. Results: We found that pullulan covered nanoparticles did not interact with endothelial cells, while those coated with xantane induced green fluorescence in the endothelial cells of blood vessels of portal triad. However, nanoparticles coated with chondroitin sulphate stimulated green fluorescence in the endothelial cells of sinusoids. Conclusion: Endothelial cells of liver tissue expressed different proteins in their surface depending if there are in the blood vessels of portal triad or in the sinusoid. Finally, xantane/chondroitin sulphate nanoparticles could be used to deliver drug for liver disease to specific endothelial cells.

65 ETHAMSYLATE TREATMENT IN ENDOTOXIN-INDUCED UVEITIS

(1) Solís Ruiz, J.; (2) Mérida Donoso, S.; (3) Mayordomo Febrer, A.; (3) López Murcia, M.; (2) Ramirez Lamelas, T.; (2,4) Bosch-Morell, F.; (1,5) Sancho-Tello Valls, M.

(1) Departament de Patologia, Facultat de Medicina i Odontologia, Universitat de València, Valencia; (2) Instituto de Ciencias Biomédicas, Departamento de Ciencias Biomédicas, Facultad de Ciencias de la Salud, Universidad CEU Cardenal Herrera, Valencia; (3) Departamento de Medicina y Cirugía Animal, Facultad de Veterinaria, Universidad CEU Cardenal Herrera, Valencia; (4) FISABIO, Oftalmología Médica, Valencia; (5) INCLIVA, Hospital Clínico Universitario, Valencia.

INTRODUCTION. Ethamsylate is a haemostatic non-thrombogenic agent involved in the inhibition of prostaglandin synthesis, which has also several anti-inflammatory effects. Thus, the aim of the present study was to investigate the possible anti-inflammatory effect of ethamsylate in an experimental model of endotoxin-induced uveitis. **MATERIAL AND METHODS.** Twenty adult New Zealand male rabbits, weighting between 1.2 and 1.5 kg, were used. Rabbits were randomly assigned to 4 different experimental groups: Control (C), Uveitis (E), Uveitis plus Ethamsylate (EF) and Ethamsylate (F). All rabbits received 2 intravitreal injections: a first injection contained 10 µl of saline solution in the absence (groups C and F) or presence (groups E and EF) of 1 µg of Endotoxin. Immediately after the first injection, all animals received a second intravitreal injection of 100 µl of saline solution in the absence (groups C and E) or presence (groups F and EF) of 12.5 mg of Ethamsylate. Twenty-four hours after treatment, rabbits were sacrificed and enucleation was immediately carried out in order to fix the eyes in formaldehyde. After fixing, a sagittal section of the eyeball was done, the lens was removed, and samples were processed with standard paraffin embedding procedure. Finally, 5 µm-thick sections were obtained and they were stained with both haematoxylin-eosin and Masson's trichrome. Two evaluators blindly studied all samples in order to measure the presence of inflammatory cells with a 4 levels-scale (0 absence, 1 light, 2 mild, 3 severe). **RESULTS.** Control samples (C) responded adequately to the treatment, not showing any kind of inflammatory reaction, setting a good standard for comparison. The samples treated with Endotoxin (E) showed clear signs of uveitis, with mild or severe presence of inflammatory cells in the ciliary body and in the anterior, posterior, and vitreous chambers. Ethamsylate plus Endotoxin-treated samples (EF) showed a reaction similar to that observed in the E group, with the presence of inflammatory cells in the same places and with a similar intensity in both groups. Finally, samples treated only with Ethamsylate (F) showed a light inflammatory reaction, which was lower than in samples treated with Endotoxin (E and EF) but higher than controls (C). Retinas showed a slight or mild infiltration of inflammatory cells in E and EF groups. In addition, there was a great vasodilation, especially in the ciliary processes of E and EF groups, while it was lower in F samples and absent in controls. **CONCLUSIONS.** Ethamsylate administration induces a light uveitis 24 hours after its administration, but it does not seem to modify the inflammatory process in endotoxin-induced uveitis. **ACKNOWLEDGEMENTS.** This study was partly supported by PRCEU-UCH 13/17 (CEU ? BANCO SANTANDER).

94 ALCOHOL INGESTION IN RATS WITH MILD BILE DUCT LIGATION PRODUCE HEPATIC ENCEPHALOPATHY WITH COGNITIVE AND MOTOR IMPAIRMENT

(1,3) Giménez-Garzó, C; (2,3) Ruíz-Sauri, A; (3) Agustí, A; (3) Mangas-Losada, A; (1,3) Garcia-García, R; (3) Urios, A; (2,3) Carda, C; (1) Felipo, V; (2,3) Montoliu, C.

(1) CIPF (2) UV (3) INCLIVA

Background and Aims: Studies in animal models allow identifying mechanisms and treatments for cognitive and motor alterations in hepatic encephalopathy (HE). Liver diseases leading to HE in humans have different aetiologies (alcoholic, viral, etc). The International

Society for Hepatic Encephalopathy points out that satisfactory model for HE resulting from alcoholic cirrhosis are lacking.

Methods: This work aimed to develop and characterize an animal model for HE in alcoholic liver cirrhosis. To potentiate the effects of alcohol on liver we administered it (5, 8 or 10% in drinking water) to rats showing mild liver damage induced by “mild” bile duct ligation (MBDL), obtained by sectioning 3 out of 5 bile ducts.

Results: MBDL rats show increased markers of cholestasis and liver damage, hyperammonemia and inflammation. MBDL rats also show motor in-coordination, hypokinesia, impaired learning ability in a Y maze and reduced spatial memory in the Morris water maze.

Ingesting 10% ethanol does not induce relevant liver damage in control rats but potentiates liver damage in MBDL rats. In contrast, ethanol did not enhance the biochemical or neurological alterations in MBDL rats. This supports that the combination of certain levels of hyperammonemia and inflammation is enough to induce mild cognitive impairment, even in the absence of liver cirrhosis.

Conclusions: Rats with MBDL and MBDL-OH survived more than 3 months, allowing performing longterm studies on cognitive and motor alterations and on underlying mechanisms. MBDL-OH rats are a good model to study the mechanisms of ethanol-induced liver cirrhosis and the factors making the liver susceptible to ethanol damage.

105 MAY CANNABINOIDS PREVENT THE DEVELOPMENT OF CHEMOTHERAPY-INDUCED DIARRHOEA AND INTESTINAL MUCOSITIS? EXPERIMENTAL STUDY IN THE RAT

(1) De Andrés, R.; (3) Pérez-García, I.;(2, 3, 4, 5) Vera, G.; (2, 3, 4, 5) Girón, R.; (2, 3, 4, 5) Martín-Fontelles, MI.; (2, 3, 4, 5) Abalo, R.; (1, 2, 5)Uranga, J. A.

(1) **Histología y Anatomía Patológica (URJC)**, (2) **Unidad Asociada al CIAL (CSIC)**. (3) **Farmacología y Nutrición (URJC)**, (4) **Unidad Asociada al IQM (CSIC)**, (5) **Grupo de Excelencia de Investigación en Dolor URJC-CSIC-Santander. Fac. Ciencias de la Salud. Univ. Rey Juan Carlos, Avda. de Atenas s/n, 28922 Alcorcón, Madrid (Spain)**.

Introduction: 5-fluorouracil (5-FU) is an antimetabolite drug used for treatment of solid tumours. However, it may induce important adverse effects comprising stomatitis, oesophagitis, anorexia, nausea, vomits, diarrhoea and enteritis. To our knowledge, a thorough assessment of the effects of 5-FU on gastrointestinal histological architecture and its physiology has never been previously performed. On the other hand, activation of CB1 and CB2 cannabinoid receptors reduces gastrointestinal motility, secretion and inflammation. Therefore, cannabinoids might be useful to counteract the adverse effects of 5-FU on the gastrointestinal tract. Our aim was to characterise the effects of 5-FU, alone or in combination with the synthetic mixed cannabinoid agonist WIN 55,212-2 (WIN) by means of histological and non-invasive (radiographic) motility methods in the rat.

Methods: Male adult Wistar rats (250-400 g, n=8 rats/group) received saline or 5-FU (150 mg/Kg, ip) for two consecutive days (cumulative dose, 300 mg/Kg). WIN (0.5 mg/Kg, ip) or its vehicle were injected for four days, starting 30 min before the first antineoplastic drug administration. On day 4, gastrointestinal motility was analysed radiographically after barium administration (Cabezos et al, 2008). At the same time-point, gut wall alterations were analysed on histological cross sections with HE, PAS and Van Gieson staining. General damage of ileum wall, villi size, number of goblet cells and submucosa and muscular layers thickness were evaluated.

Results: Four days after 5-FU, animals showed less weight than their controls, and diarrhoea was clinically and radiographically apparent. Mucositis was evident in ileum after 5-FU treatment with an increase in the general histological damage. Similarly, villi size was reduced significantly in the groups treated with 5-FU. Number of the epithelial goblet cells and thickness of both muscular layers were also decreased. On the contrary, submucosa thickness was increased with 5-FU. These functional and histological effects were not prevented in WIN-treated animals.

Conclusions: The antineoplastic drug 5-FU induces weight loss and intestinal mucositis in the rat with important damage to the three main structures of the intestinal wall. This was associated to diarrhoea which could be detected radiographically. WIN did not prevent the histological or functional effects of 5-FU in the gut, although this could be due to the low dose used.

Acknowledgements: Supported by: SAF2012-40075-C02-01 (MINECO), S2010/BMD-2308, and PRIN13-CS20 (URJC). Thanks to Raquel Franco, Julio Paredes, Antonio Márquez and M^a Carmen Merino for technical assistance.

106 TISSUE EFFECTS OF HIGH FAT DIETS ON ORGANS RELATED WITH METABOLIC SYNDROME AND DIET-RELATED CANCERS

(1, 2, ·) Uranga, J.A; (1) de Andrés, R; (6) Moreno, S; (6) Fernández, F ; (2, 3, 4, 5) Girón, R; (2, 3, 4, 5) Herradón, E; (5)González C; (2, 3, 4, 5) Vera, G; (2, 3, 4, 5) Abalo, R; (6) Miguel, M ; (2, 3, 4, 5) López-Miranda, V

(1)Histología y Anatomía Patológica, Fac. Ciencias de la Salud. Univ. Rey Juan Carlos (URJC), Madrid (2) Unidad Asociada al CIAL (CSIC), (3) Grupo de Excelencia de Investigación en Dolor URJC-Banco de Santander, (4) Unidad Asociada al IQM (CSIC), (5) Farmacología y Nutrición (URJC), (6) Instituto de Investigación en Ciencias de la Alimentación (CIAL-CSIC).

Introduction: Dietary habits play a key role in the development of the metabolic syndrome (MS). Similarly, an increased body mass index, the reduced intake of fiber and high fat diets are risk factors in cancer and patients with diabetes mellitus 2 show increased susceptibility to aggressive tumors like those affecting the pancreas, liver and colon. Correction of these metabolic problems would eventually make it possible to prevent these problems. We have used an experimental model of MS induced by cafeteria-diet in rats to look for a relationship between tissue markers, functional, and plasma parameters with the risk for developing some types of cancer, namely pancreas, liver and colon.

Methods: Male Wistar rats, 8 weeks of age, were fed ad libitum with a high-caloric and high-fat diet (22% fat, 48% carbohydrates, 20% proteins) and filtered tap water with no sugar or 25% fructose or 25% dextrose added for 18 weeks. A fourth group was fed with the same diet with fructose except that fat was hydrogenated. Control animals were fed with a standard diet (5% fat, 53% carbohydrates, 23% proteins) with no added sugars. At the end of the experimental period, pancreas, liver, colon, kidneys, epididimal fat and brown interscapular adipose tissue were fixed and stained with H&E, PAS and Van Giesson. Antibodies against CD163, GLUT2, COX2, leptin, insulin and Lgr5 were assayed as tissue or precancerous markers.

Results: Animals fed with high fat and sugar diets increased their body weight. Appearance of white adipose tissue was normal with no lymphocyte infiltrates. However, adipocytes were hypertrophied in all fat diets compared to controls, especially in the hydrogenated fat group and when sugars were added. Brown fat was highly infiltrated with white adipocytes, mainly in the groups fed with fructose. Similarly, the liver showed a moderate steatosis, which increased with sugars and hydrogenated fat. There were no differences between groups regarding COX2 expression or kidney damage. On the contrary, pancreas showed a decrease in islets size when animals were fed with sugars. Finally, colon showed an increased damage with small ulcers and a larger size of Peyer's patches when animals were fed with hydrogenated fat and/or sugars. No differences were appreciated regarding CD163, leptin or Lgr5.

Conclusions: The consumption of high fat and sugar diets increases body weight and generates adipocyte hypertrophy and liver steatosis. It did not involve an increased expression of oxidative stress (COX2), irritable bowel syndrome (leptin) or colorectal cancer (Lgr5) markers.

Acknowledgements: Supported by SAF2012-40075-C02-01 (MINECO) and Mapfre 2013 (Fundación Mapfre). Thanks to Raquel Franco, Julio Paredes, Antonio Marquez and M^a Carmen Merino for technical assistance.

136 RESVERATROL IMPROVES MITOCHONDRIAL INNER MEMBRANE INTEGRITY AND POTENTIAL AFTER HIPOXIA-ISCHEMIA

(1) Arteaga Cabeza, O.; (1) Revuelta Aramberri, M. ;(2) Urigüen Echevarria, L.; (3) Martínez Ibarguen, A; (1) Álvarez Díaz, A and (1) Hilario Rodriguez, E.

(1) Cell Biology & Histology, (2). Pharmacology, (3).Otorrhinolaryngology, School of Medicine & Dentistry, University of the Basque Country (UPV/EHU), Leioa, Bizkaia, Spain.

INTRODUCTION: Perinatal cerebral hypoxia-ischemia (HI), a common neurologic injury, is a major cause of morbidity in survivors. Resveratrol (RVT) is a natural polyphenol found in grapes with several anti- apoptotic, anti-inflammatory and antioxidants properties. The aim of the present study was to investigate whether resveratrol was neuroprotective in a rat model of HI. **MATERIAL AND METHODS:** By permanent ligation of the left common carotid artery and then by asphyxia for 135 minutes with 8% O₂ hypoxic-ischemic brain injury was provoked when rats were P7. Then they were randomly assigned to: sham, hypoxia-ischemia (HI) and HI animals that received a single dose of 20 mg/kg of RVT 10 minutes before hypoxia (HI+RVT). Animals were sacrificed immediately (0 h), 3 h and 12 h after HI event in order to evaluate

mitochondrial state by flow cytometry. Mitochondrial inner membrane integrity was determined by using the fluorochrome Nonyl Acridine Orange (NAO) and mitochondrial transmembrane potential was analyzed by Rhodamine 123 (Rh 123). P14 brains were stained with Nissl and immunolabelled with GFAP. RESULTS: Regarding mitochondrial integrity, at 12 h, while HI group underwent a diminishment with statistical differences with respect to the Control group in the percentage of NAO positive cells, pretreated ones maintained mitochondrial inner membrane integrity. In regard to mitochondrial transmembrane potential, pups subjected to the HI event showed an important decrease in the percentage of Rh 123 positive cells, but rats pretreated with RVT presented similar values to controls. On P14, HI animals showed swollen and deformed neurons especially in the ipsilateral CA 1 and CTX areas, while only mild cell loss and a few damaged neurons were observed in slices from animals pretreated with RVT. A substantial increase of ipsilateral GFAP immunostaining was observed in hippocampus and parietal cortex of animals that underwent hypoxia-ischemia respect to controls, but RVT pretreatment avoided this increase. CONCLUSIONS: Our results suggest that resveratrol protects against hypoxic-ischemic brain injury reducing cell damage, minimizing astroglial response and maintaining mitochondrial inner membrane integrity and potential. Acknowledgments: This work was supported by grant from the Basque Government IT 773/13 and BFI-2011-129.

139 PLACENTAL OXIDATIVE STRESS CAUSED BY TWO DIFFERENT STRAINS OF TRYPANOSOMA CRUZI INDUCES TROPHOBLAST ALTERATIONS

Triquell MF, Díaz-Luján CM, Moreira-Espinoza MJ, Mezzano L., Benizio E, Piegari M, Fretes R.

Departamento de Biología Celular, Histología y Embriología - Facultad de Ciencias Médicas - Universidad Nacional de Córdoba

Placenta is an organ physiologically exposed to high levels of oxidative stress and several pathologies like preeclampsia, diabetes and infectious diseases exacerbate this condition. *Trypanosoma cruzi* (*T. cruzi*) is the causative agent of Chagas disease that could be transmitted in a low percentage from the Chagasic pregnant mother to the fetus through the placenta. Nitric oxide (NO) and oxidative stress are mechanisms that prevent microorganism invasion and fetal infection, but the effect of these mechanisms in chagasic pregnancies and specifically in placental infection is actually unknown. Thus, the objective of the present work is to study the effect of oxidative stress caused by two different strains of *T. cruzi* in the placental tissue and their participation in the infection.

Materials and Methods. Placental villi explants were co-cultured for 24 hs with 1×10^6 trypomastigotes of Tulahuen and Lucky strains (isolated from a congenital case) and with addition of endothelial Nitric Oxide Synthase (eNOS) inhibitor L-NAME (1mM, 0,1mM), addition of N-acetyl Cysteine (NAC) as reactive oxidant species (ROS) scavenger (5mM – 10 mM) and addition of H_2O_2 (200 μ M – 500 μ M). Controls: without parasites in similar conditions as above. Histological analysis and quantification of the detachment area of Syncytiotrophoblast (STB) and eNOS and Nitrotyrosine expression were done. In culture media: quantification of NO (Griess), hCG with ELISA quimioluminescence. Tissue

homogenates: Gamaglutamiltranspeptidase (GGT) activity to measure oxidative stress. Real time PCR quantifying *T. cruzi* using TCZ primers was also performed.

Results. The infection of placental villi with both strains of *T. cruzi* caused an increment in more than two fold NO production than control, eNOS RNA and protein expression and protein nitrosilation ($p < 0.05$). Detachment of STB was increased significantly with both strains of *T. cruzi* and this phenomenon was similar in cultures with addition of H_2O_2 . ($p < 0.05$) and the concentration of hCG decrease. The activity of GGT increased the presence of both strains of *T. cruzi*. When eNOS was inhibited with L-NAME we observed a significant augment of detachment of STB and parasite infection respect to control. STB detachment was diminished with addition of NAC.

Conclusions. These data suggest that NO participate in the control of *T. cruzi* infection, because when the production of NO was inhibited with L-NAME the quantification of infection was higher, that might explain the low incidence of congenital transmission. On the other hand, the STB detachment induced by both strains of *T. cruzi*, which alters the structure of placenta barrier in placental villi, seems to be caused by NO and oxidative stress, and could establish a parasite gateway to the placenta.

Aknowledgments: To Gina Mazzudulli for her technical assistance. Grants: FONCyT-PICT 2012-1061, SECyT-Universidad Nacional La Rioja, SECyT-Universidad Nacional Cordoba.

144 EXPRESSION AND LOCALIZATION OF ENZYMES INDOLEAMINA 2,3-DIOXYGENASE AND ARYL HYDROCARBON RECEPTOR IN CHAGASIC PLACENTAS

Moreira-Espinoza, M.J. (1), Triquell, M.F.(1), Moran, J.P.(1), Piegari, M.(1), Mezzano, L.(1), Díaz-Lujan, C.(1), Fretes, R.E.(1)(2)

(1)Laboratory of Placenta and Chagas, Cell Biology, Histology and Embryology Department, School of Medical Sciences, Universidad Nacional Córdoba-INICSA (CONICET), Argentina. (2)Histology, Embryology and Genetic - IICSHUM, Universidad Nacional La Rioja, Argentina.

Indoleamine 2,3-dioxygenase (IDO) is an intracellular enzyme, that is constitutively expressed in placenta. It is implicated in depleting Tryptophan (Trp). The product, kynurenines are substrate for Aryl Hydrocarbon Receptor (AhR) enzyme, which is also expressed in placenta. Both IDO and AhR are crucial for modulating immune response in pregnancy. This system is involved in the resistance to *Trypanosoma cruzi* infection, the causal parasite of the Chagas disease, in experimental conditions. Therefore, this system might be participating in the congenital transmission of the Chagas disease. Objective: to analyze the expression and localization of IDO and AhR in placentas from chagasic pregnant women (CPW). Methods: Paraffin-embedded placental tissues from healthy pregnancies (control) (PN) (n=5) and CPW (n=14), who transmitted (CHWT) (n=5) or not (CHNT) (n=9) the infection to their new born were used. Slices of placental tissue were stained with anti-IDO and anti-AhR by Immunohistochemistry. Primary antibodies were replaced for control of the technique. Immunodetection was analyzed at 40X and semi-quantified employing ImageJ software.

Statistical analysis was performed using GraphPad Prism by Student's t Test and ANOVA, with Bonferroni post-hoc differences with p-value of <0.05. Pearson's Correlation Coefficient (r) between the IDO and AhR proteins levels was performed. Results: The strongest IDO staining was seen in PN, located in endothelial cells of all types of blood vessels. There are also some positive mark in stromal cells (SC). In CHNT there was a weak staining in endothelia of small or larger vessels and SC. An intermediate positive staining was observed in CHWT in small vessels and SC. IDO was not expressed at Syncytiotrophoblast (STB). The expression of IDO was significantly reduced in CPW (mainly in CHNT) respect to PN. There are significantly differences in IDO protein levels between PN and CPW, as well as between CHNT and CHWT. A moderate AhR staining was observed in PN, located at STB and SC. Weak AhR staining was found in CPW, localized in SC and some endothelium of small blood vessels. No difference in AhR proteins levels was found between PN and CPW. No significant correlations was found between IDO and AhR. Conclusion: Reduced activity of IDO in CPW, and specifically in those placentas from pregnant who not transmitted the congenital infection may deplete Trp in a deficient manner with production reduced of kynurenines. However, there was not modification of AhR expression in CPW respect PN. This work analyzed two key enzymes of the immune system in pregnancy, finding significantly modifications in the protein expression in chagasic placentas related to congenital transmission of the Chagas disease.

Grants: FONCyT-PICT 2012-1061, SECyT-Universidad Nacional La Rioja, MINCyT-PID (Cba), SECyT-Universidad Nacional Córdoba.

Keywords: IDO, AhR, Chagasic disease, placenta.

148 HEALTH DIAGNOSTIC IN THE LIVER OF CATFISH (*Ariopsis felis*) ASSOCIATED WITH POLLUTION OF THE ENVIROMENT

Román-Zepeda, P., Arteaga Silva, M., Jiménez Morales, I., Hernández Calderas, I., Jerónimo-Juárez, J. R., Ramírez Romero, P. & Guzmán García, X.

Universidad Autónoma Metropolitana. Unidad Iztapalapa. División de Ciencias Biológicas y de la Salud.

Environmental perturbations affect aquatic organisms, which are proposed as biomarkers that provided pollution-environment relationship. Histopathology, with another biomarkers, is a useful tool to evaluate exposition or damage to environmental stress. Hepatosomatic (HI) and gonadosomatic (GI) indexes, condition factor (FC) and the use of biomarkers allow establishing health state of organisms. The aim of this work was to assess some morphometric parameters and tissue structure, alterations and physiological responses in the liver of catfish from two monitoring sites (Río Tecolulta, Ver and Ría Celestún, Yuc). Water physicochemical parameters of each study site were registered. Five catfish (*Ariopsis felis*) of each area were collected and biological data, like macroscopic lesions, parasites and morphometric parameters, per sample was recorded. Hepatosomatic index (IH), gonadosomatic index (IG) and condition factor were calculated. The liver of each organism was histologically processed, fixing it with formalin buffered at 10 %, then dehydrated, cleared and infiltrated, for subsequent embedding in paraffin wax. Each sample was cut in three serial tissue sections, which were stained with Hematoxylin

and eosin (H&E stain), seen at optical microscopy, making a damage level table and digitalizing images. Physicochemical characteristics, registered for water in the study area, matches with the reported for brackish estuarine aquatic systems. IG, IH and condition factor showed that the organisms were suitable for merchandising. We observed presence of hepatic parenchyma formed by hepatocytes, veins, arteries, bile ducts and hepatopancreas. Histopathological analysis suggests that organisms have disturbances in their hepatic structures, mainly inflammation, melano- macrophage centres, infiltrations and atrophy. Collected organisms at Tecolutla, Ver. show more prevalence of injuries that organisms collected in Ría Celestún, Yuc., although later samples have wounds that jeopardize their health. Injuries seen were categorized like reversible, and exposition biomarkers expression suggest activation of metabolic mechanisms in response to environmental stress, however is necessary to continue monitoring to establish the health diagnosis of the organisms and the health of the study site.

149 HEALTH DIAGNOSIS USING BIOMARKERS IN THE LIVER AND MUSCLE OF *Scomberomorus cavalla*.

(1) Ramírez-Trejo, V., (1) Ramírez-Romero, P., (2) Vazquez Botello, A., (1) Hernández Calderas, I., (1) Jerónimo-Juárez, J. R., & (1) Guzmán-García, X.

(1) Universidad Autónoma Metropolitana. Unidad Iztapalapa. División de Ciencias Biológicas y de la Salud. Departamento de Hidrobiología. Lab. de Ecotoxicología. Av. San Rafael Atlixco. No. 186. Colonia Vicentina. C.P. 09340. Delegación Iztapalapa. México. D.F. (2) Universidad Nacional Autónoma de México. Instituto de Ciencias del Mar y Limnología. Circuito exterior S/N. Ciudad Universitaria. Delegación Coyoacán. Código postal 04510. Ciudad de México

The Gulf of Mexico basin has been severely impaired, by the presence of contaminants such as oil and heavy metals, among others, which generate adverse effects on organisms. For this reason, in ecotoxicological studies, tissue biomarkers have been proposed and utilized to evaluate the effect of environmental stress. The aim of this work was to carry out a health diagnosis using biomarkers in the liver and muscle of *Scomberomorus cavalla* caught in the Tecolutla area, Veracruz. Ten organisms of commercial size were collected according to the recommendation of Padrós (2005); morphometric, biological and status index (Barnabé *et al.*, 1996) parameters were obtained. Quantification of Hg, Pb and Cr were obtained for liver and muscle through Inductively Coupled-Plasma Mass Spectroscopy (ICP-MS) technique. The samples were processed histopathologically. 75 liver and 129 muscle serially cuts stained with hematoxylin-eosin were analyzed with microscope. A lesion prevalence table was elaborated in which an impact factor was associated to them (Bernet *et al.*, 1999). With an immunohistochemical analysis the presence of Hsp70 and Metallothioneins was determined. With the data obtained evidence analysis was conducted to establish the health diagnosis. The average of total weight and length was 83 cm and 3400 g respectively. Index status was 0.6 ("thin and elongated"). Biological parameters showed an absence of parasites and macroscopic lesions. The average of Hg for both tissues was within the same order of magnitude; in liver 1.19 mg/Kg and muscle 0.92 mg/Kg wet weight Hg; there was no significant difference in the concentration of the two organs analyzed ($t = 0.8098$, $P = 0.46$). Pb was registered below the detection limit (<0.01 mg/Kg) in liver and muscle. Regarding Cr, the average in liver (0.46

mg/Kg wet weight) compared to muscle (0.45 mg/Kg wet weight), was not significantly different ($t = -0.2850$; $P = 0.79$). Hg muscle values exceeded the reference standard established for the consumption of fish meat in the EU and only one exceeded the national legislation. The liver showed the characteristic tissular structure; hepatocytes with central nuclei and blood vessels with nucleated erythrocytes were observed. The muscle presented muscle fibers with characteristic striations surrounded by connective tissue and peripheral ovoid nuclei; the connective tissue presented blood vessels with oval nucleated erythrocytes. Some of the lesions observed in the liver were congestive vessels, infiltration, focal inflammation, eosinophilic secretions, melanomacrophage centers and granulomas; lesions with impact factor between 1 and 3 (minimal, moderate and severe pathological importance). The muscle presented congestive vessels with impact factor of 1. The immunohistochemical technique revealed the presence of Hsp70 in the cytoplasm of hepatocytes but not in the muscle; with respect to metallothioneins, they were not immunodetected. Biomarkers used showed evidence a low status index, progressive and reversible damage and the presence of Hsp70, associated with the presence of Hg and Cr. The muscle is not compromised; however, the presence of Hg may represent a risk to consumers, therefore it is necessary to continue monitoring in the area of Tecolutla, Veracruz

INGENIERÍA TISULAR

28 TITANIUM LAMINA GRAFT SEEDED WITH ADIPOSE TISSUE-DERIVED MESENCHYMAL STEM CELLS INCREASES MANDIBULAR BONE REGENERATION Gayoso del Villar, J.; Garrosa García, M.; Gayoso Rodríguez M.J.

Department of Cell Biology, Histology and Pharmacology. Faculty of Medicine and INCYL. University of Valladolid. Spain

INTRODUCTION The scarce regenerative capability of mandibular bone tissue is a limitant factor in a number of pathological and therapeutic processes in current odontology. Our aim is to analyze the effect that titanium laminae seeded with adipose tissue-derived mesenchymal stem cells (ASCs) can exert on the regenerative capability of the mandibular bone tissue. **METHODOLOGY AND MATERIALS** We have used the critical size (4mm) defect model in the rat mandible. Titanium laminae were grafted in such bone defects made in the posterior third of the mandible body, with or without the addition of autologous ASCs, and left for 30 days. Each half of the mandible were studied without decalcification and included in epoxyresin. Sections were stained with hematoxylin, alizarin, von Kossa and toluidine blue for light microscopy, and also processed for scanning electron microscopy and energy dispersive X-ray spectroscopy (EDX). **RESULTS AND CONCLUSIONS** Our results show that titanium laminae favour mandibular bone regeneration and when these laminae are seeded with ASCs, repairing of the mandibular bone defect occurs faster and a higher volume of newly formed bone is produced.

46 TISSUE ENGINEERING FOR CARTILAGE REGENERATION IN LARGE MAMMALS

(1,2) Sancho-Tello Valls, M.; (3) Vikingsson, L.; (4) Martínez Díaz, S.; (4,5) García, F.; (3) Gómez-Tejedor, J.A.; (3,6) Gallego Ferrer, G.; (1,2) Ruiz Saurí, A.; (4,7) Monllau, J.C.; (3,6) Gómez Ribelles, J.L.; (1,2) Carda Batalla, C.

(1) Departament de Patologia, Facultat de Medicina i Odontologia, Universitat de València; (2) INCLIVA, Hospital Clínico Universitario, Valencia; (3) Center for Biomaterials and Tissue Engineering (CBIT) Universitat Politècnica de València; (4) Hospital Clínic Veterinari, Universitat Autònoma de Barcelona; (5) Departament de Medicina i Ciurgia Animals, Bellaterra; (6) Ciber en Bioingeniería, Biomateriales y Nanomedicina (CIBER-BBN), Valencia; (7) Hospital Santa Creu i Sant Pau, Barcelona.

INTRODUCTION. Articular cartilage is poorly repaired and its pathologies have a high incidence in our population. Tissue engineering techniques has been widely employed, using different biomaterials, both in vitro and in vivo in small animals, but few studies have been performed in larger ones. Thus, the aim of the present study was to investigate the in vivo regenerative ability of articular cartilage by using biodegradable implants in large animals by means of histological techniques. **MATERIALS AND METHODS.** The device synthesized consisted in a porous Polycaprolactone discoid scaffold, attached to a biocompatible Poly(L-lactic) pin for anchoring to the subchondral bone. This device is based on patent EP201131625 PCT/WO2013/178852. Scaffolds were implanted in the femoral condyle of 6 adult female sheep, after two defects with the same size of the device and microfracture were performed (2 scaffolds in one knee of each animal). Contralateral knees were used as controls. Four and a half months after surgery, animals were sacrificed and femoral condyles were obtained, macroscopically studied, and immersed in a decalcifying solution. When samples were decalcified, they were processed following standard histological procedures, utilizing a low-melting embedding wax in order to preserve the biomaterials. **RESULTS.** Macroscopic study showed that most of the defects (75%) exhibited the articular surface completely or almost completely repaired with a neotissue with macroscopic aspect of cartilage, although they had a rougher appearance than controls. Besides, only 2 samples (16%) presented a cystic cavity, which was in the deeper end of the pin. These results shows an improvement of previous studies where scaffolds were implanted without any anchoring pin, that resulted in a high incidence of cystic cavities, as it has been reported in animal models of cartilage tissue engineering using large mammals. Histological study reveals an active repair process in the injured surface as well as around the pin. All samples presented neocartilage formation at the edges of the injury, that eventually covered the whole surface in some cases, although the cartilage observed had an immature aspect at the time of study (4,5 months after surgery) most of the times. Around the pin, fibrous, loose or mesenchymal connective tissues were observed along with an active process of primary ossification. **CONCLUSIONS.** Articular surface shows an active reparative process 4,5 months after scaffold implant containing an anchoring pin. Subchondral bone shows an active process of bone formation around the pin, and it presents a reduced formation of cystic cavities. Therefore, the device implanted improves tissue regeneration in large mammals, although it needs to be optimized. **ACKNOWLEDGEMENTS.** This study was supported by MAT2013-46467-C4 grant from Ministerio de Economía y Competitividad, Spain.

51 A GENE EXPRESSION PROFILE OF HUMAN ORAL MUCOSA AND CORNEA FOR USE IN TISSUE ENGINEERING

(1) Garzón, I.; (1) Martín-Piedra, M.A.; (2) Rico, L.; (1) Campos, F.; (1,3) Oyonarte, S.; (4) Medialdea, S.; (1) García, J.M.; (1) Campos, A.; (1) Alaminos, M.

(1) Tissue Engineering Group, Department of Histology, University of Granada, Spain, and Instituto de Investigación Biosanitaria ibs.GRANADA, Spain; (2) Andalusian Initiative for Advanced Therapies -IATA-, Consejería de Igualdad, Salud y Políticas Sociales, Sevilla, Spain; (3) Blood and Tissue Bank of Sevilla-Huelva, Sevilla, Spain; (4) Division of Ophthalmology, University Hospital of Granada, Spain

Background: Previous reports suggest that oral mucosa epithelial cell sheets can be used for the clinical treatment of corneal limbus stem-cell deficiency, and oral mucosa epithelial stem cells are able to adapt and integrate in the corneal environment following transplantation. However, the reasons why these cells resemble the normal cornea epithelium are not known. In the present study, we have analyzed the gene expression profile of human oral mucosa biopsies and compared this profile with the human cornea and skin to determine which structures are genetically more similar and establish putative clinical uses. Methods: Sclero-corneal limbus, oral mucosa and skin tissue biopsies were obtained from human donors and total RNA was extracted by using the Trizol method. RNA was retrotranscribed to cDNA and quantified by q-RT-PCR using Bio-Rad systems for 45 genes with a role in epithelial differentiation, extracellular matrix synthesis and development and cell proliferation. Results were analyzed by using the Bio-Rad CFX Manager Software 3.1 and samples were classified according to their gene expression profile using the Cluster mode of the program. Histological analysis of the sclero-corneal limbus, oral mucosa and skin tissues was carried out by haematoxylin-eosin staining. Results: As expected, the human oral mucosa was histologically analogue to the human skin, with the presence of a stratified keratinized epithelium with more than 15 cell layers and a vascular stroma with epithelial rete ridges and stromal papillae. In contrast, limbal tissues had a non-keratinized epithelium with 7-8 cell layers without epithelial rete ridges and stromal papillae, and the corneal stroma was avascular. However, the gene expression analysis revealed that corneal tissues clustered in the same branch than oral mucosa tissues and were genetically more similar to oral mucosa than to human skin. The highest gene expression similarities between cornea and oral mucosa were found for LAMA1, LAMC1, JUP, KRT7, COL5A1, VIM, KRT19, KRT8 and KRT13 genes. Conclusions: These results confirm the hypothesis that epithelial and extracellular matrix gene expression may be similar for oral mucosa and corneal limbus, despite their histological dissimilarities. This support the use of tissue-engineered epithelial cells fabricated ex vivo from autologous oral mucosal epithelium for reconstruction of the ocular surface of patients with bilateral stem-cell deficiencies. Acknowledgements: Supported by the Spanish Plan Nacional de Investigación Científica, Desarrollo e Innovación Tecnológica (I+D+i) from the National Ministry of Economy and Competitiveness (Instituto de Salud Carlos III), grant FIS PI14-0955. Co-financed by Fondo Europeo de Desarrollo Regional (FEDER), European Union.

52 CORNEAL ENDOTHELIUM SELECTION FOR ENDOTHELIAL CELL CULTURE IN TISSUE ENGINEERING

(1,2) Ramos, J.F.; (1) Megías, I.; (1,2) Muñoz-Ávila, J.I.; (3) González-Andrades, M.; (3) Martín-Piedra, M.A.; (3) Crespo, P.V.; (3) García, J.M.; (4) Sánchez-Montesinos, I.; (3) Alaminos, M.

(1) Granada Institute of Ophthalmology (IOG), Granada, Spain; (2) Division of Ophthalmology, University Hospital of Granada, Spain; (3) Tissue Engineering Group, Department of Histology, University of Granada, Spain, and Instituto de Investigación Biosanitaria ibs.GRANADA, Spain; (4) Department of Human Anatomy and Embryology, University of Granada, Spain

Introduction: The human cornea endothelium may be damaged during different surgical procedures of the cornea, especially in cataract surgery. However, numerous previous works suggest that the human corneal endothelium has very limited in vivo regeneration capability, and this is one of the main limitations of the use of endothelial cell cultures for cornea tissue engineering purposes. The purpose of this study is to evaluate the regenerative capability of the human cornea endothelium in patients subjected to cataract surgery by phacoemulsification. **Materials and methods:** 20 patients with low-grade cataract were included in this study. All patients received cataract surgery by phacoemulsification and the following parameters were evaluated before surgery and up to one year after surgery by using a noncontact specular microscope: corneal endothelial cell density (CECD), coefficient of variation (CV), and mean cell area (MCA). Results corresponding to the youngest patients were compared to the eldest patients by using a statistical t test. **Results:** The analysis showed that the surgical procedure was associated to an initial decrease of the CECD in both study groups. Whereas the group of elder patients was not able to recover this cell count decrease, a number of patients corresponding to the youngest group demonstrated to have certain degree of cell regeneration. **Conclusions:** These results suggest that the human endothelium might have certain regeneration capability in vivo, especially in young patients. The use of human cornea biopsies to establish primary endothelial cell cultures should preferentially select the youngest donors. **Acknowledgements:** Supported by the Spanish Plan Nacional de Investigación Científica, Desarrollo e Innovación Tecnológica (I+D+i) from the National Ministry of Economy and Competitiveness (Instituto de Salud Carlos III), grant FIS PI14-0955. Co-financed by Fondo Europeo de Desarrollo Regional (FEDER), European Union.

53 INFLUENCE OF SURFACE PHOTOACTIVATION AND LUBRICANT CONTAMINATION IN THE OSSEOINTEGRATION PROCESS OF TITANIUM DENTAL IMPLANTS

(1,2) Martín de Llano, J.J.; (3) Cano Tebar, A.B.; (1, 2) Carda, C.; (3) Sánchez-Pérez, A.

(1) Departament de Patologia, Facultat de Medicina i Odontologia, Universitat de València, Spain. (2) Instituto de Investigación Sanitaria INCLIVA, València, Spain. (3) Departamento de Dermatología, Estomatología, Radiología y Medicina Física. Universidad de Murcia, Spain.

Important efforts have been made to improve osseointegration in an attempt to secure the best possible results. This has led the manufacturing companies to conduct expensive investigations with the purpose of improving the implant surfaces. However, such efforts may prove futile if the surgical procedure used is inadequate. A lack of early osseointegration is not always the fault of the surgeon; indeed, there may be shortcomings in the procedures and protocols used. An example of this is represented by inadequate application of the lubricants used to improve the performance and durability of the surgical rotary instruments. On the other hand, osseointegration can be improved by modifying the implant surface. This has led to the investigation and development of a broad range of surface treatments. One of the options is photoactivation, which can alter implant wettability, accelerating clot formation and improving cell recruitment and differentiation.

Materials and methods

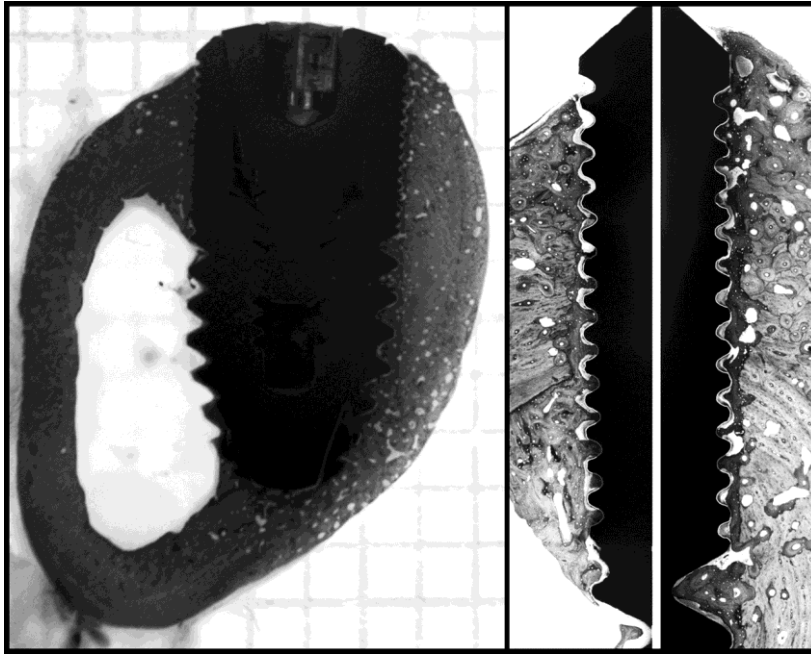
Animal model were adult New Zealand rabbits. Standard surgical procedures were followed. 3 cavities were drilled in both the right and left tibia of each of 5 animals using a milling speed of 800 rpm and a 40-Ncm torque, flushing continuously with a physiological solution. 30 titanium implants (Mozo-Grau, Valladolid, Spain), 3.3 mm in diameter and 6 mm long were aleatory distributed in the animals. Implant groups were: (1) 10 control implants (implant inserted in a bone cavity drilled without lubricant or UV-C exposition); (2) 10 UV-photoactivated implants (implant irradiated for 15 min with UV-C -200 to 280 nm wavelength- light); (3) 10 lubricant contaminated implants (implant inserted in a bone cavity drilled using an oleaginous lubricant). Animals were sacrificed 2 months after the surgery. Fragments of the tibias containing the implants were fixed, dehydrated, embedded in methyl methacrylate and, after polymerization, sawed, grinded to reach the central portion of the implant, polished and the bone surface stained with toluidine blue pH 3.5. Digital images of the cortical bone surrounding the implant threads were recorded with a bright field microscope and bone-implant contact (BIC) was evaluated using the image processing program ImageJ 1.48 (figure). The SPSS version 19.0 statistical package (SPSS Inc., Chicago, IL, USA) was used for the statistical comparisons and calculations. Statistical significance was considered for $p < 0.05$.

Results

All animals completed the healing phase. There were no postoperative complications. No inflammation was detected in any of the 30 samples. BIC could be measured in all the samples. BIC values were similar to that described by other groups using a similar experimental approach. BIC mean values (in %) were 25.5 (CI 21.6 to 29.5). BIC values found were as follows: Control 24.2 (CI 19.1 to 29.3), photoactivated 26.9 (CI 18 to 35.8) and contaminated 25.5 (CI 16.8 to 34.3). No statistically significant differences were found among the 3 experimental groups.

Conclusions

The experimental model used was effective for comparing BIC values. UV-C treatment markedly enhanced the hydrophilicity and seemed to yield a more reactive surface at the moment of insertion. However, the treatment of the surface of titanium implants with UV-C radiation did not improve osseointegration although a lower dispersion was found. The use of an oleaginous lubricant during the milling procedure had not a detrimental effect on the osseointegration process.



56 PLURIPOTENCY AND CONTRIBUTION OF HUMAN DENTAL PULP STEM CELLS (DPSC) TO BONE-LIKE TISSUE IN ORGANOTYPIC CULTURE

(1) Marquez Clavijo, J.; (2) Fernández Piñeiro, I.; (1) Unda Rodríguez, F.; (1) Ibarretxe Bilbao, G.; (2) Sánchez Barreiro, A., (1) Badiola Etxaburu, I.

(1) Department of Cell Biology and Histology. Faculty of Medicine and Dentistry. University of the Basque Country. Universidad del País Vasco/Euskal Herriko Unibertsitatea. Leioa 48940, Bizkaia. SPAIN. (2) Department of Pharmacy and Pharmaceutical Technology. Faculty of Pharmacy. Praza Seminario de Estudos Galegos, s/n. Campus sur. 15782 Santiago de Compostela. SPAIN

Introduction: Dental pulp stem cells (DPSC) are a powerful tool for tissue engineering. The aim of this work was to study the osteogenic potential DPSCs for bone regeneration. Material and Methods: DPSCs cells were isolated from third molars of healthy adult human donors and we characterized these cells using pluripotent and differentiation markers by RT-PCR and immunocytochemistry. Cells were culture in the presence of differentiation reagents such as dexamethasone, ascorbate and β -glycerolphosphate. Formation of mineralized tissue was quantified by Alizarin Red staining. In addition, DPSCs cells were labeled with fluorescent DiI/DiO lipophilic tracers and transplanted into embryo mouse first molars, and mouse mandibular bone explants. After 1 week in culture organotypic cultures were analyzed by histology and fluorescence microscopy. Results: Freshly-plated DPSCs formed adherent colonies, which proliferated to eventually create a uniform collagen I-containing monolayer. DPSC were positive for bone markers collagen I, osteocalcin and osteonectin. Interestingly, these cells also expressed a wide range of pluripotent stem cell markers, such as Oct-4 and Sox-2. Therefore, DPSCs cells in the presence of osteogenic differentiation factors significantly increased the production of mineralized tissue, when compared to controls. DiI/DiO-labeled DPSCs were transplanted into embryo alveolar bone and molar organotypic cultures. In bone

explants, the generation of bone-like tissue containing transplanted cells was detected. In tooth explants, DPSC integrated within the host dental pulp and periodontal tissues. Conclusion: Our results demonstrated that DPSCs can be readily induced to generate in vitro bone-like mineralized tissue and histointegrate into hard and soft tissues. These findings shows new strategies for the use of DPSCs use in cellular therapies for bone regeneration.

9 MORPHOLOGICAL AND MOLECULAR PROPERTIES OF A HUMAN OSTEOBLAST-LIKE CELL LINE CULTURED ON SURFACE-TREATED TITANIUM DISCS AND THE EFFECT OF MELATONIN

(1,2) Martín de Llano, J.J.; (3) Pérez-Martínez, C.; (3) Labaig-Rueda, C.; (3) Fons, A.; (3) Solá-Ruiz, M.F.; (1,2) Carda, C.

(1) Departament de Patologia, Facultat de Medicina i Odontologia, Universitat de València, Spain. (2) Instituto de Investigación Sanitaria INCLIVA, Valencia, Spain. (3) Departament d'Estomatologia, Universitat de València, Spain

INTRODUCTION: Gastric cancer is the fourth most common malignant disease and the second leading cause of cancer-related death worldwide (Matsuoka T, 2015). Despite some advances in the prevention and treatment of the disease, the five year survival in most parts of the world still remains around 20%. The poor survival rate is mainly explained by the advanced stage of the disease at the time of diagnosis (Jørgensen JT, 2012). We reached the point where the only treatment available is the paliative one. HER2 is the first targeted therapy succesfully tested in gastric cancer. Patients with HER2 overexpressed and/or amplified tumours derived the greatest benefit from trastuzumab therapy (Rüschoff J, 2012), an humanized HER2 antibody, in combination with chemotherapy. The HER2 overexpression is assessed by semiquantitative immunohistochemistry: 0 and 1+ are defined as negative, 2+ as borderline, and 3+ as positive. In order to determinate whether borderline cases are positive or negative, HER2 gene an d centromere 17 (CEN17) status must be assessed. Due to the high percentage of cases with heterogenity in gastric cancer, some authors recommend the use of chromogenic methods (i.e., DuoCISH) to assess HER2 gene status instead of fluorescent ones (FISH) (Rüschoff J, 2010). But the development of new methods such as automated IQFISH that allows us to obtain results in just 3.5 hours, in contrast to DuoCISH which takes 2 days, makes it a very attractive technique for the laboratory daily routine. The implementation of new methods in the selection of patients for this kind of treatments depends on the use of reliable and validated methods (Gomez-Martin C, 2014). The main goal of this work is to validate the automated IQFISH method in the determination of HER2 gene status in gastric cancer. **METHOLOGY AND MATERIALS:** We selected 55 consecutive endoscopic biopsies diagnosed with gastric cancer from the Pathology archive of the Complexo Hospitalario Universitario de Santiago in the period 2012-2013. We performed 4 ?m sections to determine the HER2 gene status by DuoCISH (Dako-Agilent) and automated IQFISH in the Omnis system (Dako-Agilent). Assays were performed according to the manufacturer recomendations. DuoCISH results were evaluated in a light microscopy at x60 magnification. Automated IQFISH results were evaluated at x100 magnification in a fluorescence microscopy equiped with a dual filter for TexasRed and FITC, and a filter for DAPI. Samples with HER2/CEN17 ratios ? 2 were considered amplified. **RESULTS:** The automated IQFISH method showed clear discernible signals for HER2 gene

and CEN17. The results obtained by both techniques were concordant in all cases ($\kappa = 1.0$), indicating a perfect agreement between them. All cases that revealed amplification by DuoCISH were also amplified by automated IQFISH. The Wilcoxon's test for paired data did not show significant differences between the means of HER2/CEN17 ratios by both methods ($p = 0.851$). CONCLUSION: Using as reference the results of the HER2 expression by immunohistochemistry in gastric cancer, the possibility to obtain results in just 3.5 hours with minimal technician involvement makes the automated IQFISH a fast, reliable and robust alternative to chromogenic methods.

78 EFFECTS OF HEPARIN AND LOW MOLECULAR WEIGHT HEPARIN-LOADED HYDROGELS ON THE DIABETIC CICATRIZATION PROCESS IN A RAT WOUND HEALING MODEL

Cifuentes, A.; Gómez-Gil, V.; Mesa-Celler, C.; del Castillo, E.; García-Honduvilla, N.; Buján, J.

Dept. of Medicine and Medical Specialities, Faculty of Medicine and Health Sciences. University of Alcalá. Alcalá de Henares (Madrid, Spain). Networking Research on Biomaterials, Bioengineering and Nanomedicine. (CIBER-BBN).

INTRODUCTION Diabetes mellitus is associated to impairments in the normal process of cutaneous cicatrization. Diabetic wounds often fail to progress through the classical phases of healing (inflammatory, proliferative and maturation/remodeling), remaining in an inflammatory status, which usually leads to ulcer formation. Topical therapies with bioactive dressings could ameliorate this situation, allowing a better healing of diabetic wounds. In this work, the effects of chitosan hydrogels functionalized with two types of heparin (unfractionated heparin and bemiparin, a low molecular weight heparin) in a diabetic excisional wound rat model were evaluated. **MATERIALS AND METHODS** 30 female Wistar rats (healthy or streptozotocin-induced diabetic) were divided in five groups and received treatments as described in Table 1. A circular, full-thickness cutaneous excisional defect ($\phi = 1,5$ cm) was made in the dorsum of the animals, followed by the administration of chitosan hydrogels (in PLCB, HEP and BEM groups). Animals were euthanized 21 days after surgery, and cicatrization tissue samples were obtained and processed for histological and morphometric studies. The thickness of the neoepidermis and granulation tissue was measured, and macrophages and their subpopulations were characterized by a double fluorescent immunostaining of CD68 and CD206. ANOVA followed by Tukey- Kramer post-test were used for statistical analysis. **RESULTS** CTRL-S showed features of an advanced maturation status of the granulation tissue, with reduced cellularity and vascularization, while CTRL-D neoformed tissues displayed higher inflammation and reduced matrix deposition and organization. A slight improvement of the healing process was observed in PLCB group, but the best results in diabetic animals were those observed in HEP and BEM, which displayed lower levels of inflammation and tissues with a more mature profile. The thickness of the granulation tissue of HEP and BEM was similar to that found in CTRL-S, while CTRL-D and PLCB showed a thinner neodermis. All diabetic groups exhibited greater numbers of macrophages than healthy animals, but groups treated with unfractionated and low molecular weight heparin-loaded hydrogels showed higher proportions of the pro-reparative M2 phenotype. **CONCLUSIONS** The administration of unfractionated

heparin and bemiparin-functionalized chitosan hydrogels seemed to improve the impaired healing of diabetic wounds, promoting the progression from an inflammatory chronic status to a reparative and more mature stage, and enhancing the amount and quality of the healing tissues.

GROUP	DESCRIPTION	DIABETIC	HYDROGEL	HG LOAD
CTRL-S	Healthy control	No	No	-
CTRL-D	Diabetic control	Yes	No	-
PLCB	Placebo hydrogel	Yes	2% chitosan	No
HEP	Unfractionated heparin hydrogel	Yes	2% chitosan	0.2% Heparin
BEM	Bemiparin (LMWH) hydrogel	Yes	2% chitosan	0.2% Bemiparin

79 REMODELING OF NON-CROSSLINKED PORCINE DERMAL MATRICES IN AN EXPERIMENTAL MODEL OF VENTRAL HERNIA REPAIR

(1,3) Pascual, G.; (1,3) Sotomayor, S.; (2) Adel, F.; (1,3) del Castillo E.; (2,3) Pérez-Köhler, B.; (2,3) Rodríguez, M.; (2,3) Bellón, J.M.

(1) Depts. of Medicine and Medical Specialties and (2) Surgery and Medical and Social Sciences, Faculty of Medicine and Health Sciences, University of Alcalá. Madrid. Spain. (3) Networking Biomedical Research Centre in Bioengineering, Biomaterials and Nanomedicine. (CIBER-BBN), Madrid, Spain.

INTRODUCTION. Bioprosthesis represent a significant advance in the abdominal wall reconstruction since they become degraded until their complete elimination in the recipient organism. This study examines remodeling in the host of three non-crosslinked porcine dermal collagen biomeshes: Strattice™ (St) (LifeCell™), XCM Biologic Tissue Matrix™ (XCM) (Synthes CMF) and Protexa® (Pr) (Deco Med S.R.L.). **MATERIAL AND METHODS.** Partial ventral hernia defects created in New Zealand White rabbits were repaired using the biomeshes that were placed in a sublay preperitoneal position. At 14 and 90 days postimplant, explants were assessed in terms of their host tissue incorporation by morphological studies, collagen gene/protein expression (qRT PCR/immunofluorescence), macrophage response (immunohistochemistry) and biomechanical strength. **RESULTS.** There were no cases of mortality or infection in any of the animals of the different groups. Among our macroscopic findings, of note was mesh detachment detected in one-third of the Pr implants at 90 days. The host tissue response to all the biomeshes was similar at both time points, with a tendency observed for their encapsulation. There were no appreciable signs of mesh degradation. The extent of host tissue infiltration and collagenization was greater for St and Pr than for XCM. Macrophages were observed in zones of inflammation and tissue infiltration inside the mesh. XCM showed the greater macrophage response at 90 days. Improved tensile strength was observed for St over Pr and unrepaired defects. **CONCLUSION.** St showed the best behavior, featuring good collagenization and tensile strength while also inducing a minimal foreign body reaction. **Acknowledgments:** This study was supported by the company LIFECCELL EME Ltd., (Kidlington, UK).

85 OBTENCIÓN DE CELULAS TRONCALES A PARTIR DE LIGAMENTO PERIODONTAL HUMANO.

Trejo CG(1), Ramírez OR(1), Gómez-Clavel JF(2) .

(1) Laboratorio De Investigación En Odontología Almaraz, Facultad De Estudios Superiores Iztacala, Universidad Nacional Autónoma De México (2) Laboratorio De Investigación En Educación Y Odontología, Facultad De Estudios Superiores Iztacala, Universidad Nacional Autónoma De México

INTRODUCTION: The periodontal ligament (PDL) is a highly specialized connective tissue that holds the tooth articulated in its socket; It meets physical, nutritional, and sensory functions. The Periodontal Ligament Stem Cells (PDLSCs) fulfill the function of tissue renewal; not only of the collagen fibers, but also in bone remodeling and formation of new cementum (Hopkins., 2011).

Mesenchymal stem cells (MSC) are multipotent non-hematopoietic cell population with the capacity for self-renewal, and expressing the criteria established by the International Society for Cellular Therapy (ISCT); between the expression of surface markers CD73, CD90 and CD105; also they have the multipotent to differentiate into osteoblasts, adipocytes and chondrocytes (E. Horwitz, 2006). The PDL can be a source de MSC; therefore the objectives of this study were: Get a population of MSC derived from PDL, standardize the cell culture and take the relevant evidence postulated the ISCT.

METHODOLOGY: Cells were obtained from 12 PDL biopsies taken from healthy premolars extracted from patients (17 and 25 years of age) from the University Clinic of Orthodontics "Naucalpan" prior informed consent. The extracted cells were grown under standard conditions. In the first passage morphology and cell viability tests they were performed and immunohistochemically studies. Proliferation curves were performed using the MTT technique. Subsequently, the cell population was induced osteogenic differentiation for 2 weeks and immunocytochemical and histological tests were performed to analyze the osteogenic phenotype.

RESULTS: The cell population is able to obtain using a new standardized methodology, that, after at least 10 trials of trial and error; (patients not counted in the study). In primary cultures, cells first appeared at 72 hours under standard conditions, cells appeared fibroblastoid morphology that reached confluence in 5-7 days, In tests with MTT cell proliferation kept rising for 14 days in culture. The ability of cell migration by testing In vitro repair injuries where it was observed that cells invaded again assessed the injured to cover 100% the injury caused to the area 72 hours. The CD90 positive cell population was more than 80%, of CD105 in 60% more anti-vimentin and 90%, CD73 in 70%, also not showing the hematopoietic markers CD34 and CD11b.

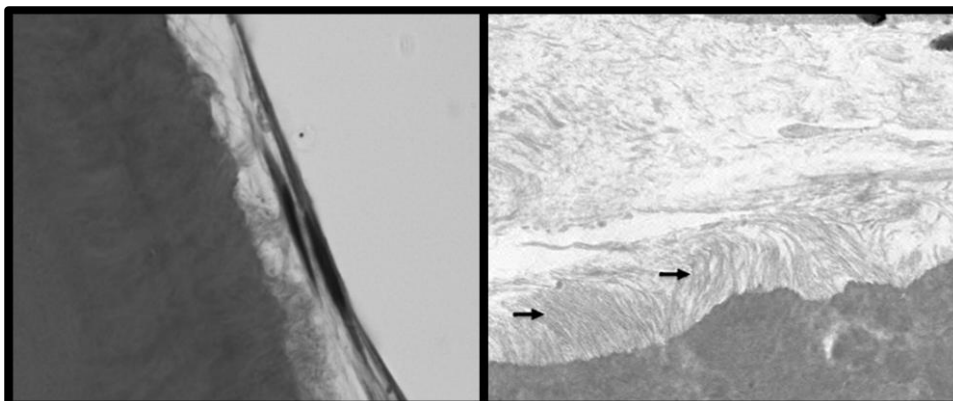
CONCLUSIONS: The cell population obtained has a high percentage of cells of mesenchymal type, so we can say that the periodontal ligament is an affordable source of mesenchymal cells.

92 HUMAN DENTAL PULP STEM CELLS ADHESION AND DIFFERENTIATION ON DENTAL CEMENTUM

(1) Peydró, S.; (1,2) Sancho-Tello, M.; (1,2) Ruiz-Sauri A.; (1,2) Mata, M.; (1,2) Carda, C.; (1,2) Martín de Llano, J.J.

(1) Departament de Patologia, Facultat de Medicina i Odontologia, Universitat de València, Spain. (2) Instituto de Investigación Sanitaria INCLIVA, Valencia, Spain.

Introduction Human dental pulp stem cells (hDPSC) capacity to differentiate into several cell lineages has prompted its possible use as an alternative therapy for tissue regeneration. We are currently determining the influence of several factors on the fate and differentiation of hDPSC. The specific three dimensional structure and composition of the environment in which a cell develops could be one of those factor. Thus, we are analyzing the effect that mineralized components of the dental tissue have in hDPSC adhesion, growth, morphology and eventually differentiation. Herein we summarized the results observed when hDPSC are grown on human dental cementum. **Materials and methods** hDPSC were obtained from the pulp of third molars extracted for prophylactic reasons. Cell growth and morphology were as previously described. Furthermore, they exhibited expected molecular markers as determined by flow cytometry analysis. Transversal sections of dental roots were obtained from human teeth from which the soft tissues, dental pulp and periodontal ligament, had been mechanically removed. Cells and dental sections were co-cultured, from 1 to 6 weeks, in cell culture basal media containing ascorbic acid. Samples were processed for both light and transmission electron microscopy using standard procedures. Cell adhesion, proliferation, morphology and secretion activity were evaluated. **Results** Phase contrast microscopy observation of the samples showed a high cell proliferation rate and adhesion to the cementum at the early stages of cell culture. Nevertheless, when these early samples were processed for paraffin embedding most of the cells were lost during the sample processing. At six weeks of cell culture, cells developed as dense and complex layers that completely surrounded the dental surfaces. The strong adhesion to the surface allowed the light and electron microscopy processing of the samples. On the cementum surface the cells adopted a flattened disposition and secreted an abundant collagen matrix associated to the dental surface. The electron microscopy analysis of the samples corroborated these findings. Furthermore, the ultrastructural study showed that the cells carried out a high secretory activity. Both the light microscopy and ultrastructural studies demonstrated an asymmetrical distribution of the collagen fibers (see figure). Interesting, collagen fibers associated to the cementum surfaces were predominantly perpendicular to that surface, resembling the collagen bundles found in vivo in the periodontal ligament. **Conclusions** Dental cementum constitutes a biological environment that favors hDPSC adhesion and proliferation. The asymmetrical deposit of the newly synthesized collagen fibers surrounding the cementum surface as well as the secretory activity of the cultured cells point out to the possible differentiation of hDPSC into a cell type similar to that found in the periodontal ligament.



100 DECELLULARIZED TRACHEAS FOR TISSUE ENGINEERING

(1)(2)(3) Mata, M., (2) Milian, M.;(2, 4) Galan, A.; (5) Garzón, I.;(1) (2) Ruiz Saurí, A.; (1)(2) Sancho-Tello, M; (1)(2) de Llano, J.J. and (1)(2) Carmen Carda.

(1) Departament de Patologia, Facultat de Medicina i Odontologia, Universitat de València. (2) INCLIVA, Hospital Clínico Universitario de Valencia. (3) Ciber de enfermedades respiratorias (CIBERES). (4) Servicio de Cirugía Torácica. Hospital Clínico Universitario de Valencia. (5) Departamento de Histología. Facultad de Medicina. Universidad de Granada.

Background/Objective: Extrapulmonary airway obstruction, including tracheal stenosis, leads to dyspnoea and can, sometimes, lead to the death if a correct and timely treatment is not performed. Surgery for tracheal stenosis is limited to a maximum length of 6-7 cm and it is not exempt of morbidity. Although there are different approaches of tissue engineering for the development of tracheal substitutes, unfortunately we are still too far to propose a realistic solution for these patients. One of the approximations of the tissue engineering is the use of decellularized matrix. The limitation in the use of these constructs includes the potential risk of immunogenic reaction due to cell debris permanence and the disturbance of the extracellular matrix occasioned by the detergent agent used to remove resident cells. In this study we have exposed porcine tracheas to different combinations of detergents to obtain decellularized scaffolds as a starting point to obtain a substitute potentially useful for the treatment of tracheal stenosis. Methods: Porcine tracheas were cut in 3 cm rings and exposed to the following detergent combinations: Triton X100 2% + SDS 0.3%, Triton X100 0.2% + SDS 0.3%, SDC 0.25% and SDC 2% for up to four weeks. Cell debris was evaluated by DAPI weekly. Haematoxylin Eosin, Masson Trichrome, and Orcein staining were performed in paraffin embedded formalin fixed tissue to analyse the effect of the different combinations of detergent. PAS staining was performed in OCT frozen tissues to evaluate GAGs. Ultrastructure of tracheas was studied by electron microscopy. Results: All the combinations of the detergents tested removed completely the cells present in the mucosa and submucosa, but only Triton X100 2% + SDS 0.3% and SDC 2% removed completely chondrocytes from hyaline cartilage. Regarding the extracellular matrix, SDC was the detergent which had a lower impact in the extracellular matrix composition according to collagen and elastic fibers and GAGs content and distribution. Conclusion: In conclusion, our results point the usefulness of SDC 2% to remove the cells conforming the different tissues in the trachea exhibiting a minimal disturbance of the extracellular matrix. This detergent may be useful to generate decellularized scaffolds for airway tissue engineering applications.

109 DEVELOPMENT OF DIFFERENT TECHNIQUES FOR THE STUDY OF TISSUE SAMPLES CONTAINING OPAQUE SCAFFOLDS

(1) Roa Ibarra, A.P.; (1,2) Martín de Llano, J.J.; (3) Pérez-Martínez, C.; (3) Fons, A.; (3) Sola-Ruiz, M.F.; (1,2) Carda, C.

(1) Departamento de Patología, Facultad de Medicina i Odontologia, Universidad de Valencia, Spain. (2) Instituto de Investigacion Sanitaria INCLIVA, Valencia, Spain. (3) Departamento de Estomatologia, Universidad de Valencia, Spain.

INTRODUCTION: The success of new tissue engineering techniques applied to regenerative medicine is based on the correct relationship between various components of the tissue, namely cells and scaffold, as well as the existence of some bioactive molecules that facilitate or enhance the biological response.

Among the different strategies that are developed in the field of tissue engineering, we are interested in the study of the adhesion and interaction of cells with biocompatible scaffolds. The histologic analysis of these samples can be carried out through two different approaches, either by cutting the sample in sequential slices, or by observing the surface of the full sample, i.e. whole mount analysis. The whole mount analysis provides information that cannot be easily obtained from the sequential slices approach.

Some of the materials commonly used as scaffolds are very hard and cannot be cut using standard microtomy techniques. Furthermore, the opaque or translucent characteristic of some materials used in tissue engineering hinders the observation of the samples by optical microscopy. Herein we describe the process developed for the analysis of whole mount samples.

MATERIALS AND METHODS: Dental pulp stem cells (DPSC) as well MG63 cell line were used. Cells were grown in 24-well plates and seeded on the selected biocompatible material, titanium discs. The samples were analyzed at several incubation time points. Cell culture media was removed and samples were fixed in 2.5% glutaraldehyde for 30 minutes and sequentially stained with hematoxylin and eosin for 5 minutes and incubated with 30 microM DAPI for 10 minutes.

The construct was placed on a slide (upright or upside down, depending on the microscopic technique used) and observed by using a stereomicroscope, an inverted microscope, a direct microscope or a fluorescence microscope and analyzed using the morphometric analysis program Image-Pro Plus version 6.0 software (MediaCybernetics). Data are shown as mean \pm SD. Statistical significance was considered for $p < 0.05$.

RESULTS: The opaque titanium discs avoided the direct in vivo observation of cells growing on them. After staining the cells with hematoxylin or cresyl violet it was possible to observe them, both by using an inverted microscope or a direct microscope. The stained cells could be distinguished from the scaffold background, but it was difficult to carry out a morphometric study as the limits of the cells were not clearly observed. The use of fluorescent dyes, such as DAPI and eosin, greatly improved the resolution. This allowed us to obtain images of the samples from which cell morphology parameters, based on the cell components staining with eosin, were calculated.

Thus, the MG63 cells adhered and proliferated similarly on different titanium discs. At 72 hours of cell culture the cell density on the O-type discs was significantly lower. Furthermore, the superficial differences of the titanium discs significantly affected some morphological features of the cells, as cell area, mean diameter and perimeter. The samples could be subsequently processed for SEM.

CONCLUSIONS: In this communication we describe the procedures that we have developed to obtain the maximum histological information from cells growing on opaque materials, using the whole mount approach. The methodology described in this work can be applied in studies focusing on the in vivo behavior of cells grown on different biomaterials.

110 IN SITU AND EX VIVO PHENOTYPIC EVALUATION OF UMBILICAL CORD STEM CELLS

(1) Garzón, I.; (1) Campos, F.; (1) Alfonso-Rodríguez, C.A.; (1) Jaimes-Parra, B.D.; (1) Carriel, V.; (1) Martín-Piedra, M.A.; (2) Rico, L.; (1) Sánchez-Quevedo, M.C.; (1) Alaminos, M.

(1) Tissue Engineering Group, Department of Histology, University of Granada, Spain, and Instituto de Investigación Biosanitaria ibs.GRANADA, Spain; (2) Andalusian Initiative for Advanced Therapies -IATA-, Consejería de Igualdad, Salud y Políticas Sociales, Sevilla, Spain

Introduction: Umbilical cord stem cells are easy to obtain with few ethical concerns and have large differentiation and proliferation capabilities. One of the main cell types of the umbilical cord is the Wharton's jelly stem cell population (WHJSC), which has been used in different tissue engineering protocols. In particular, WHJSC are thought to be in an early differentiation state and may retain some of the primitive stemness properties of embryonic cells. Although several WHJSC populations have been described in the umbilical cord, the specific properties of each population are not well understood. In this work, we have analyzed three different WHJSC cell populations in the umbilical cord in order to identify their intrinsic capability to differentiate into epithelial-like cells and to determine the most adequate cell population for epithelial differentiation. Materials and Methodology: Six human umbilical cords were fixed in formalin and embedded in paraffin for in situ histological studies. For ex vivo studies, primary cell cultures of WHJSC were obtained by enzymatic digestion of umbilical cord Wharton's jelly biopsies using type-I collagenase and trypsin-EDTA. Isolated cells were seeded and expanded using Amniomax culture medium. Histological and genetic analyses included detection of several undifferentiation and epithelial markers in cells located in situ in different zones of the umbilical cord -in situ analysis- and in primary cell cultures -ex vivo analysis- by microarray and immunofluorescence. Results: The results revealed that WHJSC showed positive expression of CD90 and CD105 stem cell markers in situ. In addition, cytokeratins 3, 4, 7, 8, 12, 13, 19, desmoplakin and zonula occludens 1 were expressed at the RNA and protein levels by cells in the umbilical cord and cell cultures. However, topographical differences were found among the different areas of the umbilical cord, with higher presence of epithelial cell markers in cells allocated at the Wharton's jelly region of the umbilical cord. Conclusion: These results suggest that umbilical cord mesenchymal cells have intrinsic expression of epithelial cell markers both in situ and ex vivo and confirm that cells of the Wharton's jelly region may be more committed to epithelial differentiation than cells at other regions. Acknowledgments: This study was supported by the Spanish Plan Nacional de Investigación Científica, Desarrollo e Innovación Tecnológica from the Spanish Ministry of Economy and Competitiveness (Instituto de Salud Carlos III), grant FIS PI14/0955 (co-financed by FEDER funds, European Union), and Fundación Benéfica Anticáncer San Francisco Javier y Santa Cándida, Granada, Spain.

112 EVALUATION OF THE OPTICAL PROPERTIES OF A BIOMIMETIC ARTIFICIAL CORNEA MODEL WITH WHARTON'S JELLY MESENCHYMAL STEM CELLS

(1) Ionescu, A.M.; (1) Cardona, J.C.; (1) Ghinea, R.; (2) González-Andrades, M.; (2) Jaimes-Parra, B.D.; (2) Campos, A.; (2) Alaminos, M.; (1) Pérez, M.M.; (2) Ga rzón, I.

(1) Department of Optics, University of Granada, Spain; (2) Tissue Engineering Group, Department of Histology, University of Granada, Spain, and Instituto de Investigación Biosanitaria ibs.GRANADA, Spain

Introduction: Numerous stem cells sources with low immunogenicity have been tested experimentally for corneal epithelium replacement. Recently, human Wharton's jelly mesenchymal stem cells (WJSC) were proved to be able to differentiate into cornea epithelial-like cells and to be efficiently used to generate an artificial anterior human cornea using tissue engineering strategies with results similar to the use of native cornea epithelial cells. Nevertheless, the capability of this new human artificial cornea model to transmit the incoming light was not yet evaluated. Therefore, the purpose of the present study was to determine the transparency of a biomimetic artificial cornea model using WJSC during its development in culture and also, after three months of in vivo implantation. **Materials and Methods:** First, primary cell cultures of human Wharton's jelly mesenchymal stem cells (WJSC), rabbit corneal epithelial cells (CEC) and corneal keratocytes were cultured. Then, three-dimensional orthotypic (using CEC) and heterotypic (using WJSC) rabbit cornea models were generated with fibrin-agarose scaffolds by tissue engineering. After 7 days in culture, both types of cornea models were implanted in 6 New Zealand rabbits. Pre and 3 months post-evaluation of the transparency characteristics of the bioengineered cornea models was performed using the Inverse-adding doubling (IAD) method. The transparency was determined for 4 wavelengths of the visible spectrum 457nm, 488nm, 514nm and 633nm. **Results:** During the time of development in culture, the orthotypic corneas (OC) displayed transparency values higher than the heterotypic corneas (HC) for all wavelengths studied, as shown in Figure 1. In addition, no differences were found between the different periods of time in culture (7-28days) studied. Interestingly, once implanted in rabbits, an increase in transparency was produced for both types of bioengineered corneas. OC displayed an overall 30% increase in the transparency values once implanted, whereas the HC doubled their transparency values after three months implantation, reaching values between 55 and 71%. In addition, the in vivo cornea models based on WJSC showed the closest values of transparency when compared to the control native corneas. Although the OC samples increased their transparency values once implanted, stretching the gap with the control corneas, their overall transparency values were found to be smaller than the HC. **Conclusion:** According to the results of our study, the heterotypic cornea model generated using Wharton's jelly mesenchymal stem cells and fibrin-agarose scaffolds improved its transparency once implanted in vivo, reaching values between 55 and 70% of transparency, values close to the ones of the native rabbit control cornea. **Acknowledgments:** This study was supported by the Spanish Plan Nacional de Investigación Científica, Desarrollo e Innovación Tecnológica from the Spanish Ministry of Economy and Competitiveness (Instituto de Salud Carlos III), grant FIS PI14/0955 (co-financed by FEDER funds, European Union).

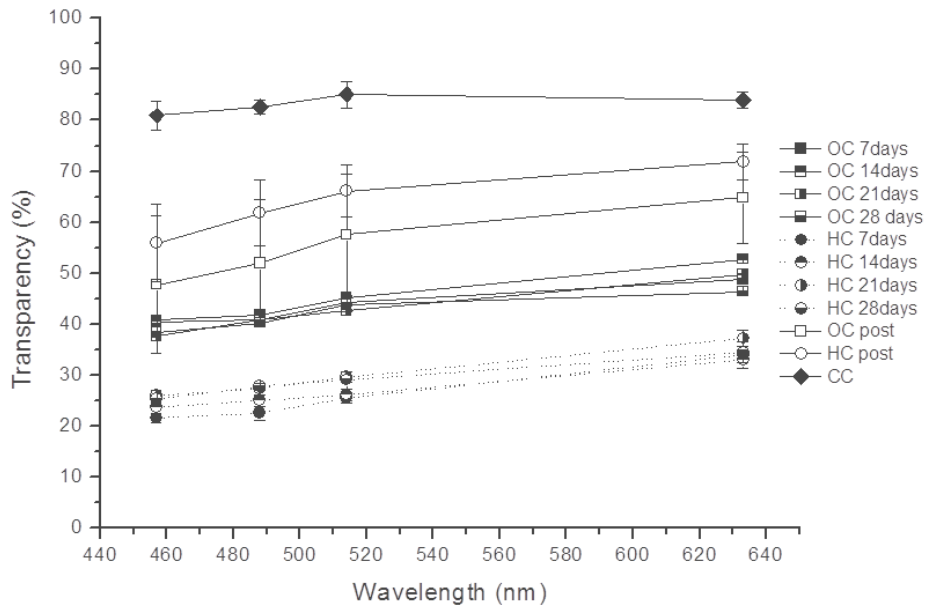


Figure 1. *Transparency of the orthotypic (OC) and heterotypic (HC) cornea during the time of development in culture (7 to 28 days) and after 3 months of implantation in rabbits (post). These values are also compared with the transparency values of a native rabbit control cornea (CC).*

113 HISTO-FUNCTIONAL CORRELATION OF REINNERVATION FINDINGS IN TWO MODELS OF PERIPHERAL NERVE REGENERATION

(1) Carriel, V.; (2) Miralles, E.; (3) Roda, O.; (2) Sáez-Moreno, J.A.; (1) Jaimes-Parra, B.D.; (4) Kretschmer, T.; (4) Cornelissen, M.; (1) García-Martínez, L.A.; (1) Campos, A.

(1) Tissue Engineering Group, Department of Histology, University of Granada, Spain, and Instituto de Investigación Biosanitaria ibs.GRANADA, Spain; (2) Division of Clinical Neurophysiology, University Hospital of Granada, Spain; (3) Department of Human Anatomy and Embryology, University of Granada, Spain; (4) Department of Basic Biomedical Sciences, Histology, Faculty of Medicine, Ghent University, Belgium.

Introduction: Following a structural injury, peripheral nerves have the capacity to partially regenerate their components and reinnervate distal target organs. Skeletal muscle reinnervation is a progressive and relatively slow process which theoretically depends on the complete regeneration of the affected nerve. On the other hand, peripheral nerve regeneration is a complex process which ends with the myelination of the newly-formed nerve fibers. The aim of this work is to correlate the electromyographic and histological findings that take place during short term peripheral nerve regeneration. Materials and methods: In this study, 5 mm of the left sciatic nerve were surgically excised from 48 male Wistar rats under general anesthesia, and the gap was repaired using autografts (group 1) or clinically used hollow collagen conduits (group

2). After 20, 30 and 50 days, animals were subjected to electromyography and then euthanatized for histological and histochemical analyses. Results: Electromyography revealed clear signs of muscle denervation 20 days after the surgical procedure in both groups, while histology showed degeneration of the grafted nerve in group 1 (autograft) and the cellular phase of regeneration on group 2 (conduit repaired). After 30 days, we observed a decrease of muscle denervation and some signs of reinnervation in group 1, which correlated with positive histological signs of nerve regeneration in this group. After 50 days, electromyography showed signs of muscle reinnervation in both groups, especially in group 1. These findings correlated well with the presence of histological signs of nerve regeneration in both groups, which were characterized by the presence of newly-formed nerve fascicles, but an incomplete or absent myelination of these fascicles. Conclusion: This study demonstrated that autograft repair is superior to hollow conduits at electromyographic and histological levels. In addition, muscle reinnervation began before a complete myelination of the regenerated nerve fibers took place in both study groups. Finally, this study highlights the importance of both the electromyography and histology, which allowed us to analyze and characterize the peripheral nerve regeneration process and muscle reinnervation with high accuracy along the time. Funding: This study was supported by the Spanish Plan Nacional de Investigación Científica, Desarrollo e Innovación Tecnológica (I+D+i) from the National Ministry of Economy and Competitiveness (Instituto de Salud Carlos III), grant FIS PI14-1343, co-financed by Fondo Europeo de Desarrollo Regional (FEDER), European Union.

114 IDENTIFICATION OF A NOVEL MARKER OF PERIPHERAL NERVE REGENERATION AT THE CENTRAL NERVOUS SYSTEM

(1) Carriel, V.; (2) García-García, S.; (2) Miralles, E.; (2) Sáez-Moreno, J.A.; (3) Roda, O.; (1) Campos, F.; (4) Katati, M.J.; (5) Rodríguez, I.A.; (1) Campos, A.

(1) Tissue Engineering Group, Department of Histology, University of Granada, Spain, and Instituto de Investigación Biosanitaria ibs.GRANADA, Spain; (2) Division of Clinical Neurophysiology, University Hospital of Granada, Spain; (3) Department of Human Anatomy and Embryology, University of Granada, Spain; (4) Division of Neurosurgery, University Hospital of Granada, Spain; (5) Cátedra de Histología B, University of Córdoba, República Argentina.

Introduction: Peripheral nerves are complex organs which connect the central nervous system to distal target organs at the motor, sensitive and vegetative levels. These organs can be structurally affected by a variety of conditions, which trigger a progressive process of peripheral nerve regeneration. Some of the cellular and molecular processes that are involved in peripheral nerve regeneration have been elucidated to the date. However, little is known about the histological and molecular changes that take place at the central level. The aim of this study is to perform a time-course histological and histochemical analysis of the spinal cord following a critical nerve gap regeneration process. Materials and methods: In this study, 10 mm of the left sciatic nerve of 9 male Wistar rats was removed under general anesthesia and the gap was repaired by using commercially available collagen conduits. After 10, 20 and 30 days, the animals were euthanatized, perfused with 4% paraformaldehyde, and the spinal cord, the right control sciatic nerve and the implanted conduits were harvested for histological analyses. In

addition, three healthy Wistar rats were used as healthy controls. MCOLL histochemical method was used to evaluate the collagen matrix, cell morphology and myelin, while the growth-associated protein 43 (GAP-43) was identified by immunohistochemistry and used for the identification of regenerated axons. Results: Histological analysis of the implanted conduits revealed progressive peripheral nerve regeneration over the time, with the presence of newly-formed nerve fascicles after 20 and 30 days. These fascicles showed positive expression of GAP-43, but negative histochemical reaction for myelin (MCOLL), pointing out an incomplete regeneration. The spinal cord showed some histological changes in the gray and white matters, which suggests the existence of neuronal damage from day 10 to day 30. Myelin was minimally affected in the dorsal white matter, but an increase in the immunohistochemical expression of GAP-43 was clearly observed in the left ascending dorsal pathways of the white matter from 20 to 30 days post-repair. Conclusion: This study demonstrates that early peripheral nerve regeneration is associated to progressive morphological changes of the spinal cord with a differential expression of GAP-43 on specific ascending pathways. Therefore, GAP-43 could be used as a marker to identify affected regions of the spinal cord following a peripheral damage and neural regeneration. Funding: This study was supported by the Spanish Plan Nacional de Investigación Científica, Desarrollo e Innovación Tecnológica (I+D+i) from the National Ministry of Economy and Competitiveness (Instituto de Salud Carlos III), grant FIS PI14/1343, co-financed by Fondo Europeo de Desarrollo Regional (FEDER), European Union.

115 HISTOLOGICAL AND BIOMECHANICAL CHARACTERIZATION OF AN ARTIFICIAL MULTILAYERED NERVE GUIDE CONTAINING MESENCHYMAL STEM CELLS

(1) Carriel, V.; (1) Campos, F.; (2) García-García, S.; (1) Scionti, G.; (3) Cornelissen, M.; (4) Rodríguez, I.A.; (1) Garzón, I.; (1) Sánchez-Quevedo, M.C.; (1) Campos, A.

(1) Tissue Engineering Group, Department of Histology, University of Granada, Spain, and Instituto de Investigación Biosanitaria ibs.GRANADA, Spain; (2) Division of Clinical Neurophysiology, University Hospital of Granada, Spain; (3) Department of Basic Biomedical Sciences, Histology, Faculty of Medicine, Ghent University, Belgium; (4) Cátedra de Histología B, University of Córdoba, República Argentina.

Introduction: Neural tissue engineering is focused on the design of novel biocompatible substitutes to bridge critical nerve gaps. Over the recent years, several biomaterials were used to generate different kinds of nerve substitutes and nerve conduits. Hollow conduits have been used with promising results, but the lack of internal supportive structures and biological properties to promote nerve regeneration make necessary the search of more bioactive systems. The aim of this study was to perform an *ex vivo* characterization of a novel multilayered nerve guide containing human adipose-derived mesenchymal stem cells (HADMSC) by using biomechanical and histological techniques. Materials and Methods: HADMSC were isolated, characterized by flow cytometry and used for the elaboration of fibrin-agarose hydrogels. These hydrogels were nanostructured and rolled to form cellular multilayered nerve guides (MNG). Some nerve guides were subjected to tensile test (n=10) and compared with rat sciatic nerves (controls). Other MNG were kept in culture for 2, 8 and 16 days for histological analysis. We evaluated the cellularity of the MNG with DAPI, cell proliferation with PCNA, and cytoskeletal

remodeling by identifying cortactin. Finally, the synthesis of acid proteoglycans and collagen type I were determined by alcian blue staining and immunohistochemistry, respectively. Uncompressed cellular fibrin-agarose hydrogels were used as controls for all histological analyses. Results: Tensile test demonstrated that MNG were resistant, flexible and elastic, but they were not comparable to the tensile properties of native rat sciatic nerves. However, MNG showed significantly higher deformation capability than the sciatic nerves. Histological analysis revealed a decrease of the cellularity of the MNG during the first four days in culture, but a significant increase of this parameter was observed after 8 days, accompanied by positive expression of PCNA. Interestingly, histological analysis revealed that cells were able to synthesize proteoglycans and collagen type I inside the MNG, especially after 16 days in culture. Conclusion: This *ex vivo* study demonstrated that it is possible to elaborate MNG by using fibrin-agarose hydrogels, HADMSC and nanostructuring techniques. These novel MNG are mechanically stable and biologically active, but *in vivo* analyses are needed to demonstrate their potential usefulness for peripheral nerve repair. Funding: This study was supported by the Spanish Plan Nacional de Investigación Científica, Desarrollo e Innovación Tecnológica (I+D+i) from the National Ministry of Economy and Competitiveness (Instituto de Salud Carlos III), grant FIS PI14/1343, co-financed by Fondo Europeo de Desarrollo Regional (FEDER), European Union.

117 GENERATION OF BIOENGINEERED ELASTIC CARTILAGE USING NANOSTRUCTURED FIBRIN-AGAROSE HYDROGELS

(1) García-Martínez, L.A.; (1) Campos, F.; (1) Garzón, I.; (2) Antúnez, C.; (2) Hernández-Lamas, M.C.; (3) Godoy, C.; (1) Sánchez-Quevedo, M.C.; (1) Campos, A.; (1) Carriel, V.

(1) Tissue Engineering Group, Department of Histology, University of Granada, Spain, and Instituto de Investigación Biosanitaria ibs.GRANADA, Spain; (2) Malaga Blood and Tissue Bank, Malaga, Spain; (3) Department of Histology, Faculty of Medicine, University of Santiago, Chile

Introduction: Elastic cartilage is a specialized connective tissue with limited regeneration capability. However, this tissue is often affected by several pathological conditions. Tissue engineering is currently focused on the generation of 3D models of EC for the reconstruction of different organs composed by EC. In this regard, different biomaterials were evaluated with promising results, but it is still necessary to find an efficient combination of elastic chondrocytes and appropriate biomaterials for use in regenerative medicine. In this sense, the aim of this study is to evaluate the ability of human elastic chondrocytes to grow in nanostructured fibrin-agarose hydrogels and to analyze their chondrogenic phenotype in these biomaterials. Materials and methods: Human elastic chondrocytes were isolated from small biopsies taken from healthy donors and cultured in fibrin-agarose hydrogels (FAH) 3D systems. FAH were subjected to nanostructuring and samples were harvested after 1, 2, 3, 4 and 5 weeks of *ex vivo* development for histological analysis using H&E staining. To identify acid proteoglycans and elastic fibers, alcian blue and orcein methods were used. Protein S-100, type I and II collagens, decorin, biglycan and aggrecan were identified by immunohistochemistry. Results: Histological analysis showed a progressive growth and development of the elastic chondrocytes in FAH, which were found scattered along the hydrogel or forming clusters. In

general, cells tended to remodel and degrade the surrounding biomaterial. Histochemical analysis revealed a weak reaction for acid proteoglycans, but clear elastic fibers were observed after some weeks of culture. Immunohistochemical analysis confirmed that the cells preserved their chondrogenic lineage with a positive reaction for S-100. In addition, elastic chondrocytes were able to synthesize type I and II collagens, biglycan and aggrecan over the time. Conclusion: This *ex vivo* study demonstrates that nanostructured FAH is an adequate biomaterial for 3D culture of elastic chondrocytes. These cells preserved their chondrogenic phenotype and synthesized essential extracellular matrix molecules. For these reasons, we hypothesize that FAH could be a useful biomaterial for the generation of a 3D model of elastic cartilage. Funding: This study was supported by grant SAS PI-0653-2013, Consejería de Igualdad, Salud y Políticas Sociales, Junta de Andalucía, Spain.

118 CORRELATION ANALYSIS OF THE BIOMECHANICAL AND HISTOLOGICAL FEATURES OF TWO TYPES OF HUMAN SKIN

(1) Campos, F.; (1) García-Martínez, L.A.; (1) Martín-Piedra, M.A.; (1) Alfonso-Rodríguez, C.A.; (1) Sánchez-Quevedo, M.C.; (2) Osorio, R.; (2) Toledano, M.; (3) Arias-Santiago, S.; (1) Garzón, I.

(1) Tissue Engineering Group, Department of Histology, University of Granada, Spain, and Instituto de Investigación Biosanitaria ibs.GRANADA, Spain; (2) Department of Stomatology, University of Granada, Spain; (3) Division of Dermatology, University Hospital of Granada, Spain

Introduction: The human skin is the largest organ in the body. This strong and flexible organ consists of three layers: epidermis, dermis and hypodermis. Several pathologies may affect the normal histology and physiology of human skin, and the efficient generation of an artificial human skin based on tissue engineering techniques could contribute to the management of these diseases. However, skin tissue engineering requires the entire knowledge of histological and biomechanical characteristics of the different skin types that exist in the human body. In this study, we have analyzed two regions of the human foreskin using histological and biomechanical methods. Material and Methods: To analyze the main histological and biomechanical properties of outer and inner human foreskin, 3 human biopsies of each of these skin types were fixed and stained with hematoxylin and eosin, and histochemical studies were performed using picosirius, Verhoeff, alcian blue (AB) and Schiff Periodic Acid (PAS) to analyze the fibrillar and non fibrillar components of the skin extracellular matrix. To evaluate the biomechanical properties of the outer and inner foreskin, the stiffness and deformability of both skin types were measured under tensile tests by determining the Young's modulus, stress at fracture and strain at fracture parameters using fresh samples. Results: Our histological results demonstrated that the epithelium of the outer foreskin was characterized by the presence of deep and well-developed dermal papillae and epithelial rete ridges that were generally absent from the inner foreskin. Moreover, the number of epithelial cell layers tended to be higher in outer skin as compared to inner skin. In addition, our picosirius results revealed that the concentration and location of collagen fibers was different in outer and inner foreskin. On the other hand, the presence of elastic fibers was higher in inner foreskin as compared to outer foreskin, especially in the reticular dermis. In contrast, non-fibrillar components of the

extracellular matrix did not show any difference between both types of human skin. Regarding the biomechanical analysis, our analysis performed by tensile tests showed that the average values of the Young's Moduli of the outer and inner skin were similar (27.36 MPa and 28.45 MPa, respectively). However, the stress and strain at fracture of the external skin, equal to 21.48 MPa and 186.47 % respectively, were higher than the corresponding average values of the internal skin, equal to 17.54 MPa and 149.97 % respectively, suggesting that the external skin samples could resist higher tensile forces and deformations before fracturing. Conclusions: Our results confirm the heterogeneity of the different types of skin that co-exist in the human body and imply the need of studying each specific native skin before generating artificial biomimetic models of these skins. Both the structure of the epithelium and the composition of the dermal extracellular matrix demonstrated to play a crucial role on the biomechanical behavior of the different types of human skin. These features should be reproduced in artificial skin models generated by tissue engineering in order to obtain the specific biomechanical characteristics of native tissues. Acknowledgments: This study was supported by the Spanish Plan Nacional de Investigación Científica, Desarrollo e Innovación Tecnológica from the Spanish Ministry of Economy and Competitiveness (Instituto de Salud Carlos III), grant FIS PI13/2576 (co-financed by FEDER funds, European Union).

128 HISTOPATOLOGÍA EXPERIMENTAL KARWINSKIA HUMBOLDTIANA INDUCES PANCREATIC ACINAR DESTRUCTION WITH ISLETS OF LANGERHANS PRESERVATION IN A RAT MODEL

(1) Carcaño Díaz, K.; (1) García García, A.; (1,2) Segoviano Ramírez, J.C.; (1) Rodríguez Rocha, H.; (1) Loera Arias, M.J.; (1) Salazar Leal, M.E. ; (1,2) García Juárez, J.

(1)Unit of Bioimage, Center for Research and Development in Health Sciences (CIDICS), UANL (Monterrey, Nuevo León, México); (2)Histology Department, Faculty of Medicine, UANL, (Monterrey, Nuevo León, México); (3) Immunology Department, Faculty of Medicine, UANL, (Monterrey, Nuevo León, México).

INTRODUCTION: Accidental ingestion of fruit *Karwinskia humboldtiana* (Kh) induces systemic damage, that causes severe respiratory failure and death. There is evidence of histological lesions in the lung, liver and kidney; in addition to those already described in the nervous system. However, the pancreas has not been studied. Acute inflammatory damage of the pancreas is closely related to systemic inflammatory response syndrome (SIRS), which may then lead to multiple organ dysfunction syndrome (MODS), the most common cause of mortality in acute pancreatitis. The objective of this work is to find histological evidence of damage to the pancreas in an animal model of acute intoxication for the purpose of correlate it with the severity of the poisoning. **METHODS AND MATERIALS:** It was administered an aqueous suspension of dry, ground and sieved fruit Kh, in a single dose of 5 g / kg weight to 15 Wistar rats of 225 ± 25 g, by oral catheter. The rats in the control group (n = 5) received only water. All animals were sacrificed under general anesthesia. Pancreas samples were obtained from three intoxicated and one untreated rats every 24 hours for 5 days. Pancreas samples, were fixed in 4% formaldehyde and processed to paraffin embedding. Sections of 5 micron thick were obtained and then stained with hematoxylin-eosin. It was recorded the weight of animals every 24 hours from the administration of Kh. This work has the approval of the Ethics Committee of the Faculty of Medicine of the UANL (Registration HT14-004). **RESULTS:** The average weight of the control group was maintained between $226,7 \pm 2,9$ and $230,7 \pm 9,0$ g during all treatment. At 48 h the mean weight of control group was $229,7 \pm 10,8$ g, while Kh

group was $222,8 \pm 13,5$ g. At 120 h after administration of Kh the mean weight of control group was $230,7 \pm 9,0$ g, and the mean weight of the Kh group was $200,3 \pm 8,1$ g, representing a significative difference of 12,9% .

MODELOS EXPERIMENTALES

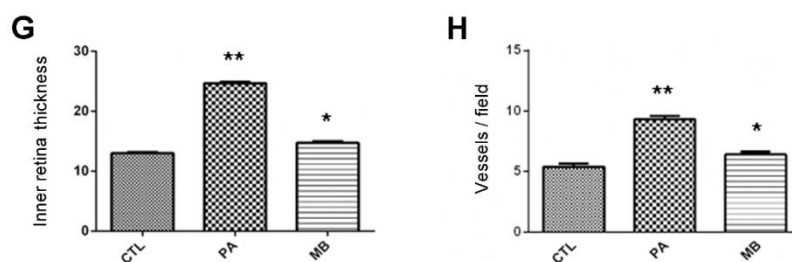
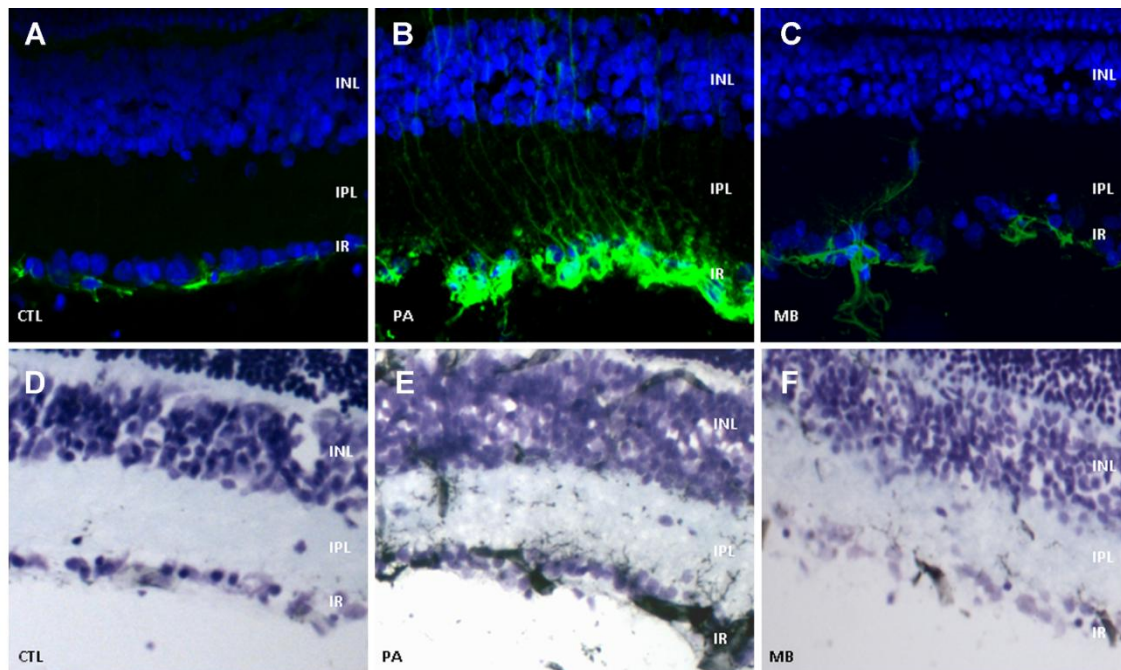
10 CHEMICAL PREVENTION OF RETINAL DAMAGE IN A RAT MODEL OF RETINOPATHY OF PREMATURITY (ROP)

Larrayoz, I.M.(1) , Rey-Funes, M.(2) , Fernández, J.C.(5) , Contartese, D.S.(2) , Rolón, F.(2) , Inserra, P.(3) , López-Costa, J.J.(2) , Dorfman, V.B.(3) , Martínez, A.(1) , Loidl, F.(2,4)

(1) Angiogenesis, Centro de Investigacion Biomedica de La Rioja (CIBIR), Logroño, La Rioja, Spain; (2) Laboratorio de Neuropatologia Experimental, Instituto de Biologia Celular y Neurociencia

INTRODUCTION: Perinatal asphyxia (PA) induces retinal lesions, generating ischemic proliferative retinopathy (IPR) and ROP, which may result in blindness. Previously, we have shown that the nitregeric system was involved in the physiopathology of PA-related ROP. Here we analyze the application of methylene blue (MB), a well-known nitric oxide synthase (NOS) inhibitor, as a therapeutic strategy to prevent IPR in a rat model of ROP. **METHODS:** Male rats were treated in 3 different ways: 1) CTL group comprised born to term animals; 2) PA group comprised rats exposed to perinatal asphyxia (20 min.); and 3) MB group comprised animals born from pregnant rats treated with MB (2 mg/kg) 30 and 5 min before delivery and then the pups were subjected to PA as above. mRNA was obtained 6 h after asphyxia for molecular studies and tissue was collected 30 days later for morphological and biochemical analysis. Data were statistically analyzed by ANOVA and differences were considered statistically significant when $p < 0.05$. **RESULTS:** PA produced significant gliosis, angiogenesis, and thickening of the inner retina ($p < 0.01$). MB treatment normalized these parameters

(Fig. 1). PA resulted in a significant elevation of the nitregeric system as shown by NOS activity assays, Western blotting, immunohistochemistry for nNOS, and histochemistry for NADPH-diaphorase activity ($p < 0.05$). All these parameters were also normalized by MB treatment. In addition, MB prevented the PA-induced upregulation of MMP9 ($p < 0.05$) and induced the upregulation of the antiangiogenic peptide, PEDF ($p < 0.01$). **CONCLUSIONS:** Application of MB prevented morphological and biochemical parameters of IPR and ROP. This finding suggests the use of MB as a new treatment to prevent or decrease retinal damage in the context of IPR.



11 THE INFLUENCE OF ADRENOMEDULLIN ON COLITIS STUDIED WITH AN INDUCIBLE GENE KNOCKOUT MODEL

Martínez-Herrero S, Narro-Íñiguez J, Larrayoz IM, Martínez A.

Oncology Area, Center for Biomedical Research of La Rioja (CIBIR), 26006, Logroño, Spain.

INTRODUCTION: Adrenomedullin (AM) is a biologically active peptide which is able to improve the symptoms of inflammatory bowel diseases (IBD) in animal models and in patients with severe ulcerative colitis. A polymorphism in the AM gene leads to lower plasma levels of this hormone in carrier individuals, which could result in a greater predisposition to IBD, and greater clinical severity and / or worse response to treatments. To get a formal demonstration of the effects that endogenous levels of AM may have in IBD, a genetic approach is needed where this gene is deleted throughout the body. Our goal was to generate the first full-body AM knockout (KO) model, in order to establish whether there is a relationship between AM expression and development and degree of pathogenesis of IBD. We hypothesized that the absence of AM would lead to greater disease severity. Results from several groups have shown

that early abrogation of the gene coding for AM results in 100% embryo lethality. **METHODS:** To circumvent this problem, we have developed an inducible KO using Cre/loxP technology combined with the induction system mediated by doxycycline, tet-On. Then we carried out a colitis model with our KO animals. Acute colitis was induced in mice, males and females, by rectal instillation of 3 mg of 2,4,6-Trinitrobenzenesulfonic acid (TNBS) in 100 μ L of 50% ethanol; control mice received the same volume of saline in 50% ethanol. The procedure lasted 5 days, during which the weight of the animals and the index of disease severity were recorded. Once the procedure was completed the inflammatory response was assessed in all mice by analyzing the weight of the colon and spleen, as macroscopic inflammation markers; by histomorphometric analysis of histological sections of colon; and by the activity of the enzyme myeloperoxidase (MPO) as an indicator of leukocyte infiltration. **RESULTS:** Induction of deletion in adult mice generated viable KO animals with no apparent anomalies. TNBS administration caused in KO mice, especially females, a much more severe colitis when compared to wild-type (WT) mice treated with TNBS. Deletion of the AM gene caused more severe diarrhea, accompanied by rectal bleeding, anorexia, and a significant increase of colon weight. Histological analysis of the KO mice treated with TNBS confirmed the macroscopic study data showing large areas of lymphocyte infiltrates in the mucosa and submucosa, with loss of tissue architecture. MPO activity showed a tendency to increase in the KO mice, both treated and control, which could mean that in the absence of AM there is an increased permeability of blood vessels. **CONCLUSIONS:** All results of this study support the protective role of endogenous AM against the development of acute colitis, its effect being particularly beneficial on females. This study was supported by a grant from the Instituto de Salud Carlos III (PI13/02166).

17 SUBCUTANEOUS IMPLANTATION OF MSCS-COATED MESHES FOR REDUCING POST-SURGICAL INFLAMMATION IN A MURINE MODEL.

Blázquez Durán, R., Sánchez-Margallo, F.M., Álvarez Pérez, V., Usón Gracia, A., García Casado, J.

Introduction: Surgical meshes are widely used in clinics to reinforce soft tissue's defects, and to give support to prolapsed organs. However, the implantation of surgical meshes is commonly related with an inflammatory response being difficult to eradicate without removing the mesh. After surgical implantation, different steps are involved such as coagulum formation and platelet adherence followed by migration of fibroblasts, polymorphonucleocytes and macrophages. These macrophages fuse into multinucleated giant cells and remain in the meshes for an undetermined period of time. The failure to resolve the inflammatory response leads to foreign body reaction, granulation tissue formation and encapsulation of the implant. Here we hypothesize that the combined use of surgical meshes and mesenchymal stem cells (MSCs) could be a useful tool to reduce the inflammatory reaction secondary to mesh implantation. **Materials and methods:** An *in vivo* study using a murine model was conducted to assess the safety and efficacy of MSCs-coated meshes to reduce the inflammatory reaction. Mice were divided into two groups (n=9). In the control group, meshes without MSCs were subcutaneously implanted. In the treatment group, MSCs-coated meshes were similarly implanted. Magnetic resonance imaging, laparoscopy and histology were performed for safety assessment. For

histology, at day 7 post-implantation, animals were euthanized with CO₂ and the whole layer composed by the skin, mesh and muscular-peritoneum was fixed in paraformaldehyde 4%, paraffin-embedded and sliced in 5-8µm thickness. Histological samples were stained for Hematoxylin-Eosin and Masson Trichrome. Finally, flow cytometry and qRT-PCR were used to elucidate the immunomodulatory mechanism of MSCs-coated meshes. Results: Our results demonstrate that these biological meshes fulfill the safety aspects as non- adverse effects were observed when compared to controls. The histological comparison between control and treated animals did not show cellular evidences of acute inflammatory changes including necrosis, hemorrhage or neovascularization around the implantation site. Also, there were no noticeable signs of collagen depositions around material. Finally, there were no alterations in the adjacent tissues; although slight differences were found in the density of cells adhered to the implanted meshes. Histological analysis showed a higher density of cells adhered to MSCs-coated meshes, compared to control. Moreover, flow cytometry and qRT-PCR analyses demonstrated a local immunomodulation of implanted MSCs-coated meshes mediated by a macrophage polarization towards an anti- inflammatory phenotype was noted. Conclusions: In conclusion, the combined usage of surgical meshes with MSCs fulfills the safety requirements for a future clinical application. These MSCs-coated meshes provide an anti- inflammatory environment that could reduce the inflammatory processes commonly observed after surgical mesh implantation.

50 EFFECT OF TOPICAL POLYACETAL AND HYALURONIC ACID IN A MURINE MODEL OF WOUND HEALING - A MORPHOMETRIC STUDY

Marcos -Garcés, V. (1), Sepúlveda Sanchís, P. (2, 3), Garcia, N. A. (2, 3), Rodríguez Escalona, G. (4) , Ruiz-Saurí, A. (1, 5)

(1) Pathology Department, Faculty of Medicine and Odontology, University of Valencia (2) Medical Research Institute Hospital La Fe (IIS La Fe), Valencia (3) Cardiovascular Repair Laboratory, Príncipe Felipe Research Center, Valencia (4) Polymer Therapeutics Laboratory, Príncipe Felipe Research Center, Valencia (5) INCLIVA Biomedical Research Institute, Valencia

INTRODUCTION: The use of biopolymers in skin wound healing is a relatively new field of research that has provided promising results in the past years. Polyacetal (PA) has been used in tissue engineering, but its efficacy in skin regeneration has not been clarified yet. We aim to study the histological effects of a single topical application of hyaluronic acid (HA) with or without PA in a murine model of cutaneous wound healing.

MATERIAL AND METHODS: We used C57BL6 mice aged 8-10 weeks. After being anesthetized with sevoflurane, their back was shaved and a 5mm diameter full-thickness skin defect was made with a punch biopsy. Afterwards, topical treatment was applied - saline physiological solution for the control group (n=16) or a 50 µl water resuspension of HA with or without PA for experimental groups (each n=16). Animals were sacrificed at day 3 (n=4 for each group), day 10 and day 22 (n=6 for each group) and samples were taken for histological analysis. All procedures were approved by the Research Ethics Committee.

Samples were fixed in a 5% formaldehyde solution and embedded in paraffin. 5µm microtome sections were made and then stained with Hematoxylin-Eosin. We took 5 microphotographs

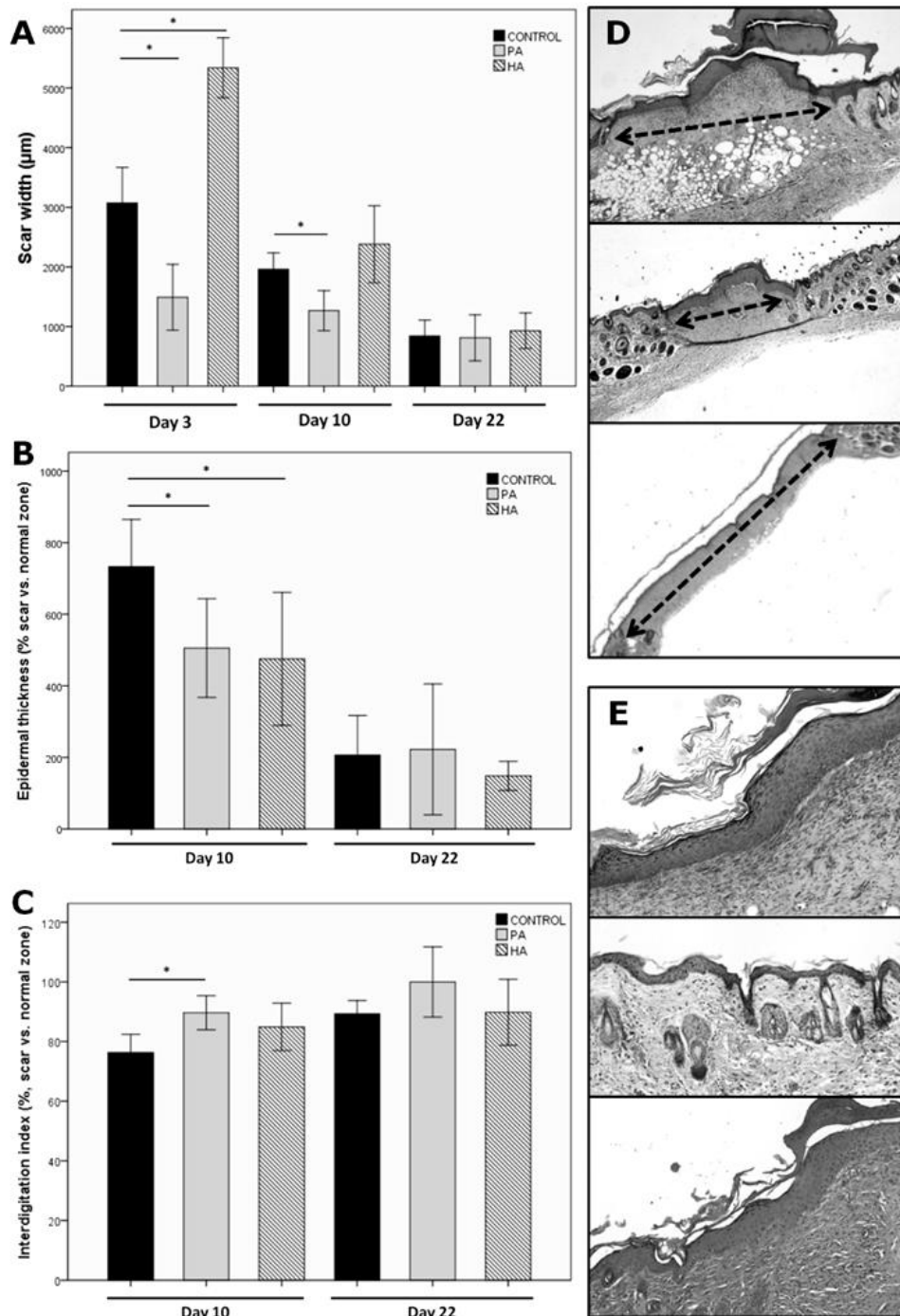
with a microscope Leica DMD108 and measured the following morphometrical parameters with IMAGE-PRO PLUS 7.0 software: scar width, hair follicle density, interdigitation index, and epidermal thickness. Semiquantitative evaluation of inflammatory infiltrate and integrity of subjacent muscle was also made. A blind protocol was used. Statistical analysis was made using Student t test for continuous variables and Chi-Square (χ^2) for categorical variables. $P < 0.05$ was considered significant.

RESULTS: An intense inflammatory infiltrate with full-thickness skin defect and scab formation was present in all groups at day 3. However, at this time scar width was increased in HA-alone and reduced in PA-HA compared to control ($p=0,008$ and $p=0,001$ respectively). Those differences are still present at day 10 in HA-PA ($p=0,009$) but not in HA-alone, suggesting an accelerated wound closing only in HA-PA. At day 10, a milder inflammatory infiltrate was seen in PA-HA and HA-alone compared to control (χ^2 , $p=0,001$), and also a less hypertrophic epidermis in the scar area ($p=0,039$ and $p=0,047$, respectively). Dermo-epidermal junction recovery increased in PA-HA at day 10 as demonstrated by the interdigitation index ($p=0,01$).

Regeneration of hair follicles was moderate at day 10 and nearly complete at day 22, with no differences between groups. At day 22, subjacent muscle regeneration was increased in PA-HA and HA-alone (χ^2 , $p=0,004$), while in control group substitution by fibrous tissue was seen in all cases.

CONCLUSIONS: Histopathological data show that a single application of topical PA-HA has beneficial effects on murine skin healing after full-thickness skin defects, as demonstrated by an accelerated wound closing at day 3 and 10, less inflammatory infiltrate, increased recovery of normal epidermal thickness and dermo-epidermal junction interdigitation at day 10, and better subjacent muscle regeneration at day 22. Most of these changes were not present in HA-alone group, suggesting that PA addition has a beneficial effect on skin wound healing.

Figure 1: histological analysis of PA-HA ,HA-alone and control groups at day 3, 10 and 22. **A**, scar width (μm). **B**, epidermal thickness (% of thickness in scar area compared to normal area). **C**, interdigitation index (% of value in scar area compared to normal area). **D**, histological images (40x magnification) of control (upper), PA-HA (middle) and HA-alone (lower) groups at day 10. **E**, histological images (100x magnification) of control (upper), PA-HA (middle) and HA-alone (lower) groups at day 10.



62 DEVELOPMENT OF AN EXPERIMENTAL MODEL OF GANGLION IN WISTAR RATS.

(1) Crespo-Lora V, (2) O'Valle Ravassa F, (3) Crespo PV, (3) García JM, (4) Fernandez Quesada F, (5) Hernández-Cortés P.

(1) Provincial Inter-center Management Unit, Department of Pathology. Granada, Spain, (2) Department of Pathology and Biopathology and Regenerative Medicine Institute

(IBIMER), School of Medicine. University of Granada. Granada, Spain. (3) Tissue Engineering Group, Department of Histology, University of Granada, Spain.(4) Surgery department, University of Granada, Spain. (5)Orthopedic Surgery Department of San Cecilio University Hospital of Granada. Spain.

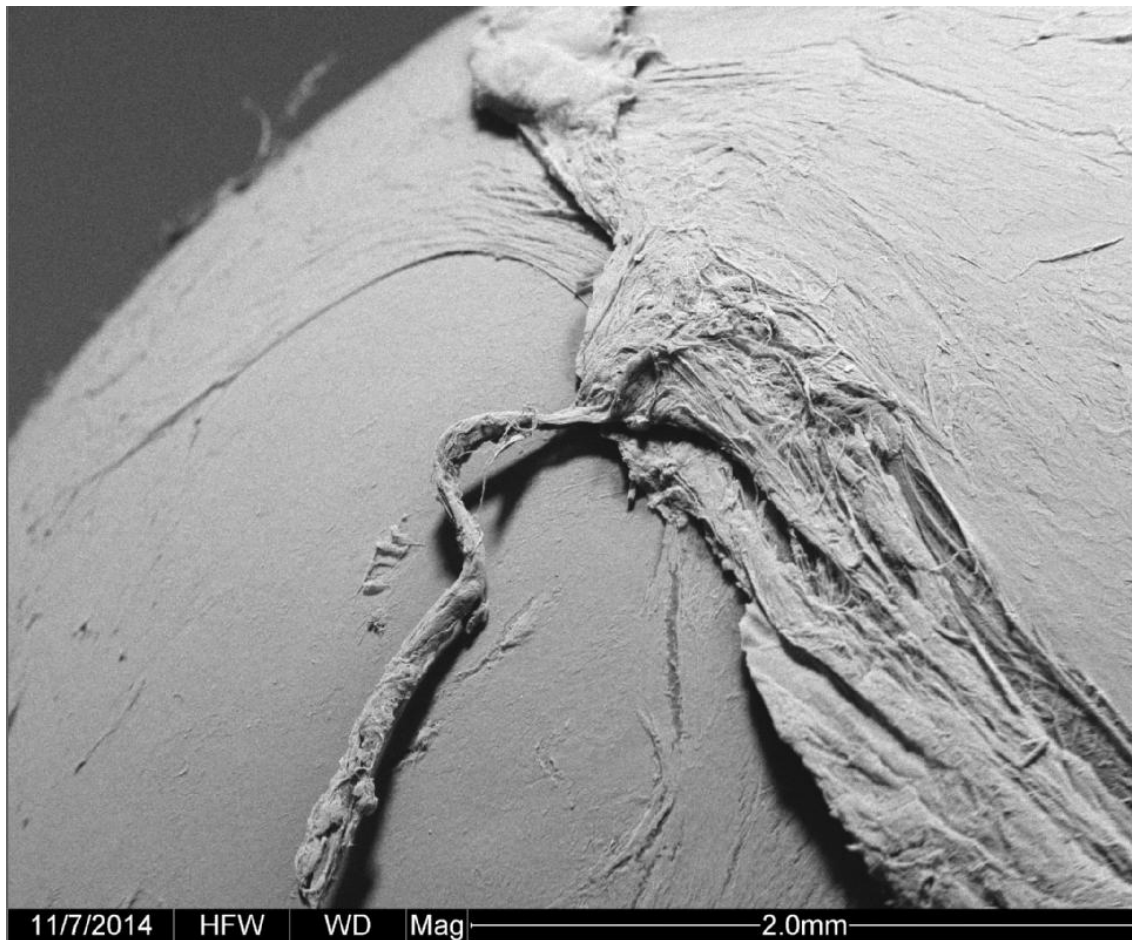
Introduction: The ganglion is a prevalent joint disease of unknown etiology characterized by presented as a pseudocystic lesion in relation to joints. It is surgical treated and shows a recurrence rate of up to 40%, and may show sometimes postoperative side effects such as neurovascular injury or hypertrophic scars that interfere with the joint mobility. At present, there is only one published model proposed by Taniguchi et al. The aim of this study is the development of a new model of ganglion more adjusted to the human for application of new minimally invasive therapies.

Material and methods: In 10 male Wistar rats weighing 250-300 g, were inserted two spherical crystal implants of 1 cm in diameter in the dorsal region (n = 20) through two medial longitudinal incisions, at 4 months implants were removed and filling the “neocyst” formed around sphere with commercial hyaluronic acid solution. After 21 days the animals were sacrificed by overdose with sodium pentobarbital, and the cysts extracted. The samples were fixed in 10% buffered formalin, embedded in paraffin and stained with hematoxylin-eosin, PAS and Masson’s trichrome for morphological studies. Cysts used for studies with a scanning electron microscope were fixed in 2.5% glutaraldehyde for 24 hours at 4°C, and subsequently maintained in cacodylate buffer. The experiment was conducted in a homologated laboratory following ethics guidelines for animal care and the current regulations issued by the European Union and the Government of Spain (EU Directive 63/2010, RD 53/2013).

Results: Out of 10 rats, 4 died during anesthesia (40%), and were replaced. Rats throughout the experiment did not show complications due to surgery, showing at the time of extraction of the crystal sphere, a thin layer of tissue with an elastic consistency and translucent appearance, which covered it entirely. The morphological and ultrastructural study showed that the layer is formed by connective tissue, mostly fibroblasts, without an inflammatory infiltrate, remains of old hemorrhage and a smooth surface, both external and internal. These histologic features resembled those found on the microscopic study of ganglion in human biopsies.

Conclusions: We believe that the experimental model proposed is a valid, reliable and reproducible model, as we induced a cystic formation that morphologically had ganglion features; Due to this similarity, this model could be used to test new minimally invasive treatments of this pathology.

Figure: Scanning electron microscope image of the external surface of one of the experimental cysts, the layer of connective tissue surrounding the entire crystal sphere is evidenced (bar 2 mm).



63 FIRST DESCRIPTION OF IMMUNOHISTOCHEMICAL EXPRESSION OF MUSASHI-1 IN EXPERIMENTAL BONE FRACTURE HEALING IN RATS.

(1) Crespo Lora V, (2) Cándido Corral C, (3) Hernández Cortés P, (2) Rodríguez Martínez MD, (1) Aneiros Fernández J, (2) Aguilar Peña M, (4) Padial Molina M,(4) Galindo Moreno P, (1) O?Valle Ravassa F.

(1) Provincial Inter-center Management Unit, Department of Pathology. Granada, Spain. (2) Department of Pathology and Biopathology and Regenerative Medicine Institute (IBIMER), School of Medicine. University of Granada. Granada, Spain. (3) Orthopedic Surgery Department of San Cecilio University Hospital of Granada. Spain. (4)Associate Professor, Oral Surgery and Implant Dentistry Department, School of Dentistry, University of Granada. Granada, Spain.

Introduction: Mesenchymal stem cells (MSCs) play a crucial role in providing progenitor cells from which osteoblasts, bone matrix forming cells, differentiate. The mechanical environment plays an important role in regulating stem cell differentiation into osteoblasts. However, the mechanisms by which MSCs respond to mechanical stimuli are yet to be fully elucidated. Musashi-1 (Msi1) is an RNA-binding protein that plays an important role in regulating the maintenance and differentiation of stem/precursor cells. Its presence in reparative

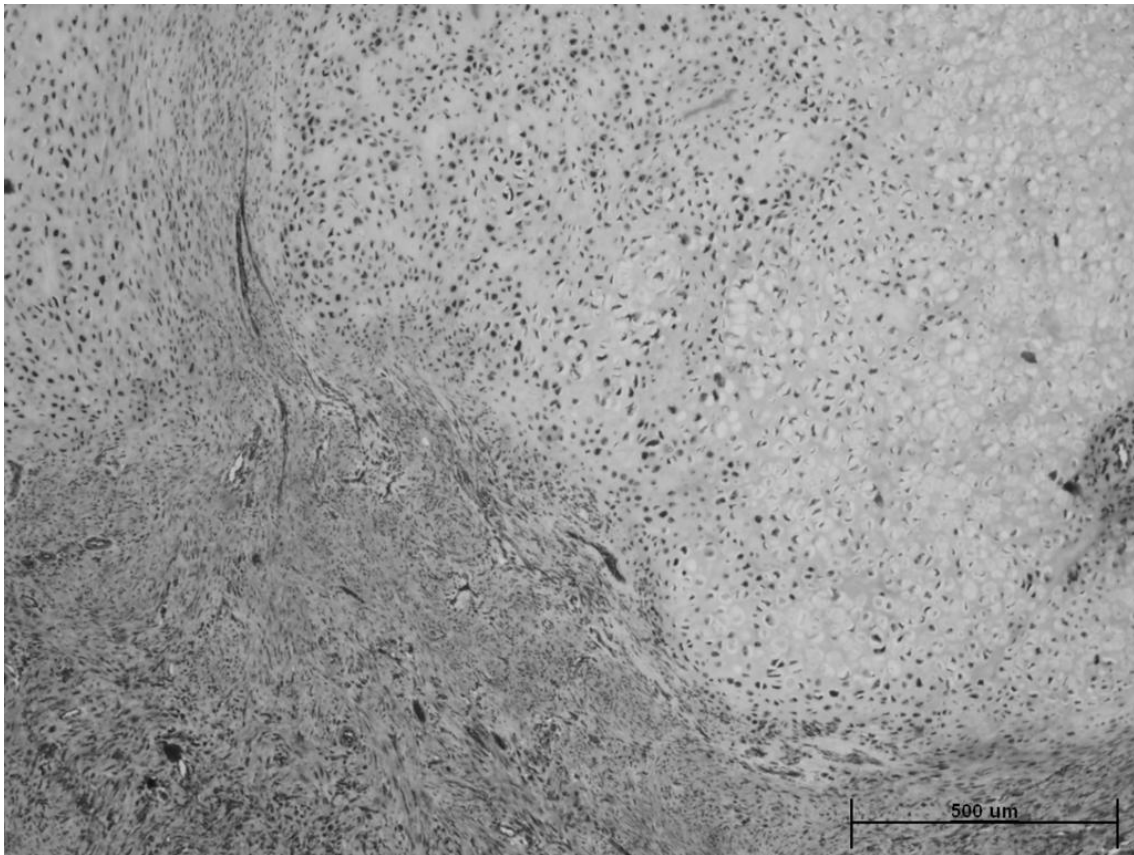
fibrocartilaginous tissue of callus has not been yet communicated; on the other hand, small animal fracture models have gained increasing interest in fracture healing studies as a dynamic and mechanically challenged environment. Therefore, the objective of this investigation was to determine the immunohistochemical expression of Msi1 protein in an experimental rat model of femoral bone fracture.

Material and methods: Internal fracture without fixation was used as endochondral repair model (modified from Bonnarens F. & Einhorn TA., 1984). Diaphyseal femur fractures were induced in the right hind limb of 10 rats; 10 right hind limbs without fractures were used as controls. After six weeks Tjips disjointed were fixed in 10% buffered formalin, decalcified with EDTA (Surgipath I), embedded in paraffin and stained with hematoxylin-eosin for morphological study and Masson's trichrome for morphometric study. Ten images of the fracture callus per rat were captured with the 10x objective in a BX51 microscope equipped with a digital camera DP70 (Olympus Optical Company). Images were evaluated using the software ImageJ (version 1.48), and quantified each cellular types separately from callus. For the immunohistochemical study, paraffin sections were treated with 1 mM EDTA at pH 8 and 95°C for 20 minutes in a PT module to induce antigen retrieval. Sections were incubated with polyclonal antibody against Musashi-1 (Sigma-Aldrich) during 16 hours at 4°C. The polymer-peroxidase-based method (Ultravision Quanto) followed by development with diaminobenzidine (Master Diagnostica) were performed in an automated immunostainer. A millimeter scale in the eyepiece of a BH2 microscope (Olympus, Optical Company, Ltd, Tokyo, Japan) with a 40x objective was used to count nuclear Msi1 positive osteocytes, osteoblasts, mature chondrocytes, immature chondrocytes and mesenchymal cells per mm².

Results: In this model, the calli were constituted by mesenchymal tissue (24.39% of area), cartilage (41.74%) and newly formed bone tissue (41.74%). Msi1 was expressed by osteoblasts, osteocytes, immature chondrocytes and mesenchymal cells, which was statistically significant compared to controls (512.0 ± 48.3 vs. 131.7 ± 53.4; 373.0 ± 77.9 vs. 8.0 ± 5.7; 426.6 ± 75.8 vs. 104.6 ± 44.0; 383.0±173 vs. 0.0±0.0 positive cells/mm², respectively, P<0.001, Mann Whitney U-test) (Figure 1). A significant direct correlation between the expression of mesenchymal cells and Msi1 in osteogenic cells was observed (rho = 0.841, P <0.0001, Spearman test).

Conclusions: Higher Msi1 expression in the cells that compose the callus suggests its role in the differentiation of mesenchymal stem cells into bone tissue forming cells and bone healing.

Figure: Immunohistochemical nuclear expression of Msi1 in bone fracture callus. Note the positivity in mesenchymal cells, immature chondrocytes and negativity in mature chondrocytes (asterisk) (polymer-peroxidase-based method plus Masson's trichrome x4).



64 MORPHOLOGICAL STUDY IN GUINEA PIGS MODEL OF VASCULAR REPAIR THROUGH PATCH EXPANDED AND REINFORCED POLYTETRAFLUOROETHYLENE.

(1) Crespo-Lora V, (2)Bravo Molina A, (1) Gonzalez Sanchez JF, (1) Rios Pelegrina R, (1) Caba Molina M, (3) O'Valle Ravassa F.

(1) Provincial Inter-center Management Unit, Department of Pathology. Granada, Spain. (2) Department of Angiology and Vascular Surgery, Complejo Universitario hospitalario de Granada, Spain, (3) Department of Pathology and Biopathology and Regenerative Medicine Institute (IBIMER), School of Medicine. University of Granada. Granada, Spain

Introduction: The experimental study of peripheral vascular disease is an unexplored field with high technical difficulty: indeed, few studies have been conducted on mammals, mainly in pigs, with its concomitant limitations. We present a morphological study of a new experimental model based on rodents.

Material and Methods: The study was performed with male guinea pigs of Hartley strain (n = 15) with an average weight of 350 g pretreated with iv heparin weight adjusted at the time of the surgery. After designing a learning curve in 20 animals, we laparotomized the animals, dissected the previously clamped infrarenal, aorta placing a PTFE prosthetic patch of 0.6 micrometers. A preventive 10 mg/day oral acetylsalicylic acid treatment was indicated. The animals were sacrificed after two weeks after surgery with an overdose of sodium pentobarbital.

The experiment was conducted in a homologated laboratory following ethics guidelines for animal care and the current regulations issued by the European Union and the government of Spain (EU Directive 63/2010, RD 53/2013). For morphological study, samples were fixed in 10% buffered formalin and subsequently embedded in paraffin. Serial sections of 4 micrometres of the treated area with PTFE patch and the normal abdominal aorta, that was used as a control, were performed. The sections were stained with hematoxylin-eosin, Masson's trichrome and orcein for elastic fibers.

Results: After surgery, six guinea pigs died within 72 hours (40%), in three cases (20%) at necropsy found mural thrombus in the abdominal aorta in relation to the prosthesis. Nine animals survived until the end of the experiment (60%), showing a good vascular permeability without secondary vascular complications appear to intervention. Microscopic examination showed in treated areas maintenance of arterial lumina and a preservation of the internal elastic lamina, lined by endothelial cells. The muscle fibers of the arterial wall showed no abnormalities, at the same time there was no evidence of elastic fibre duplication or bleeding in the arterial wall. Surrounding the PTFE prosthesis on its external surface, a mild giant cell granulomatous foreign body reaction was observed.

Conclusions: Despite the limitations of the model and considering the need optimization, the study shows that this experimental animal model that uses easy handling in a animal facilities, may be useful for testing prosthesis with future clinical application, despite the technical difficulty implied of the model and own morbidity. The maintenance of the morphological integrity of the arterial wall with endothelialization, internal elastic lamina preserving and properly oriented muscular fibers was in relationship with the clinical result obtained.

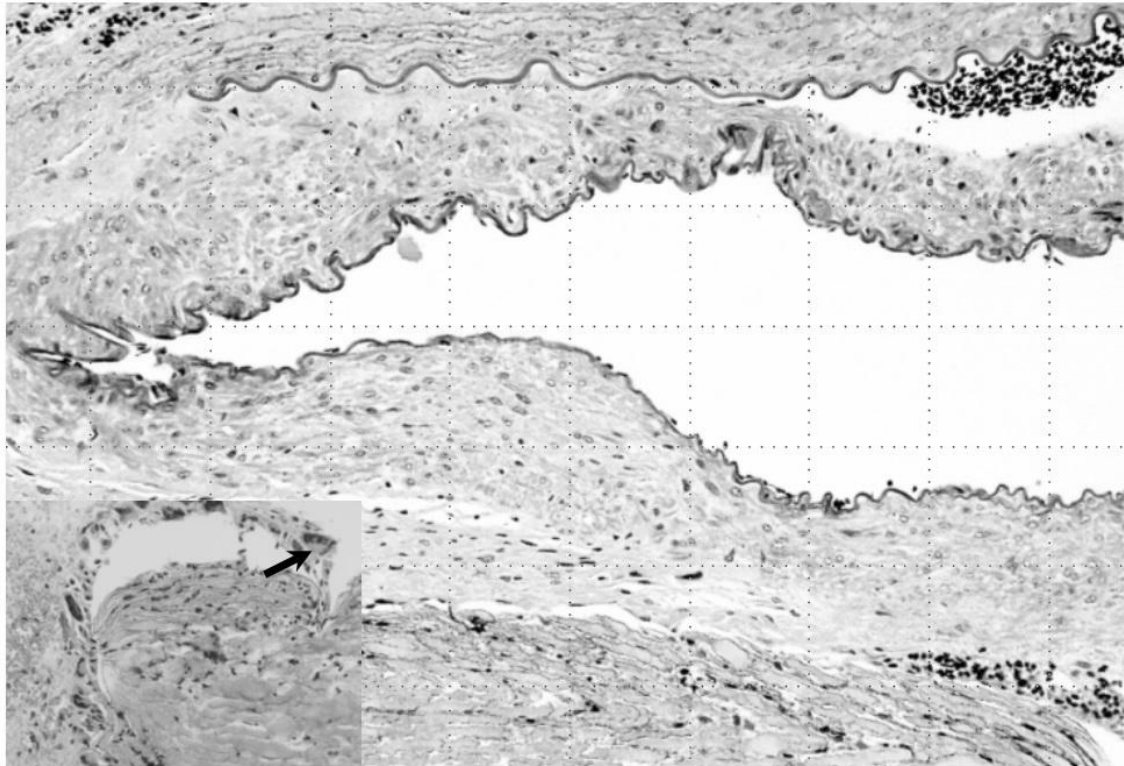


Figure: Microphotograph of the arterial lumen showing the integration of the PTFE patch, preservation of the internal elastic lamina and endothelial cells without myointimal injury. Insert: Picture with evidenced of a small accumulation of giant cells externally surrounding PTFE patch (Arrow) (Masson's trichrome method, original magnification x10)

73 HYPOXIA-ISCHEMIA IN NEWBORN PIGLETS. A NOVEL MODEL TO STUDY AUDITORY SYSTEM IMPAIRMENT

(1) Revuelta, M.,(1) Arteaga, O.,(2) Alvarez, F.J.,(2) Lafuente, H.,(3) Santaolalla, F.,(1) Alvarez, A.,(1) Hilario, E.,(3) Martinez-Ibargüen, A3

(1) Department of Cell Biology and Histology, Faculty of Medicine and Dentistry, University of the Basque Country, Leioa, 48940-Bizkaia, Spain. (2) Research Unit on Experimental Perinatal Physiopathology, Hospital de Cruces, Barakaldo, 48080-Bizkaia, Spain (3).Department of Otorrhinolaryngology, Faculty of Medicine and Dentistry, University of the Basque Country, Leioa, 48940-Bizkaia, Spain.

Introduction Hypoxia?ischemia is a major perinatal problem that results in severe damage to the brain. In humans, 80% of the growth of the CNS takes place in the last two months of gestation and the first few months of life, periods during which this system is particularly damaged by the effects of a low blood flow. In line with this, hypoxic/ischemic brain injury that takes place during this perinatal period is one of the most common causes of long-term severe neurological impairments. Objective The objective of the present study was to develop a new animal experimentation model to study the effect of perinatal asphyxia on the auditory system. Material and methods Hypoxia-ischemia was induced to 1.3 day-old piglets by clamping both carotid arteries by vascular occluders and lowering the fraction of inspired oxygen. We compared the Auditory Brain responses (ABRs) of newborn piglets exposed to acute hypoxia/ischemia (n=6) and a control group with no such exposure (n=10). Results The Auditory Pathway as assessed by ABR was altered during the hypoxic-ischemic insult but recovered 30-60 minutes later. Hypoxia/ischemia seemed to induce auditory functional damage by increasing I-V latencies and decreasing wave I, III and V amplitudes, although differences were not significant. Conclusion The hypoxic-ischemic experimental model in newborn piglets is a suited model for studying the functional effects of perinatal asphyxia on the auditory system. Moreover, the development of this model will allow us, in the future, to study the effect of more severe damage and the effects of treatment strategies for the prevention of hearing impairment.

83 HISTOLOGICAL ASSESSMENT OF THE CHONDRAL LESION IN PORCINE MODEL

Usón Gracia, A., Tapia-Araya, A., Álvarez Pérez, V., Blázquez Durán, R., Vela F.J., Borrega Hernández, M., García Casado, J., Sánchez-Margallo, F.J.

Centro de Cirugía de Mínima Invasión Jesús Usón

Objective: This study aimed to create a uniform and reproducible model of chondral lesion on the knees of a porcine model. This model is currently used to evaluate the combined use of Mesenchymal Stem Cells (MSCs) and absorbable scaffolds therapies. In this work, histological analysis was assessed in chondral tissue lesions with and without scaffolds. **Materials and Methods:** A total of three female Large White pigs were included in this study. At the initial stage, animals were 3 months old and weighted approximate 30 kg. In both medial femoral condyles a chondral defect was performed of 6 mm diameter and 2 mm deep. On the right knees scaffolds were implanted on the condral defect and left knee was used as control. The animals were observed daily to ensure they were eating and drinking regularly. The hind limbs were examined and evaluated regularly and range of motion. Animals were followed for three months. For histology, after fixing with formalin, samples were processed and embedded in paraffin using standard techniques. Cross sections of the defect area of the femoral condyle, to a thickness of 10 µm were performed. These cuts were made with a semi-automatic microtome. Samples were stained with Hematoxylin-Eosin for observation of nuclei and tissue structures and Toluidine Blue as specific technique for observing chondroblasts. After washing the samples with alcohols resin they mounted with DPX. Images of the samples taken at 10X - 20X magnification were obtained. The histological analysis will be completed with the determination by semi-quantitative PCR of the expression of the COL2A1, Sox9 and Aggrecan Pig genes. **Results:** In all cases, the outcome was excellent: no intraoperative or postoperative complications. Regarding the histological findings in the left knee (without scaffolds) there was a defect filled with fibrocartilage tissue. It was observed normal structures of fibrocartilage as blood vessels, elastic fibers or fibroblasts and lack of perichondrium. On the contrary, in the right knee (with scaffolds) was found that these filled entire the condral defect with fibrocartilaginous tissue. **Conclusions:** Histological examination proved to be an excellent tool for assessment and evolution of chondral defects. The histological study confirmed that in the case of control samples, the cut size was between 3-5 µm, while the minimum size necessary to cut the chondral defect with scaffolds were 10 µm. Finally, this thickness does not affect the histological evaluation.

86 OSTONECROSIS DE LOS MAXILARES ASOCIADA A BIFOSFONATOS. UN MODELO EXPERIMENTAL DE EXTRACCIÓN.

Trejo CG(1), Bolaños MA(1), Gómez-Clavel JF(2).

(1) Laboratorio de Investigación en Odontología Almaraz, Carrera de Cirujano Dentista, Facultad de Estudios Superiores Iztacala, Universidad Nacional Autónoma de México. (2) Laboratorio de Investigación y Educación en Odontología, Carrera de Cirujano Dentista, Facultad de Estudios Superiores Iztacala, Universidad Nacional Autónoma de México.

INTRODUCTION: Zoledronic acid (AZ) is a bisphosphonate (BF) used for treatment of bone diseases related to osteoclast activity (osteoporosis, myeloma, bone metastases and Paget's disease); newly found relationship between BF and bisphosphonate-related osteonecrosis of the jaws (BRONJ). Ersan et al. (2013) conducted an evaluation of a model of osteonecrosis associated with AZ performed in rats, in their study they not found clinical manifestations of BRONJ, however, in histological evaluation if found developing BRONJ and increased the number, size and osteoclast apoptosis. Yoshiga D. et al. (2014) evaluated the use of BF as a

etiology to BRONJ in 192 patients, they found that 57% of these patients had BRONJ in seven months, average time, these patients were given treatment and only 36% of them, osteonecrosis not budge and even progress. Bi Y. et al. (2010) reported that BF cause BRONJ because of the effects of these drugs in angiogenesis and bone remodeling, especially at high dosages, long-term and in combination with chemotherapy and immuno / suppressing drugs. Marino K. et al. (2012) reported that the degradation of collagen and bacteria are BRONJ by AZ characteristics. Ulteja et al. (2010) reported that a relationship exists between dental extractions and BRONJ development. Given the above, the aim of this study was to develop a rat model, translational of BRONJ.

METHODOLOGY: 16 rats were divided into 2 groups (n = 4) were used. Group 1: Control who underwent the administration of saline solution, later, we perform the extraction of the second molar tooth; and Group 2: translational 66µL doses of AZ was administered 14 and 7 days before the tooth extraction. Study times were 15 and 30 days. Samples were processed for histological study.

RESULTS: A clinical evaluation in the groups to 15 days could not determine BRONJ; however, at 30 days in the group administered AZ 50% of the specimens had no epithelialization and open alveolus was observed, accompanied by 50% loss of the outer table.

CONCLUSIONS: he results presented are preliminary, this clinical evaluation determined that the jaw necrosis was increasing with time to form a study in experimental groups when these

91 SUBLETHAL EFFECTS OF JELLYFISH (*Chrysaora* sp.) VENOM IN ZEBRAFISH (*Danio rerio*).

Becerra Amezcua, M.P., López Vite, S.A., Guzmán-García, X., González Márquez, H., Guerrero Legarreta, I., Hernández Calderas, I.

Universidad Autónoma Metropolitana

SUBLETHAL EFFECTS OF JELLYFISH (*Chrysaora* sp.) VENOM IN ZEBRAFISH (*Danio rerio*). Becerra Amezcua, M.P., López Vite, S.A., Guzmán García, X., González Márquez, H., Guerrero Legarreta, I., Hernández Calderas, I. The jellyfish of the *Chrysaora* sp. genus are present worldwide, but the toxicity of their venoms has not yet been described. On the other hand, this model has been used for investigation of toxicological impact of many drugs and chemicals. The aim of this study is to observe the effect of *Chrysaora* sp. venom in zebra fish (*Danio rerio*) tissues, to understand the mechanisms of poisoning. Zebra fish were administered with three sublethal dose of the venom (2, 20 and 200 µg/g) by intraperitoneal injection. The principal macroscopic effect, at the highest concentration (200 µg/g) of crude venom on *Danio rerio*, was the appearance of eye hemorrhage. Meanwhile the histological analysis revealed liver was the most affected, presenting infiltration and congestion, gills showed lumen dilatation and capillary blood congestion. The blood analysis showed hemolysis, nuclear abnormalities and echinocytes. The Venom of *Chrysaora* sp. alter circulatory system of zebra fish, disturbing liver and gills, asociated with vascular dilatation due to localized release of inflammatory mediators. Erythrocytes were affected by the action of phospholipase A2, present in venom.

101 ROLE OF MIRNAS IN ENDOTHELIAL TO MESENCHYMAL TRANSITION INDUCTION IN CULTURED HUMAN PRIMARY ENDOTHELIAL CELLS.

Mata, M. (1)(2)(3); Sarrion I. (4), Milian, M.(2); Ruiz Saurí, A.(1)(2); Sancho-Tello, M.(1)(2); de Llano, J.J. (1)(2) and Carmen Carda(1)(2).

(1) Departament de Patologia, Facultat de Medicina i Odontologia, Universitat de València. (2) INCLIVA, Hospital Clínico Universitario de Valencia. (3) Ciber de enfermedades respiratorias (CIBERES). (4) Universidad Católica de Valencia.

Background/Objective: Human pulmonary arterial hypertension (PAH) is a vascular disease that is largely restricted to small pulmonary arteries. The pathogenesis of PAH is characterized by vascular remodelling that leads to an increase in vascular resistance with devastating effects on patient. Vascular remodelling involves predominantly the accumulation of α -smooth muscle actin-expressing mesenchymal-like cells in obstructive pulmonary vascular lesions in a process known as endothelial to mesenchymal transition (EnMET). Molecular mechanisms involved in this process are actually under investigation. Recently, the role of miRNAS controlling the pathophysiology of the disease have been described in different in vivo and in vitro models, as well as in circulating blood of IPAH patients. In this study we have analysed the global expression changes of miRNAS in cultured primary pulmonary endothelial cells exposed to transforming growth factor beta (TGF- β) and endothelin (ET) which are two key regulators of EnMET. Methods: Small vascular human endothelial cells were isolated and cultured in the absence or presence of TGF- β 5 ng/ml or ET 20 nM for up to 72 hours. Gene expression of ASMA, CD31, vEGF, vECADHERINA, SNAIL and SLUG was determined by real time RT-PCR. miRNA expression was determined using Affymetrix's miRNA arrays. Results: We have observed an increase of the expression of ASMA, CD31, vEGF, vECADHERINA, SNAIL and SLUG as consequence of TGF- β and ET-1 exposure of cultured endothelial cells compared to non-exposed cultures. Regarding microarray analysis we have detected differential changes in 52 miRNAs (18 down-regulated and 34 up-regulated). Hierarchical clustering and PCA analysis of the data obtained indicated a good separation of the three experimental groups included. Among data obtained there are well known pulmonary hypertension implicated miRNA like miR130-301, miR-21, miR17-92 and miR204 as well as several new miRNAs non-related to the pathogenesis of the disease. Conclusion: Our data enforce the implication of miR130-301, miR-21, miR17-92 and miR204 in the pathological events affecting the endothelium in pulmonary hypertension. On the other hand we propose new molecules which may be involved in the cellular events leading to EnMET.

140 PRIMARY CO-CULTURES OF DOPAMINERGIC NEURONS AND GLIAL CELLS OF HEALTHY ADULT RATS FOR TWENTY DAYS.

(1) Hernández Zúñiga, D.; (2) Godínez Fernández, J. R.; (3) Beltrán Vargas N. E., (4) Jiménez Anguiano A. y (4) García Lorenzana

(1) Doctorado en Biología Experimental, Universidad Autónoma Metropolitana. (2), (3), (4) y (5) Universidad Autónoma Metropolitana.

Introduction: Primary neuron cultures have been a popular research tool for decades. They offer the advantage to do dose-response handling and long-term studies. Neuroscience works with embryonic, neonatal, and adult neurons. Obtaining cultures of adult origin is difficult due to strong adhesion of cell bodies, thousands of synapses, and fragmentation of axons and dendrites. Dopaminergic adult neurons (DN) show different response to pharmacological and electrophysiological stimuli than embryonic and neonatal neurons. The DN are involved in initiation and control of movement, and their death is associated with Parkinson's disease (PD). Actually, they are missing studies describing the establishment and description of primary co-cultures of dopaminergic neurons and glial cells obtained from healthy adult rats for future studies, that would provide relevant information on the generation of new therapeutic strategies for PD.

Objective : To develop a primary co-cultures of dopaminergic neurons and glial cells of healthy adult rats.

Methodology and materials: Male Wistar rats were used (200 g). They were anesthetized, and euthanized humanely (NOM-033-ZOO-1995). SN was dissected, and placed in cold Hanks solution. Subsequently, crushing and disintegration of the tissue were done mechanically, and enzymatically (trypsin 0.25%), recovered and seeded in boxes. The co-cultures were maintained at 37 °C, and 5% CO₂. The cells were quantified. Viability cellular test with the kit Calcein AM, and ethidium homodimer was developed during 20 days, with some different temperatures. ND morphology was described by atomic force microscope. ND identification was confirmed by tyrosine hydroxylase (TH) immunostaining. The material was observed in the Divisional Confocal Microscope from UAM-Iztapalapa.

Results: Primary cultures were maintained in vitro for twenty days. A total of 5,680,000 cells were quantified. Viability of extraction protocol was 59%. Survived cells keep viable until day 20. Viability decreased when cells are maintained at 5 °C compared to others at 37 °C. Dopaminergic neurons were identified by atomic force microscope and TH immunoreactivity.

Discusion and Conclusion: The extraction protocol increased cell viability in a 9% compared with neonatal cell extraction. The neurons are dopaminergic because they have a characteristic morphology and TH expression, a key enzyme in dopamine synthesis.

This work generated a new culture system to examine various dopaminergic neurons' aspects such as their interactions with glial cells, pathogenesis of PD, and evaluation of new drugs or therapeutic alternatives.

This work was conducted as part of "The PhD in Experimental Biology at the Universidad Autonoma Metropolitana , member of the National Quality Graduate Program (PNPC) of CONACyT, registration 001482, in the Consolidated level, and is supported by the same Council , DAFCYT-2003IDPTNNN0020 "key. Deisy Hernandez Zuniga student received support from CONACyT under the number 26578 with fellow 420 480 CVU.

146 HISTOPATHOLOGICAL ANALYSIS OF CLAM (*Polymesoda caroliniana*) EXPOSED TO CADMIUM.

Vázquez Castro, J.A., Guzmán García X., Hernández Calderas I. Jerónimo Juárez, J. R.

Universidad Autónoma Metropolitana. Unidad Iztapalapa. División de Ciencias Biológicas y de la Salud. Departamento de Hidrobiología. Laboratorio de Ecotoxicología. Av. San Rafael Atlixco. No. 186. Colonia Vicentina. C.P. 09340. Delegación Iztapalapa. México. D.F.

In México there are major problems of pollution in coastal areas. These problems are caused principally because of dumping of potentially toxic waste, like cadmium. Aquatic organisms, such as bivalves, are sessile filter feeders, therefore pollution affects their physiological condition. Tecolutla, Veracruz has few studies of environmental monitoring biological diversity and ecological importance. The aim of this study was to conduct a histopathological analysis of clam *Polymesoda caroliniana* from Tecolutla Veracruz, exposed to cadmium. Thirty organisms were collected, registering their morphometric parameters, such as length, width, height and weight. The clams were transferred alive to the laboratory where they were acclimated for 40 days with controlled feed (*Chlorella* sp. at 909.935 cells/mL), aeration, salinity (2 ‰) and constant temperature (24 °C). Later were exposed to 300 mg/L of cadmium per 96 h in devices with and without sediment. They were harvested at 24 and 48 hours recording mortality and behavior patterns. Clams harvested were fixed with 10 % buffered formalin performing dissections in three regions: anterior, middle and posterior. The cuts were made at 5 microns and stained with H-E. Each histological sample was observed with the optical microscope focusing on five target organs: mantle, gills, foot, digestive gland and gonad. Tissue responses observed were recorded and prevalence matrix was constructed. The tissue changes were related to impact factor Bernet (1999). The data was treated statistically to corroborate the significant differences between the variables of the bioassay and tissue responses. The collected clams had an average length of 52.8 mm, 47 mm wide, a full weight of 50 g, and height of 30 mm. During the acclimatization a mortality of 13% (4 organisms) was registered. Behavior patterns were: affinity for sediment and complete closure of the leaflets. The main tissue responses were: brown cells, atrophy, spherical inclusions, loss of cilia and eosinophil digestive secretions in gill, mantle, gonad, and digestive gland. No statistical difference was found ($P= 0.1429 \neq 0.05$ $t= 1.7025$). Organs with worse tissue responses were gill and digestive gland, in organisms with sediment, possibly because this metal settled and buried bivalves had more contact with this metal. According to Bernet, (1999) tissue responses are type 2, that is, reversible moderate, thus the tissue can be repaired in optimal conditions in a given time. We suggest to continue with biomonitoring studies to evaluate the presence of metals and their effects in Tecolutla, Veracruz.

NEUROHISTOLOGÍA

23 STIMULATION OF THE MYOGENIC ABILITY IN NORMAL AND ATROPHIC SKELETAL MUSCLES

Jimena, I (1,2,3); Ruz-Caracuel, I (1,2); Leiva-Cepas, F (1,2); Giovanetti-González R (1,2); Cambrón-Carmona, M.A (1,2); Casado-Ruiz, J (1,2); Luque, E (1,2,3); Peña, J (1,2,3)

(1) Department Morphological Sciences, Section of Histology, Faculty of Medicine and Nursing, University of Córdoba. Spain (2) Research Group in Muscle Regeneration, University of Córdoba, Spain (3) Maimónides Institute for Biomedical Research IMIBIC, Reina Sofia University Hospital, University of Córdoba. Spain

Introduction The myogenic potential of skeletal muscle is determined by the existence of a satellite cells population and possibly other related precursors located in the muscle connective tissue. Get strategies to encourage these cell populations without inducing muscle injury, it is essential to try to recover the atrophic muscles. In previous studies we have demonstrated that an extract from denervated muscle can induce changes in the tissue microenvironment in vivo to promote myogenic differentiation in adult skeletal muscle in absence of injury. The aim of this study was to determine whether the rate of myogenic capacity can be increased in muscle atrophy treatment with muscle extracts. **Material & methods** Normal and denervated Wistar rats were treated with denervated muscle extract during 10 days; similar groups without treatment were used as normal and denervated controls. Soleus muscles were then dissected and processed for light microscopy (histological, histochemical and immunohistochemical). The index of myogenic capacity was evaluated by desmin staining, since it is a very useful marker to detect early activated muscle precursor cells in vivo. The morphological characteristics of the response from satellite cells population and other potential myogenic precursors were established with ultrastructural analysis and also a quantitative analysis of changes observed was performed. **Results** We observed isolated or grouped mononucleated cells desmin⁺ in the interstitial space and also satellite cells desmin⁺ were located in the muscle fibers surface; the quantitative analysis showed significant differences between controls and experimental groups. The ultrastructural study confirmed the immunohistochemical observations microscopy and showed that a part of the population of satellite cells were activated and also with morphological evidence of the involvement of pericytes in the myogenic response. **Conclusion** In our opinion, the results show that our experimental model may be useful for testing experimental strategies in permanently atrophic denervated muscle.

25 ENTERIC GLIA AND PRIMARY CILIUM

Junquera C., Monzón M., Iruzubieta P., Luesma MJ., Cantarero I., Guillorme A., Castiella T.

University of Zaragoza

INTRODUCTION Enteric nervous system (ENS) is formed of neurons and their axons, as well as glial cells constituting a complex neural network, mainly distributed in two ganglionated plexuses. Enteric glial cells are smaller than neurons and have innumerable processes of different shapes and sizes. These glial cells in gut are more similar in structure and morphology to the astrocytes than to other glial-cell types of the peripheral nervous system. Some types of glial cells maintain a progenitor potential even in adults (astrocytes in subventricular zone in the lateral ventricles and those in subgranular zone of dentate gyrus of hippocampus). Although

neurogenesis is a known physiological function of some adult glial cell types, the presence of these properties in enteric glial cells remains as a matter for discussion. Since the existence of a single cilium characterizes neural progenitor cells in the subventricular zone of the adult mouse, it could be also a feature of precursor glial cells in the ENS. The purpose of this study is to present evidence of a primary cilium (PC) in glial cells from human colon. MATERIAL AND METHODS Samples corresponded with those healthy edges from resection of surgical intestine tissues not presenting inflammatory pathology. They were provided by the Hospital Clínico Lozano Blesa from Zaragoza. Standard protocols for transmission electron microscopy (TEM) have been applied on serial ultrathin sections from all samples with the aim of developing a three-dimension reconstruction of PC. RESULTS Glial cells are more numerous than ganglion neurons. They can be located in direct contact with neuron membranes in the enteric ganglia but also extending their cytoplasmic prolongations around intraganglionar axons. The ganglion is surrounded by cytoplasmic prolongations of interstitial cells of Cajal. Glial cells were also found in the nerve strands, where lack myelin sheaths. The intraganglionar cells presenting PC have large round nuclei with fine granular euchromatin. PC origin is a region next to the nucleus and dictiosome and its length about 2 - 3 μ m. The axoneme is a direct extension of a typical basal body and contains nine outer doublet microtubules; it exhibits a 9+0 pattern because the central pair of microtubules is not observed in any of the serial sections, and it lacks motility-related components such as inner and outer dynein arms and radial spokes. The mother centriole converts into the basal body, and structures that include the transition fibers, basal foot and striated rootlet are observed. The transition fibers tether the basal body to the plasma membrane in the transition zone. Even a 2/3 proportion of the proximal region of the cilium can be located within an invagination of the plasma membrane, the ciliary pocket. CONCLUSIONS Each enteric glial population in gut wall compartments represents a morphological, and presumably functional, distinct subtype. We propose that single cilia could be a characteristic of glial precursor cells in the ENS. Figure 1.- Transmission electron microscopy. Myenteric plexus of human colon. A) Glial cells in the myenteric ganglia. B) Magnification of the white square in Figure A. Primary cilium projects towards the extracellular space from the membrane of a glial cell. gc: glial cells; lm: longitudinal muscle; bb: basal body; cp: ciliary pocket; ax: axoneme

27 NEUROPATHOLOGICAL FINDINGS IN A SUBJECT WITH SPORADIC PRESENILIN-1 GENE MUTATION (P264L) WHICH CAUSED ALZHEIMER'S DISEASE AND SPASTIC PARAPARESIS

(1) Navarro, A; (1) del Valle , E; (2) Martínez- Pinilla, E; (3) Astudillo, A; (3) Junceda, S; (4) Corte-Torres, MD; (1) Tolivia, J

(1) University of Oviedo (2) CIMA, University of Navarra (3) University Central Hospital of Asturias (4) Biobank of the University Central Hospital of Asturias

In familial Alzheimer's disease (FAD), it has been shown that mutations in the amyloid precursor protein (APP), presenilin-1 (PSEN-1), and presenilin-2 (PSEN-2) genes cause an excessive production and accumulation of the amyloid β -peptide (A β). According to the "amyloid cascade" hypothesis, APP and PSEN mutations promote formation of the highly insoluble A β 42 variant from APP, whose progressive aggregation triggers synaptic abnormalities and neuronal loss. A second postulate for FAD-linked mutations is the

“endangerment hypothesis”, which proposes that APP and PSEN mutations enhance neuronal sensitivity to degeneration and dysfunction.

Among the 200 mutations that have been described for PSEN-1, half of them displays symptoms of presenile dementia. Despite to this marked genetic heterogeneity, pathological brain lesions associated with the mutations have not been characterized so far. We described here the brain pathology for a subject affected by Alzheimer’s disease (AD) with spastic paraparesis who presented PSEN-1 (P264L) mutation.

For this purpose, brain and spinal cord of one patient was fixed in 4% phosphate-buffered formaldehyde. Representative tissue samples were embedded in paraffin and stained with hematoxylin-eosin or Congo red. Immunohistochemistry (IHC) study for the typical biomarkers of AD like Tau, A β , Apolipoprotein D (Apo D) and gliofibrillar acid protein (GFAP) was performed and visualized with diaminobencidine.

At macroscopic level the examination of the brain revealed a general atrophy, especially in the hippocampus and an enlargement of the lateral ventricles. Histopathological analysis showed amyloid angiopathy (AA), neurofibrillary tangles (NFT) and abundant “cotton wool plaques” (CWP) similar to those described in other FAD variants (Fig. 1). Although neuronal loss was observed in all areas of isocortex, it was particularly pronounced in the hippocampus and entorhinal cortex. Amyloid angiopathy was visualized in the meningeal and cortical blood vessels and it was particularly extensive in the precentral cortex and in the cerebellum. Interestingly, the majority of neocortical plaques were large diffuse CWP without cores or dystrophic neurites. The CWP display immunoreactivity for A β , Apo D and GFAP but not for Tau. Despite the lack of neurites within CWP, a significant number of NFT in several cerebral and hippocampal cortex were found using IHC for Tau. We also found scarcely diffuse or cored “neuritic plaques” (NP) with dystrophic A β positive neurites in the deeper cerebral layers. Noteworthy, we have demonstrated the occurrence of kuru-like plaques (KP), predominantly in cerebellar cortex, and a new type of “compact plaque” (CP), not described previously, without neurites or glia, in the white matter. This type of plaque was positive for A β and Apo D.

Several data suggest that the type of PSEN-1 mutation may determine not only the type, size, biochemical properties or the overall level of A β but also may influence the morphology and distribution of A β plaques. Our data support the link between spastic paraparesis and presence of CWP in cerebral cortex. However we also found abundant kuru-like plaques. In this sense, many works have shown a marked variability in clinical and neuropathological findings between subjects with the same pedigree. This discrepancy could be due to the existence of other factors, still unknown, that influence pathophysiology of FAD.

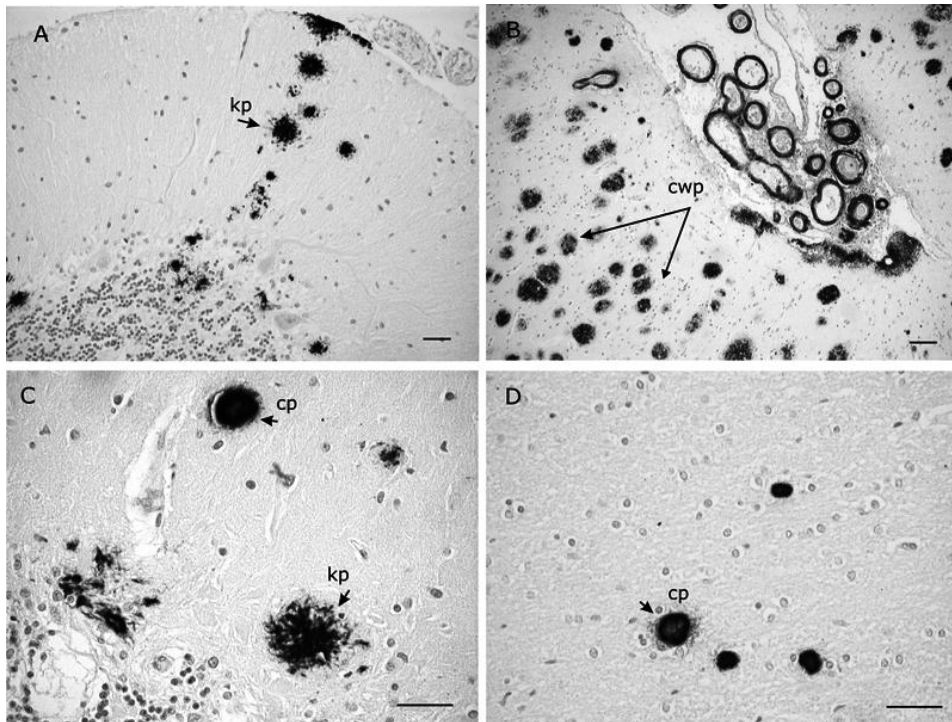


Fig. 1. Different types of amyloid plaques positives to $A\beta$. Sections were counter-stained with Toluidine blue. (A) Kuru-like plaques (kp) in cerebellum. 20x (B) Cotton wool plaques (cwp) in entorhinal cortex. Note the amyloid angiopathy. 20x (C) Kuru-like, diffuse and compact plaques in cerebellum. 40x (D) Characteristic compact plaques located in white matter of frontal cerebral cortex. 40x. Scale bar: 40 micrometers.

69 NEURONAL DIFFERENTIATION MODEL OF HUMAN SH-SY5Y CELL LINE USING EC23 AND BDNF

Cordero, M.; Palomares, T. and Alonso-Varona, A.

Department of Cell Biology and Histology. Department of Surgery, Radiotherapy and Physical Medicine. Faculty of Medicine and Dentistry. University of the Basque Country.

Introduction. The human neuroblastoma cell line SH-SY5Y can be induced to neuronal differentiation using appropriate differentiation agents, such as retinoids. In particular, mostly studies use all-*trans* retinoic acid (ATRA) as an effective agent to induce differentiation of this cell line. However, this natural retinoid derivative of vitamin A is unstable and very susceptible to photoisomerisation, resulting in its degradation. New synthetic retinoids has been designed to overcome this ATRA limitation, maintaining its biological activity and obtaining increased reliability in the process of neuronal differentiation. A good example of this type of compounds is the ec23, which possess higher chemical and physical stability.

In order to optimize the neural differentiation of SH-SY5Y cell line, brain-derived neurotrophic factor (BDNF) has been used in combination with ATRA, demonstrating an increase in expression of key synaptic genes comparing to ATRA alone.

Based in the fact that ec23 induces neuronal differentiation in a manner similar to ATRA, along with the important role of BDNF in this differentiation process, the aim of this study was to evaluate the combination of ec23 and BDNF in order to improve the neuronal maturation of SH-SY5Y cells.

Materials and Methods. The SH-SY5Y human neuroblastoma cells were seeded on multiwell-plates pre-coated with laminin (10µg/ml) and incubated for 24 h to allow cell adhesion. For cell differentiation, ATRA or ec23 was added the day after plating at a final concentration of 10µM and 1µM, respectively. In order to improve neuronal maturation, we add 2 nM Brain Derived Neurotrophic Factor (BDNF) to culture media on day 6 (SH-SY5Y_d). Cell viability was determined by trypan blue exclusion method. Reactive oxygen species (ROS) were detected using 2'-7'-dichlorofluorescein diacetate (H₂-DFC-DA). For immunofluorescent staining, SH-SY5Y_d were fixed by the addition of methanol (-20°C) for 10 min, incubated 30 min in blocking buffer and after overnight (4°C) with NF-200 antibody (1:160). Cells were rinsed and incubated for 1 h at room temperature with Alexa Fluor 488 Goat antiRabbit (1:200). Nuclei were counterstained with Hoechst 33342 DNA stain.

Results. ATRA and ec23 induced a similar reduction in cell proliferation (2.1- and 1.9-fold, respectively; $p < 0.001$) at day 7; this reduction was more evident at 10 days (5.3- and 4.3-fold, respectively; $p < 0.001$), with no significant differences between the two retinoids. Only in the case of ATRA-treated cells we found a significant increase in ROS levels (1.8-fold at 60 min; $p < 0.01$) compared to control, suggesting a higher oxidative stress state induced by this natural retinoid compared to the synthetic one. Both agents induced similar morphological changes towards neuronal phenotype, assessed by the presence of cells with neurite-like extensions and NF-200 immunostaining positivity.

The combination of ec23+BDNF reduce proliferation rate (1.2 ± 0.05 vs 1.6 ± 0.06 ; $p < 0.001$), and increase ROS levels (2.9-fold) compared to ec23 alone ($p < 0.001$). At a morphological level, we observed the development of longer and interconnected neurites, which correspond with the acquisition of a higher neuronal maturation morphology.

Conclusion. In conclusion, the combination ec23+BDNF provides a useful method to induce a functional and morphological SH-SY5Y neuronal differentiation.

75 EXPLORING THE SPATIAL CORRELATION BETWEEN ?ETA-AMYLOID AND APOLIPOPROTEIN D IN AMYLOID DEPOSITS: A NEW INSIGHT INTO THEIR FUNCTIONAL INTERACTIONS (1) del Valle, E; (1) Navarro, A; (2) Marinez-Pinilla, E; (1) Tolia, J

(1) Universidad de Oviedo (2) CIMA, Univeridad de Navarra

The discovery that some of the apolipoproteins synthesized in the human nervous system, i.e. Apo E, Apo J and Apo D are elevated in Alzheimer's disease (AD), was followed by the analysis of the role that these proteins could play in the pathophysiology of the disease. In these studies the focus is placed in the relationship between apolipoproteins and the amyloid- β (A β), a peptide that self-aggregates and whose deposition as senile plaques and cerebral amyloid angiopathy is key for AD pathology, according to the "amyloid cascade hypothesis". In this sense, apolipoproteins, due to their proven function as transporters of lipophilic molecules, could facilitate the amyloid clearance or in contrast promote the A β fibrillogenesis. The exact mechanism has not been clarified yet. Specifically, Apo D is a neuroprotective and antioxidant protein that has been shown to be located in senile plaques of AD, A β -related pathologies and aging brains. The distribution pattern of Apo D in all different types of amyloid plaques in

relation with A β has not been studied in detail and would give us an idea about the functional interactions between them.

In the present study, we sought to determine the possible relationship between Apo D and A β in several types of amyloid deposits of some diseases, as late onset AD, familiar AD (FAD), amyloid angiopathy (AA), fronto-temporal dementia (FTD) and fatal familial insomnia (FFI), using immunohistochemistry for Apo D and A β combined with Congo Red stain for A β -pleated sheet protein conformation.

We found that Apo D is located in all different types of amyloid deposits: vascular plaques (vp) in CCA and AD, diffuse and neuritic plaques (np) in AD and FTD, kuru-like plaques (kp) and cotton wool plaques (cwp) in FFI or FAD. Interestingly, Apo D is not present in all A β senile plaques; we observed that it colocalizes with A β in the core of neuritic plaques and more compact senile plaques but only in those with high content of A β , stained with Congo Red. In FAD, we found that all neuritic and compact plaques are positive for Apo D, whereas only a sixty percent of the diffuse cwp, without A β dense core, presents this protein (Fig. 1).

In this work we have studied in depth the spatial correlation between A β and Apo D in amyloid deposits of AD as well as other neurodegenerative diseases. It should be noted that the commercially antibody against A β , that we have used, recognizes all peptide species (40/42). Despite the fact that that we cannot discriminate the nature of A β peptide that interacts with Apo D, it seems clear that Apo D binds to A β folded sheet of Congo Red positive core. These data suggest that Apo D may be involved more in the A β removal than in the fibrillogenesis since it is primarily attached to a more hydrophobic and aggregating A β . If Apo D was able to bind soluble early aggregation stages of A β 40 and A β 42, then we should expect to see a greater number of cwp and diffuse neuritic plaques positive for Apo D.

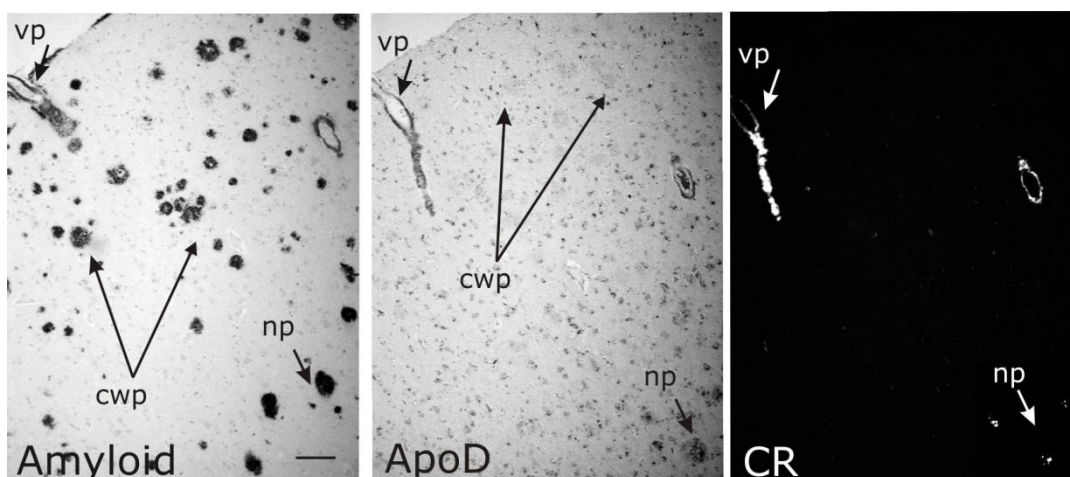


Fig. 1. - Motor cortex in a subject with FAD. Consecutive sections immunolabeled for A β and Apo D. Counterstain with Congo Red (CR) for the visualization of A β -pleated sheet protein conformation. X20. Scale bar: 40 micrometers.

76 APOLIPOPROTEIN D NEURONAL CONTENT IS INFLUENCED BY CELL SIZE IN BRAINSTEM (3) Pascual, G.; (2) Fernández-Gutiérrez, M.; (1) Rodríguez, M.; (3) Sotomayor, S.; (1) Pérez-Köhler, B.; (1) Kuhnhardt, A.; (2) San Román, J.; (1) Bellón, J.M.

(1) Universidad de Oviedo (2) CIMA, Universidad de Navarra

Amount of intracellular Apo D and neuronal size

Apolipoprotein D (Apo D) is a transporter lipocalin mainly expressed in mammalian brain where it has been shown a progressive increase of this protein in the development and aging. Neuronal Apo D presence in central nervous system (CNS) seems to be part of a cellular defence system in regions affected of neuropathology changes in certain neurodegenerative and neuropsychiatric disorders. In the brainstem, we previously demonstrated that Apo D expression is significantly higher in somatomotor nuclei than in the visceromotor and sensory nuclei and that these levels do not change with age. Due to the different neuronal shape and size between functional nuclei of brainstem, one possible explanation is that Apo D expression could be influenced by the cell size. Thus, in this work we performed an extensive immunohistochemical study for Apo D, discriminating between different nuclei of brainstem and estimating cell size.

Tissues from twenty-six patients, without previous inner ear or neurological disease, were provided by Biobank of the University Central Hospital of Asturias with a range between 32 and 92 years-old. We performed an immunohistochemical study of Apo D in brainstem quantifying its signal and describing the immunostaining pattern in all cell types and neuropile. For the immunohistochemistry, paraffin sections were cut at 10 μm of thickness and incubated with the antibody against human Apo D overnight at 4 °C. Immunoreactivity was detected using the Extravidin biotin peroxidase staining kit and the peroxidase activity visualized by incubation with Sigma Fast DAB at room temperature for 30 minutes. For quantification of Apo D expression, the chromogenic signal was selected using Adobe Photoshop CS 8.0.1 and density measured by ImageJ 1.37c according to a procedure developed by our group. As in previous studies, neurons were divided into three groups according to the cross-sectional surface. Small: below to 200 μm^2 , medium: 200–500 μm^2 and large: over to 500 μm^2 .

We found that, unlike other areas of the CNS, the majority of neurons of brainstem are positive for Apo D, showing a finely distributed signal throughout the cytoplasm. The percentage of negative neurons for Apo D is 9.5% in the sensory nuclei and 4.9% in the motor nuclei. Interestingly, we demonstrated that Apo is expressed in a cell size dependent manner; we observed that neurons with greatest amount of Apo D were the largest. This statistically significant correlation was found in both brainstem nuclei, motor and sensory (Fig. 1). However we did not find significant differences in the Apo D expression between these two functional nuclei.

It is difficult to infer a motive for these data. In this context Apo D has been related with the maintenance and reparation of the cell membrane due to its role as a lipid carrier, so it seems justified that a higher content of Apo D in the largest cells could contribute to the greater complexity of this neuronal membrane integrity.

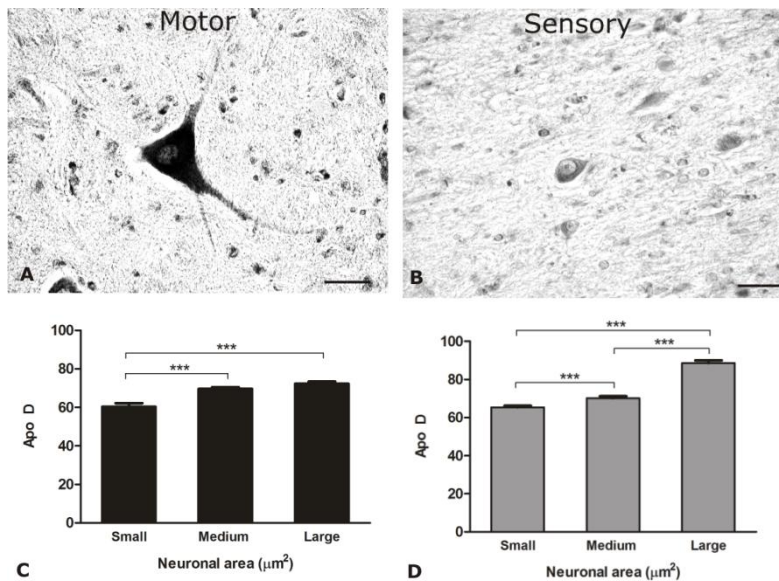


Fig. 1. Immunohistochemistry and densitometric quantification for Apolipoprotein D. (A) Positive Apo D neuron in Hippoglossal Nucleus as example of motor nucleus. 40x. (B) Slightly positive neurons in Superior Vestibular Nucleus as example of sensory nucleus. 40x (E, D) Percentage of Apo D immunohistochemical signal in relation to neuronal size. (***) $p < 0.001$ compared with small neurons). Scale bar: 40 micrometers.

132 EXPRESSION OF THE LIM-HOMEODOMAIN TRANSCRIPTION FACTOR ISLET-1 IN THE DEVELOPING AND MATURE VERTEBRATE RETINA

Martín Partido, G.; Bejarano Escobar, R.; Álvarez Hernán, G.; Pavón Muñoz, T.; Francisco Morcillo, J.

Departamento de Anatomía, Biología Celular y Zoología, Facultad de Ciencias, Universidad de Extremadura, 06071 Badajoz.

INTRODUCTION: The LIM-homeodomain transcription factor Islet-1 (Isl1) orchestrates cell fate decisions in a variety of systems. Different studies have shown that this transcription factor is detected in mature and differentiating retinal cell types, suggesting that it plays a pivotal role in their maturation. Although there is compelling evidence for the expression of Isl1 in the developing and mature retina in the chick and in the mouse, little is known about the expression of Isl1 in the retinas of other species. The main goal of the present study is to examine whether the expression of Isl1 in the developing and mature retina is conserved across vertebrate species. MATERIAL AND METHODS: Embryos and post-natal specimens of tench (*Tinca tinca*), Senegalese sole (*Solea senegalensis*), small-spotted catshark (*Scyliorhinus canicula*), South African clawed frog (*Xenopus laevis*), Mediterranean pond turtle (*Mauremys leprosa*), chick (*Gallus gallus*), and mouse (*Mus musculus*) were fixed in PFA 4% in PBS for 12 to 24h, depending on their size, at 40C. Tissues were washed in PBS, then cryoprotected, soaked in embedding medium, frozen, and freeze-mounted onto aluminium sectioning blocks. Cryostat

sections, 15 µm thick, were cut in the frontal plane. Single and double immunohistochemical studies were performed. The primary antibodies used in this report have been widely used in neuroanatomical studies in the central nervous system of different groups of vertebrates. They cross react with antigens present in the retina of all species tested. The sections were observed using an epifluorescence, brightfield Nikon Eclipse E600 microscope, and photographed with a digital camera (AxioCam HRc). Some of the double immunolabelings were photographed with a Nikon D-Eclipse C1 confocal laser scanning microscope. Graphical enhancement and preparation for publication were performed in Adobe Photoshop (v.CS4). **RESULTS:** We have found that the pattern of Isl1 expression is very similar in the mature and developing retinas of multiple vertebrate species. Thus, Isl1 is detected in the nuclei of subpopulations of differentiating and mature ganglion, amacrine, bipolar, and horizontal cells in different species of fish, amphibians, reptiles, birds, and mammals. However, Isl1 is not detected in horizontal cells in the developing and mature mouse retina. Surprisingly, we have detected a transient expression of Isl1 in the outer nuclear layer during retinal development in the turtle and in the chick. During retinal development, the expression of Isl1 is consistent with that expected for a transcription factor involved in retinal neuroblast differentiation, following the gradients of maturation described during vertebrate retinogenesis. **CONCLUSIONS:** Comparative analyses demonstrate that the LIM homeodomain transcription factor Isl1 shows similar but not identical patterns of expression throughout vertebrate phylogeny. It seems to play a highly conserved role in cell specification, differentiation, and maintenance of phenotypes of the ganglion, amacrine, bipolar, and horizontal cells in the retina from fish to mammals.

133 EXPRESSION OF CATHEPSINS B AND D IN THE DEVELOPING MOUSE CEREBELLUM

Martín Partido G.; Bejarano Escobar R.; Gil Redondo J.C.; Díaz Chamorro S.; González García R.; Francisco Morcillo, J.

Departamento de Anatomía, Biología Celular y Zoología, Facultad de Ciencias, Universidad de Extremadura, 06071 Badajoz.

INTRODUCTION: The cathepsin family consists of cysteine, aspartate, and serine lysosomal proteases that play an important role in many physiological and pathological processes. Among these, cathepsin B is involved in the degradation of cellular proteins in lysosomes. It is also found in extralysosomal sites, where it participates in several cell processes including cancer metastasis and inflammation. The major function of cathepsin D is the digestion of peptides and proteins within the lysosomes, although it contributes to other physiological roles, such as hormone and antigen processing, cell proliferation and tissue renewal, or cell differentiation. The main goal of the present study is to examine the expression of cathepsins B and D in the developing mouse cerebellum.

MATERIAL AND METHODS: Embryos and postnatal Swiss/ICR albino mice of different ages were used in the present study. They were fixed by immersion or intracardiac perfusion with 4% paraformaldehyde solution, in 0.1 M phosphate buffered saline (PBS) (pH 7.4), at 4°C. The fixed specimens were cryoprotected in 10% sucrose solution in PBS and embedded in 10% gelatine 10% sucrose solution in the same buffer. The blocks were frozen for 3 min in

isopentane cooled at -70°C by dry ice, and then stored at -80°C . Serial sections $20\ \mu\text{m}$ thick were cut in a cryostat, collected on Super-Frost Plus slides, and stored at -80°C until use. In situ hybridization was carried out as described in Schaeren-Wiemers and Gerfin-Moser (1993). Sections were incubated overnight with an alkaline phosphatase-conjugated anti-digoxigenin antibody. Staining reactions were developed with NBT and BCIP. For double labeling purposes, the ISH was performed first followed by the single or double immunolabeling, the TUNEL assay, or tomato lectin histochemistry.

RESULTS: Here in our study, we have found a highly coincident spatiotemporal distribution of the gene expression pattern and morphological features between cathepsin B- and cathepsin D-expressing cells in the developing cerebellum. Cathepsin B/D expressing cells showed a rounded or amoeboid morphology, demonstrating that cathepsins B and D are a valuable marker for macrophages and microglial precursors. The entry of microglial precursors into the cerebellum anlage was through the pial surface and, to a lesser extent, through the fourth ventricle. Once inside the cerebellum, cathepsin B/D-expressing microglial precursor cells migrated along axons in the white matter of the cerebellum between P2 and P10. Subsequently microglial precursors migrated radially to reach their final locations within the cerebellar cortex, where they morphologically differentiated into microglia. We found that as microglial precursors differentiated the expression of both cathepsins was down-regulated. Cathepsin B/D-expressing microglial precursors engulfed apoptotic cells which they found on their way through the white matter and nearby regions. However, they were not involved in the phagocytosis of the many apoptotic cells located in the external granule layer of the developing cerebellum.

CONCLUSIONS: Our findings point to a role for cathepsin D and B in cell debris degradation after apoptotic processes rather than promoting cell death. Additionally their pattern of expression suggests a role in the maturation of the microglial precursors.

137 IMMUNOHISTOCHEMICAL CHARACTERIZATION OF PUTATIVE ADULT NEURAL STEM CELLS IN THE BRAIN OF THE TELEOST *Gymnotus omarorum*.

(1)(2)Olivera-Pasilio, V. (1) Radmilovich Cabrera, M., (1) Barreiro-González, I., (1)
(2)Castelló Gómez, M.E.

(1) Facultad de Medicina Universidad de la República (UdelaR) (Montevideo, URUGUAY) (2) Instituto de Investigaciones Biológicas Clemente Estable Ministerio de Educación y Cultura (MEC) (Montevideo, URUGUAY)

1. INTRODUCTION. The brain of adult *G. omarorum*, like many other teleost fishes, shows a widespread distribution of proliferation zones composed by at least four putative cell types: stem cells, intermediate amplifying progenitor cells, quiescent cells and neuroblasts, as evidenced by double thymidine analog labeling with short and long chase between analogs (Olivera-Pasilio et al., 2014). Neural stem cells are highly heterogeneous as their phenotypes vary along development and evolution, and between brain regions of the teleost *Danio rerio*, in the adulthood. In this teleosts, unlike mammals, some adult neural stem show a radial glial phenotype and express glial markers while other neural stem cells retain the phenotype and

express markers of neuroepithelial cells (Than-Trong & Bally-Cuif, 2015). To test if this is a conserved feature of adult teleosts' neural stem cells, we decided to study the phenotype of putative adult stem cells in the brain of *G. omarorum*, an American weakly electric fish.

2. MATERIALS AND METHODS. Putative neural stem cells were identified by means of a double thymidine analog labeling and the expression of the transcription factor Sox2, a conserved marker of neural stem cells. To depict the cellular phenotype we also analyzed the colocalization of markers of radial glial cells. Animals received 5 daily i.p. injections of 50 mg/kg of CldU and 5 daily i.p. injections of 50 mg/kg of IdU, separated by a chase of 21 days between both series. After this treatment, animals were deeply anesthetized (500 mg/L of MS-222) and fixed by transcardial perfusion of 10% paraphormaldehyde followed by overnight postfixation. Frontal serial brain sections were obtained with a vibratome (70 microns) and processed for triple immunohistochemistry to reveal the colocalization of both thymidine analogs (to evidence the reentry into the cell cycle after a long chase) and Sox2 or markers of radial glial cells (the intermediate filament Vimentin, or brain lipid binding protein (BLBP)). Preparations were observed by confocal microscopy. Images were sequentially acquired, and colocalization was evidenced by orthogonal projections in xz and yz planes of z stacks or by overlay of single confocal sections.

3. RESULTS. We found few double thymidine analog labeled cells in all studied ventricular and extraventricular brain proliferation zones in adult *G. omarorum*. Ventricular proliferation zones in all main brain divisions (telencephalon, mesencephalon diencephalon and rombencephalon) were populated with Sox2+, Vimentin+ and BLBP+ cells (usually exceeding the boundaries of the proliferation zones). Many proliferating cells of the ventricular proliferation zones were Sox+, but very few putative neural stem cells (IdU+/CldU+) colocalize with SOX, Vimentin or BLBP.

4. CONCLUSIONS. We confirmed the widespread distribution of neural stem cells in the brain of adult *G. omarorum* by double thymidine analog labeling and colocalization of Sox2. According to their phenotype and markers' expression, some of *G. omarorum* neural stem cells might correspond to radial glia as occurs in other teleosts. Further studies will be required to elucidate if other neural stem cells retain the neuroepithelial phenotype and expression of epithelial markers in the adulthood in this species too.

TÉCNICAS HISTOLÓGICAS

9 ASSESSMENT OF HER2 STATUS BY IQFISH IN GASTRIC CANCER: A COMPARISON OF DUOCISH AND A NOVEL AUTOMATED IQFISH METHOD.

(1) García-Caballero, T.; (2) Araújo-Correia, S.E. ; (3) Vázquez-Boquete, A.; (4) Viaño, P.; (5); Ínsua Santamaría, D.C.; (6) Pérez Costoya, M.; (7) Pisco Neira, M.; (8) Antúnez, J.R.

(1 y 2) Universidade de Santiago de Compostela; (3, 4, 5, 6, 7 y 8) Hospital Clínico-Universitario de Santiago.

INTRODUCTION: Gastric cancer is the fourth most common malignant disease and the second leading cause of cancer-related death worldwide (Matsuoka T, 2015). Despite some advances in the prevention and treatment of the disease, the five year survival in most parts of the world still remains around 20%. The poor survival rate is mainly explained by the advanced stage of the

disease at the time of diagnosis (Jørgensen JT, 2012). We reached the point where the only treatment available is the paliative one. HER2 is the first targeted therapy succesfully tested in gastric cancer. Patients with HER2 overexpressed and/or amplified tumours derived the greatest benefit from trastuzumab therapy (Rüschoff J, 2012), an humanized HER2 antibody, in combination with chemotherapy. The HER2 overexpression is assessed by semiquantitative immunohistochemistry: 0 and 1+ are defined as negative, 2+ as borderline, and 3+ as positive. In order to determinate whether borderline cases are positive or negative, HER2 gene an d centromere 17 (CEN17) status must be assessed. Due to the high percentage of cases with heterogenity in gastric cancer, some authors recommend the use of chromogenic methods (i.e., DuoCISH) to assess HER2 gene status instead of fluorescent ones (FISH) (Rüschoff J, 2010). But the development of new methods such as automated IQFISH that allows us to obtain results in just 3.5 hours, in contrast to DuoCISH which takes 2 days, makes it a very attractive technique for the laboratory daily routine. The implementation of new methods in the selection of patients for this kind of treatments depends on the use of reliable and validated methods (Gomez-Martin C, 2014). The main goal of this work is to validate the automated IQFISH method in the determination of HER2 gene status in gastric cancer. METHODOLOGY AND MATERIALS: We selected 55 consecutive endoscopic biopsies diagnosed with gastric cancer from the Pathology archive of the Complejo Hospitalario Universitario de Santiago in the period 2012-2013. We performed 4 ?m sections to determine the HER2 gene status by DuoCISH (Dako-Agilent) and automated IQFISH in the Omnis system (Dako-Agilent). Assays were performed according to the manufacturer recomendations. DuoCISH results were evaluated in a light microscopy at x60 magnification. Automated IQFISH results were evaluated at x100 magnification in a fluorescence microscopy equiped with a dual filter for TexasRed and FITC, and a filter for DAPI. Samples with HER2/CEN17 ratios ? 2 were considered amplified. RESULTS: The automated IQFISH method showed clear discernible signals for HER2 gene and CEN17. The results obtained by both techniques were concordant in all cases (kappa =1.0), indicating a perfect agreement between them. All cases that revealed amplification by DuoCISH were also amplified by automated IQFISH. The Wilcoxon\'s test for paired data did not show significant differences between the means of HER2/CEN17 ratios by both methods (p=0.851). CONCLUSION: Using as reference the results of the HER2 expression by immunohistochemistry in gastric cancer, the possibility to obtain results in just 3.5 hours with minimal technician involvement makes the automated IQFISH a fast, reliable and robust alternative to chromogenic methods.

45 HISTOPATHOLOGICAL AND MORPHOMETRIC EVALUATION OF ARTICULAR CARTILAGE REGENERATION WITH A BIOMATERIAL IMPLANT IN AN OVINE MODEL

(1,2) Ruiz-Saurí, A.; (1,2) Sancho-Tello Valls, M.; (1) Martín Buigues, D.; (1,2) Martín de Ll ano, J.J.; (1,2) Mata Roig, M.; (3) Vikingsson, L.; (3) Gómez-Tejedor, J.A.; (3,4) Gallego Ferrer, G; (3,4) Gómez Ribelles, J.L.; (1,2) Carda Batalla, C.

(1) Departament de Patologia, Facultat de Medicina i Odontologia, Universitat de València; (2) INCLIVA, Hospital Clínico Universitario de Valencia; (3) Center for

Biomaterials and Tissue Engineering, CBIT, Universitat Politècnica de València; (4) CIBER en Bioingeniería, Biomateriales y Nanomedicina, Valencia.

INTRODUCTION: Articular cartilage has a poor intrinsic capacity for regeneration because of its avascularity and a very slow cellular turnover. Defects caused by trauma or joint disease have a tendency to be repaired with fibrocartilage rather than with hyaline cartilage. The aim of this work is to study *in vivo* articular cartilage regeneration with biomaterial implant in an ovine model through histopathological and morphometric evaluation.

MATERIALS AND METHODS: We studied 10 adult sheep who underwent two cylindrical lesions in the medial femoral condyle of a knee. The lesion size was 4 mm in diameter and 4 mm depth, which originated microfracture of the subchondral bone resulting in bleeding. Furthermore, in 7 of the 10 sheep, a porous mesh made of Polycaprolactone (PCL) was located in each lesions immediately after the injury was performed. Contralateral knees received no treatment and were used as controls. Therefore, we studied 20 lesions (14 with microfracture+mesh and 6 with microfracture only) and 20 zones of normal articular cartilage. Four and a half months after surgery, animals were sacrificed and articular samples were processed with standard histological procedure including Alcian Blue staining. In all cases, morphometric study was performed to determine the thickness and percentage of the regenerated articular cartilage, as well as the number of cells. By using Alcian blue, strongly acidic sulfated mucosubstances stain blue, nuclei stain pink and cytoplasm pale pink. To better suit our purposes, the counterstain was made with Hematoxylin, resulting in a darker overview, and thus a higher contrast between cartilage and bone tissue was observed, useful for morphometric scrutiny.

RESULTS: The regeneration of articular cartilage in injuries treated only with microfracture or with microfracture plus PCL mesh was evaluated and compared with zones of uninjured normal hyaline cartilage by morphometric analysis and stained with Alcian Blue. We have found that the average thickness of normal articular cartilage was 1.41 μm , while the thickness of regenerated articular cartilage in lesion areas treated with microfracture plus mesh was 0.64 μm and in areas treated only with microfracture was 0.60 μm . These differences were statistically significant when compared normal cartilage with treated groups. The percentage of regenerated cartilage was of 68.7% in the microfracture plus mesh group and 53.0% in the microfracture group, which was a difference statistically significant ($p < 0.05$). Regarding cell density, we have found that in normal cartilage cells average was 366.2 cells/ μm^2 , in microfracture plus mesh group was 960.4, and 1306.1 in microfracture group, with a statistically significant difference in all cases ($p < 0.05$).

CONCLUSIONS: The implant of polycaprolactone mesh along with microfracture promotes regeneration of articular cartilage injury in an ovine model and induces cell proliferation at 4.5 months after surgery. Further research is needed in this regard to have more conclusive results.

ACKNOWLEDGEMENTS: This study was supported by MAT2013-46467-C4 grant from Ministerio de Economía y Competitividad, Spain.

67 QUANTIFICATION OF FIBRONECTIN. A PRELIMINARY STUDY IN NEUROBLASTOMA

(1) Burgos-Panadero, R.; (1) Blanquer-Maceiras, M.; (2) Lilao, J.; (2) Costell, M.; (1) Fos, S.; (1) Noguera, R.

(1) Department of Pathology, Medical School, University of Valencia; Medical Research Foundation INCLIVA. Valencia, Spain. (2) Department of Biochemistry and Molecular Biology. Faculty of Biological Science, University of Valencia, Valencia, Spain.

Introduction: The importance of quantification of fibronectin (FN) resides in the fact that is a glycoprotein with the ability to interact with several cells, and macromolecules through integrin receptors. FN is related to adhesion control, migration, proliferation and cellular growth in development as well as with tumor growth and metastasis. Its presence in fibrillar networks not only provides a primary scaffold that allows survival and cellular growth, but also supplies signals that promote migration and cellular invasion. For this reason, it is of interest to quantify the FN using morphometric techniques in cancer. The objective of this work is to know the quantification value of FN and other macromolecules of the extracellular matrix (ECM) and their relation with clinicobiological factors that have a prognostic value in neuroblastoma (NB).

Material and methods: The quantification of FN in NB was performed in 20 samples included in a tissue microarray (TMA). The TMA was stained by indirect immunofluorescence, using as primary antibodies anti-EDA (only detects the cellular-FN), and anti-FN (detects cellular and plasmatic forms of FN), given that the objective was to distinguish between the two FN forms. The images are taken at 60x with cell-B (Olympus Image System) software and quantified by Image Pro-Plus v.6.0 (Media Cybernetics) software. These samples of NB were also analyzed with Gomori and Alcian blue stains to detect reticulin fibers and glycosaminoglycans (GAGs), respectively, digitized with Aperio ScanScope XT (Aperio technologies) software and quantified by Image Pro-Plus v.6.0 (Media Cybernetics) software.

Results: The relation between FN and macromolecules of MEC found was variable. The form that contains EDA domain had an isolated distribution, whereas FN without this domain made fibrillary networks. Within the analyzed cases two tendencies were observed regarding FN and age: a greater quantity of FN (mean: 26.22) was connected with a lower quantity of EDA (mean: 5.41) in the subgroup of ≤ 18 months, and inversely in the subgroup of > 18 months, EDA (mean: 24.85) and FN (mean: 7.81).

Conclusions: Communication between the elements that constitute the ECM in tumor stroma seems to generate signals related to the age of the patients, which can influence in tumor cell behavior. Therefore, the quantitative analysis of FN as well as its relation with macromolecules of the ECM in a higher cohort of NB is essential to establish a relation with tumor progression.

Grants: RD12/0036/0020 and PI14/01008, both from ISCIII.

68 MORPHOMETRIC IDENTIFICATION OF TERTIARY LYMPHOID ORGANS IN PRIMARY ADRENAL GLAND NEUROBLASTOMA

(1) Zúñiga V., (1) Tadeo I.,(2) Cañete A.,(2) Navarro S., (1) Noguera R.

(1)Department of Pathology, Medical School, University of Valencia; Medical Research Foundation INCLIVA. Valencia, Spain (2) Pediatric Oncology Unit, University and Polytechnic Hospital La Fe, Valencia, Spain

Introduction: Tertiary lymphoid organs (TLO) are ectopic lymphoid tissues generated by chronic inflammatory processes, in contrast to those of secondary lymphoid organs (SLO), which arise during embryogenesis at specific sites of the organism (lymph node, spleen, tonsils and Peyer's patches). An antitumoral role of TLOs has been shown in some tumors such as lung cancer. However, to our knowledge, TLOs have not been characterized in neuroblastoma (NB), the most common extracranial pediatric cancer. TLOs have several characteristics which allow their identification, as follows: presence of different, but adjacent regions of T and B lymphocytes, a network of fibroblastic reticular cells (FRC), presence of high endothelial venules (HEV) in the T cell region, B cell class switching and germinal center reactions (GC) in the B regions, presence of the Activation-Induced cytidine Deaminase (AID) enzyme and presence of dendritic cells (DC). We aim to identify these structures and their cellular patterns in NB with morphometry, as these structures are believed to be an organism adaptation as a consequence of an increased demand for a localized immune response.

Material and Methods: We analyzed 20 primary adrenal gland NB, 8 with and 12 without TLOs. Serial sections were stained by immunohistochemistry using anti-CD4, CD7, CD8, CD11c, CD20 and CD45 for detecting T and B lymphocytes, dendritic cells and general leukocytes. The stained tumor sections were digitized with Panoramic Midi (3D Histech) and the positive cells were quantified with Panoramic Viewer (3D Histech).

Results: Of the 8 cases with TLOs, 7/8 had T and B cell regions with more than 50 cells; all cases had reticulin fibers, an indicator of the presence of FRCs; 5/8 had HEV; 4/8 had GCs; 5/8 were CD4⁺ T_H lymphocytes. Since T_H17 lymphocytes are capable of synthesizing the AID enzyme, this marker can be an indirect clue to the presence of AID; and, finally, all cases had CD11c⁺ cells, a marker for DC. TLOs had a mean of 313 T cells (CD4⁺, CD8⁺ and CD7⁺), 769 CD20⁺ cells and 98 CD11c⁺ per node, whereas controls had a mean of 71 T cells, 9 CD20⁺ cells and 39 CD11c⁺ per core. There were differences in the infiltration cell patterns of the TLOs. Some were T cell rich (>700 cells) and some were B cell rich (>2500 cells).

Conclusions: Although not all the criteria for TLO are fulfilled, it is possible to detect organized structures that can function as TLO in NB through the identification of the different cell characteristics by using immunohistochemistry and morphometry.

Grants: RD12/0036/0020 from ISCIII and PI14/01008 from ISCIII

129 CONTROL OF NATURAL AND FORMALDEHYDE INDUCED AUTOFLUORESCENCE BY NaBH₄ IN SKIN BIOPSIES

(1 y 2)Segoviano-Ramírez, J.C., (1 y 2)García-Juárez, J., (2)Carcaño-Díaz, K., (2)Cárdenas-Vega, R., (2)López-Altamirano, D.F., (1 y 3)Medina-de la Garza, C.E.

(1)Unit of Bioimage, Center for Research and Development in Health Sciences (CIDICS), UANL (Monterrey, Nuevo León, México); (2)Histology Department, Faculty of Medicine, UANL, (Monterrey, Nuevo León, México); (3) Immunology Department, Faculty of Medicine, UANL, (Monterrey, Nuevo León, México).

INTRODUCTION. Use of formaldehyde for tissue fixation is a worldwide standard. The ever-growing use of fluochrome-conjugated antibodies for diagnostic immunofluorescence of autoimmune and neoplastic diseases demands high levels of sensibility and specificity, for histopathological analysis will determine not only diagnosis but staging and further therapeutics. In many cases, after morphological analysis of slides stained with H & E, pathologists decide to perform an immunofluorescent stain, with biopsy tissue fixed with formaldehyde and processed by routine protocols. Tissues may show natural fluorescence when stimulated with ultraviolet light or with laser with specific wavelength. Furthermore, aldehyde fixation induce autofluorescence of tissue. To avoid possible "cross-talk" of signals it is necessary to sting both natural and induced auto- fluorescence, without damaging epitopes against which immunostainig is directed. **MATERIAL AND METHODS.** Four micrometers thick histological sections, from human skin biopsies fixed with formaldehyde and processed in paraffin, were obtained. The slides were deparaffinized and then incubated in darkness to test Sodium Borohydride (NaBH₄) at three different concentrations: 0.1%, 0.5% and 1.0% incubated 4 minutes. Slides were incubated in distilled water pH5 as negative control. Another series of slides were processed identically but then were stained with indirect immunofluorescent technique, using Cy3-conjugated antibodies. Slides were mounted with glycerol and analyzed by multiphoton confocal microscopy. Using a Plan-apochromatic 20x/0.8 M27 objective, samples were put into focus and a spectral scanning from 417 to 719 nm, using simultaneously as excitation source three lasers (458 nm, 488 nm and 514 nm) was performed. A 32-channel spectral detector was used to record images. Also we acquired five images in stack from six random fields, to quantify remaining fluorescent intensity and signal from conjugated antibodies. Calibration of lasers and photomultiplier was done with a smear of FITC-conjugated microbeads. ZEN software for spectral analysis of image and quantification of signal from fixative-induced autofluorescence and from Cy3 was used. **RESULTS.** Slides incubated with distilled water showed high levels of induced autofluorescence. This native and induced autofluorescent signal was reduced in 70% with NaBH₄ 0.1%. This signal decreased almost totally (95%) with NaBH₄ 1.0%. **CONCLUSIONS.** 1. NaBH₄ 1.0% reduces almost totally autofluorescence induced by formaldehyde in skin slides. 2. In skin slides, treatment with NaBH₄ does not affect antigenic sites nor interfere with signal from fluorochromes used in immunofluorescent stains.

OTROS

12 EVALUATION OF NOVEL MONETITE SCAFFOLDS IN SHEEP. EFFECT OF THE HYDROXYAPATITE CONTENT.

Benito Garzón, L. (1), Collía Fernández, F. (2), Padilla Mondéjar, S. (3), García de Castro, A. (3), Díaz-Guemes, I. (4), Enciso Sanz, S. (4), De Pedro Moro J.A. (1), García Carrodegas R. (3,5).

(1) Surgery Department, University of Salamanca, Spain. (2) Human Anatomy and Histology Department, University of Salamanca, Spain. (3) Azurebio S.L. Madrid, Spain. (4) CCMI Jesús Usón, Cáceres, Spain. (5) Instituto de Cerámica y Vidrio (ICV), CSIC, Spain.

INTRODUCTION In this work novel resorbable materials containing monetite (Mon, CaHPO₄), HAp and silica gel (SG, (-OSi(OH)₂-)_n) are evaluated in vivo. HAp is well known as a bioactive, osteoconductive and scarcely resorbable bone repairing material. Mon and SG are incorporated for their biodegradability and osteoinductive properties, respectively. In order to regulate the resorption rate, materials with different ratios of HAp/Mon were compared with regard to local tissue response, bone regeneration and material resorption employing a critical size bone defect model in sheep. **EXPERIMENTAL METHODS** Granule-shaped experimental scaffolds (size 0.25-1.0 mm) were implanted in critical size defects, drilled in the femur, tibia and humerus condyles of adult sheep. Materials: HA0, HA15 and HA30. Commercial bovine HAp granules (Bio-Oss®) and empty defects were used as positive and negative controls, respectively. CT scans were registered at 0, 4, 8, 12 and 16 weeks after implantation. Sacrifice was carried out 16 weeks after surgery. Bone samples were removed and processed for histological evaluation (Goldner's Trichromic and Von-Kossa stains). **RESULTS AND DISCUSSION** Empty critical defects showed little regeneration and were mostly invaded by adipose tissue. Sites treated with Bio-Oss® appeared full of the implanted material, with no apparent resorption, osteointegrated in a new bone characterized by disorganized and anastomosed thin trabeculae. New bone appeared mostly mineralized with little osteoid and abundant vascularization. Defects implanted with HA0 showed hardly any remaining material and partial bone regeneration in the defect borders, with the remainder of the defect occupied by connective tissue. Differently to other materials, CT scans showed marked reabsorption of HA0 as early as 4 weeks. In contrast, sites implanted with HA15 and HA30 showed almost full bone regeneration with little remaining material which appeared well osteointegrated. Newly formed bone showed disorganized and anastomosed thick trabeculae, intense osteogenic activity and high vascularization along the entire defect. No adverse reactions were observed for any of the studied materials. **CONCLUSION** Critical bone defects filled with scaffolds made of Mon, HAp, and SG combinations were regenerated after 16 weeks with no adverse reactions. Scaffolds appear to be almost totally resorbed giving way to the formation new bone. The presence of HAp appears to be an essential feature in these materials.

33 INITIALS STEPS TOWARDS THE CONSTRUCTION OF A EXTRACELLULAR MATRIX MODEL IN CANCER. AN EXAMPLE USING NEUROBLASTOMA

Berbegall A P, Tadeo I, Víctor Zúñiga, Blanquer-Maceiras M, Martín-Vanó S, Navarro S and Noguera R

Universitat de Valencia

BACKGROUND: Cells and the surrounding extracellular matrix (ECM) are subject to forces with a profound influence on biological processes. Any cell has the capacity to convert mechanical stimuli into biological signals. This process is based on the biotensegrity principle, a mechanism determining tensional integrity. To date, this principle has been demonstrated to act in physiological processes such as mechanotransduction and mechanosensing at different scales, including the relation of the cells with the extracellular matrix compounds. However, little is known about how biotensegrity influences pathological processes. Clearly though, the tumour microenvironment must impose and experience distinct tensional forces compared to normal tissue.

M&M: To analyse the relationship between tumour cells and the extracellular matrix in neuroblastic tumours quantitative and topological analyses of the elements that drive traction and resistance of the extracellular matrix, including the fibrous scaffolding, blood vascularization, fundamental substance and immune and stem cells, were developed. Stored pools of samples from neuroblastoma patients to correlate the prognostic impact of the quantitative information obtained from the statistical and mathematical models applied to the microscopic images through databasing were used

RESULTS: We applied a novel approach that will capture tissue elements morphology, topology and genetic patterns, aiming to find relevant features that can be associated with the severity of the pathology. This includes the implication of chromosomal copy number changes and their breakpoints.

CONCLUSIONS: Distinguishing the contribution of each biological factor into prognosis is complicated given the heterogeneity of the neoplasia. More innovative and more comprehensive research approaches are need. Future tissue engineering methods that aim to create a 3D ECM model to mimic tumor behavior and progression should take into account not only the ECM components but also the genetic background of tumor cells and their interactions.

FUNDING: This study was supported by FIS (PI14/01008) and RTICC (RD12/0036/0020) grants from ISCII.

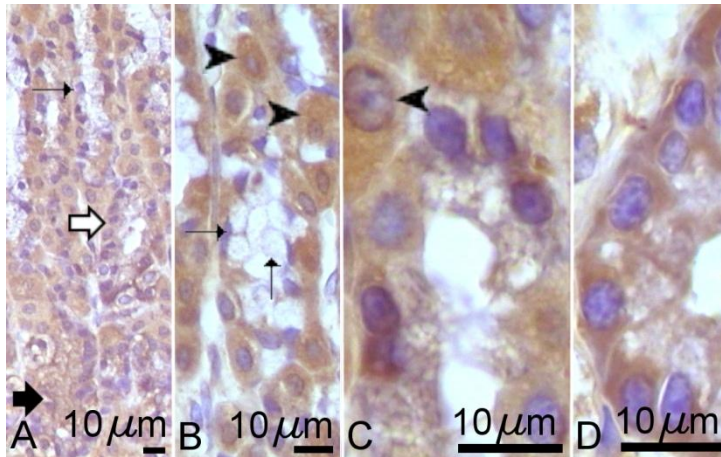
41 THE DIFFERENTIATION OF CHIEF CELLS FROM MUCOUS NECK CELLS IN FUNDIC GASTRIC GLANDS: EVIDENCE BY GNA LECTIN HISTOCHEMISTRY

(1) Gómez-Santos L., (1) Alonso E., (1) Bizkarguenaga M., (2) Díaz-Flores L, (3) Madrid J. F., and (1) Sáez F . J.

(1) Department of Cell Biology and Histology, UFI 11/44, University of the Basque country UPV/EHU, Leioa (Vizcaya), Spain, (2) Department of Anatomy, Pathology, Histology and Radiology, University of La Laguna (Tenerife), Spain, and (3) Department of Cell Biology and Histology, Regional Campus of International Excellence “Campus Mare Nostrum”, IMIB-Arrixaca, University of Murcia, Espinardo (Murcia), Spain.

The epithelium of the gastric mucosa and its glands is an example of self-renewing epithelium. This epithelium contains mucous surface cells (MSCs), parietal cells, mucous neck cells (MNCs), zymogenic or chief cells (ZCs) and several types of enteroendocrine cells. Recent research works have established that all cell types in the gastric epithelium arise from the same somatic stem cell (SSC), not yet identified, located at the isthmus of the gland. This SSC produces the precursor cells of MSCs, MNCs and parietal cells. Most of the evidences indicate that MNCs, located at the top of the gland, are the precursor cells of ZCs, located at the bottom of the gland. In addition, cells with characteristics between MNCs and ZCs are located between both regions, and these intermediate cells are called transitional or prezymogenic cells (pre-ZCs). The aim of our work was to analyze the expression of Mannose (Man) in the rat gastric glands by means of lectin histochemistry to identify the differences between MNC, pre-ZCs and ZCs and to establish the relationships between them. Methodology and materials Histochemistry with biotinilated lectin from *Galanthus nivalis* (GNA) was performed on histological sections from rat gastric corpus. The staining intensity in the gastric cells was evaluated and classified into six pre-established categories: no labeling (0), very weak (1), weak (2), moderate (3), strong (4), and very strong (5). Results GNA labeling of MNCs, pre-ZCs and ZCs was analyzed. No cell shows strong (4) or very strong (5) labeling, thus, cells were labeled in a scale from 0 (no labeling) to 3 (moderate labeling). Most of the cytoplasm of MNCs, plenty of secretion granules, was negative for GNA histochemistry (fig 1A,B). Intensity of GNA labeling in the gastric gland showed a graduation from pre-ZCs (labeling intensity 1 or 2), which are close to the top, under MNCs (fig 1A,C), to ZCs (labeling intensity 3) at the bottom (fig 1A,D). Labeling of ZCs was stronger at the perinuclear cytoplasm and at the apical secretion granules located near the cell apical surface (fig 1D). Conclusions Two hypotheses about the origin of ZCs have been proposed. The first hypothesis suggests that chief cells might differentiate directly from undifferentiated SSC. The second hypothesis considers that chief cells differentiate from MNCs, which are originated from the SSC. In rat stomach, cells intermediate between MNCs and ZCs have been found. These cells show secretory granules with some ultrastructural and histochemical properties that partially resembles those of MNCs and those of ZCs. In the last years, strong evidence has been reported supporting that ZCs originates from MNCs through pre-ZCs. Our work also support the origin of ZCs from MNCs, because the GNA labeling graduation might be due to oligosaccharides which are not expressed in MNCs, start to express in pre-ZCs and are more abundant in ZCs, indicating that differentiation from MNCs to ZCs is a process in which glycans with Man moieties are synthesized. Acknowledgements This work was supported by the UPV/EHU (EHUA13/15 and UFI 11/44), and Fundación Séneca (04542/GERM/06).

Figure legend: GNA lectin histochemistry of gastric glands. A: lower magnification of a gastric gland. B: MNCs. C: pre-ZCs. D: ZCs. Arrowhead: parietal cells. Thin arrows: MNCs. Black arrows: ZCs. White arrows: pre-ZCs.



48 MORPHOMETRIC STUDY OF MICROVASCULAR DENSITY IN CLEAR-CELL RENAL-CELL CARCINOMA INFLUENCED BY EXPOSURE TO CHRONIC PERSISTENT LOW-DOSE IONIZING RADIATION.

(1,2) Ruiz-Saurí, A.; (1,3) Valencia-Villa, G. (4) Romanenko, A. (3) Pérez, J. (3) García, R., (5) García, H.; (1) Benavent, J.; (1,2) Sancho-Tello, M.; (1,2) Carda, C.; (1,2) Llombart-Bosch, A.

(1) Departament de Patologia, Facultat de Medicina i Odontologia, Universitat de València; (2) INCLIVA, Hospital Clínic de Valencia. (3) Universidad del Norte, Medical School, Barranquilla, Colombia; (4) Departamento de Patología, Instituto de Urología. Academia de Ciencias Médicas. Ukraine, Kiev; (5) Universidad Libre, Facultad de Medicina, Barranquilla, Colombia. Departamento de Medicina Legal, Barranquilla, Colombia

INTRODUCTION Tumor angiogenesis is an essential factor for tumor growth and metastasis and its increase is related to worse prognosis. ?Chronic Persistent Low-Dose Ionizing Radiation? (CPLDIR) exposure increases incidence and aggressive behavior of clear-cell renal-cell carcinoma (CCRCC).. Our purpose is to study the behavior of the Microvascular Density (MVD), Vascular Endothelial Grow Factor (VEGF) and Hipoxy Induced Factor-1? (HIF-1?) in Clear Cell Renal Cell Carcinoma (CCRCC) from radio-contaminated geographical area (after Chernobyl accident) and compare the renal carcinomas from areas non-contaminated regions of Europe. **METHODS.** MVD, VEGF and HIF-1? expression was examined in 75 patients diagnosed with CCRCC from two geographical areas, 50 from the highly contaminated area and 25 from the low contaminated area of Ukraine, by means of immunohistochemical and digital micro-imaging and computerized analysis. Additionally, 50 tumors from areas that have not received radioactive contamination were studied comparatively (Spain and Colombia). **RESULTS.** The microvascular density within the CCRCC presented statistically significant progression (median p value p=0.00) when comparing the non-radiated and the radiated groups: Colombia: 407 vessels/mm²; Spain: 517 vessels/mm²; Ukraine low contaminated: 633 vessels/mm²; Ukraine high contaminated: 754 vessels/mm². When considering positive cells by tumor groups, we found that expression of VEGF in cases from the contaminated area of Ukraine was significantly higher than in the rest of the tumors, with statistical significance. A

significant increase in MVD was seen in CCRCC exposed to CPLDIR (754 capillaries/mm²), associated with high VEGF expression (49%) and HIF-1 α (31%). The Ukrainian group with low CPLDIR showed a persistent increase in MVD (633 capillaries/mm²) associated with a simultaneous increase in VEGF (28%) and HIF-1 α (22%) expressions. **CONCLUSIONS** We confirm that higher intratumoral MVD, together with high expression of VEGF and HIF-1 α are the more discriminating factors associated with the aggressiveness of CCRCC. Moreover, these factors discriminate between tumors from CPLDIR regions of Ukraine and tumors diagnosed in radiation-free countries such as Spain and Colombia.

66 STRUCTURAL ALTERATIONS OF THE NUCLEAR ENVELOPE. A STUDY IN NEUROBLASTOMA.

(1) Martín-Vañó, (1) S., Berbegall, A.P., (1) Tadeo, I. , (2) Cañete, A., (1) Noguera, R.

(1) Department of Pathology, Medical School, University of Valencia; Medical Research Found ation INCLIVA. Valencia, Spain. (2) Pediatric Oncology Unit, University and Polytechnic Hospital La Fe, Valencia, Spain

BACKGROUND. Molecular features such as high chromosomal instability (HCIN) of some genomes can be reflected in the morphological changes of the nuclear envelope (NE). These NE changes can be used by the pathologists for cancer diagnosis and include pleomorphism in shape and size, deep infoldings, intranuclear cytoplasmic inclusions and micronuclei. The presence of chromothripsis or a great number of genomic amplifications are characteristics of HCIN in cancer. Chromothripsis is defined by the presence of tens to hundreds of genomic rearrangements acquired in a single catastrophic event. This phenomenon is observed in at least 2-3% of all cancers. In neuroblastoma (NB) it has been recently shown to occur in 18% of high-stage NB associated with a poor prognosis. We aimed to study the different morphological changes in the NE of 2 types of HCIN in NB samples.

MATERIAL AND METHODS. Two sets of patient samples were analyzed in order to evaluate morphologic changes at the nuclear level: 18 NB samples with chromothripsis and 20 samples with 4 to 22 amplifications detected by genome analysis using aSNP (~250K aSNP Affymetrix or ~300K aSNP Illumina). Tumors were morphologically re-analyzed by 3 researchers under a microscope. Morphological changes of NE were established by the observation of 5 areas at 40X magnification in Hematoxylin and Eosin slides.

RESULTS. Morphological changes in NE were detected in all the tumors analyzed with HCIN. The main changes of NE observed in chromothripsis samples were intranuclear cytoplasmic inclusions and infoldings (11/18), NE fragility with granular chromatin distribution and evident nucleoli (9/18) and pleomorphism with micronuclei (5/18). In samples with high number of amplifications the characteristics of NE observed were the presence of inclusions or infoldings (5/20) and granular chromatin distribution with NE fragility and evident nucleoli (11/20) while micronuclei were barely detected (2/20).

CONCLUSIONS. There is a link between HCIN and morphological changes of NE in NB. The findings indicate that changes detected in the NE are differently associated with the two types of

chromosomal instability NB samples. Performing similar studies in a higher cohort and in other types of tumors might reveal new associations between morphological changes of NE and genetics.

Grants: RD12/0036/0020 from ISCIII and PI14/01008 from ISCIII

77 BIOASSAY OF CYANOACRYLATE TISSUE ADHESIVES USED FOR INTRAPERITONEAL MESH FIXATION

(3) Pascual, G.; (2) Fernández-Gutiérrez, M.; (1) Rodríguez, M.; (3) Sotomayor, S.; (1) Pérez-Köhler, B.; (1) Kuhnhardt, A.; (2) San Román, J.; (1) Bellón, J.M.

(1) Department of Surgery, Medical and Social Sciences, Faculty of Medicine and Health Sciences, University of Alcalá. Networking Biomedical Research Centre on Bioengineering, Biomaterials and Nanomedicine (CIBER-BBN). Madrid, Spain. (2) Polymeric Biomaterials Group. Polymer Science and Technology Institute-Consejo Superior de Investigaciones Científicas (ICTP-CSIC), Networking Biomedical Research Centre on Bioengineering, Biomaterials and Nanomedicine (CIBER-BBN), Madrid, Spain. (3) Department of Medicine and Medical Specialities, Faculty of Medicine and Health Sciences, University of Alcalá. Networking Biomedical Research Centre on Bioengineering, Biomaterials and Nanomedicine (CIBER-BBN). Madrid, Spain.

INTRODUCTION. During laparoscopic/endoscopic hernia repair, the use of a tissue adhesive to fix a prosthetic material is a feasible option. However, scarce data exist for the use of a synthetic adhesive in this setting. This study examines the intraperitoneal behavior of two cyanoacrylate tissue adhesives: Ifabond® and a new, non-marketed octyl cyanoacrylate adhesive (OCA) used for the intraperitoneal fixation of an expanded polytetrafluoroethylene (ePTFE) mesh.

MATERIALS AND METHODS. In 36 New Zealand White rabbits, 3x3 cm (n=24) or 1,5x3 cm (n=12) fragments of ePTFE mesh (PrecludeR, Gore, Flagstaff, USA) were fixed to the parietal peritoneum using OCA or Ifabond®. Peritoneal fluid was obtained at the time of implant and at 2 weeks postimplant for cytokine determinations (IL-6 and TNF- α). At 14 or 90 days postsurgery, the animals were euthanized and the meshes excised *en bloc* with the anterior abdominal wall to assess host tissue incorporation (light microscopy and scanning electron microscopy), the macrophage response (immunolabeling with the rabbit monoclonal anti-RAM 11 antibody), apoptosis (TUNEL) and fixation strength (T-peel tensiometry).

RESULTS. Peritoneal fluid IL-6 and TNF- α concentrations were similar in the OCA and Ifabond® groups. Both adhesives gave rise to adequate mesothelialization of the ePTFE and their degradation was visible at 90 days. Macrophage counts were similar for the two study groups, but a significantly increase in macrophage response was observed from 14 to 90 days for Ifabond®. At 90 days postimplant, apoptotic cell counts was lower for the implants fixed with OCA (p<0.05) and a fixation strength was significantly lower for OCA (p<0.0001).

CONCLUSION. Despite similar cytokine levels at 2 weeks and similar host tissue incorporation observed for the meshes fixed with the two adhesives, the use of Ifabond® gave rise to a greater apoptosis rate, although this adhesive provided a stronger fixation bond.

Acknowledgments: Financial support for this research was provided by the Spanish Ministry of Economy and Competitiveness through the research project SAF2014-55022-P

80 INFLUENCE OF CHRONIC VENOUS INSUFFICIENCY ON PLACENTAL DEVELOPMENT: VILLI AND SYNCYTIAL KNOTS.

(1) Mesa-Ciller, C.; (1) Álvarez-Rocha, MJ.; (2) Asúnsolo, A.; (1) Cifuentes, A.; (1) García-Honduvilla, N.; (1) Buján, J.

Departments of (1) Medicine and Medical Specialities and (2) Surgery, Medical and Social Sciences, Faculty of Medicine and Health Sciences, University of Alcalá, Alcalá de Henares, Madrid, Spain. Networking Research Center on Biomaterials and Nanomedicine (CIBER-BBN), Madrid, Spain.

Introduction: Placenta is a unique organ derived from both the mother and the fetus, and it is of prime importance throughout the period of gestation. The main functions of the placenta are transport, metabolism, protection and endocrine. The placenta acts to provide oxygen, water, carbohydrates, amino acids, lipids, vitamins, minerals and other nutrients to the fetus, whilst removing carbon dioxide and other waste products.

Maternal blood enters at high pressure into the chorionic plate, and then slowly flows around the villous area when the pressure lowers, allowing the exchange of substances, returning afterwards through the veins. Changes in the hemodynamics of the maternal blood flow can seriously affect the growth of the placenta, and indirectly, of the fetus.

The aim of this study was to evaluate the possible histological changes of placental villi on pregnant women with varicose pathology.

Materials and Methods: Human full-term placentae (n=35) were collected after delivery and divided into two groups: control (n=15, women without varicose veins), and varicose (n=20, women with varicose pathology). Each group was subdivided into young pregnant women (<35 years) and aged pregnant women (≥35 years). Histological sections were stained with hematoxylin-eosin (H-E), and light microscopy images (5 micrographs per sample, 100x) were analyzed to determine the number of villi and syncytial knots. Results were expressed as mean ± standard error of the mean, and were analyzed using the Mann-Whitney *U* test.

Results: Placentae from women suffering varicose pathology showed a higher number and a smaller size of villi than control group ($p \leq 0.05$). However, the analysis of the groups split by age did not reveal significant differences in the number of villi. The measurement of the numbers of syncytial knots revealed a higher abundance in the varicose group when compared with control ($p \leq 0.01$). Taking the age of the mothers into account, greater number of knots were also observed in young varicose vs. young control groups ($p \leq 0.01$). Fibrinoid deposits did not show significant differences between varicose and non-varicose populations.

Conclusions: Observed differences between control and varicose groups suggest a relationship between chronic venous insufficiency and the number of placental villi and syncytial knots. However, while this raise in the number of villi seems to happen regardless of the age of the pregnant mother, the increment in the amount of syncytial knots could be mainly attributable to differences between young healthy and varicose populations.

Acknowledgements: This work was supported by a FIS PI13/01513 grant.

87 MELATONIN DECREASES NO LEVELS AND GLIAL REACTIVITY IN A MODEL OF BRAIN HYPOBARIC HYPOXIA INJURY

Peinado MA, Hernández R, Lamelas L, Blanco S

Department of Experimental Biology, University of Jaen. Las Lagunillas s/n 23071 Jaén, Spain.

Nitric oxide (NO) is a gaseous neurotransmitter with many physiological effects. In fact, and due to its dual neuroprotective-neurotoxic role, in which free radicals play a main role, NO is key in brain response to hypoxic and ischemic injuries. In this sense, many studies have demonstrated a neuroprotective effect for the antioxidant melatonin against hypoxic insults. We analyzed the response of neuronal-NO system in the brain of rats treated with melatonin and submitted to a model of hypobaric hypoxia (HH) followed by two reoxygenation periods of 0 and 2 hours (0h and 2h). Specifically, we determined: 1) the amount of NO by means of a Nitric Oxide Analyzer (NOA); 2) the expression and localization of nNOS isoform and; 3) glial reactivity (GFAP localization and expression). Our results show that after the hypoxic insult, the administration of melatonin decreases NOx levels at both reoxygenation periods. Concurrently, GFAP expression is decreased in the melatonin-treated group immediately after HH, but not at further periods (2h). On the other hand, melatonin administration enhanced nNOS expression straightway after HH but not at 2h. In summary, the administration of melatonin in our model of cerebral hypobaric hypoxia modulates both glial and NOS responses. Supported by MICINN (SAF2008-03938).

102 CANNABIONOIDS RECEPTOR AGONISTS INHIBIT PROLIFERATION IN PULMONARY PRIMARY CANCER CELLS.

Mata, M. (1)(2)(3); Milian, M.(2); Carretero J.(5); Galvis J. (4); Ruiz Saurí, A.(1)(2); Sancho-Tello, M.(1)(2); de Llano, J.J. (1)(2) and Carmen Carda(1)(2).

(1) Departament de Patologia, Facultat de Medicina i Odontologia, Universitat de València. (2) INCLIVA, Hospital Clínico Universitario de Valencia. (3) Ciber de enfermedades respiratorias (CIBERES). (4) Servicio de Cirugía Torácica. Hospital de Alzira, valencia. (5) Departament de Fisiologia, Facultat de Medicina i Odontologia, Universitat de València.

Background/Objective: Cannabinoids are bioactive lipids that have a range of interesting activities mediated by two G-protein- coupled receptors (CNR1 and CNR2). These molecules have been proposed as direct inhibitors of tumour growth in vitro and in animal tumour models through several pathways. Different mechanisms have been implicated in the actions of endocannabinoids and include cytotoxic or cytostatic effects, apoptosis induction, etc. These effects have been described in several types of cancers including glioma, glioblastoma, breast cancer, prostate cancer, thyroid cancer, colon carcinoma, leukaemia, and lymphoid tumours. Unfortunately, the implication of this molecules in lung cancer are poorly studied. In this study we have analysed the relative gene expression of CNR1 and CNR2 receptors in 157 non-small lung cancer samples as well as the antiproliferative effects of different combinations of THC and cannabidiol in A549 cells as well as in primary cultured lung cancer cells. We have also analysed the effects of these compounds regulating the gene expression of CNR1, CNR2, EGFR, Bcl2 and APAF. Methods: CNR1, CNR2, EGFR, Bcl2 and APAF gene expression was analysed by Real Time RT-PCR. A549 cells were obtained from the ATCC while primary tumour cultures were established using lung cancer tumour-spheres. Proliferation was evaluated according to BrdU incorporation. Results: Human lung cancer patients were separated according to the relative expression of CNR1 and CNR2. Survival analysis demonstrate that patients with high levels of CNR1 and/or CNR2 exhibited a longer survival than those patients with lower levels of CNR1 and/or CNR2. Exposure of A549 and primary lung cancer cultures to different combinations of THC and cannabidiol resulted in a dose dependent inhibition of cell proliferation as well as in a down-regulation of EGFR and Bcl2 as well as in an increase of the apoptotic activator APAF. Conclusion: Results presented here support the implication of the cannabinoid system in lung cancer as well as the potential use of cannabionoid agonists for the treatment of non-small lung cancer.

121 HISTOLOGICAL, IMMUNOHISTOCHEMICAL AND GENETIC PATTERNS OF HUMAN LOOSE, DENSE AND FIBROTIC CONNECTIVE TISSUE. THE DUPUYTREN'S DISEASE AS A MODEL

(1) Alfonso-Rodríguez, C.A.; (1) Martín-Piedra, M.A.; (1) Garzón, I.; (1) García-Martínez, L.A.; (1) Jaimes-Parra, B.D.; (1) Vela-Romera, A.; (1) Sánchez-Quevedo, M.C.; (1) Alaminos, M.; (1) Campos, A.

(1) Tissue Engineering Group, Department of Histology, University of Granada, Spain, and Instituto de Investigación Biosanitaria ibs.GRANADA, Spain

Introduction: Dupuytren's Disease is a very prevalent disease of the hand palm and one of the most common hereditary diseases of the connective tissue. In severe cases, the disease leads to a permanent flexion contracture of the metacarpophalangeal and proximal interphalangeal joints of the digits, leading to loss of function and deformity of the hand. Despite its clinical relevance, the specific alterations found in the extracellular matrix (ECM) of the hand tissues affected by this disease are not fully understood. In the present study, we have analyzed all major components of the ECM of tissues affected by Dupuytren's disease in order to determine the ECM alterations associated to this disease. Materials and Methods: Three types of tissues were analyzed in patients with Dupuytren's Disease: the fibrotic connective tissue corresponding to the hand contracture cord (DDC), the dense connective tissue of the palmar fascia clinically

unaffected by Dupuytren's disease contracture (NPF) and the loose connective tissue of the normal forehand fascia (NFF). Tissue biopsies corresponding to each tissue type were histologically analyzed by Masson's trichrome staining, picrosirius, Gomori's reticulin, orcein, Schiff Periodic acid staining (PAS) and alcian blue histochemistry and immunohistochemistry for decorin, versican, aggrecan and laminin. In addition, total RNA was extracted from each tissue type and quantified using oligonucleotide microarrays. Results: The results showed that DDC samples had abundant fibrosis with numerous reticular fibers and few elastic fibers, and contained abundant laminin and glycoproteins. In contrast, control NFF had lower amounts of these components. Interestingly, NPF tissues had more collagen, reticular fibers, laminin and glycoproteins than NFF, although at lower level than DDC, with similar elastic fibers than DDC. Immunohistochemical expression of decorin was high in DDC, whereas versican was highly expressed NFF, with no differences were found for aggrecan. The global expression profile showed that NPF was very similar to DDC and different to control NFF. Conclusions: The results of the present study show that DDC tissues have important ECM alterations, including fibrillar and non-fibrillar components. In addition, we found that NPF tissues are also affected and they should not be considered as normal tissues. Acknowledgments: This study is supported by CTS-115, Tissue Engineering Group, University of Granada, Spain.

152 PLACENTAL BARRIER INDEMNITY PLAY A KEY ROLE IN THE INFECTION OF PLACENTAL TISSUE BY TRYPANOSOMA CRUZI

(1) Díaz-Luján C., (1) Triquell MF, (3) Castillo C, (3) Kemmerling U,(4) Hardisson D.,(1, 2) Fretes RE

(1)Cell Biology, Histology and Embryology Department, Facultad Cs. Médicas. Universidad Nacional de Córdoba-INICSA (CONICET), Argentina. (2)Histology, Embryology and Genetic-IICSHUM, Health Department, Universidad Nacional de La Rioja. Argentina. (3)Programa de Anatomía del Desarrollo, Instituto de Ciencias Biomédicas. Facultad de Medicina. Universidad de Chile. Chile. (4) Hospital La Paz. Universidad Autónoma de Madrid. España.

Trypanosoma. cruzi is an obligate intracellular parasite that can be transmitted from pregnant women to feta, causing the congenital transmission of the Chagas disease. The American trypanosomiasis is one of the neglected disease which is endemic in LatinAmerica, but nowadays congenital Chagas disease it has been spread outside this region to cause a global health problem. The infection of placental tissue and the vertical transmission of *T. cruzi* seem to depend on several factors although its initial steps are still relatively unknown. Therefore, it is important to research the relevance of the first structure of the placental barrier presence in the chorionic villi infection by *T. cruzi*, the agent of the congenital Chagas disease and to define which placental cells are mainly infected when this parasite accesses within the chorionic villi in the initial steps of the infection.

Material and methods: Explants of human chorionic villi placenta from healthy pregnant women at term, were denuded of their syncytiotrophoblast (STB) with trypsin and then were co-cultured for 3h, 24h and 96h with 800,000 trypomastigotes (Tulahuen strain). Denudation was verified by hCG- β and placental alkaline phosphatase activity in culture media and

immunostaining for syncytin and analyzed remanent area of STB. *T. cruzi* infected cells were identified by immunohistochemistry for cytokeratin-7 (+ cytotrophoblast) and CD68 (+ macrophages) and infection was quantified as area occupied by the parasite, nests of parasites and amastigotes per nest. Parasite load was analyzed by qPCR and viability in the culture medium. Statistics: Student t-test and ANOVA.

Results: In chorionic villus denuded of syncytiotrophoblast: total area occupied by the parasite ($451,23 \mu\text{m}^2$, 1,33%) and parasite load (RQ: 87) were significantly higher ($p < 0.05$) in the entire villous ($5,98 \mu\text{m}^2$, 0,016%) (RQ:1). Stromal cells were infected among cytotrophoblast (cytokeratin-7 +), and some macrophages (CD68 +), without significant differences in the level of infection. The parasite viability was significantly higher ($p < 0.05$) in denuded culture explant from 24 to 96h hours of culture.

Conclusion: The complete human chorionic villi limited the infection. Detaching the syncytiotrophoblast (first placenta barrier), the villous stroma infection is increased along with the viability of the parasite in the placental environment. Therefore indemnity chorionic villous controls the infection, and structural and functional alterations could favor the parasite to reach the fetal circulation, hence participating in congenital transmission.cases.

Aknowledgements: To Gina Mazzudulli for her technical assistance. Grants: SECyT-UNLaR, SECyT-UNC, MINCyT-Córdoba, PICT-2012-1061, MINCyT (Argentina)-CONICYT (Chile).

153 ESTIMATE OF THE K FUNCTION AND ISOTROPY OF ACINI IN HUMAN NORMAL PROSTATE AND PROSTATE ADENOCARCINOMA

(1) Santamaría Solís, L.*; (2) Ingelmo Ingelmo, I.;(3) Rodríguez Ramos, R.; (4) Sinues Ojas, B.; (4) Martínez Blázquez, L.; (5) Teba del Pino, F.

(1) Department of Anatomy, Histology, and Neuroscience. School of Medicine, Autonomous University of Madrid, Madrid, Spain. (2) Department of Anesthesiology. Hospital Ramón y Cajal, Madrid, Spain. (3) Department of Medical Basic Sciences, School of Medicine, San Pablo University, CEU, Madrid, Spain.(4)Service of Urology. Hospital del Henares, Madrid, Spain. 5Department of Surgery (Urology). Hospital de La Princesa, School of Medicine, Autonomous University of Madrid, Spain

Introduction: Second-order stereology was employed to investigate the spatial distribution of acini in normal prostate and adenocarcinoma. The distribution of glandular profiles in a tissue could be assimilated to the spatial arrangement of a random set of points, and then might be studied by methods of stochastic geometry.

Second-order functions provide a series of values as a function of the interpoint distance r . These functional values indicate which kind of interaction between acini prevails at a certain distance. This interaction may consist of attraction (clustering) or repulsion, or otherwise there may be no interactive effects between the points at all at a certain distance. Second-order stereology could bring in this respect, valuable information about the spatial distribution of

acini of malignant or premalignant lesions, and probably contribute to an appropriate gradation of tumor aggressiveness.

Material and methods: Sections from normal prostate (ctr) and adenocarcinoma (ca) were immunostained to cytokeratin 18 (ck18) for visualization of prostate epithelium.

Strips formed by adjacent quadrats chosen by systematic random sampling were explored for each section from both groups. The result was a series of images, sized 512 x 4600pixels. The images were binarized, and the volume fraction (v_v) of epithelium ck18 immunoreactive was estimated.

After digitizing the coordinates of the mass centre of the acini, the correlation k function, $k(r)$ was applied to characterize the two-dimensional point process of the profiles. This function represents the mean number of other points of the process lying within a circle of radius r , centred about a typical point of the process. As reference model a stationary poisson point process was used.

Besides to estimating $k(r)$, the isotropy of the distribution of acini population was investigated. Anisotropy analysis is the study of whether spatial pattern differs along different cardinal axes, for this purpose the angular correlation between the distribution of the acini and certain directions in the plane was estimated.

All the analysis were performed using the software for spatial statistics, passage (version 2.0).

Results: There was not significant differences for v_v between ctr and ca groups. In both groups, the $k(r)$ function indicates that the distribution of acini is not poisson type, i.e. Having absence of complete spatial randomness, showing a significant tendence to the clustering of the acini, this was more relevant in ctr cases than in cancer, but the difference between them was not significant. The angular correlation analysis show a mild but significant anisotropy in the distribution of normal acini, this anisotropy dissapears in the tumor group.

Conclusions:

- 1- the first order parameter v_v of epithelium does not apport differential information between normal and cancer prostate acini.
- 2- in both normal and cancer cases the acinar distribution shows tendency to clustering and does not show complete spatial randomness.
- 3- the structure of $k(r)$ was similar from both ctr and ca groups, but the clustering was more relevant in normal acini.
- 4- the tumor acini show lost of anisotropy in their directional orientation when comparing with normal glands.